

Dissertation zur Erlangung des Doktorgrades der Fakultät für Chemie
und Pharmazie der Ludwig-Maximilians-Universität München

**Entwicklung und Anwendung von
MS-Bindungsassays zur Charakterisierung der
Bindung von MB327 und anderer Verbindungen an
die MB327-Bindestelle des nikotinischen
Acetylcholinrezeptors**

vorgelegt von

Sonja Andrea Sichler

aus

Immenstadt i. Allgäu, Deutschland

2018

Erklärung

Diese Dissertation wurde im Sinne von § 7 der Promotionsordnung vom 28. November 2011 von Herrn Professor Dr. Klaus T. Wanner betreut.

Eidesstattliche Versicherung

Diese Dissertation wurde eigenständig und ohne unerlaubte Hilfe erarbeitet.

München, 13.11.2018

.....
Sonja Sichler

Dissertation eingereicht am: 13.11.2018

1. Gutachter: Professor Dr. Klaus T. Wanner

2. Gutachter: Professor Dr. Franz F. Paintner

Mündliche Prüfung am: 11.12.2018

Die vorliegende Arbeit entstand in der Zeit von März 2014 bis Oktober 2017 am
Department für Pharmazie – Zentrum für Pharmaforschung – der Ludwig-
Maximilians-Universität München auf Anregung und unter Leitung von

Herrn Prof. Dr. Klaus T. Wanner

Für die hervorragende und sehr engagierte Betreuung und Förderung meiner Arbeit,
sowie die ausgezeichneten Forschungsbedingungen danke ich
Herrn Prof. Dr. Klaus T. Wanner sehr herzlich.

Herrn Prof. Dr. Franz F. Paintner danke ich herzlich
für die Übernahme des Koreferats

- Für meine Eltern,

für Marco -

Danksagung

Ich danke allen Mitarbeitern und Kollegen des Arbeitskreises von Herrn Prof. Dr. Klaus T. Wanner für die gute Zusammenarbeit.

Ein besonderer Dank gilt Dr. Georg Höfner für seine Unterstützung, für viele, viele konstruktive Anregungen und alles, was ich von ihm lernen durfte. Ein großer Dank geht auch an meine Laborkollegen Paddi, Marc, Thomas und Jürgen für die großartige Arbeitsatmosphäre. Paddi und Marc verdanke ich insbesondere, dass ich in dieser Zeit kein musikalisches Schmankerl verpasste.

Für vielfältige Unterstützung geht mein Dank außerdem an Oberfeldapothekerin Karin V. Niessen und Ihrer Arbeitsgruppe, insbesondere an Bea Boch und Gerda Engl, am Institut für Pharmakologie und Toxikologie der Sanitätsakademie der Bundeswehr in München.

Ein spezieller Dank gilt außerdem Sebastian Rappenglück für die hervorragende Zusammenarbeit und seinen beständigen, ansteckenden Optimismus.

Für die netten Gespräche und dafür, dass ich mich schon in der ersten Woche im Arbeitskreis aufgenommen gefühlt habe, danke ich Anne Kärtner.

Ein besonderer Dank geht an Maren Schaarschmidt. Ich danke dir für die Freundschaft und dafür, dass du immer ein offenes Ohr für mich hattest.

Mein größter Dank gilt schließlich meinen Eltern und meinem Freund Marco, ohne deren bedingungslose und stetige Unterstützung die vorliegende Arbeit nicht hätte entstehen können. Euch ist diese Arbeit gewidmet.

Diese kumulative Doktorarbeit basiert auf folgenden Originalpublikationen:

Erste Publikation:

Sonja Sichler, Georg Höfner, Sebastian Rappenglück, Thomas Wein, Karin V. Niessen, Thomas Seeger, Franz Worek, Horst Thiermann, Franz F. Paintner, Klaus T. Wanner; *Toxicology Letters* **2018**, 293, 172-183 (DOI: 10.1016/j.toxlet.2017.11.013). Copyright Elsevier B.V. © 2018. Dieses Manuskript wird durch die CC-BY-NC-ND 4.0 Lizenz zur Verfügung gestellt [<http://creativecommons.org/licenses/by-nc-nd/4.0/>]

“Development of MS Binding Assays targeting the binding site of MB327 at the nicotinic acetylcholine receptor”

Zweite Publikation:

Sebastian Rappenglück, **Sonja Sichler**, Georg Höfner, Thomas Wein, Karin V. Niessen, Thomas Seeger, Franz F. Paintner, Franz Worek, Horst Thiermann, Klaus T. Wanner; *ChemMedChem* **2018**, 13, 1806-1816 (DOI: 10.1002/cmdc.201800325). Copyright Wiley-VCH Verlag GmbH & Co. KGaA. Die Genehmigung zum Nachdruck liegt vor.

“Synthesis of a Series of Structurally Diverse MB327 Derivatives and Their Affinity Characterization at the Nicotinic Acetylcholine Receptor”

Drittes Manuskript:

Sebastian Rappenglück, **Sonja Sichler**, Georg Höfner, Thomas Wein, Karin V. Niessen, Thomas Seeger, Franz F. Paintner, Franz Worek, Horst Thiermann, Klaus T. Wanner. Angenommen von *ChemMedChem* (DOI: 10.1002/cmdc.201800539). Copyright Wiley-VCH Verlag GmbH & Co. KGaA. Die Genehmigung zum Nachdruck liegt vor.

“Synthesis of a Series of Non-Symmetric Bispyridinium and Related Compounds and Their Affinity Characterization at the Nicotinic Acetylcholine Receptor”

Teile dieser Arbeit wurden bereits auf nationalen und internationalen Konferenzen präsentiert:

Präsentation eines Posters auf der „12. Tagung über Iminiumsalze“ 2015, Goslar

Sebastian Rappenglück, **Sonja Sichler** und Klaus T. Wanner

“Entwicklung neuer Modulatoren für den nikotinischen Acetylcholinrezeptor zur Therapie von Vergiftungen mit phosphororganischen Verbindungen”

Präsentation eines Posters auf dem „47. Kongress der Deutschen Gesellschaft für Wehrmedizin und Wehrpharmazie (DGWMP)“ 2015, Neu-Ulm

Sonja Sichler, Georg Höfner, Thomas Wein, Karin V. Niessen, Thomas Seeger und Klaus T. Wanner

„Entwicklung von MS-Bindungsassays zur Charakterisierung der Bindung von MB327 als Modulator am nikotinischen Acetylcholinrezeptor“

Präsentation eines Posters auf der „16. Medical Chemical Defense Conference“ 2016, München

Sonja Sichler, Georg Höfner, Thomas Wein, Sebastian Rappenglück, Karin V. Niessen, Thomas Seeger, Franz Worek, Horst Thiermann und Klaus T. Wanner

“Development of MS Binding Assays targeting the binding site of bispyridinium compounds at the nicotinic acetylcholine receptor”

Inhaltsverzeichnis

1. Einleitung	1
1.1 Phosphororganische Verbindungen als chemische Kampfstoffe	1
1.2 Symptome einer Organophosphatvergiftung	4
1.3 Standardtherapie von Organophosphatvergiftungen	6
1.4 Der nAChR als Target alternativer Therapieoptionen	7
1.4.1 Struktur und Funktion des nAChR	7
1.4.2 Therapie durch allosterische Modulation des nAChR	10
1.5 MB327 als potentielltes Antidot gegen OP-Vergiftungen	12
1.5.1 MB327 als positiv allosterischer Modulator am Muskeltyp-nAChR	12
1.5.2 Pharmakologische Wirkung von MB327 in <i>ex vivo</i> und <i>in vivo</i> Studien	14
1.6 Entwicklung neuer Antidote ausgehend von MB327 als Leitstruktur	15
1.6.1 Die rationale Wirkstoffentwicklung	15
1.6.2 Radioligand-Bindungsassays als Testsystem der rationalen Wirkstoffentwicklung	17
1.6.3 MS-Bindungsassays als Label-freie Alternative	19
1.6.4 Anwendung von Bindungsassays zur Bestimmung von Affinitätskonstanten	19
2. Zielsetzung	23
3. Ergebnisse und Diskussion	28
3.1 Erste Publikation	28
Development of MS Binding Assays targeting the binding site of MB327 at the nicotinic acetylcholine receptor	28
3.1.1 Zusammenfassung der Ergebnisse	28
3.1.2 Erklärung zum Eigenanteil	30
3.2 Zweite Publikation	31
Synthesis of a Series of Structurally Diverse MB327 Derivatives and Their Affinity Characterization at the Nicotinic Acetylcholine Receptor	31
3.2.1 Zusammenfassung der Ergebnisse	31
3.2.2 Erklärung zum Eigenanteil	33
3.3 Drittes Manuskript	34
Synthesis of a Series of Non-Symmetric Bispyridinium and Related Compounds and Their Affinity Characterization at the Nicotinic Acetylcholine Receptor	34

3.3.1 Zusammenfassung der Ergebnisse	34
3.3.2 Erklärung zum Eigenanteil	36
3.4 Unveröffentlichte Ergebnisse	37
3.4.1 Allgemeiner Teil	37
3.4.2 Experimenteller Teil	40
4. Zusammenfassung der Arbeit	45
5. Abkürzungsverzeichnis	50
6. Literaturverzeichnis	52

EINLEITUNG

1. Einleitung

1.1 Phosphororganische Verbindungen als chemische Kampfstoffe

Im ersten Weltkrieg wurden chemische Kampfstoffe erstmals als Massenvernichtungsmittel instrumentalisiert. Wie am 22. April 1915 im belgischen Ypern, als deutsche Soldaten den chemischen Kampfstoff Chlorgas im Großmaßstab gegen französische Stellungen einsetzten, was mehreren Tausend Menschen das Leben kostete, waren die Folgen stets verheerend^{1,2}. Um dem entgegenzuwirken, wurde im Jahr 1925 das Genfer Protokoll verabschiedet, in dem sich alle Vertragsparteien zu einem Verzicht auf den Einsatz erstickender, giftiger und sonstiger Gase sowie Biologischer Waffen verpflichteten. Nichtsdestotrotz befeuerte die Entdeckung neuer, noch giftigerer Agenzien, die sich für den militärischen Einsatz eigneten, auch weiterhin das internationale Wettrüsten mit Chemiewaffen, denn die Entwicklung sowie das Bevorraten chemischer Kampfstoffe war durch das Genfer Protokoll noch nicht explizit verboten worden.³ Anfang der 1990er Jahre wurde deshalb ein neues internationales Übereinkommen, die Chemiewaffenkonvention, mit dem Ziel verabschiedet, eine Welt frei von Chemiewaffen zu schaffen.⁴ Diese trat am 29. April 1997 in Kraft. Um sicherzustellen, dass alle bis heute 192 Unterzeichnerstaaten ihre vertraglichen Verpflichtungen einhalten, hierzu zählen neben dem Verbot Chemiewaffen einzusetzen nun auch das Verbot von Entwicklung, Produktion, sowie Lagerung und schließt außerdem die Vernichtung vorhandener Arsenale mit ein, ist die OPCW (Organisation for the Prohibition of Chemical Weapons) mit Sitz in Den Haag beauftragt. Für ihre Arbeit wurde die OPCW im Jahr 2013 mit dem Friedensnobelpreis ausgezeichnet.⁵ Die Zeiten in denen Chemiewaffen zur Massenvernichtung im internationalen Konflikt eingesetzt wurden sind heute Vergangenheit. Gleichzeitig werden Chemiewaffen vermehrt im Kontext terroristischer Straftaten eingesetzt. In einem letzten prominenten Fall, der sich im März 2018 in Salisbury Großbritannien ereignete, wurden ein ehemaliger, russischer Doppelagent und dessen Tochter Opfer eines Angriffs mit einem Nervenkampfstoff vom Typ Nowitschok.^{6,7} Im Jahr zuvor erfolgte ein Attentat auf Kim Jong-Nam, Halbbruder des nordkoreanischen Machthabers Kim Jong-Un, mit dem Nervenkampfstoff VX in Malaysia, das in diesem Fall tödlich endete.⁸ Dass im Zuge des syrischen Bürgerkriegs

ebenfalls ein chemischer Kampfstoff - das Nervengift Sarin - eingesetzt wurde, bestätigte sich nach gründlicher Untersuchung durch die OPCW.^{9,10}

Chemische Kampfstoffe lassen sich nach ihrer Wirkweise bzw. den, nach Exposition primär betroffenen, Körperarealen grob in Irritantien, Nerven-, Lungen-, Blut-, Haut-, Nerven- sowie Psychokampfstoffe einteilen.² Bei den bereits obengenannten Kampfstoffen VX, Sarin bzw. solchen vom Typ Nowitschok handelt es sich um Nervenkampfstoffe. Namensgebend für diese Verbindungen, es handelt sich dabei um phosphororganische Verbindungen deren Struktur typischerweise einer allgemeinen Formel nach Schrader genügt (vgl. Abb. 1), ist ihre toxische Wirkung durch Störung der Reizübertragung im Nervensystem.^{1,11,12} Der erste Nervenkampfstoff, der 1936 zufällig von Gerhard Schrader, einem deutschen Chemiker des damaligen IG Farben Konzerns in Leverkusen, entdeckt wurde, war die Verbindung Ethyl-dimethylphosphoramidocyanidat, heute besser bekannt als Tabun. Das eigentliche Ziel der Forschungsarbeit Schraders war die Entwicklung potenter Insektizide.¹³ In den darauffolgenden Jahren wurden von Schrader und Kollegen ebenfalls die Nervengifte Sarin (1938), Soman (1944) sowie Cyclosarin synthetisiert.

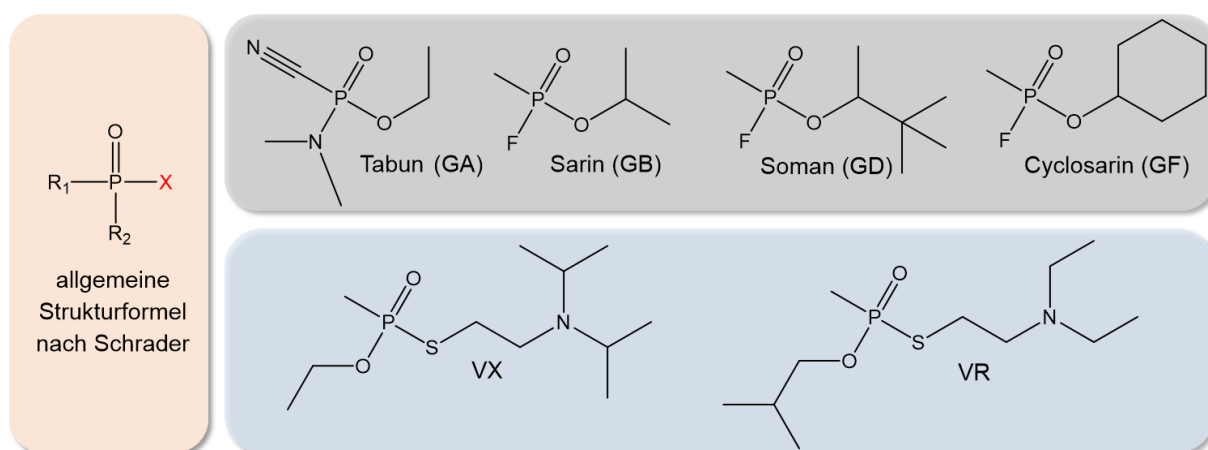


Abbildung 1: Allgemeiner Aufbau von Nervenkampfstoffen gemäß Schrader^{1,11,12} (rot hinterlegt) und Strukturformeln bekannter Nervenkampfstoffe der G- (grün hinterlegt) und V-Reihe (blau hinterlegt). Dargestellt sind Tabun, Sarin, Soman, Cyclosarin, VX und VR. Die Abgangsgruppe ist rot markiert.

Tabun (GA), Sarin (GB), Soman (GD) und Cyclosarin (GF) bilden die G-Reihe der Nervenkampfstoffe, wobei das G für das Herstellungsland „Germany“ steht.^{14, 15}

Verbindungen der V-Reihe der Nervenkampfstoffe wurden ab Mitte der 1950er Jahre im Vereinigten Königreich Großbritannien entwickelt, darunter VX als wohl bekanntester und potentester Vertreter (vgl. Abb. 1 und Tab. 1). VR, eine phosphororganische Verbindung, die ebenfalls zur V-Reihe der Nervenkampfstoffe gezählt wird, wurde unabhängig davon in der Sowjetunion entwickelt und ist auch unter dem Namen russisches VX bekannt.¹⁶

Tabelle 1: Physikalische und biologische Eigenschaften der Nervenkampfstoffe Tabun, Sarin, Soman und VX nach Newmark¹⁴ und Worek¹⁷

Nervenkampfstoff	Dampfdruck [mm Hg, 20 °C]	Tödliche Dosis [mg × min/m ³]	Persistenz im Boden	Reaktionsrate „Alterung“ [h ⁻¹]
Tabun	0,037	400	1 – 1,5 Tage	0,036
Sarin	2,1	100	2 – 24 Std.	0,228
Soman	0,4	50	relativ persistent	6,6
VX	0,0007	10	2 – 6 Tage	0,019

Phosphororganische Verbindungen vom Typ Nowitschok bilden die jüngste Klasse der Nervenkampfstoffe. Der Großteil des heutigen Wissens zu diesen Verbindungen stammt aus Memoiren eines, ehemals an deren Entwicklung beteiligten, russischen Chemikers namens Vil S. Mirzayanov.^{18,19} Nervenkampfstoffe vom Typ Nowitschok, der Name leitet sich vom russischen Wort für Neuling ab, wurden ab Mitte der 1970er Jahre im Rahmen eines geheimen russischen Militärprojekts mit dem Namen FOLIANT entwickelt.²⁰ Diese Verbindungen umfassen sowohl Einkomponenten-Kampfstoffe als auch binäre Kampfstoffe, deren Strukturen aber nur teilweise bekannt bzw. veröffentlicht sind. Nach Angaben von Mirzayanov sind Nowitschok-Kampfstoffe um ein Vielfaches potenter und noch toxischer als VX.^{19,20}

Für die Herstellung vieler Organophosphat(OP)-Kampfstoffe z.B. von Tabun ist nur ein erschreckend geringer apparativer Aufwand sowie ein Minimum an fachlicher Expertise nötig.^{1,16} Aus diesem Grund kann leider auch zukünftig nicht ausgeschlossen werden, dass es, insbesondere im Kontext terroristischer Straftaten, zum Einsatz von Nervenkampfstoffen kommt. Umso wichtiger ist es daher, dass Antidote zur schnellen und wirksamen Therapie einer Organophosphat(OP)-Vergiftung zur Verfügung stehen.

1.2 Symptome einer Organophosphatvergiftung

Die Vergiftungssymptome infolge einer Nervenkampfstoff-Exposition lassen sich auf eine Reizübertragungsstörung im zentralen und peripheren Nervensystem zurückführen. Da im militärischen bzw. terroristischen Kontext meist eine inhalative Exposition erfolgt, erreicht der chemische Kampfstoff als Dampf oder Aerosol zunächst die Augen sowie Schleimhäute von Nase, Mund und Rachen.¹⁴ Erste Symptome sind entsprechend eine Pupillenengstellung (Miosis) mit teilweise eingeschränkter, vernebelter Sicht, ein starker Tränen- und Speichelfluss, Rhinorrhö und Bronchorrhö, sowie eine Verengung der Luftwege (Bronchokonstriktion), letztere hervorgerufen durch die Kontraktion der glatten Atemmuskeln.^{12,21} Auch Gerhard Schrader bekam die toxische Wirkung von Tabun zu spüren, als er sich in einem Syntheseversuch versehentlich leicht vergiftete. Analog zur zuvor beschriebenen Symptomatik beobachtete er eine „starke pupillenverengende Wirkung“, ein eingeschränktes Sehvermögen und das „Auftreten von Asthma-Erscheinungen“ sowie „starke Beklemmungsgefühle im Brustkorb“.²²

Über die sogenannte Blut-Luft-Schranke gelangt der Nervenkampfstoff von der Lunge in den Blutkreislauf und verteilt sich schnell im ganzen Körper.²³ Dabei treten bald Übelkeit, Erbrechen, Durchfall bzw. Abdominalkrämpfe als Folgen einer parasympathischen Überstimulation im Verdauungstrakt auf.^{12,23,24} Im Herz-Kreislauf-System ist bei OP-Vergiftungen durch sympathische Überaktivierung oft initial ein (Nor)adrenalin-vermittelter Anstieg von Puls und Blutdruck zu beobachten.²¹ Störungen im zentralen Nervensystem äußern sich mitunter als Kopfschmerzen, Verwirrung oder Schwindel.²⁵ Im peripher-somatischen Nervensystem verursacht das Organophosphat eine Überreizung der neuromuskulären Endplatte. Als Folge kommt es zunächst zu Faszikulationen und Krämpfen der Skelettmuskulatur, die schließlich, nachdem muskuläre Energiespeicher aufgebraucht sind, in eine allgemeine Muskelschwäche mit verringerten muskulären Reflexen übergeht.¹² Die Lähmung der Atemmuskulatur, in Verbindung mit Bronchokonstriktion, Bronchorrhö und einer zentralen Hemmung des Atemantriebes, führt bei schweren OP-Vergiftungen schließlich zum Tod durch Ersticken.

Ursächlich für die skizzierte Symptomatik - das sogenannte cholinerge Syndrom - auf molekularer Ebene ist eine Inaktivierung von Cholinesterasen, insbesondere der

Acetylcholinesterase (AChE). Die AChE, eine Serinesterase, ist für den Abbau des Neurotransmitters Acetylcholin (ACh) zuständig. Durch eine schnelle Hydrolyse von präsynaptisch freigesetztem ACh im synaptischen Spalt ermöglicht die AChE, dass Reizübertragungen an der cholinergen Synapse (vgl. Abb. 2) in möglichst hoher Frequenz erfolgen können.

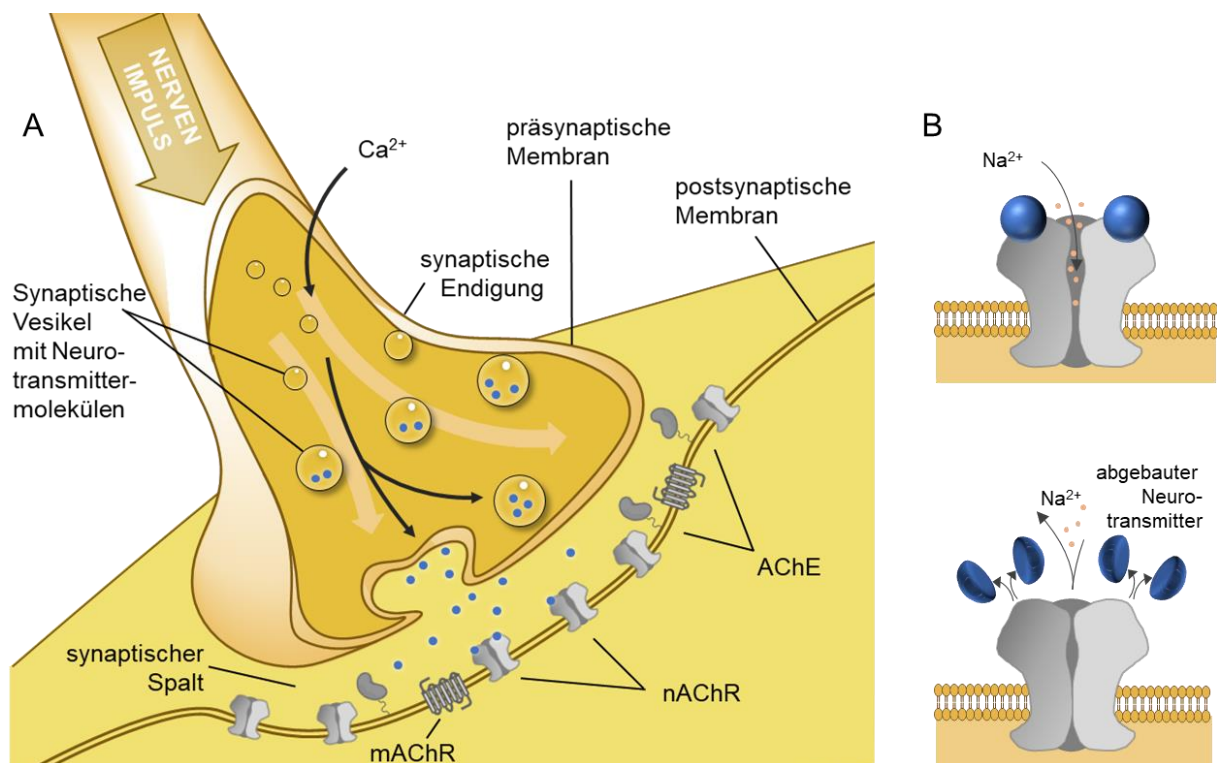


Abbildung 2: Chemische Reizübertragung an der cholinergen Synapse nach Campbell und Reece²⁶: (A) Ein ankommender Nervenimpuls führt, durch Einstrom von Calciumionen in das synaptische Endköpfchen, zur Freisetzung von Neurotransmittermolekülen in den synaptischen Spalt. Der Neurotransmitter bindet an ionotrope (Ionenkanäle) und metabotrope Rezeptoren der postsynaptischen Membran. (B) Mit der Neurotransmitter-Rezeptor-Bindung, im Fall der Ionenkanäle kommt es zum Einstrom von Natriumionen, wird eine Depolarisation der postsynaptischen Membran ausgelöst. Die Acetylcholinesterase (AChE) ist zuständig für den schnellen enzymatischen Abbau des Neurotransmitters und beendet so die Signaltransmission.

Phosphororganische Verbindungen inaktivieren die AChE indem sie an den Serinrest im aktiven Zentrum binden, wie in Abbildung 3 am Beispiel von Soman schematisch dargestellt.

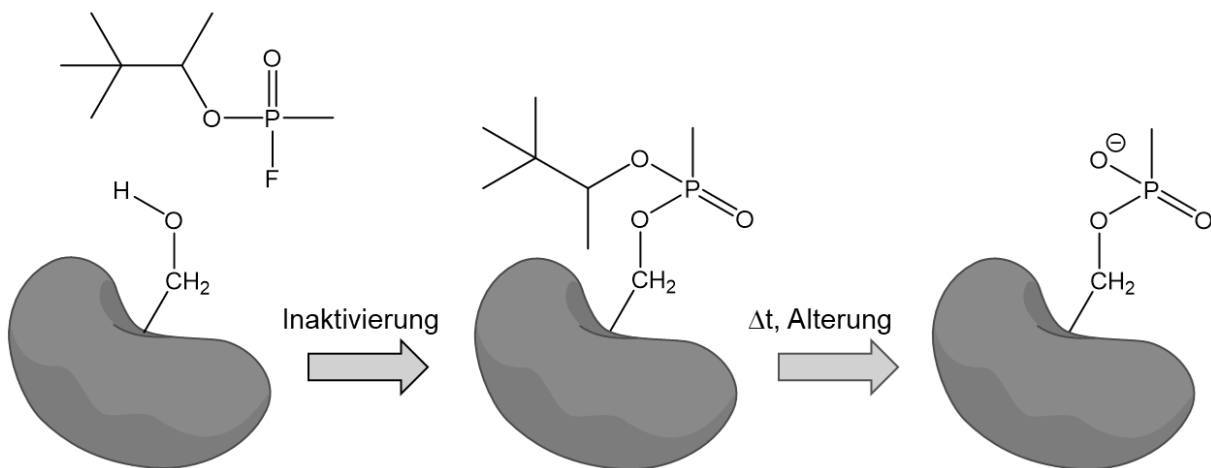


Abbildung 3: Inaktivierung der Acetylcholinesterase durch Organophosphate am Beispiel von Soman nach Sirin²⁷. Die sogenannte Alterung als konsekutive, zeitabhängige Reaktion des OP-AChE-Komplexes ist ebenfalls dargestellt. Im gealterten OP-AChE-Komplex ist das Enzym irreversibel inhibiert, sodass keine Reaktivierung durch Oxime mehr möglich ist.

In der Folge akkumuliert Acetylcholin im synaptischen Spalt und an postsynaptischen Acetylcholinrezeptoren und aktiviert letztere dauerhaft. Von dieser Überaktivierung sind sowohl die metabotropen, G-Protein gekoppelten muskarinischen als auch die ionotropen nikotinischen Acetylcholinrezeptoren (mAChRs bzw. nAChRs) betroffen.

1.3 Standardtherapie von Organophosphatvergiftungen

Mit Atropin, einem Extrakt des Nachtschattengewächses *Atropa Belladonna* und altem Heilmittel für verschiedenste Leiden, war früh ein erstes Antidot identifiziert, das zur Therapie der Symptome einer OP-Vergiftung eingesetzt werden konnte.^{28, 29} Das Alkaloid verdrängt den Neurotransmitter ACh kompetitiv von der Bindungsstelle am muskarinischen AChR und beendet damit die Daueraktivierung des Rezeptors. Da die Bindung selektiv am mAChR erfolgt, vermag Atropin gegen die Daueraktivierung des nikotinischen AChR jedoch nichts auszurichten. Neben Atropin ist deshalb außerdem die Gabe eines Oxims z.B. Obidoxim, Pralidoxim oder HI-6, ein wichtiger Bestandteil der modernen Standardtherapie von OP-Vergiftungen.³⁰ Diese Wirkstoffe vermitteln die Abspaltung des Organophosphats vom aktiven Zentrum der AChE und ermöglichen damit eine Reaktivierung des Enzyms.³¹ Somit kann die AChE die Neurotransmitterüberlast abbauen und die Signaltransduktion sowohl über muskarinische als auch nikotinische Acetylcholinrezeptoren wiederherstellen. Zur

Behandlung von Krampfanfällen, zur Beruhigung und Angstlösung sowie zur Prävention gegen neurologische Schäden wird außerdem Diazepam, ein Arzneistoff aus der Gruppe der Benzodiazepine, verabreicht.^{32,33}

Ein Nachteil bei Verwendung der Oxime als Antidot besteht darin, dass deren pharmakologische Potenz stark davon abhängt, auf welche phosphororganische Verbindung die Vergiftung zurückzuführen ist. So zeigten Vergiftungsstudien mit der humanen, erythrozytären AChE *in vitro* beispielsweise, dass die Enzym-Reaktivierungsrate nach Tabunvergiftung grundsätzlich niedrig ist, unabhängig davon welches Oxim, getestet wurden hier Obidoxim, Pralidoxim, HI-6 und HIö-7, zur Reaktivierung eingesetzt wird.^{17,31} Eine Oxim-vermittelte AChE-Reaktivierung steht darüberhinaus in Konkurrenz mit der sogenannten Alterung, einer konsekutiven Reaktion des OP-Enzymkomplexes. Es handelt sich um eine spontane Dealkylierung am OP-Addukt im aktiven Zentrum der AChE (vgl. Abb. 3), wodurch das Enzym irreversibel gehemmt wird, sodass auch eine Oxim-vermittelte Reaktivierung nicht mehr möglich ist. Bei Vergiftung mit Soman altert der OP-AChE-Komplex innerhalb von wenigen Minuten.³⁴

Ist eine Oxim-vermittelte AChE-Reaktivierung und damit der Abbau des akkumulierten Neurotransmitters nicht möglich, führt die Überreizung des nAChR letztlich dazu, dass der Rezeptor in einen inaktiven Zustand der Desensitisierung übergeht. In diesem Zustand bleibt der Ionenkanal trotz Neurotransmitterbindung undurchlässig für Ionen, sodass es zum vollständigen Depolarisationsblock an der cholinerg-nikotinischen Synapse kommt.

1.4 Der nAChR als Target alternativer Therapieoptionen

Da bislang kein Oxim mit universaler Wirksamkeit als AChE-Reaktivator identifiziert werden konnte, wird zunehmend in die Richtung alternativer, AChE-unabhängiger Therapiemöglichkeiten einer OP-Vergiftung geforscht. Attraktiv erscheint hier insbesondere der Ansatz einer direkten pharmakologischen Interaktion am nAChR.

1.4.1 Struktur und Funktion des nAChR

Anders als beim metabotropen mAChR handelt es sich bei dem nAChR um einen ionotropen Rezeptor. Er ist Teil der Cys-Loop Superfamilie Liganden-gesteuerter

Ionenkanäle, zu der unter anderem auch der GABA_A-, der Glycin- sowie der 5-HT₃-Rezeptor zu rechnen sind.^{35,36} Mehrere Strukturmerkmale, wie beispielsweise der namensgebende Cys-Loop, dabei handelt es sich um eine kurze Aminosäuresequenz mit zwei Cysteinen, die durch knapp ein Dutzend Aminosäuren getrennt, über ein Disulfid verbrückt, besagte Schleife bilden, sind innerhalb dieser Familie konserviert. Der nAChR wird aus 5 Untereinheiten (UEs) gebildet, die kreisförmig angeordnet sind, sodass sich mittig eine Pore bildet (vgl. Abb. 4). Jede UE setzt sich dabei aus einer großen extrazellulären Domäne, vier aufeinanderfolgenden Transmembrandomänen (TM1 – TM4) und einer zytoplasmatischen Domäne (zwischen TM3 und TM4) zusammen.

Der nAChR kommt entweder als Homopentamer, mit 5 identischen UEs wie im Fall des neuronalen ($\alpha 7$)₅-AChR, oder als Heteropentamer, wie im Fall des neuromuskulären nAChR, vor. Nikotinische Acetylcholinrezeptoren sind im ZNS, im somatomotorischen Nervensystem, in sympathischen sowie parasympathischen Ganglien, aber auch im Gefäßgewebe und in Immunzellen lokalisiert.^{37,38,39} Durch seine breite Verteilung im Körper ist der nAChR an einer Vielzahl verschiedener, physiologischer Prozesse, wie der Muskelkontraktion, der Gedächtnisbildung, der Immunantwort, der Blutgefäßbildung, dem Lernprozess, sowie dem Schmerzempfinden beteiligt.^{40,41} Es ist deshalb keine Überraschung, dass der Rezeptor in vergangenen Jahren auch zunehmend in Zusammenhang mit einer Vielzahl verschiedener Krankheitsbilder wie der Alzheimer-Krankheit, Schizophrenie, Depression, Myasthenia gravis und Krebs gebracht wurde und für assoziierte Forschungsfeldern daher auch ein interessantes therapeutisches Target darstellt.^{42,43,44,45}

Bei OP-Vergiftungen beeinflusst die Desensitisierung des neuromuskulären nAChR, als Ursache für die Lähmung der Atemmuskulatur, entscheidend den Verlauf des cholinergen Syndroms. Dementsprechend steht insbesondere der neuromuskuläre bzw. Muskeltyp-nAChR als potentiell Target im Fokus der Antidotforschung.

Der Großteil dessen, was heute zu Struktur und Funktion des humanen Muskeltyp-nAChR bekannt ist, basiert auf Studien am nAChR des Zitterrochens (Familie der Torpedinidae) als Modell. Der sogenannte Elektroplax, das Organ mit dem der Zitterrochen elektrische Entladungen generiert um seine Beute zu betäuben, ist durch

eine besonders hohe Dichte an nikotinischen Acetylcholinrezeptoren, der nAChR macht knapp 40 % des Gesamtproteingehalts aus, charakterisiert.⁴⁶ Der *Torpedo*-nAChR hat eine hohe strukturelle Ähnlichkeit zum humanen Muskeltyp-nAChR,^{47,48,49} weshalb er gerne als Modell dessen verwendet wird.^{50,51} Hinzu kommt, dass das bislang einzig vollständige, dreidimensionale Strukturmodell eines nAChR, das für computergestützte Simulationen beispielsweise im Rahmen des strukturbasierten Wirkstoffdesigns zur Verfügung steht, auf elektronenmikroskopischen Bildern des nAChR von *Torpedo marmorata* basiert.⁵²

Der heteromere Muskeltyp-nAChR setzt sich aus den Untereinheiten $\alpha 1$, $\beta 1$, γ bzw. ϵ und δ zusammen. Dabei ist die Zusammensetzung abhängig davon, ob es sich um die fötale ($(\alpha 1)_2\beta 1\gamma\delta$) oder adulte Form ($(\alpha 1)_2\beta 1\delta\epsilon$) des Muskeltyp-nAChR handelt.^{37,46,53} Der Agonist bindet an zwei sogenannte orthosterische Bindestellen in der extrazellulären Domäne des Muskeltyp-nAChR, jeweils am Interface zwischen den Untereinheiten α und $\gamma(\epsilon)$ bzw. zwischen α und δ .^{54,55} (vgl. Abb. 4)

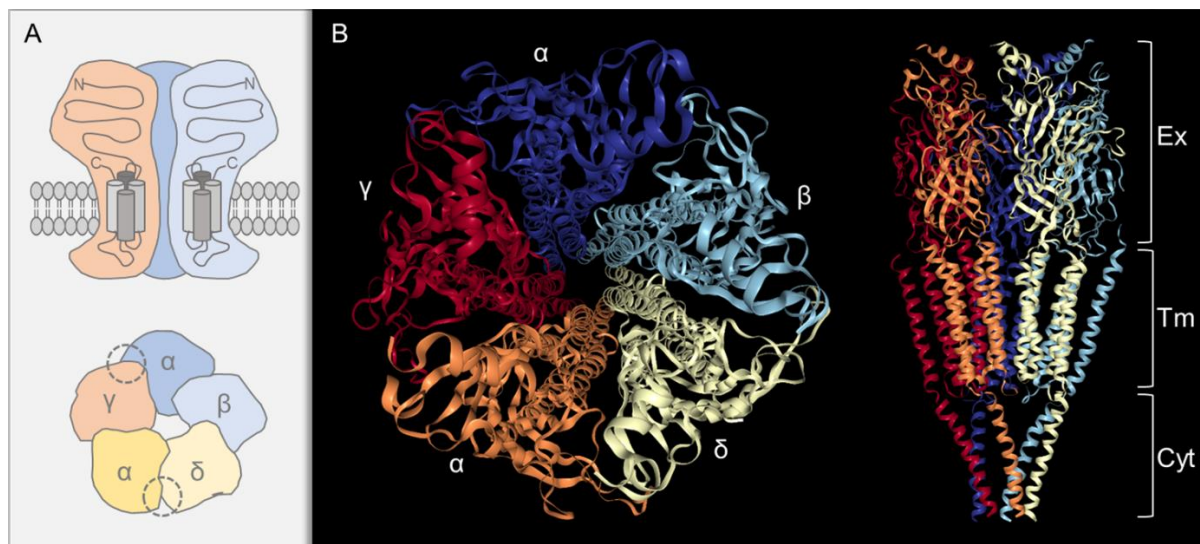


Abbildung 4: Schema des neuromuskulären, nikotinischen Acetylcholinrezeptors in der fötalen Form nach Hurst⁶⁵ (A) und 3D-Strukturmodell des Muskeltyp-nAChR aus *Torpedo marmorata* (B) jeweils in Draufsicht und Seitenansicht. Orthosterische Bindestellen sind durch gestrichelte Kreise markiert. Darstellung der 3D-Strukturmodelle ausgehend von der ID 2BG9 der Protein Datenbank⁵⁶ mithilfe der NGL Software⁵⁷. Ex = extrazellulärer Teil, TM = transmembranärer Teil, Cyt = cytosolischer Teil

Bezüglich einer direkten pharmakologischen Interaktion am nAChR als alternativer Therapieoption bei OP-Vergiftungen stellt sich die Frage, ob analog zum Wirkmechanismus von Atropin am mAChR auch mit dem Einsatz nAChR-selektiver Antagonisten positive therapeutische Effekte zu erzielen sind. Beispielsweise könnte das Muskelrelaxans Rocuronium zur Competition von ACh an der orthosterischen Bindestelle des nAChR eingesetzt werden. Aus Sicherheitsgründen bedürfte es hierbei allerdings, im Gegensatz zur mAChR-Antagonisierung, der kontinuierlichen, künstlichen Beatmung, da das therapeutische Fenster zwischen adäquater Antagonisierung des nAChR und vollständiger Muskelparalyse als relativ klein einzuschätzen ist. Somit empfiehlt sich der Einsatz nAChR-selektiver Antagonisten als Antidot nur im Einzelfall, wenn eine entsprechende apparative Ausrüstung vorhanden und eine intensive, individuelle Behandlung möglich ist.⁵⁸

Eine attraktive Alternative zur nAChR-Antagonisierung, mit der ebenfalls am nAChR interveniert werden kann, jedoch ohne, dass der Wirkstoff mit dem Neurotransmitter um dieselbe Bindestelle am nAChR konkurrieren muss, bietet die allosterische Modulation.

1.4.2 Therapie durch allosterische Modulation des nAChR

Allosterische Modulatoren sind typischerweise selbst nicht in der Lage den Rezeptor zu aktivieren, sondern modulieren die Rezeptorantwort, die durch die Bindung eines Agonisten angestoßen wird.^{37,59} Lassen sich die Effekte des Agonisten am Rezeptor durch allosterische Modulation steigern, handelt es sich bei entsprechenden Liganden um positiv allosterische Modulatoren (PAMs), werden die Effekte abgeschwächt, handelt es sich um negativ allosterische Modulatoren (NAMs). Insbesondere PAMs gewinnen in der modernen Wirkstoffentwicklung durch ihre modulatorischen Eigenschaften zunehmend an Interesse beispielsweise im Hinblick auf die Therapie neurodegenerativer bzw. neurologischer Erkrankungen wie der Alzheimer Krankheit und der Schizophrenie. Für einige PAMs, die selektiv an neuronale nAChRs binden, konnte bereits eine Verbesserung kognitiver Leistungen und sensorischer Prozesse *in vivo* nachgewiesen werden.^{60,61,62} AVL-3288, ein $\alpha 7$ -nAChR-selektiver PAM, befindet sich bereits in klinischen Studien der Phase I als vielversprechender Wirkstoffkandidat zur Therapie von Schizophrenie.⁶³

Grundsätzlich basieren alle Modelle zur positiv allosterischen Modulation am nAChR auf der Annahme, dass sich der Rezeptor als allosterisches Protein nach Monod, Wyman und Changeux verhält.^{64,65} Deren Modell folgend, lässt sich die Funktion des nAChR als Konformationszustand in Abhängigkeit der Agonistbindung abbilden:

In Abwesenheit von Neurotransmitter bzw. Agonist kommt der nAChR überwiegend in einem geschlossenen Zustand, dem sogenannten „resting state“, vor.^{54,65} In diesem Zustand ist der Rezeptor aktivierbar d.h. mit der Bindung des Agonisten an die orthosterischen Bindungsstellen des nAChR öffnet sich der Ionenkanal (offener Zustand). Ist der Rezeptor dem Agonisten dagegen dauerhaft ausgesetzt bzw. häufen sich hohe Agonistkonzentrationen am Rezeptor an, geht dieser in einen energetisch äußerst stabilen, desensitisierten Zustand über. In diesem Zustand ist der Rezeptor nicht aktivierbar. Zwar bindet der Agonist weiterhin am Rezeptor, in diesem Fall scheinbar sogar mit erhöhter Affinität,⁶⁶ allerdings führt diese Bindung nicht zur Öffnung des Ionenkanals.

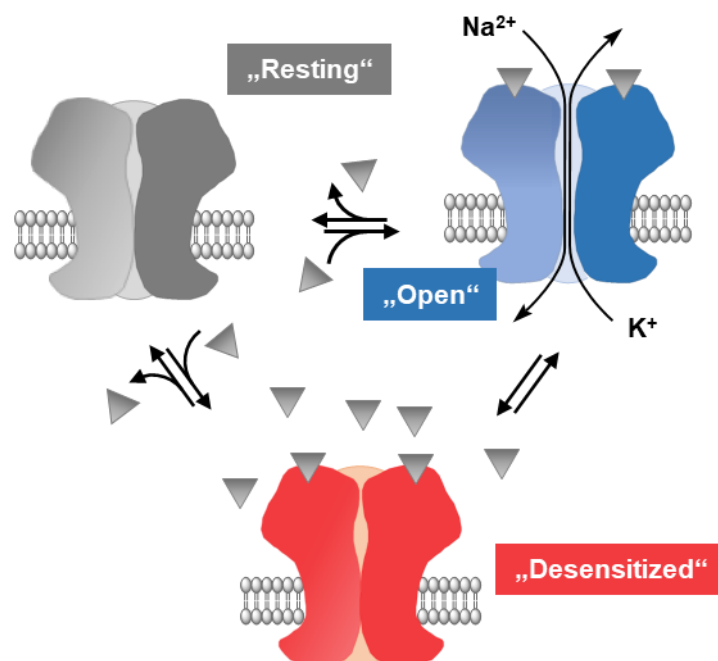


Abbildung 5: Minimalmodell der nAChR-Konformationszustände nach Corradi und Bouzat⁶⁵. Gezeigt sind die wichtigsten funktionellen Zustände des nAChR: der geschlossene, aktivierbare (resting state), der offene (open state) und der desensitisierte Zustand (desensitized state).

Über das Minimalmodell, dargestellt in Abbildung 5, mit den wichtigsten funktionellen Konformationszuständen des nAChR, hinaus existiert eine Vielzahl komplexer Modelle mit weiteren, intermediären Zuständen.^{66,67} Um zu verstehen wie positiv allosterische Modulatoren am nAChR wirken, ist das Minimalmodell als Grundlage zunächst aber ausreichend.

Positiv allosterische Modulatoren sind dadurch gekennzeichnet, dass sie die Agonist-induzierte Rezeptorantwort verstärken. Einigen PAMs wird zugeschrieben, die Agonistbindung oder den Übergang des Agonist-gebundenen Rezeptors in den offenen Zustand, durch Senkung der entsprechenden Energieschwelle, zu erleichtern. Einige PAMs zeigen sich sogar in der Lage, den Übergang des nAChR aus dem Agonist-gebundenen, desensitisierten Zustand in den offenen Zustand zu vermitteln.⁶² Ein spontaner Übergang des desensitisierten Rezeptors in den offenen Zustand ist in Gegenwart hoher Agonistkonzentrationen äußerst unwahrscheinlich. Im Kontext einer OP-Vergiftung erscheint es deshalb besonders attraktiv diese modulatorische Eigenschaft zu nutzen. PAMs mit der Fähigkeit zur „Resensitisierung“ des nAChR werden gegenüber PAMs, die dazu nicht in der Lage sind (PAMs der Klasse I) als positiv allosterische Modulatoren der Klasse II bezeichnet.³⁷ Um einen PAM der Klasse II handelt es sich beispielsweise bei PNU-120596. Das Harnstoffderivat zeigte sich in elektrophysiologischen Studien am $\alpha 7$ -nAChR in der Lage, den desensitisierten Rezeptor, sogar in Anwesenheit hoher Agonistkonzentrationen ($100 \mu\text{mol L}^{-1}$ Nikotin) zu reaktivieren.⁶² Da PNU-120596 selektiv am $\alpha 7$ -nAChR bindet, lassen sich dessen modulatorischen Eigenschaften allerdings nicht zur Reaktivierung des desensitisierten, neuromuskulären nAChR nutzen.

1.5 MB327 als potentielltes Antidot gegen OP-Vergiftungen

1.5.1 MB327 als positiv allosterischer Modulator am Muskeltyp-nAChR

Bislang bzw. zu Projektbeginn war nur eine einzige Verbindung - das Bispyridiniumsalz MB327 - mit den Charakteristika eines positiv allosterischen Modulators der Klasse II am Muskeltyp-nAChR bekannt.

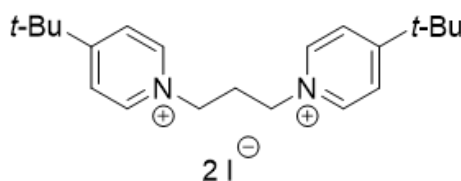


Abbildung 6: Struktur des Bispyridiniumsalzes MB327

Dass MB327 in der Lage ist, den desensitisierten Muskeltyp-nAChR zu reaktivieren zeigte Niessen in zellfreien, elektrophysiologischen Messungen am *Torpedo*-nAChR mittels einer neuen Membranbilayer-basierten Technologie auf einer sogenannten Surface-Electrogenic-Event-Reader(SURFE²R)-Plattform.⁶⁸ Für diese Messmethode werden Vesikel aus nAChR-reichen Membranfragmenten des *Torpedo* Elektroplax auf eine artifizielle Membrandoppelschicht aufgebracht, die selbst wiederum auf goldbeschichtete Sensorchips aufgelagert wurde. Über die Vesikelmembran wird ein Ionengradient induziert, sodass mit der nAChR-Aktivierung durch Agonistbindung Ionen in die Vesikel einströmen. Indem die Vesikelmembran direkt mit der artifiziellen Membrandoppelschicht verbunden ist - die Membranen sind sozusagen kapazitativ gekoppelt - kann die nAChR-Aktivierung und Depolarisierung der Vesikelmembran als Signal am Sensor gemessen werden.

Wie typischerweise für allosterische Modulatoren beobachtet, zeigte sich MB327 selbst, d.h. in Abwesenheit eines Agonisten, nicht in der Lage den nAChR zu aktivieren. Agonist-induzierte Ionenströme waren in Anwesenheit von MB327 allerdings deutlich erhöht. Dieser Effekt war bei einer Konzentration von 10 $\mu\text{mol L}^{-1}$ MB327 am größten. Nach Desensitisierung des Rezeptors mithilfe eines Agonistüberschusses (100 $\mu\text{mol L}^{-1}$ Carbachol) konnte MB327 den nAChR reaktivieren und den Ionenstrom über die Vesikelmembran wiederherstellen. In Analogie zu elektrophysiologischen Experimenten mit PNU-120596 am $\alpha 7$ -nAChR, zeigte MB327 die Fähigkeit zur Rezeptor-„Resensitisierung“ auch in Anwesenheit hoher Agonistkonzentrationen. Eine Desensitisierung des nAChR konnte sogar im Vorfeld verhindert werden, wenn steigende Konzentrationen Carbachol (bis 10 mmol L^{-1}) in Anwesenheit von 1 mmol L^{-1} MB327 appliziert wurden.

Dass die Bispyridiniumverbindung MB327 nicht bzw. nur mit geringer Affinität an die orthosterischen Bindestellen des Muskeltyp-nAChR bindet, konnte in Radioligand-

Bindungsstudien am *Torpedo*-nAChR gezeigt werden ($K_i > 100 \mu\text{mol L}^{-1}$).⁵¹ Informationen dazu, an welcher Bindestelle bzw. mit welcher Affinität die Bindung von MB327 an den Muskeltyp-nAChR erfolgt, waren bis dato nicht verfügbar.

1.5.2 Pharmakologische Wirkung von MB327 in *ex vivo* und *in vivo* Studien

Ein therapeutischer Effekt des positiv allosterischen Modulators MB327 zeigte sich auch in elektrophysiologischen Messungen am isolierten, OP-vergifteten Muskel im Organbad.⁶⁹ Hier wurde die Muskelkraft von Zwerchfelldiaphragmen der Ratte sowie von Biopsien des humanen Interkostalmuskels nach Elektrostimulation bzw. nach Somanvergiftung und Elektrostimulation gemessen. Die Vergiftung mit Soman hatte eine nahezu vollständige Hemmung der AChE (mit 1% Restaktivität) zur Folge, sodass vergiftete Muskelpräparationen nicht weiter zur Kontraktion angeregt werden konnten. Auch nach Auswaschen des Nervenkampfstoffs aus dem Organbad konnte die Muskelkraft nicht wiederhergestellt werden. Durch Zugabe von MB327, allerdings, ließ sich in beiden Muskelpräparationen konzentrationsabhängig ein beträchtlicher Teil der Muskelkraft wiederherstellen. Die effektivste MB327-Konzentration lag bei $200 \mu\text{mol L}^{-1}$ für den humanen Interkostalmuskel und $300 \mu\text{mol L}^{-1}$ für die Zwerchfelldiaphragmen der Ratte. Der humane Interkostalmuskel erlangte so bei einer Stimulationsfrequenz von 25 Hertz 46.5 % seiner ursprünglichen Muskelkraft zurück.⁶⁹

Der therapeutische Effekt der Bispyridiniumverbindung MB327 zeigte sich auch *in vivo* an OP-vergifteten Mäusen bzw. Meerschweinchen. In einer Kombinationstherapie mit Scopolamin, einem Anticholinergikum, und Physostigmin, einem reversiblen AChE-Hemmer, steigerte MB327 konzentrationsabhängig (1.66, 9.7 bzw. 16.57 mg kg^{-1}) die Überlebensrate Soman-vergifteter Meerschweinchen.⁷⁰ Die Kombinationstherapie mit 16.57 mg kg^{-1} MB327 sicherte das Überleben aller acht Versuchstiere über den gesamten Beobachtungszeitraum der Studie, während vier der acht Versuchstiere innerhalb einer Stunde verstarben, wenn lediglich Physostigmin und Scopolamin in Kombination verabreicht wurden. Ein vergleichbarer protektiver Effekt von MB327 zeigte sich auch bei Vergiftungsversuchen mit anderen Nervenkampfstoffen wie Sarin und Tabun.^{69,71,72,73} In einer Studie an Tabun-vergifteten Meerschweinchen zeigte sich die therapeutische Wirksamkeit von MB327 sogar der des Oxims HI-6 überlegen, wenn beide Antidote in äquimolarer Dosis und als Teil einer Kombinationstherapie mit Scopolamin und Physostigmin verabreicht wurden.

In den bislang durchgeführten *in vivo* Studien lag die pharmakologisch effektivste MB327-Dosis im Bereich um 9 - 30 mg kg⁻¹. Untersuchungen zur Toxizität von MB327 in Meerschweinchen kamen dabei zu dem Ergebnis, dass eine Dosis von 100 mg kg⁻¹ bereits tödlich wirkt, während die Atemfunktion schon ab einer Dosis von 30 mg kg⁻¹ MB327 teilweise beeinträchtigt war.⁷² Eine weitere Studie zur Toxizität von MB327 an Mäusen ermittelte einen LD₅₀-Wert von 160 mg kg⁻¹.⁷¹

In Bezug auf mögliche Nebenwirkungen bei Anwendung von MB327 als Antidot ist außerdem zu beachten, dass die Bispyridiniumverbindung in höheren Konzentrationen auch als Ionenkanalblocker zu wirken scheint.⁷³ Dies wurde auch bereits als potentieller pharmakologischer Wirkmechanismus von MB327 bei OP-Vergiftungen vorgeschlagen. Allerdings korrelieren die in entsprechenden Versuchen für den Ionenkanalblock ermittelten K_d -Werte (um 44 µmol L⁻¹) weder mit funktionellen Daten zur MB327-Interaktion am nAChR in SURFE²R-Studien⁶⁸, noch mit Dosis-Wirkungsbeziehungen zur Muskelkraft-Wiederherstellung am vergifteten Muskel *in vitro*.⁶⁹ Beobachtungen einer rückläufigen pharmakologischen Wirkung bei Konzentrationen > 300 µmol L⁻¹ in funktionellen Studien, sprechen allerdings durchaus dafür, dass die Bispyridiniumverbindung in höheren Konzentrationen als Ionenkanalblocker agiert.⁷⁴ Daneben wurde gezeigt, dass MB327 auch die orthosterische Bindestelle an muskarinischen Acetylcholinrezeptoren (hM₅-Subtyp; K_i = 3.3 µmol L⁻¹) adressiert.⁷⁵

Insgesamt erscheint MB327 aufgrund der geringen Potenz und Selektivität am nAChR bzw. einer geringen therapeutischen Breite nicht für den Einsatz als Antidot bei OP-Vergiftungen geeignet. Nichtsdestotrotz handelt es sich bei der Bispyridiniumverbindung um den bislang einzig bekannten „Resensitisierer“ des Muskeltyp-nAChR, sodass sich eine Entwicklung neuer Antidote auf Basis von MB327 als Leitstruktur durchaus anbietet.

1.6 Entwicklung neuer Antidote ausgehend von MB327 als Leitstruktur

1.6.1 Die rationale Wirkstoffentwicklung

Die moderne, rationale Wirkstoffentwicklung beginnt typischerweise mit der Identifizierung eines Targets, d.h. eines potentiellen Angriffspunkts für eine

medizinische bzw. pharmakologische Intervention (vgl. Abb. 7). Im nächsten Schritt muss eine Leitstruktur gefunden werden, die mit dem Target interagiert und dadurch einen gewünschten therapeutischen Effekt herbeiführt. Da die Leitstruktur meist noch nicht das gewünschte Wirkstoffprofil besitzt, wird sie anschließend medizinalchemisch modifiziert bis Derivate entsprechende pharmakokinetische bzw. pharmakodynamische Eigenschaften aufweisen. Aussichtsreiche Wirkstoffkandidaten gehen dann in die vorklinische bzw. klinische Testung ein. Im Idealfall kann zuletzt ein hochwirksamer, gut verträglicher Wirkstoff zugelassen werden.⁷⁶

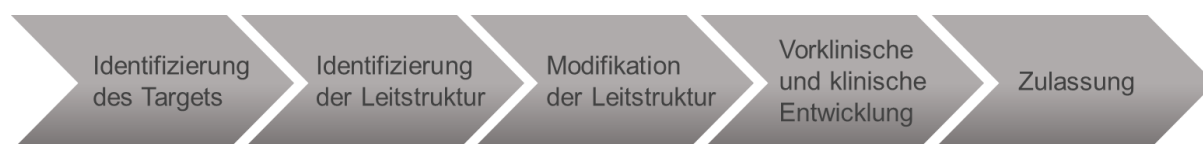


Abbildung 7: Prozess der modernen, rationalen Wirkstoffentwicklung von der Identifizierung des Targets bzw. der Leitstruktur bis zur Zulassung des klinisch geprüften Medikaments nach Silverman und Holladay⁷⁶

Für eine rationale Entwicklung neuer, potenter Antidote gegen OP-Vergiftungen, die analog zu MB327 wirken, wurden mit dem Muskeltyp-nAChR und der Bispyridiniumverbindung MB327 bereits Target und Leitstruktur identifiziert. Nun muss – entsprechend Schritt 3 des rationalen Drug Designs (vgl. Abb. 7) - die Leitstruktur MB327 an verschiedenen Stellen des Molekülgerüsts chemisch modifiziert werden, indem neue funktionelle Gruppen eingeführt bzw. die Position der Substituenten am Molekülgerüst variiert wird. Ob die neu-synthetisierten MB327-Derivate verbesserte Wirkstoffeigenschaften zeigen, muss im Anschluss in geeigneten biologischen Testverfahren geprüft werden. Diese biologischen Daten fließen wiederum in die Synthesepanung zur weiteren Optimierung der Leitstruktur ein. Auch bietet sich eine Kombination mit computergestützten Modellen an. So kann beispielsweise die Identifizierung putativer Bindestellen durch Ligand-Docking an einem dreidimensionalen Strukturmodell des Targets *in silico* wertvolle Informationen für die Synthesepanung liefern. Für die Modifikation von MB327 als Modellverbindung steht, wie bereits diskutiert, zunächst eine Verbesserung von Potenz und Selektivität im Vordergrund. Je potenter die Verbindung, desto geringere Konzentrationen des

Wirkstoffe müssen verabreicht werden, um den gewünschten pharmakologischen Effekt zu erzielen. Mit einer Erhöhung der Selektivität ließen sich zudem off-Target-Effekte und damit mögliche Nebenwirkungen minimieren.

1.6.2 Radioligand-Bindungsassays als Testsystem der rationalen Wirkstoffentwicklung

Für die Wirkstoffentwicklung gilt typischerweise, dass eine verbesserte Bindungsaffinität am Target auch zu einer höheren Potenz sowie Selektivität führt.^{77,78,79,80} Zur Bestimmung von Bindungsaffinitäten bzw. der Charakterisierung der Bindung eines Liganden an einen Rezeptor kommen sogenannte Rezeptor-Ligand-Bindungsassays zum Einsatz.^{78,81,82} Den Goldstandard stellen hierbei die in den 1970er Jahren entwickelten Radioligand-Bindungsassays dar. Hier ist der Reporterligand bzw. die Markerverbindung mit einem radioaktiven Label, typischerweise mit Tritium, markiert. So kann der Reporterligand im Anschluss mittels Szintillationszählung in Bindungsproben quantifiziert werden.

Die Durchführung von Rezeptor-Ligand-Bindungsassays verläuft allgemein, wie auch in Abbildung 8 schematisch dargestellt, nach folgendem Prinzip: Rezeptor und Reporterligand werden inkubiert bis sich ein Bindungsgleichgewicht eingestellt hat. Anschließend werden der Target-gebundene Anteil und der ungebundene Anteil des Reporterliganden getrennt. Die Trennung kann beispielsweise durch Filtration oder Zentrifugation erfolgen, wobei der Target-Reporterligand-Komplex bei der Filtration gemäß Größenausschluss auf dem Filter verbleibt, während er bei Zentrifugation der Bindungsproben sedimentiert und in einem Pellet am Boden des Reagiergefäßes eingeschlossen wird. Typischerweise wird im Anschluss der gebundene Reporterligand z.B. mittels Szintillationszählung oder mithilfe spektrometrischer Methoden quantifiziert.

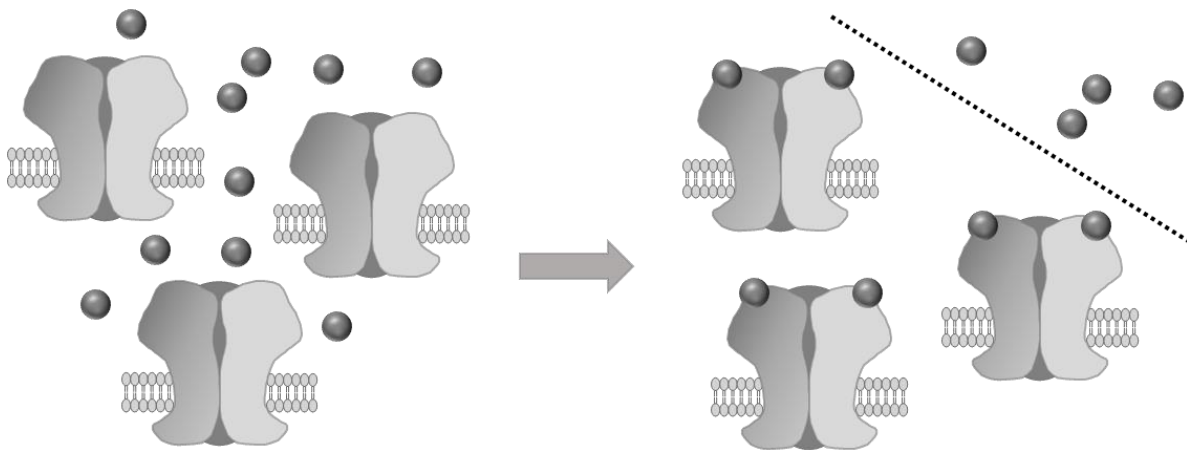


Abbildung 8: Schematische Darstellung eines Bindungsexperiments: Rezeptor und Reporterligand werden inkubiert. Nach Erreichen des Bindungsgleichgewichts werden ungebundener und gebundener Reporterligand getrennt. Im Anschluss wird typischerweise der gebundene Anteil des Reporterliganden quantifiziert.

Im Verlauf der Inkubation bindet der Reporterligand nicht nur an spezifische Bindestellen am Rezeptor (spezifische Bindung, SB), sondern zu einem bestimmten Teil auch nicht-spezifisch an andere Komponenten der Targetpräparation sowie an verwendete Verbrauchsmaterialien (nicht-spezifische Bindung, NB). Die gemessene Reporterligand-Target-Bindung im Bindungsversuch - die sogenannte Gesamtbindung (GB) - setzt sich dementsprechend aus der spezifischen Bindung und der nicht-spezifischen Bindung zusammen (1).

$$GB = SB + NB \quad (1)$$

Um die eigentliche, spezifische Bindung des Reporterliganden zu bestimmen, müssen Gesamtbindung und nicht-spezifische Bindung separat für eine bestimmte Konzentration Reporterligand bestimmt werden und anschließend die letztere von der ersteren abgezogen werden.

Die nicht-spezifische Bindung wird meist mithilfe der Kompetitor-Methode ermittelt. Ein Kompetitor, der mit dem Reporterliganden um dieselbe Bindestelle am Target konkurriert, wird dem Bindungsansatz in deutlichem Überschuss (z.B. $1000 \times K_d$) zugesetzt, sodass alle spezifischen Reporterligand-Bindestellen belegt sind und nur noch die nicht-spezifische Reporterligand-Bindung erfasst wird.^{77, 83} Eine weitere, attraktive Möglichkeit zur Bestimmung der nicht-spezifischen Bindung besteht in der

Zerstörung spezifischer Bindestellen durch Hitzedenaturierung der Targetpräparation vor dem Bindungsversuch.

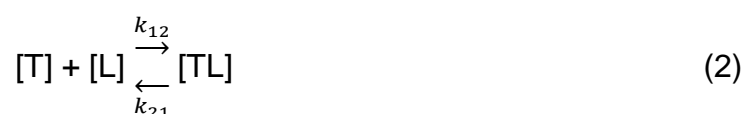
1.6.3 MS-Bindungsassays als Label-freie Alternative

Obwohl Radioligand-Bindungsassays sehr häufig zur Untersuchung von Rezeptor-Ligand-Interaktionen zum Einsatz kommen, hat diese Methode aufgrund der Notwendigkeit der radioaktiven Markierung des Reporterliganden einige Nachteile. Die Anschaffung von Radioliganden, beispielsweise, ist äußerst kostenintensiv. Zudem erfordert das Arbeiten mit radioaktiv markierten Substanzen die Einhaltung überaus aufwendiger Sicherheitsstandards und Entsorgungsrichtlinien.

Als Alternative zu den Radioligand-Bindungsassays haben sich in den letzten Jahren Massenspektrometrie(MS)-basierte Bindungsassays etabliert.^{82,84,85,86,87,88} Der Aufbau von MS-Bindungsassays entspricht grundsätzlich dem der Radioligand-Bindungsassays, unterscheidet sich von diesen aber im Kern dadurch, dass eine native d.h. unmarkierte Verbindung als Reporterligand eingesetzt werden kann, die im Anschluss massenspektrometrisch, typischerweise mittels LC-MS, quantifiziert wird. So erübrigt sich die kostspielige Anschaffung, umständliche Handhabung und aufwendige Entsorgung von Radioliganden. Durch das charakteristische Retentionsverhalten auf der Säule im HPLC-System in Kombination mit MS-Detektion, die meist im sogenannten Tandem-MS(MS/MS)-Modus d.h. auf Grundlage des Masse-zu-Ladung(m/z)-Verhältnisses des ionisierten Moleküls bzw. im Massenspektrometer erzeugter spezifischer Fragment-Ionen erfolgt, wird eine hohe Selektivität erreicht.

1.6.4 Anwendung von Bindungsassays zur Bestimmung von Affinitätskonstanten

Im Bindungsversuch gilt für die bimolekulare Assoziationsreaktion von Target und Reporterligand, ausgehend vom Massenwirkungsgesetz und unter der Prämisse reversibler Bindung:⁷⁷



Die Reaktionsgeschwindigkeit, mit welcher der Target-Ligand-Komplex (TL) gebildet wird, ist definiert durch $k_{12} \times [T] \times [L]$, mit [T] und [L] als Konzentration des freien Targets bzw. Reporterliganden und k_{12} als Assoziationskonstante. Für die Geschwindigkeit

der Rückreaktion gilt $\frac{d[TL]}{dt} = k_{21}x[TL]$, wobei $[TL]$ die Konzentration an Target-Reporterligand-Komplex und k_{21} die Dissoziationskonstante darstellt. Das Verhältnis $\frac{k_{12}}{k_{21}}$ wird im Bindungsgleichgewicht als Gleichgewichts-Assoziationskonstante (K), der inverse Term $\frac{k_{21}}{k_{12}}$ als Gleichgewichts-Dissoziationskonstante (K_d) bezeichnet.

Ist ein Bindungsgleichgewicht erreicht, d.h. halten sich Bildung und Zerfall des Target-Reporterligand-Komplexes die Waage, gilt $k_{12}x[T]x[L] = k_{21}x[TL]$ bzw. $[TL] = \frac{1}{K_d} x [T]x[L]$. Nach erneuter Umformung und unter Berücksichtigung der Massenerhaltung mit $[TL] + [T] = [T_{\text{gesamt}}]$ lässt sich der sogenannte Langmuir-Term formulieren:

$$[TL] = \frac{[T_{\text{gesamt}}]x[L]}{K_d + [L]} \quad (3)$$

Die Gleichgewichts-Dissoziationskonstante K_d , eine gebräuchliche Kenngröße für die Affinität eines Liganden an sein Target, entspricht dabei derjenigen Ligandkonzentration, bei der die Hälfte aller Targetmoleküle $[T_{\text{gesamt}}]$ Ligand-gebunden vorliegen. Dies lässt sich auch anhand des Langmuir-Terms nachvollziehen: Erreicht die Konzentration an freiem Reporterligand $[L]$ den K_d -Wert, lässt sich die Gleichung zu $[TL] = \frac{[T_{\text{gesamt}}]}{2}$ vereinfachen. Aus der Target-Gesamtkonzentration $[T_{\text{gesamt}}]$ ergibt sich auch die Anzahl maximal verfügbarer Bindestellen (B_{max}) der Targetpräparation.

Zur Bestimmung von K_d - und B_{max} -Werten werden typischerweise Sättigungsexperimente durchgeführt d.h. eine bestimmte Targetkonzentration wird mit steigenden Konzentrationen Reporterligand inkubiert. Nach Bestimmung der spezifischen Reporterligand-Target-Bindung (SB) als Differenz von Gesamt- und nicht-spezifischer Bindung (GB bzw. NB) und graphischer Auftragung gegen die freie Ligandkonzentration ergibt sich eine sogenannte Sättigungsisotherme. Abbildung 9 zeigt eine Sättigungsisotherme für ein simuliertes Bindungsexperiment mitsamt B_{max} - und K_d -Wert. Der B_{max} -Wert ergibt sich als Grenzwert auf der y-Achse, an den sich die Sättigungskurve mit steigenden Reporterligandkonzentrationen annähert. Entsprechend zeigt der K_d -Wert die Reporterligandkonzentration an, bei der die y-Abszisse $\frac{[B_{\text{max}}]}{2}$ erreicht wird.

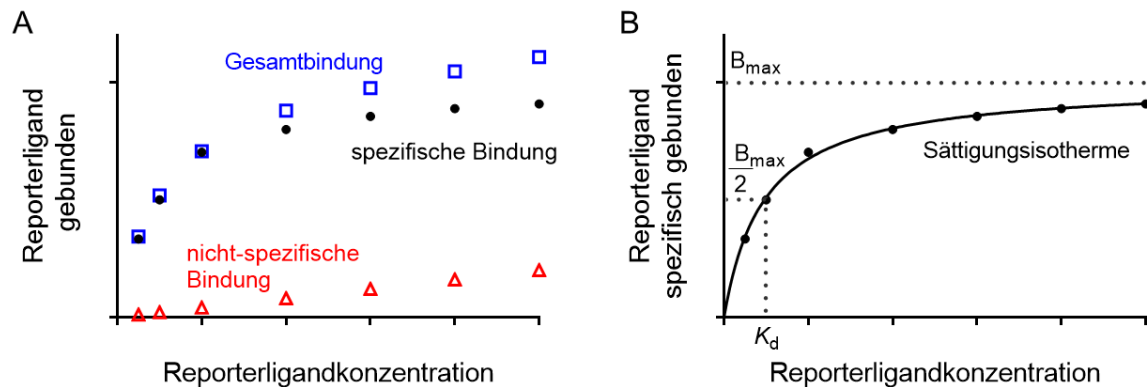


Abbildung 9: Simulation eines Sättigungs-Bindungsexperiments. (A) Gesamt-, nicht-spezifische und spezifische Bindung in Abhängigkeit der Reporterligandkonzentration. Die spezifische Bindung ergibt sich als Differenz von GB und NB. (B) Sättigungsisotherme auf Basis der spezifischen Bindung ($y = (B_{max} \cdot X) / (K_d + X)$) zur Bestimmung des B_{max} als Grenzwert auf der y-Achse und K_d als Reporterligandkonzentration mit der eine halbmaximale Sättigung des Targets erreicht wird.

Zur Vereinfachung wird für die Darstellung einer Sättigungsisotherme üblicherweise anstelle der freien Reporterligandkonzentration dessen Nominalkonzentration aufgetragen. Hierbei wird angenommen, dass der Anteil an gebundenem Reporterligand in Relation zur eingesetzten Nominalkonzentration vernachlässigbar klein ist. Um das Risiko einer Reporterligand-Depletion zu minimieren wird in Bindungsversuchen üblicherweise eine Targetkonzentration $< 0.1 \times K_d$ eingesetzt.⁷⁷ Die Darstellung einer Sättigungsisotherme, auf Basis derer eine sinnvolle Kalkulation von B_{max} - und K_d -Werten erfolgen kann, erfordert außerdem die Wahl eines ausreichend großen Reporterligand-Nominalkonzentrationsbereichs. Dieser sollte in etwa zwischen $0.1 \times K_d$ und $10 \times K_d$ liegen.⁷⁷

Während sich das Sättigungsexperiment hervorragend zur Bestimmung der Bindungsaffinität eines Liganden an sein Target bzw. zur Bestimmung der Anzahl verfügbarer Bindestellen einer Targetpräparation eignet, kommen im Zuge der Wirkstoffentwicklung z.B. für das Screening von Substanzbibliotheken, dagegen, bevorzugt Konkurrenzexperimente zum Einsatz. Hier wird die Bindungsaffinität einer Testverbindung indirekt, über den Rückgang der Reporterligand-Bindung mit steigenden Konzentrationen der Testverbindung in der Bindungsprobe, bestimmt.

Dementsprechend werden Target und Reporterligand, jeweils in einer festen Konzentration, in Anwesenheit steigender Konzentrationen einer weiteren

Testverbindung inkubiert. Binden sowohl Reporterligand als auch die Testverbindung an dieselbe Bindestelle am Target, nimmt die Reporterligand-Target-Bindung mit steigender Konzentration der Testverbindung ab, wie in Abbildung 10 anhand eines simulierten Kompetitions-Bindungsexperiments dargestellt.

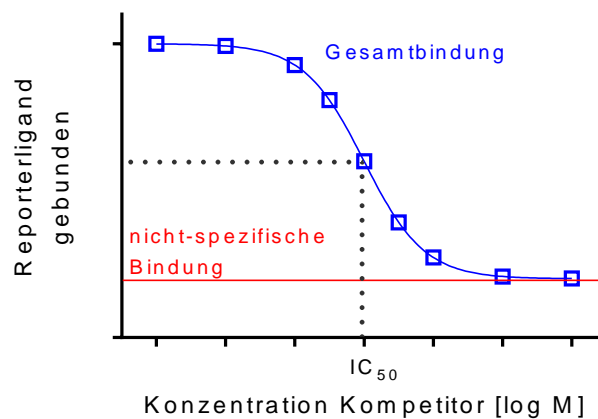


Abbildung 10: Simulation eines Kompetitions-Bindungsexperiments. Die Gesamtbindung des Reporterliganden ergibt eine sigmoidale Kompetitionskurve in Abhängigkeit steigender, logarithmisch aufgetragener Kompetitorkonzentrationen. Der IC₅₀-Wert entspricht derjenigen Kompetitorkonzentration, bei der der Reporterligand zur Hälfte vom Target verdrängt wurde.

Bei Auftragung der gemessenen Reporterligand-Target-Bindung gegen den Logarithmus der Testverbindungskonzentrationen (sogenannte Kompetitionskurve) ergibt sich ein sigmoidaler Verlauf zwischen einem oberen und einem unteren Plateau. Das obere und untere Plateau entspricht der Gesamt- bzw. nicht-spezifischen Bindung des Reporterliganden bei der im Assay eingesetzten Konzentration. Der IC₅₀-Wert entspricht der Konzentration der Testverbindung, bei der eine halbmaximale Verdrängung des Reporterliganden erreicht ist. Gemäß Cheng und Prusoff⁸⁹ kann ausgehend vom IC₅₀-Wert, mithilfe des K_d -Werts des Reporterliganden sowie der freien Reporterligandkonzentration [L], die Inhibitionskonstante K_i der Testverbindung bestimmt werden:

$$K_i = \frac{IC_{50}}{\left(1 + \frac{[L]}{K_d}\right)} \quad (4)$$

ZIELSETZUNG

2. Zielsetzung

Wie in der Einleitung geschildert, zeigte die Bispyridiniumverbindung MB327 in mehreren Studien *in vitro* sowie *in vivo* einen therapeutischen Effekt bei Vergiftungen mit phosphororganischen Verbindungen. Verantwortlich für diese pharmakologische Wirkung scheint dabei eine direkte Intervention am desensitisierten, nikotinischen Acetylcholinrezeptor (nAChR) zu sein. MB327 ist der erste und bislang einzig bekannte positiv allosterische Modulator am Muskeltyp-nAChR mit der Fähigkeit, den Rezeptor aus dem desensitisierten Zustand in einen funktionalen Zustand zurückzubringen. Aufgrund der geringen Potenz und Selektivität ist MB327 allerdings kaum für einen sicheren Einsatz als Antidot am Menschen geeignet.

Um ausgehend von MB327 als Modellverbindung Antidote mit verbessertem, therapeutischen Wirkprofil zu entwickeln müssen in erster Linie Potenz und Selektivität am Target erhöht werden. Eine höhere Potenz und Selektivität folgt typischerweise einem Gewinn an Bindungsaffinität an das Target. Deshalb sollten Bindungsassays mit MB327 als Reporterligand und dem nAChR als Target entwickelt werden, und diese anschließend zur Bestimmung der Bindungsaffinitäten von MB327 und Derivaten an die MB327-Bindestelle des nAChR angewendet werden.

Aufgrund diverser Vorteile, die bereits ausführlich in der Einleitung erörtert wurden, erhielten bei diesem Vorhaben die Massenspektrometrie-basierten Bindungsassays (MS-Bindungsassays) den Vorzug gegenüber klassischen Radioligand-Bindungsassays. In Bezug auf die Bindung der Bispyridiniumverbindung am nAChR war bislang lediglich gezeigt worden, dass diese nicht-kompetitiv d.h. nicht an die orthosterischen Bindestellen am Muskeltyp-nAChR erfolgt. Darüber hinaus standen zu Projektbeginn allerdings noch keine Daten zur MB327-Bindungsstelle bzw. zur Bindungsaffinität der Bispyridiniumverbindung am nAChR zur Verfügung.

Ziel dieser Arbeit war zunächst die Entwicklung von MS-Bindungsassays zur erstmaligen Charakterisierung der MB327-Bindung am Muskeltyp-nAChR. Im Anschluss daran sollten die Bindungsaffinitäten weiterer Testsubstanzen an die MB327-Bindestelle bestimmt werden, sodass der Aufbau erster Struktur-Affinitätsbeziehungen am Muskeltyp-nAChR bzw. gegebenenfalls bereits die

Identifizierung von Testverbindungen mit höherer Affinität an die besagte Bindestelle möglich ist.

Entwicklung einer geeigneten LC-MS-Methode

Für die Entwicklung eines MS-Bindungsassays muss zunächst eine geeignete LC-MS-Methode zur sensitiven und zuverlässigen Quantifizierung des Reporterliganden etabliert werden. Als Reporterligand wurde das sechsfach deuterierte Analogon [$^2\text{H}_6$]MB327 eingesetzt. Da der Reporterligand am Ende des MS-Bindungsexperiments mitsamt der Matrix der Bindungsprobe über das HPLC-System in das Massenspektrometer gebracht wird, muss die LC-MS-Methode gewährleisten, dass dieser auch in Anwesenheit von Matrixbestandteilen wie z.B. Puffersalzresten zuverlässig quantifiziert werden kann. Eine geeignete Kombination von stationärer Phase und Fließmittelzusammensetzung im HPLC-System sollte bereits vor der MS-Analyse für eine ausreichende chromatographische Trennung von Matrixbestandteilen und Markerverbindung sorgen. Um bei der massenspektrometrischen Detektion suppressive Effekte von Matrixbestandteilen auf das Reporterligand-Signal (sogenannte Matrixeffekte) gegebenenfalls ausgleichen zu können, wurde das deuterierte MB327-Analogon [$^2\text{H}_{18}$]MB327 als Interner Standard (IS) eingesetzt. Für eine möglichst selektive und sensitive Detektion des Reporterliganden im Massenspektrometer, sollte, wie in MS-Bindungsassays üblich, im Tandem-MS-Modus gearbeitet werden. Hierbei wird der Reporterligand nach Übergang in die Gasphase im ersten Quadrupol (Q1) des Massenspektrometers als sogenanntes Mutter-Ion isoliert. Der Q1 fungiert als Massenfilter und lässt ausschließlich Ionen mit einem bestimmten Masse-zu-Ladung(m/z)-Verhältnis passieren. Das Mutter-Ion wird im nachfolgenden Quadrupol (Q2) mithilfe eines inerten Gases fragmentiert. Nach Selektion im dritten Quadrupol (Q3) als Massenfilter können am Detektor ausgewählte Fragment-Ionen des Mutter-Ions betrachtet werden. Das Prinzip der Tandem-MS-Messung ist in Abbildung 11 nebst Schema eines Triple-Quadrupol Massenspektrometers dargestellt.

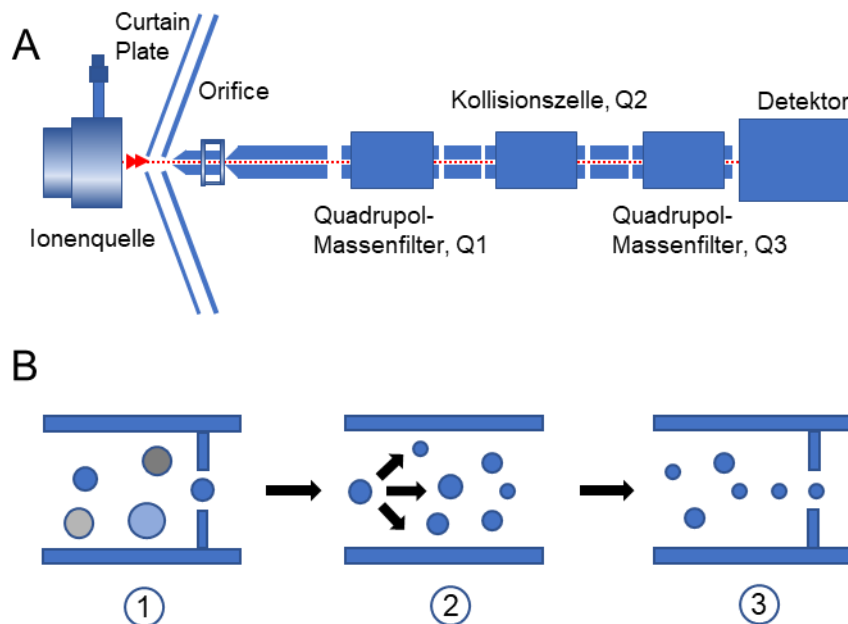


Abbildung 11: Aufbau eines Triple-Quadrupol-Massenspektrometers, modifiziert nach AB Sciex⁹⁰, (A) und Darstellung des Tandem-MS-Messprinzips (B). (A) Nach Ionisierung gelangt das sogenannte Mutter-Ion über die Curtain Plate und das Orifice in das Massenspektrometer und passiert die Quadrupole Q1 – Q3 mit anschließender Quantifizierung im Detektor. (B) Der Aufbau des Triple-Quadrupol-Massenspektrometers kann genutzt werden, um im Tandem-MS-Modus zu messen. Dazu wird im Q1 zunächst das Mutter-Ion selektiert (1). Im Q2 als Kollisionszelle erfolgt die Fragmentierung des Mutter-Ions mithilfe eines inerten Gases (2) und im Q3 die Selektion eines spezifischen Fragment-Ions (3). Für ein bestimmtes Mutter-Ion kann so ein spezifischer Massenübergang aufgezeichnet werden.

Damit bei Anwendung der MS-Bindungsassays zur Bestimmung von Bindungsaffinitäten an die MB327-Bindestelle schließlich ein hoher Probendurchsatz möglich ist, sollte die Laufzeit der LC-MS-Methode möglichst kurz sein. Die LC-MS-Quantifizierungsmethode sollte zuletzt noch gemäß Richtlinien⁹¹ des CDER (Center for Drug Evaluation and Research) der FDA (Food and Drug Administration) für bioanalytische Methoden in Bezug auf Selektivität, Linearität, Richtigkeit und Präzision validiert werden.

Identifikation geeigneter Parameter für die Bindungsassays

Nach Entwicklung einer sensitiven und robusten LC-MS-Methode zur Quantifizierung des Reporterliganden müssen im nächsten Schritt geeignete Versuchsbedingungen für das eigentliche Bindungsexperiment gewählt werden. Mangels Verfügbarkeit des humanen neuromuskulären nAChR für das Bindungsexperiment, wurde auf den Muskeltyp-nAChR aus *Torpedo californica* als Modell zurückgegriffen. Der *Torpedo*-

nAChR wird seit Jahrzehnten in Studien bevorzugt als Modell des humanen, neuromuskulären nAChR eingesetzt,^{50,51} da sich beide Rezeptoren strukturell sehr ähnlich sind und der *Torpedo*-nAChR außerdem in großen Mengen aus dem elektrischen Organ des Zitterrochens gewonnen werden kann. Auf dem nAChR aus *Torpedo marmorata* basiert außerdem das einzige vollständige 3D-Strukturmodell eines nAChR in adäquater Auflösung für *in silico* Docking- bzw. Molecular Modeling-Studien.

Die Bindungsaffinität von Reporterliganden in Bindungsassays liegt typischerweise im niedrig nanomolaren Bereich und darunter.^{79,87,88} Für die Bindung von MB327 am nAChR war stattdessen, ausgehend von der geringen Potenz der Bispyridiniumverbindung in *in vitro* und *in vivo* Studien, eine niedrige Affinität mit K_d -Wert im mikromolaren bis maximal hoch-nanomolaren Konzentrationsbereich zu erwarten. Die Verwendung einer niedrig affinen Verbindung als Reporterligand limitiert wiederum die Auswahl an Methoden, die zur Trennung von gebundenem und ungebundenem Reporterligand im Bindungsversuch zur Verfügung stehen.

Dieser Trennschritt kann grundsätzlich mittels Filtration oder Zentrifugation erfolgen. Wird der Bindungsversuch nach dem Prinzip der Gleichgewichtsdialyse durchgeführt, erübrigt sich ein separater Trennschritt, da sich das Target von vornherein nur in einer von zwei puffergefüllten Kammern befindet, die durch eine – nur für den Reporterliganden durchlässige - Membran getrennt sind. Am häufigsten kommt die Filtration als Trennschritt bzw. das sogenannte Filter-Bindungsassay zum Einsatz. Dabei werden Bindungsproben nach Inkubation über eine Filtermatte filtriert. Aufgrund des Größenausschlusses verbleibt der Target-Reporterligand-Komplex auf der Filtermatte, während ungebundener, nicht-spezifisch anhaftender Reporterligand durch mehrere Waschschrte entfernt wird. Der Reporterligand wird anschließend mittels Methanol bzw. Acetonitril aus dem Target-Ligand-Komplex freigesetzt und von der Filtermatte eluiert. Der eigentliche Trennschritt sowie anschließende Waschschrte nehmen üblicherweise einige Sekunden in Anspruch, in denen ein beträchtlicher Anteil des zuvor spezifisch gebundenen Reporterliganden vom Target dissoziieren und damit für die Quantifizierung verloren gehen kann. Dies gilt insbesondere für Reporterliganden mit einer geringen Bindungsaffinität an das Target, da in diesem Fall mit einer schnellen Dissoziation des Target-Reporterligand-Komplex

zu rechnen ist. Das Filtrations-basierte Bindungsassay wird daher nur für Reporterliganden mit einer Affinität $K_d < 3.3 \times 10^{-8} \text{ mol L}^{-1}$ (bei 0°C Arbeitstemperatur) empfohlen.⁷⁷

Anstelle der Filtration kann auch die Zentrifugation der Bindungsproben zur Trennung von gebundenem und ungebundenem Reporterliganden angewandt werden. Im Zentrifugal-Kraftfeld sedimentieren die größeren Target-Reporterligand-Komplexe und bilden ein kompaktes Pellet in der Spitze des Mikroreaktionsgefäßes. Der gebundene Anteil des Reporterliganden bleibt so in dem Raum eingeschlossen, den das Pellet im Gefäß einnimmt und kann nach Entfernen des Überstands wieder freigesetzt werden. Für die Bildung eines stabilen Pellets muss in Bindungsproben des Zentrifugations-basierten Bindungsassays allerdings eine hohe Targetkonzentration eingesetzt werden.⁷⁷ Selbiges gilt für den Bindungsversuch, wenn dieser im Zweikammersystem der Gleichgewichtsdialyse durchgeführt wird, wobei in diesem Fall noch hinzukommt, dass eine Einstellung des Bindungsgleichgewichts über beide Probenkammern vergleichsweise viel Zeit in Anspruch nehmen kann.

Anwendung der MS-Bindungsassays zur Bestimmung von Bindungsaffinitäten

Nach erfolgreicher Charakterisierung der MB327-Bindung am *Torpedo*-nAChR in entwickelten MS-Bindungsassays sollten im Anschluss die Bindungsaffinitäten strukturanaloger Testverbindungen an die MB327-Bindestelle des nAChR bestimmt werden. Hierfür waren durch Sebastian Rappenglück eine Reihe MB327-Derivate (PTM0001 – PTM0060) mit unterschiedlichem Substitutionsmuster und einer Vielzahl verschiedener funktioneller Gruppen als Substituenten synthetisiert worden. Auf Basis der gewonnenen Bindungsdaten sollten erste Struktur-Affinitätsbeziehungen an der MB327-Bindestelle abgeleitet werden. Die Erkenntnisse dieser Struktur-Affinitätsbeziehungen sollten wiederum gemeinsam mit den neuesten Daten funktioneller Testsysteme z.B. SURFE²R-basierter elektrophysiologischer Studien, unterstützt von Computermodellen des Molecular Modeling, in die Synthesepipeline neuer Testverbindungen einfließen. Damit wäre ein wichtiger Schritt in die Richtung des zielgerichteten Designs neuer, potenter „Resensitisierer“ bzw. Reaktivatoren des Muskeltyp-nAChR getan.

ERGEBNISSE UND DISKUSSION

3. Ergebnisse und Diskussion

3.1 Erste Publikation

Development of MS Binding Assays targeting the binding site of MB327 at the nicotinic acetylcholine receptor

3.1.1 Zusammenfassung der Ergebnisse

In vorangegangenen Studien zeigte die Bispyridiniumverbindung MB327 bereits - *in vitro* wie auch *in vivo* - einen therapeutischen Effekt bei Vergiftungen mit phosphororganischen Verbindungen. Dieser Effekt wird dabei dessen Fähigkeit zugeschrieben, den desensitisierten, nikotinischen Acetylcholinrezeptor (nAChR) durch allosterische Modulation zu reaktivieren bzw. zu „resensitisieren“. Für einen sicheren Einsatz als Antidot ist die Potenz der Bispyridiniumverbindung allerdings zu gering. Dem Ansatz der rationalen Wirkstoffentwicklung folgend, sollte deshalb durch chemische Modifikation der Leitstruktur vor allem die Bindungsaffinität an die MB327-Bindestelle des nAChR erhöht werden, um so potentere nAChR-„Resensitisierer“ zu entwickeln. Als Testsystem zur Bestimmung von Bindungsaffinitäten an die MB327-Bindestelle wurden in dieser Studie Massenspektrometrie(MS)-basierte Bindungsassays entwickelt. Für die Bindungsversuche wurden nAChR-reiche Membranen des elektrischen Organs aus *Torpedo californica* als Targetpräparation und das sechsfach deuterierte Analogon [$^2\text{H}_6$]MB327 als Reporterligand eingesetzt.

Zunächst wurde eine empfindliche und zuverlässige Methode zur Quantifizierung des Reporterliganden mit [$^2\text{H}_{18}$]MB327 als Internem Standard in Lösungsmittelproben entwickelt. Mithilfe einer Diol-HILIC-Säule als stationärer Phase und einem Fließmittelgemisch aus 20 mmol L⁻¹ Ammoniumformiatpuffer (pH 3.0) und Acetonitril im Verhältnis 20 : 80 als mobiler Phase im HPLC-System, und anschließender massenspektrometrischer Detektion im Tandem-MS(MS/MS)-Modus konnte die Markerverbindung ([$^2\text{H}_6$]MB327, m/z 159.2 \rightarrow 144.3) bis zu einer Konzentration von 100 pmol L⁻¹ zuverlässig bestimmt werden. Bei einer Flussrate von 800 $\mu\text{L min}^{-1}$ betrug die Analysenzeit knapp drei Minuten, womit die Methode auch für einen hohen Probendurchsatz geeignet wäre. Anschließend wurden erste Bindungsexperimente, in denen die Trennung von ungebundenem und Target-gebundenem Reporterligand nach Inkubation mittels Filtration erfolgte, durchgeführt. Höchstwahrscheinlich war es

der geringen Affinität des Reporterliganden und der damit verbundenen schnellen Dissoziation des Reporterligand-Target-Komplexes geschuldet, dass eine sichere Erfassung der [$^2\text{H}_6$]MB327-Bindung im Filter-Bindungsassay nicht möglich war. Im Gegensatz dazu erlaubten Zentrifugations-basierte Bindungsassays, in Kombination mit Hitzedenaturierung der Targetpräparation als Methode zur Bestimmung der nicht-spezifischen Bindung, eine sichere Bestimmung der spezifischen Bindung. Die Reporterligand-Quantifizierungsmethode wurde entsprechend in markerfreien Proben des Zentrifugations-basierten Bindungsexperiments, gemäß CDER-Richtlinien der FDA für bioanalytische Methoden, validiert. Die LC-MS-Methode erfüllte dabei alle Kriterien der untersuchten Validierungsparameter Selektivität, Linearität, Richtigkeit und Präzision in einem Reporterligand-Konzentrationsbereich von 100 pmol L^{-1} bis 10 nmol L^{-1} .

Unter den gewählten Assaybedingungen zeigte die spezifische Bindung allerdings zunächst keine Sättigung im untersuchten Reporterligand-Konzentrationsbereich. Es stellte sich heraus, dass ein Störfaktor in der Targetpräparation enthalten war, der die Bindung des Reporterliganden [$^2\text{H}_6$]MB327 an den *Torpedo*-nAChR negativ beeinflusste. Das „Auswaschen“ dieser Komponente aus der Targetpräparation, indem die Präparation vor dem Bindungsversuch wiederholt zentrifugiert und die pelletierten *Torpedo*-Membranen erneut in frischem Inkubationspuffer aufgenommen wurden, ermöglichte die Darstellung einer Sättigungsisotherme und die Bestimmung von Affinitätskonstanten der [$^2\text{H}_6$]MB327-Bindung im zweistelligen mikromolaren Bereich. Insbesondere Saccharose und EDTA (Ethylendiamintetraessigsäure) standen im Verdacht die [$^2\text{H}_6$]MB327-Bindung an den nAChR zu stören, da diese nicht im Inkubationspuffer enthalten waren, jedoch durch Verdünnung der Membranpräparation in nicht unerheblichen Mengen (30 mmol L^{-1} Saccharose und $50 \text{ } \mu\text{mol L}^{-1}$ EDTA) in den Bindungsansatz gelangten. Wurde ein Lagerungspuffer ohne Saccharose und EDTA im Bindungsassay verwendet, war wiederum die Darstellung von Sättigungsisothermen analog zum vorherigen „Auswasch“-Experiment möglich. Wurde in einem dieser Bindungsversuche, d.h. in Abwesenheit von Saccharose und EDTA, allerdings die Saccharose in Bindungsproben erneut in einer Konzentration von 30 mmol L^{-1} zugesetzt, stellte sich wie unter den vorherigen Assaybedingungen keine Sättigung der spezifischen [$^2\text{H}_6$]MB327-Bindung ein.

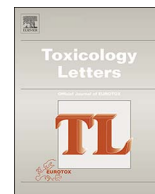
Entsprechend war keine Bestimmung von Affinitätskonstanten möglich. Damit konnte zuletzt der Nachweis erbracht werden, dass es sich bei dem gesuchten Störfaktor im Bindungsexperiment um die Saccharose handelte.

Auf Basis des modifizierten MS-Bindungsassays, in Abwesenheit von Saccharose und EDTA in Bindungsproben, war schließlich eine Charakterisierung der MB327 bzw. [$^2\text{H}_6$]MB327-Bindung an den nAChR möglich. In Sättigungsexperimenten wurde für die Bindung von [$^2\text{H}_6$]MB327 am *Torpedo*-nAChR ein K_d -Wert von $15.5 \pm 0.9 \mu\text{mol L}^{-1}$, sowie ein B_{max} -Wert von $348 \pm 18 \text{ pmol mg}^{-1}$ Protein ermittelt. Ein Vergleich der maximalen Bindestellen, bestimmt in Sättigungsexperimenten für die [$^2\text{H}_6$]MB327- bzw. die Carbacholbindung ($611 \pm 30 \text{ pmol mg}^{-1}$ Protein) deutet darauf hin, dass die Bispyridiniumverbindung, anstatt wie der Agonist an zwei Bindestellen, nur an eine Bindestelle am nAChR bindet. Autokompetitionsexperimente, zur Bestimmung der Bindungsaffinität des nativen MB327 am *Torpedo*-nAChR über die Verdrängung des Reporterliganden [$^2\text{H}_6$]MB327, lieferten einen K_i -Wert von $18.3 \pm 2.6 \mu\text{mol L}^{-1}$. Die Übereinstimmung der Affinitätskonstanten aus Kompetitionsexperimenten und Sättigungsexperimenten zeigt, dass sich die entwickelten MS-Bindungsassays gut als Testsystem zur Bestimmung von Bindungsaffinitäten an die MB327-Bindestelle des nAChR eignen.

3.1.2 Erklärung zum Eigenanteil

Alle Experimente sowie die Auswertung entsprechender Daten führte ich eigenständig durch. Die Synthese der deuterierten MB327-Analoga zur Verwendung als Reporterligand bzw. Interner Standard erfolgte durch Sebastian Rappenglück. Ich schrieb das Manuskript und erstellte alle Graphiken und Tabellen, wobei ich von Georg Höfner und Klaus T. Wanner unterstützt und angeleitet wurde. An der Korrektur des Manuskripts waren Georg Höfner und Klaus T. Wanner sowie Franz F. Paintner, Thomas Wein, Karin V. Niessen*, Thomas Seeger*, Franz Worek* und Horst Thiermann* beteiligt.

* Kooperationspartner im Rahmen eines gemeinsamen Forschungsprojekts vom Institut für Pharmakologie und Toxikologie der Sanitätsakademie in München



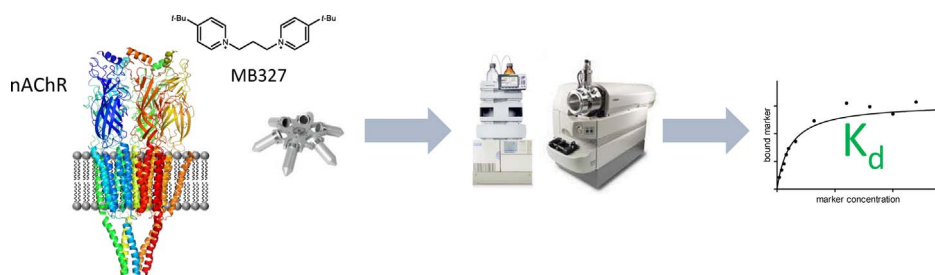
Development of MS Binding Assays targeting the binding site of MB327 at the nicotinic acetylcholine receptor

S. Sichler^a, G. Höfner^a, S. Rappenglück^a, T. Wein^a, K.V. Niessen^b, T. Seeger^b, F. Worek^b,
H. Thiermann^b, F.F. Paintner^a, K.T. Wanner^{a,*}

^a Department of Pharmacy – Center for Drug Research, Ludwig-Maximilians-Universität München, Butenandtstr. 5-13, 81377 Munich, Germany

^b Bundeswehr Institute of Pharmacology and Toxicology, Neuherbergstr. 11, 80937 Munich, Germany

GRAPHICAL ABSTRACT



ARTICLE INFO

Keywords:

MB327
MS Binding Assays
LC–MS
nicotinic acetylcholine receptor
resensitizer

ABSTRACT

The bispyridinium compound MB327 has been shown previously to have a positive pharmacological effect against poisoning with organophosphorous compounds (OPCs). The mechanism by which it exerts its therapeutic effect seems to be directly mediated by the nicotinic acetylcholine receptor (nAChR). In the present study, the development of mass spectrometry based binding assays (MS Binding Assays) for characterization of the binding site of MB327 at the nAChR from *Torpedo californica* is described. MS Binding Assays follow the principle of radioligand binding assays, but do not, in contrast to the latter, require a radiolabeled reporter ligand, as the readout is in this case based on mass spectrometric detection. For [²H₆]MB327, a deuterated MB327 analogue employed as reporter ligand in the MS Binding Assays, an LC-ESI-MS/MS method was established allowing for its fast and reliable quantification in samples resulting from binding experiments. Using centrifugation for separation of non-bound [²H₆]MB327 from target-bound [²H₆]MB327 in saturation and autocompetition experiments (employing native MB327 as competitor) enabled reliable determination of specific binding. In this way, the affinities for [²H₆]MB327 ($K_d = 15.5 \pm 0.9 \mu\text{mol L}^{-1}$) and for MB327 ($K_i = 18.3 \pm 2.6 \mu\text{mol L}^{-1}$) towards the nAChR could be determined for the first time. The almost exactly matching affinities for MB327 and [²H₆]MB327 obtained in the MS Binding Assays are in agreement with potencies previously found in functional studies. In summary, our results demonstrate that the established MS

Abbreviations: AChE, acetylcholinesterase; CE, collision energy; CXP, collision cell exit potential; DP, declustering potential; EP, entrance potential; ESI, electrospray ionization; FDA, Food and Drug Administration; FIA, flow injection analysis; HI-6, 1-[(4-carbamoylpyridin-1-ium-1-yl)methoxy]methyl-2-[(hydroxyimino)methyl]-pyridin-1-ium; HILIC, hydrophilic interaction chromatography; (HP)LC, (high performance) liquid chromatography; LLOQ, lower limit of quantification; IS, internal standard; mAChR, muscarinic acetylcholine receptor; MB327, 1,1'-(propane-1,3-diyl)bis[4-(*tert*-butyl)pyridine-1-ium] diiodide; MRM, multiple reaction monitoring; MS, mass spectrometry; nAChR, nicotinic acetylcholine receptor; NMR, nuclear magnetic resonance; NSB, nonspecific binding; OPC(s), organophosphorous compound(s); PCP, phencyclidine; PTM0001, 1,1'-(propane-1,3-diyl)bis[3-(*tert*-butyl)pyridine-1-ium] diiodide; PTM0002, 1,1'-(propane-1,3-diyl)bis[2-(*tert*-butyl)pyridine-1-ium] ditrifluoromethanesulfonate; QC, quality control; RP, reverse phase; S/N, signal-to-noise; SURFE²R, surface electronic event reader; Tris, 2-amino-2-(hydroxymethyl)propane-1,3-diol

* Corresponding author.

E-mail address: Klaus.Wanner@cup.uni-muenchen.de (K.T. Wanner).

<https://doi.org/10.1016/j.toxlet.2017.11.013>

Received 15 September 2017; Received in revised form 9 November 2017; Accepted 12 November 2017

Available online 14 November 2017

0378-4274/ © 2017 Elsevier B.V. All rights reserved.

Binding Assays represent a promising tool for affinity determination of test compounds towards the binding site of MB327 at the nAChR.

1. Introduction

Organophosphorous compounds (OPCs) are still widely used as insecticides and have to some extent also been deployed as warfare agents (Dolgin, 2013; Newmark, 2007; Worek et al., 2016). Thus, OPC poisoning still represents a serious threat to humanity. OPCs target and inactivate the enzyme acetylcholinesterase (AChE). Accumulation of acetylcholine that is not removed by AChE-promoted hydrolytic cleavage, in turn, results in overstimulation of muscarinic (mAChR) and nicotinic (nAChR) acetylcholine receptors. mAChR overstimulation can be antagonized using atropine, for instance. The nAChR, however, shifts into a state of desensitization thereby disrupting cholinergic signaling. For this pathophysiological transformation, at least in presence of constantly high amounts of agonist, no treatment is available yet, despite the nAChR being one of the best characterized ligand-gated ion channels regarding structure as well as function. (Albuquerque et al., 2009; Changeux, 2012; Unwin, 2013)

The nAChRs are composed of five distinct types of subunits α , β , δ , γ , and ϵ , assembled into homo- or heteropentamers with the composition depending on the subtype (e.g. $\alpha_2\beta\delta\epsilon$ for the adult muscle type nAChR). (Karlin, 2002; Unwin, 2005) Subtypes of the nAChR are expressed in neuronal as well as non-neuronal tissue and are involved in a wide range of physiological processes (Hurst et al., 2013; Kalamida et al., 2007). Regarding nAChR's function at least three different conformational states are important: resting, activated (also termed open) and desensitized. The conformational equilibria among these states basically vary with the level of agonist binding (Papke, 2014). If no agonist is bound, the resting state is favored. Upon agonist binding, the receptor favors the activated state. If high concentrations of agonist are present at the receptor, e.g. in the event of OPC poisoning, it ultimately favors the nonconducting, desensitized state. In addition to the agonist (also termed orthosteric) binding site, the nAChR exhibits several allosteric binding sites which may be occupied by ligands modulating nAChR function e.g. by affecting its conformational equilibrium (Arias, 2011, 2010; Changeux and Edelstein, 2005; Chatzidaki and Millar, 2015).

With the nAChR in the desensitized state in the event of OPC poisoning cholinergic signaling is disrupted, which can even result in respiratory paralysis with lethal consequences (Marrs, 1993; Thiermann et al., 2010). Since decades, the standard medication to counteract OPC intoxication is based on mAChR antagonism and restoration of nAChR mediated signaling. The latter can be achieved indirectly by reactivation of the AChE, for resumption of AChE-promoted acetylcholine hydrolysis, using oximes e.g. obidoxime. Oxime potency, however, varies strongly depending on the type of OPC causal for poisoning as well as on the time elapsed from poisoning to treatment (Worek et al., 2016, 2005). If aging of the OPC-AChE complex has already occurred, which happens particularly fast for organophosphates such as soman, the AChE inactivation is irreversible which means that the enzyme cannot be reactivated by oximes any longer. Thus, there is a therapeutic gap that calls for new antidotes capable of restoring cholinergic signaling in particular by a direct intervention at the nAChR to recover it from desensitization.

Recent studies employing electrophysiological measurements using a SURFE²R (surface electronic event reader) platform demonstrated that the bispypyridinium compound MB327 can functionally recover ("resensitize") the nAChR from desensitization (Niessen et al., 2017, 2016). Other studies further demonstrated that MB327 has a positive pharmacological effect against OPC poisoning. For soman-impaired neuromuscular transmission in human intercostal muscle and rat diaphragm preparations, MB327 could be shown to restore muscle force

(Seeger et al., 2012). Furthermore, MB327 administration was found to increase survival in tabun-poisoned guinea pigs *in vivo* versus administration of the oxime HI-6, both given in combination with physostigmine and hyoscyne (Turner et al., 2011). Despite these positive results, MB327 is not suitable for treatment of OPC poisoning as its therapeutic window is quite narrow. To induce recovery of poisoned muscle *in vitro*, MB327 has to be applied in concentrations of at least 100–200 $\mu\text{mol L}^{-1}$ to exert a clear therapeutic effect (Seeger et al., 2012), however, at concentrations only a little higher, MB327 acts also as an inhibitor of AChE (IC_{50} approx. 600 $\mu\text{mol L}^{-1}$, Niessen et al., 2011) thus giving rise to toxic side effects. Additionally, there is evidence that MB327 at higher micromolar concentrations blocks the nAChR ion channel. This could also possibly contribute to the narrow therapeutic window (Tattersall 1993; Turner et al., 2011). Furthermore, muscle force experiments using soman-poisoned rat diaphragm hemispheres showed that at higher MB327 concentrations ($> 300 \mu\text{mol L}^{-1}$) the extent of muscle force recovery started to decline again (Niessen et al., 2017).

This lack of potency of MB327 is due to a lack of affinity to the target. In consequence, for an increased therapeutic efficacy the identification of new compounds with enhanced affinity for the MB327 binding site is required. Unfortunately, the binding site of MB327 at the nAChR has not yet been characterized. Only the capability of MB327 to displace [³H]epibatidine at the orthosteric binding site of the nAChR has been examined so far yielding an $\text{IC}_{50} > 100 \mu\text{mol L}^{-1}$ (Niessen et al., 2013). Considering pharmacological effects of MB327 at low $\mu\text{mol L}^{-1}$ concentrations (Niessen et al., 2016) it seems unlikely that binding to the orthosteric binding site of nAChR is responsible for the therapeutic effect of MB327. Rather, MB327 seems to target allosteric binding sites. Hence, the aim of the present study was to develop binding assays addressing the binding site of MB327 at the nAChR as a tool for the characterization of the binding affinity of MB327 as well as of any optional test compound. The binding assays to be developed should follow the concept of MS Binding Assays, the setup of which is similar to conventional radioligand binding assays, but uses a native, non-labeled reporter ligand, that is quantified by mass spectrometry, instead of a ligand labeled with a radioisotope such as tritium (Höfner and Wanner, 2015). Both assay types share a simple working principle, provide reliable results and allow for a reasonable sample throughput (Grimm et al., 2015; Hess et al., 2011; Neiens et al., 2015). For MS Binding Assays, however, as radiolabeling of the marker is not required for detection, all disadvantages inherent to the synthesis and use of radioligands resulting e.g. from safety regulations, elaborate waste management, etc. become irrelevant. Another fundamental advantage of MS Binding Assays especially important for the present project is related to the flexibility with respect to the choice of a reporter ligand. As the latter does not require a label, it can be easily exchanged when ligands with improved affinity for the MB327 binding site at the nAChR become available.

For the development of MS Binding Assays enabling the characterization of the affinity of that compound for the MB327 binding site at the nAChR, we intended to proceed as follows. MB327 should serve as reporter ligand as it represents the most potent bispypyridinium compound for functional recovery of desensitized nAChR that has been identified so far. The human muscle type nAChR was considered as the ideal receptor source, but was not available in the required amounts. Hence instead, the *Torpedo*-nAChR, which is characterized by a high degree of homology with human muscle-type nAChRs (Millar, 2003; Navedo et al., 2004), was used as an appropriate substitute. For quantification of the reporter ligand (in the context of MS Binding Assays often termed MS Marker), a reliable, sensitive, and robust LC–MS/

MS (liquid chromatography – tandem mass spectrometry) method had to be developed and, to prove its reliability, validated according to the FDA's guideline for bioanalytical method validation. Based on this groundwork appropriate conditions for the performance of the binding assays should be developed. Here, however, it has to be mentioned that this task appeared to be challenging as previous functional studies suggested a rather low affinity for MB327 (K_d in the range of high nmol L⁻¹ to μ mol L⁻¹ concentrations, Niessen et al., 2016; Seeger et al., 2012; Turner et al., 2011), that is distinctly below the affinities that are typical for radioligands in binding assays (Davenport and Russell, 1996; de Jong et al., 2005; Hulme and Trevethick, 2010). Hence, there appeared to be a significant risk of uncontrolled loss of specifically bound MS Marker during the separation step – the separation of the marker-target complex from the non-bound marker in the incubation buffer – that could impair or even prevent the desired assay development.

2. Material and methods

2.1. Material

(+/-)-Epibatidine and carbachol (carbamoylcholine chloride) were purchased from Tocris (Bristol, UK) and Sigma-Aldrich (Taufkirchen, Germany), respectively. MB327 and analogues [²H₆]MB327 and [²H₁₈]MB327 (chemical structures see Fig. 2) were synthesized in-house by S. Rappenglück and were of $\geq 97\%$ (n/n) purity measured by ¹H NMR spectroscopy (manuscript in preparation). *T. californica* electroplaque tissue was purchased from Aquatic Research Consultants (San Pedro, CA, USA). Water for mobile phase and incubation buffers was obtained in-house by distillation of demineralized water (prepared by reverse osmosis) and subsequent filtration using 0.45 μ m filter material. For LC-MS, HPLC grade acetonitrile was purchased from VWR Prolabo (Darmstadt, Germany). Ammonium formate as additive for mobile phase buffer was obtained from Sigma-Aldrich (for mass spectrometry, $\geq 99\%$, Taufkirchen, Germany). All other chemicals were of analytical grade. Stock solutions were prepared in water if not stated otherwise (1–10 mmol L⁻¹). 96-well polypropylene microtiter plates, tubes, and tips were purchased from Sarstedt (Nümbrecht, Germany). 96-well glass fiber filter plates were supplied by Pall (AcroPrep Advance, glass fiber, 1.0 μ m, 350 μ L, Pall, Dreieich, Germany). Unless otherwise indicated, all percentages and ratios are specified as v/v ratios.

2.2. LC-MS instrumentation

Experiments for method development and validation as well as binding experiments were performed on an API 3200 triple quadrupole mass spectrometer (AB Sciex, Darmstadt, Germany) with a Turbo-V source coupled to an Agilent 1200 HPLC system (vacuum degasser, quaternary pump, column oven; Agilent, Waldbronn, Germany) and a Shimadzu SIL-HTA autosampler (Shimadzu, Duisburg, Germany). For all kinds of MS-based analyses, Q1 and Q3 were operated with unit resolution. For HPLC, a YMC-Triart Diol-HILIC (50 mm \times 2.0 mm, 3 μ m; YMC Europe GmbH, Dinslaken, Germany), protected by two in-line filters (0.5 and 0.2 μ m, IDEX, Wertheim-Mondfeld, Germany) upstream to the column were employed. For all experiments, the column temperature was set to 20 °C. The built-in syringe pump with a 1 mL syringe was used for direct infusion of analyte solutions into the mass spectrometer.

2.3. LC-MS/MS method development

All mass spectrometric investigations were performed with the pneumatically assisted ESI-probe of the Turbo-V source in the positive mode. Optimization of compound-dependent parameters (DP, EP, CE, CXP) for the precursor and product ions of [²H₆]MB327, [²H₁₈]MB327,

carbachol, phencyclidine (PCP) and (+/-)-epibatidine was performed using the Analyst v. 1.6.1 Quantitative Optimization tool by direct infusion of a 400 nmol L⁻¹ solution (in methanol and 0.1% formic acid in water, 50:50) at a flow rate of 5 μ L min⁻¹. Optimization for [²H₆]MB327 and [²H₁₈]MB327 yielded a declustering potential (DP) of 36 V for both marker and internal standard, an entrance potential (EP) of 6 V and 8 V, respectively, a collision energy of 27 V and 29 V, respectively, and a collision cell exit potential of 4 V for both compounds. Optimization of compound-dependent parameters for PCP, (+/-)-epibatidine and carbachol yielded a DP of 21 V, 36 V and 16 V, a EP of 3.5 V, 11 V and 8 V, a CE of 19 V, 37 V and 23 V, and a CXP of 2 V, 4 V and 2 V, respectively. Source-dependent parameters for MS detection in the MRM mode were determined with the Quantitative Optimization Wizard under flow injection analysis (FIA) conditions of Analyst v. 1.6.1 software analyzing injections of 10 μ L 1 nmol L⁻¹ [²H₆]MB327 as following: source temperature 640 °C, ion-spray voltage 1000 V, curtain gas (N₂) 15 psi, auxiliary gas and nebulizing gas (N₂) both 42 psi as well as collision gas (N₂) 4 psi.

Capacity factors were calculated as $k = (t_R - t_V) \cdot t_V^{-1}$ using retention time (t_R) and void time (t_V). The system void volume was determined experimentally by injection without a column. Column dead volume was calculated according to the equation $0.7 \cdot r^2 \cdot \pi \cdot l$ (Unger and Weber, 1995), where l is the column length, r the column radius and 0.7 the grade of porosity for the stationary phase. The column dead volume amounted to 110.0 mm³ for the YMC-Triart Diol-HILIC. For calculation of the distribution coefficient logD Marvin Sketch v. 6.1.4 (Chemaxon, Budapest, Hungary) was used with a weighed combination of three calculation methods (PHYSPROP[®] database; Klopman et al., 1994; Viswanadhan et al., 1989; 1:1:1).

2.4. Quantification of [²H₆]MB327 by LC-ESI-MS/MS

For quantification of [²H₆]MB327 in MS Binding Assays the YMC-Triart Diol-HILIC column was used as stationary phase, protected by two in-line filters (see above). A composition of acetonitrile and ammonium formate buffer (20 mmol L⁻¹, pH 3.0) in a ratio of 80:20 was employed as mobile phase at a flow rate of 800 μ L min⁻¹. The samples, dissolved in acetonitrile and ammonium formate buffer (20 mmol L⁻¹, pH 3.0) in a ratio of 90:10, were injected in a volume of 10 μ L to the column. The temperature at the column oven was set to 20 °C. [²H₆]MB327 (marker) and [²H₁₈]MB327 (internal standard) were monitored at the mass transitions of m/z 159.2/144.3 and m/z 165.2/147.2, respectively.

2.5. LC-ESI-MS/MS method validation

In accordance with the FDA's guidance for bioanalytical method validation selectivity, lower limit of quantification (LLOQ), linearity, precision, and accuracy were investigated. For each validation series a set of matrix standards as well as quality control (QC) samples with [²H₆]MB327 in a range of 0.1–10 nmol L⁻¹ were prepared in “IS containing blank matrix” (i.e. blank matrix containing internal standard, for generation of the matrix see [²H₆]MB327 centrifugation based binding assay). Due to the possible difference in matrix of nonspecific vs total binding samples, i.e. with and without heat treatment prior to incubation, respectively, both matrix types were investigated. For each matrix type six validation series were examined. Selectivity was examined by analysis of blank matrices (for generation of the matrix see [²H₆]MB327 centrifugation based binding assay) of all validation series. For investigation of linearity, matrix blanks, zero samples (i.e. “IS containing blank matrix”), and standards, based on “IS containing blank matrix”, spiked with marker at eight different concentration levels (0.1, 0.2, 0.5, 1, 2, 4, 7, 10 nmol L⁻¹) of all 12 validation series, that were prepared in triplicates, except for concentrations 0.1 (LLOQ) and 0.2 nmol L⁻¹, that were prepared in hexaplicates instead, were examined. Obtained area ratios (y) of [²H₆]MB327 vs [²H₁₈]MB327

were plotted against the concentration of [$^2\text{H}_6$]MB327 (x). A linear regression with a weighting of $1/x^2$ was applied to the calibration data set. QC samples at three different concentration levels (i.e., 0.25, 1 and 8 nmol L^{-1}), each prepared in hexaplicates, were used to evaluate intra- and inter-batch accuracy as well as precision. According to the guideline, intra-batch accuracy was defined as recovery obtained for QC hexaplicates at the three concentration levels of a single validation series. Inter-batch accuracy was defined as recovery for the QC samples at the three concentration levels of all validation series. Intra- and inter-batch precision was calculated as relative standard deviation (RSD) for the same QC samples used for determination of intra- and inter-batch accuracy. The LLOQ was defined as the lowest [$^2\text{H}_6$]MB327 concentration, which reached a signal-to-noise (S/N) ratio of 5:1 at minimum, an accuracy of 80 – 120%, and a precision defined by an $\text{RSD} \leq 20\%$. For all other standards and QC samples acceptance limits for accuracy and precision were 85–115% and $\text{RSD} \leq 15\%$, respectively. For all centrifugation based MS Binding Assays using [$^2\text{H}_6$]MB327 as marker, its quantification was based on the global calibration obtained during validation. On each day an MS Binding Assay was performed QC samples at three concentration levels (0.25, 1 and 8 nmol L^{-1}) were analyzed in hexaplicates. The acceptance criteria were again for accuracy (recovery) 85–115% and for precision (RSD) $\leq 15\%$, respectively.

2.6. Preparation of nAChR-enriched plasma membrane fragments from *Torpedo californica*

Membranes from frozen *Torpedo californica* electroplaque tissue were prepared according to Niessen et al. (2011) with minor modifications. Instead of a threefold volume, a twofold volume of extraction buffer was added to frozen tissue. The homogenate was centrifuged and washed twice (instead of washing three times). Before centrifugation for 10 min at 1000g, in contrast to the original procedure, the suspension was additionally homogenized in a Dounce Homogenisator (Wheaton, NJ, USA) with 50 strokes per volume. For preliminary experiments, the pellet was resuspended in storage buffer I ($120 \text{ mmol L}^{-1} \text{ NaCl}$, $5 \text{ mmol L}^{-1} \text{ KCl}$, $300 \text{ mmol L}^{-1} \text{ sucrose}$, $0.5 \text{ mmol L}^{-1} \text{ EDTA}$, $8.05 \text{ mmol L}^{-1} \text{ Na}_2\text{HPO}_4$, $1.95 \text{ mmol L}^{-1} \text{ NaH}_2\text{PO}_4$, pH 7.4) after the final centrifugation step. For experiments finally characterizing the binding site of MB327, the pellet was resuspended in storage buffer II ($120 \text{ mmol L}^{-1} \text{ NaCl}$, $5 \text{ mmol L}^{-1} \text{ KCl}$, $8.05 \text{ mmol L}^{-1} \text{ Na}_2\text{HPO}_4$, $1.95 \text{ mmol L}^{-1} \text{ NaH}_2\text{PO}_4$, pH 7.4). Preparations were rapidly frozen in liquid nitrogen and stored in the gas phase of a liquid nitrogen storage system until use. Total protein concentration was determined by the bicinchoninic acid method (Smith et al., 1985) using bovine serum albumin as standard. On the day of the binding assay aliquots of the membrane preparation were thawed (5 min on ice, 30 min at room temperature) and used in binding samples without further pretreatment. For some saturation experiments aliquots of the membrane preparation were washed prior to use in MS Binding Assays. For this purpose, aliquots were diluted 1:8 in incubation buffer ($120 \text{ mmol L}^{-1} \text{ NaCl}$, $5 \text{ mmol L}^{-1} \text{ KCl}$, $1 \text{ mmol L}^{-1} \text{ CaCl}_2$, $8.05 \text{ mmol L}^{-1} \text{ Na}_2\text{HPO}_4$ and $1.95 \text{ mmol L}^{-1} \text{ NaH}_2\text{PO}_4$, pH 7.4), centrifuged in 1.5 mL tubes for 5 min at 4°C and 23000 rpm (49088g, rotor 3331, Biofuge stratos, Heraeus, Hanau, Germany), resuspended in

incubation buffer and stored for 30 min at 4°C . This procedure was repeated five times over a period of 4 h and the washed aliquots of the *Torpedo* membrane preparation were afterwards employed in the MS Binding Assay.

2.7. MS Binding Assays – [$^2\text{H}_6$]MB327 filtration based binding assay

Aliquots of the membrane preparation from *Torpedo californica* electroplaque ($6\text{--}12 \mu\text{g}$ per well) and [$^2\text{H}_6$]MB327 were incubated in triplicates in a buffer containing $120 \text{ mmol L}^{-1} \text{ NaCl}$, $5 \text{ mmol L}^{-1} \text{ KCl}$, $8.05 \text{ mmol L}^{-1} \text{ Na}_2\text{HPO}_4$, $1.95 \text{ mmol L}^{-1} \text{ NaH}_2\text{PO}_4$, pH 7.4 according to Niessen et al. (2011) in polypropylene 96-well plates (1.2 mL well volume) in a total volume of $250 \mu\text{L}$ for 2 h in a shaking water bath at 25°C . For determination of nonspecific binding, binding samples were incubated in presence of 1 mmol L^{-1} MB327 as competitor. After incubation, $200 \mu\text{L}$ of sample volume were transferred to a filter plate on a vacuum manifold (Multi-Well Plate Vacuum Manifold, Pall, Dreieich, Germany), pretreated for 1 h with $100 \mu\text{L}$ of a 0.5% (m/v) polyethyleneimine solution per well. Filter-entrapped membrane fragments with bound marker were washed three times with $100 \mu\text{L}$ ice-cold buffer also used for incubation of binding samples. Afterwards, the plate was dried in the drying oven for 1 h at 50°C and cooled to room temperature. For liberation of target-bound marker remaining on the filter, elution in three subsequent steps, each with $100 \mu\text{L}$ acetonitrile containing [$^2\text{H}_{18}$]MB327 as internal standard, was performed. Before marker quantification by LC–MS, $33 \mu\text{L}$ ammonium formate buffer (20 mmol L^{-1} , pH 3.0) were added to the acetonitrile eluate of $300 \mu\text{L}$. The plate was sealed with aluminum foil and subjected to LC–ESI–MS/MS analysis.

2.8. MS Binding Assays – [$^2\text{H}_6$]MB327 centrifugation based binding assay

Figure 1 illustrates the basic steps of the centrifugation based [$^2\text{H}_6$]MB327 Binding Assay. Aliquots of the membrane preparation from *Torpedo californica* electroplaque ($60\text{--}120 \mu\text{g}$ protein per sample) and marker were incubated in triplicates in incubation buffer ($120 \text{ mmol L}^{-1} \text{ NaCl}$, $5 \text{ mmol L}^{-1} \text{ KCl}$, $1 \text{ mmol L}^{-1} \text{ CaCl}_2$, $8.05 \text{ mmol L}^{-1} \text{ Na}_2\text{HPO}_4$, and $1.95 \text{ mmol L}^{-1} \text{ NaH}_2\text{PO}_4$, pH 7.4) in reagent tubes (0.5 mL micro tube, Sarstedt) in a total volume of $125 \mu\text{L}$. After incubation of binding samples in a shaking water bath for 2 h at 25°C , samples were centrifuged for 5 min at 4°C and 23000 rpm (49088g, rotor 3331, Heraeus Biofuge stratos, Thermo Scientific, with adapters for 0.5 mL reagent tubes, manufactured in-house). Supernatant was removed carefully using a Pasteur pipette coupled to vacuum. The remaining pellet was washed twice very carefully by addition and subsequent aspiration of $150 \mu\text{L}$ ice-cold incubation buffer. Next, the bound marker was liberated by addition of $500 \mu\text{L}$ acetonitrile containing 167 nmol L^{-1} [$^2\text{H}_{18}$]MB327 as internal standard. Subsequently, samples were placed in an ultrasonic bath for 1 h, vortexed thoroughly and afterwards centrifuged as before. $300 \mu\text{L}$ of the individual supernatants were transferred to individual wells of a 96-well plate and diluted 1:10 in acetonitrile ($36 \mu\text{L}$ sample + $324 \mu\text{L}$ acetonitrile) in a first 96-well plate and subsequently 1:10 in acetonitrile and 20 mmol L^{-1} ammonium formate buffer, pH 3.0 in a ratio of 90:10 ($36 \mu\text{L}$ sample + $288 \mu\text{L}$ acetonitrile + $36 \mu\text{L}$ buffer) in a second 96-

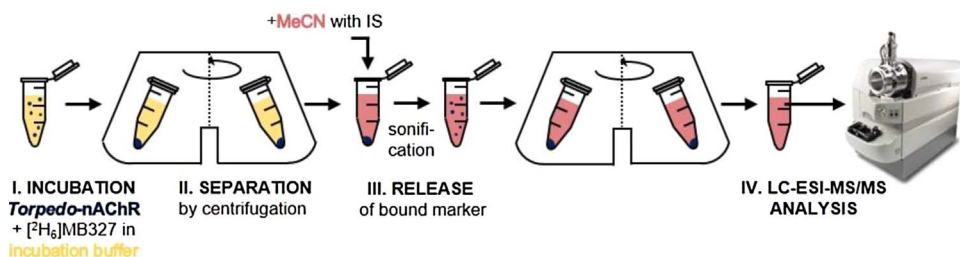


Fig. 1. Basic workflow of the centrifugation based MS Binding Assay of [$^2\text{H}_6$]MB327 towards the *Torpedo*-nAChR comprising of incubation (I), separation (II) of non-bound marker from target-bound marker using centrifugation, release (III) of target-bound marker and LC–ESI–MS/MS quantification (IV), IS = internal standard.

well plate. Finally, the plate was sealed with aluminum foil and subjected to LC-ESI-MS/MS quantification. If not stated otherwise, for each binding experiment nonspecific binding was determined by heat denaturation subjecting aliquots of the *Torpedo* membrane preparation to a temperature of 60 °C for 1 h in a shaking water bath prior to incubation with marker. Nonspecific binding was then calculated by means of linear regression (forced through the origin) based on four nominal marker concentration levels in the range of 2–20 $\mu\text{mol L}^{-1}$. In all [$^2\text{H}_6$]MB327 binding experiments, total ligand binding never exceeded 10% of the nominal concentration of the marker, so marker depletion was negligible. Blank matrices and “IS containing blank matrices” were obtained from experiments analogous to nAChR MS Binding Assays without addition of marker. In this case, after centrifugation of the samples and removal of the supernatants, pellets were resuspended therefor in pure acetonitrile (blank matrix) or in acetonitrile containing internal standard (“IS containing blank matrix”), respectively. Matrices (blank matrix and “IS containing blank matrix”) employed for preparation of validation samples (matrix blanks, zero samples, calibration standards and QC samples) were based on membrane fragments of *Torpedo californica* electroplaque in storage buffer I (see above).

2.9. MS Binding Assays – carbachol binding assay

Carbachol MS Binding Assays were conducted according to the procedure described for the [$^2\text{H}_6$]MB327 centrifugation based binding assay, except that acetonitrile, which was added to the pellet after centrifugation for liberation of bound marker, did not contain internal standard. After sonification and the final centrifugation step, 300 μL of the individual supernatants were transferred to individual wells of a 96-well plate and diluted 1:10 with acetonitrile and 20 mmol L^{-1} ammonium formate buffer, pH 3.0 in a ratio of 90:10 (36 μL sample + 36 μL buffer + 288 μL acetonitrile) in another 96-well plate. For each binding experiment nonspecific binding was determined by heat denaturation subjecting aliquots of the *Torpedo* membrane preparation to a temperature of 60 °C for 1 h in a shaking water bath prior to incubation with marker. Nonspecific binding was then calculated by means of linear regression (forced through the origin) based on four concentration levels over the full range of marker nominal concentrations (0.2–12 $\mu\text{mol L}^{-1}$). Carbachol was quantified using the LC method developed for [$^2\text{H}_6$]MB327 quantification recording the mass transition m/z 148.2/88.0. In binding samples carbachol was quantified from integrated peak areas by external calibration. On each day a binding experiment was performed, a calibration function based on matrix standards was established. For this purpose, blank matrix was obtained from experiments analogous to [$^2\text{H}_6$]MB327 MS Binding Assays, and, for generation of calibration standards, spiked with carbachol at four concentration levels in a range of 0.5–30 nmol L^{-1} . With QC samples at one concentration level examined throughout LC-MS analysis of the binding samples, quantification was accepted, if the deviation of calculated concentrations from nominal concentrations was not more than 15%, i.e. recovery of QCs was between 85–115%. Due to the amount of receptor material required for obtaining a stable pellet after centrifugation, marker depletion up to 60% of the nominal marker concentration could not be avoided. Under these conditions, instead of the nominal marker concentrations, marker concentrations calculated by subtraction of specifically bound marker from its nominal concentrations were used for calculation of the corresponding saturation isotherms.

2.10. Data analysis

Based on the determined calibration function the concentration of bound marker in the binding samples was determined using Analyst v. 1.6.1 (AB Sciex, Darmstadt, Germany). Specific binding was defined as the difference between total binding and nonspecific binding. In saturation experiments, the maximum density of binding sites (B_{max}) and the equilibrium dissociation constant (K_d) were determined from saturation isotherms calculated for specific binding with the “one-site – specific binding” regression tool by means of nonlinear curve fitting (Prism v. 5.0, GraphPad Software, La Jolla, CA, USA). Autocompetition curves were analyzed with the “one site–fit K_i ” regression tool fixing top and bottom level of the sigmoidal competition curves to total binding (in absence of competitor, $n = 3$) and nonspecific binding (determined by heat denaturation, $n = 3$). If not stated otherwise, results are given as means \pm SEM.

3. Results and discussion

3.1. LC-MS/MS method development

The aim of this work was to develop MS Binding Assays targeting the binding site of MB327 at the nAChR, hence, initially a suitable LC-MS/MS method for quantification of MB327 as reporter ligand should be developed. For method development, an API 3200 triple quadrupole mass spectrometer equipped with a pneumatically assisted electrospray ionization source, minimizing the risk of analyte degradation during transfer into the gas phase, was used. For saturation experiments marker concentrations in corresponding binding samples should be reliably determined in a range of $0.1 \times K_d - 10 \times K_d$, employing the target at a concentration below $0.1 \times K_d$. With the K_d unknown, however, it was difficult to estimate the required sensitivity. For high affinity binders (i.e. $K_d < 10 \text{ nmol L}^{-1}$), the quantification method must be able to determine marker concentrations down to low pmol L^{-1} reliably (Grimm et al., 2015; Neiens et al., 2015). Judging from recent functional studies (Niessen et al., 2016; Seeger et al., 2012; Turner et al., 2011), it seemed very unlikely that MB327 is a high affinity nAChR ligand. The K_d was rather to be expected in the range of high nmol L^{-1} to $\mu\text{mol L}^{-1}$ concentrations. With a K_d at a high nmol L^{-1} concentration, following the recommendations mentioned above, the desired lower limit of quantification (LLOQ) should be in the low nmol L^{-1} to high pmol L^{-1} range. A concentration range for marker quantification originating from this LLOQ would work as well in the event of the K_d being around $\mu\text{mol L}^{-1}$ concentrations, as by dilution of binding samples actual concentrations could still be measured in the covered concentration range of the quantification method. Therefore, we intended to establish an LC-ESI-MS/MS method enabling marker quantification down to high pmol L^{-1} concentrations. Aside from described sensitivity requirements, a run time short enough to allow for considerable sample throughput was desired.

For detection of reporter ligands in MS Binding Assays, generally, the multiple reaction monitoring (MRM) mode is used. This mode allows to filter for the precursor ion in Q1 of the triple quadrupole mass spectrometer and, after fragmentation (in Q2), to detect a specific product ion, filtered in Q3. As, ultimately, we intended to employ the developed MS Binding Assays to determine affinities of other known bispyridinium salts and of new compounds, that were planned to be synthesized, towards the MB327 binding site in competitive binding experiments, measures should be taken that these test compounds (including constitutional isomers of MB327) would not interfere with the

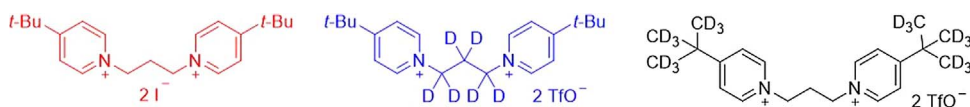


Fig. 2. MB327 (left) and deuterated analogues [$^2\text{H}_6$]MB327 (middle) and [$^2\text{H}_{18}$]MB327 (right).

marker detection in the MRM mode. In the event of coelution of constitutional isomers in particular (e.g. PTM0001 as 3-regioisomer and PTM0002 as 2-regioisomer of MB327, [Niessen et al., 2017](#)) with the MS Marker, however, those interferences were likely to occur. Therefore, we decided to use a six-fold deuterated analogue of MB327 ($[^2\text{H}_6]\text{MB327}$), with a molecular mass that is six mass units higher than the one of native MB327, making such interferences very unlikely to occur. To further enable reliable and robust quantification of $[^2\text{H}_6]\text{MB327}$ in the matrix resulting from the MS Binding Assays another deuterated analogue of MB327, $[^2\text{H}_{18}]\text{MB327}$, that coeluted with the marker (see LC-MS/MS method validation), was employed as internal standard (IS, see [Fig. 2](#)).

Fragmentation of MB327 and its deuterated analogues $[^2\text{H}_6]\text{MB327}$ and $[^2\text{H}_{18}]\text{MB327}$ in ESI-MS/MS had not been described in literature before. First, precursor ions for MB327, $[^2\text{H}_6]\text{MB327}$ and $[^2\text{H}_{18}]\text{MB327}$ were identified as m/z 156.2, m/z 159.2 and m/z 165.2, respectively, in a Q1 scan by direct infusion of the respective compounds (for experimental detail see Material and methods). Second to this, a product ion scan, that is a scan covering all product ions in a given m/z range resulting from fragmentation of the respective precursor ion, was performed to identify the most intense product ions of the precursor ions of MB327, $[^2\text{H}_6]\text{MB327}$ and $[^2\text{H}_{18}]\text{MB327}$ (see Supplementary information). The three most prominent fragments were found as m/z 141.1, 126.1 as well as 119.0 for MB327, m/z 144.3, 129.1 as well as 136.4 for $[^2\text{H}_6]\text{MB327}$ and m/z 147.2, 129.1 as well as 122.1 for $[^2\text{H}_{18}]\text{MB327}$, as illustrated in [Table 1](#). For the most abundant mass transitions observed for the marker $[^2\text{H}_6]\text{MB327}$ (m/z 159.2/144.3) and the internal standard $[^2\text{H}_{18}]\text{MB327}$ (m/z 165.2/147.2) optimization of the compound-dependent parameters of the mass spectrometer yielded optimized potential settings as listed in Material and methods. These settings were used for further method development.

A suitable HPLC method for MS Binding Assays is typically characterized by retention of the marker on the stationary phase with capacity factors (k) > 1 ([Snyder et al., 2010](#)). Using conventional reverse phase (RP) chromatography, polar components of the matrix resulting from the binding experiment typically elute close to the void time, which, in the case of coelution with marker, may cause severe suppression of the marker signal. Judging from preliminary experiments employing RP chromatography, however, to achieve marker retention as required (i.e. k > 1), a high ratio of the aqueous component in the mobile phase at costs of sensitivity under ESI conditions would have to be used ([Watson and Sparkman, 2007](#)). For a polar compound such as MB327 with a calculated distribution coefficient at pH 7.0 (logD) of −3.40 (calculated using Marvin Sketch v. 6.1.4), chromatography in HILIC (hydrophilic interaction chromatography) mode was expected to be a promising alternative, especially as the high fraction of organic solvent (most commonly acetonitrile) in the mobile phase, usually between 60–95% in combination with 5–40% of an aqueous component, typically provides high sensitivities under ESI conditions ([Hemström and Irgum, 2006](#); [Nguyen and Schug, 2008](#)). From several polar stationary phases tested in HILIC mode, a diol bonded stationary phase seemed to be best suited to achieve the intended goal (k > 1) for LC method development. With a YMC-Triart Diol-HILIC column (50 mm × 2.0 mm, 3 μm) as stationary phase and a composition of acetonitrile and ammonium formate buffer (20 mmol L^{−1}, pH 3.0) in a ratio of 80:20 as mobile phase at a flow rate of 800 $\mu\text{L min}^{-1}$ with sample injection in a volume of 10 μL at a temperature of 20 °C resulted in adequate retention of $[^2\text{H}_6]\text{MB327}$ (k = 3.9, see [Fig. 3a](#)) and detection of $[^2\text{H}_6]\text{MB327}$ concentrations down to high pmol L^{−1} concentrations could be achieved. Preliminary investigation of the marker in blank matrix (without addition of respective marker and internal standard, prepared according to an $[^3\text{H}]\text{epibatidine}$ binding experiment with the nAChR as target [Niessen et al., 2011](#)) demonstrated that the matrix effect (i.e. the reduction of signal intensity in matrix vs solvent due to the matrix) was tolerable under these conditions. Furthermore, a total run time of only 3 min could be realized, which was estimated to

be short enough to allow for considerable throughput of binding samples. As a next step, using the flow injection analysis (FIA) option of Analyst 1.6.1 Quantitative Optimization tool, employing the chromatographic conditions established before, the source-dependent parameters of the mass spectrometer for marker detection (m/z 159.2/144.3) were optimized. The settings found most appropriate are listed in Material and methods. Interestingly, we found that in addition to $[^2\text{H}_6]\text{MB327}$, several other nAChR ligands e.g. the agonists carbachol (m/z 148.2/88.0) and epibatidine (m/z 209.0/126.0), as well as the allosteric ligand phencyclidine (PCP, m/z 244.2/159.1), which was also characterized as noncompetitive antagonist ([Pedersen et al., 1999](#)), can be recorded easily with the developed LC method using the mass transitions given in the legend of [Fig. 3](#).

Retention of these nAChR ligands, employing the developed LC method, was characterized by capacity factors of 1.3, 0.4 and 0.9 for carbachol, phencyclidine, and epibatidine, respectively. From the signal-to-noise (S/N) ratio of respective 1 nmol L^{−1} standards, which were 80 ± 19 , 880 ± 171 and 601 ± 131 (mean \pm SD, n = 3, calculated by Analyst v. 1.6.1) for carbachol, phencyclidine and epibatidine, respectively, a rough estimate regarding the lower limits of quantification (LLOQs) can be made. Considering that for the LLOQ an S/N ratio of 5 is required, and further assuming a minor suppression of signal intensity in presence of binding sample matrix, quantification should be possible to about 100 pmol L^{−1} for carbachol and even down to about 10 pmol L^{−1} for phencyclidine and epibatidine. The fact that the established quantification method is easily applicable to several other nAChR ligands enables to gather additional information by usage of additional reporter ligands in MS Binding Assays without the need to develop a new quantification method for these compounds.

To guarantee reliability of the developed LC-ESI-MS/MS method for quantification of $[^2\text{H}_6]\text{MB327}$, it should be validated according to the FDA's guideline for bioanalytical method validation. However, validation of the quantification method is reasonable only in presence of matrix generated under the respective assay conditions. Therefore, prior to LC-ESI-MS/MS method validation, the conditions suited for conducting the desired binding experiments, and thereby defining the sample's matrix composition, had to be established.

3.2. Binding assay development

In MS Binding Assays – as well as in radioligand binding assays – the binding experiment is terminated by a step separating non-bound marker from target-bound marker. The separation technique in MS-based or radioligand binding assays that is best suited for this purpose strongly depends on the affinity of the reporter ligand towards its target in the individual assay. Filtration is the most commonly used technique as it offers a very simple working principle and provides a high throughput of samples ([Davenport and Russell, 1996](#); [de Jong et al., 2005](#); [Grimm et al., 2015](#); [Hulme and Trevethick, 2010](#); [Zepperitz et al., 2006](#)). According to literature, the minimum affinity constant compatible with filtration is a K_d of about 3.3×10^{-8} mol L^{−1} (at 0 °C working temperature, [Hulme, 1992](#)). In the case of higher K_d -values (i.e. lower affinities) filtration is not suited for this separation step, as the k_{off} -rate of the reporter ligand would be typically too high and therefore washing of the target-marker complex, entrapped on the filter, would cause a loss of bound marker to a non-tolerable extent. The

Table 1
Precursor and (most abundant) product ions of MB327, $[^2\text{H}_6]\text{MB327}$ and $[^2\text{H}_{18}]\text{MB327}$. The most intense product ions of respective precursors are highlighted in bold letters.

	MB327	$[^2\text{H}_6]\text{MB327}$	$[^2\text{H}_{18}]\text{MB327}$
Precursor ion (m/z)	156.2	159.2	165.2
Product ions (m/z , most abundant)	141.1 , 126.1, 119.0	144.3 , 129.1, 136.4	147.2 , 129.1, 122.1

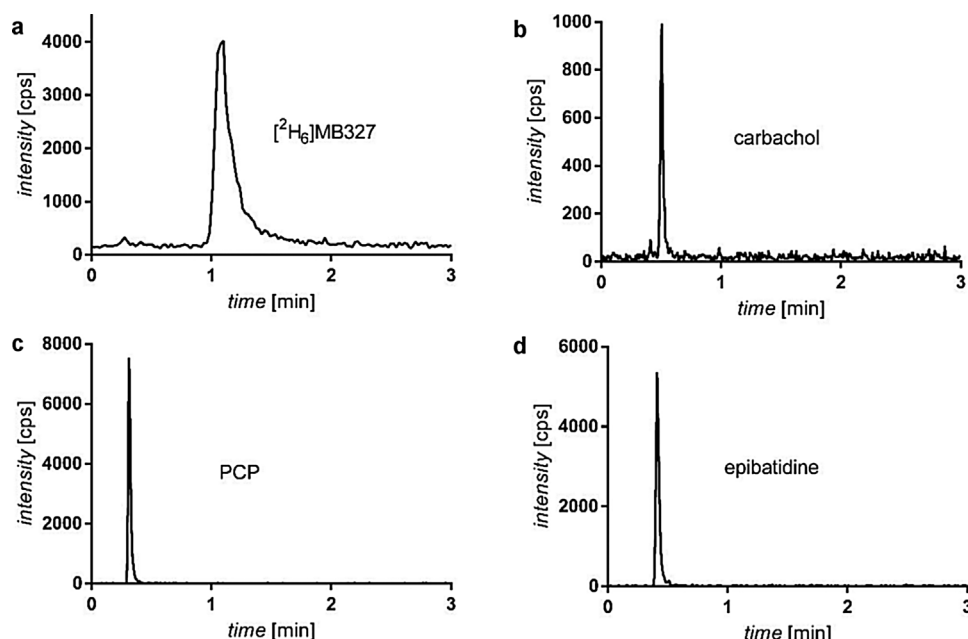


Fig. 3. MRM LC-ESI-MS/MS chromatograms of 1 nmol L⁻¹ solutions of (a) [²H₆]MB327 (*m/z* 159.2/144.3), (b) carbachol (*m/z* 148.2/88.0), (c) phencyclidine (PCP, *m/z* 244.2/159.1) and (d) epibatidine (*m/z* 209.0/126.0) using a YMC-Triart Diol-HILIC column (50 mm × 2.0 mm, 3 μm) in combination with acetonitrile and 20 mmol L⁻¹ ammonium formate buffer (pH 3.0, ratio 80:20) as mobile phase at a flow rate of 800 μL min⁻¹ at 20 °C. The injection volume was 10 μL in each case.

affinity of MB327 towards the nAChR has – as already mentioned – not been determined so far, however, data from previous functional studies suggested a *K_d*-value in the range from high nmol L⁻¹ to μmol L⁻¹ concentrations (Niessen et al., 2016; Seeger et al., 2012; Turner et al., 2011). Despite this situation, i.e. the affinity of [²H₆]MB327 appearing too low for a filtration based binding assay, we did not want to rashly exclude filtration for separation of non-bound marker from target-bound marker, as this is – as already mentioned – the by far most efficient technique for this purpose.

Therefore, we initially followed an established filtration based assay setup developed in our group (Grimm et al., 2015) for preliminary binding experiments. For preparation of nAChR-enriched membranes from *Torpedo californica* and incubation we chose the conditions previously described by Niessen et al. (2011). For determination of non-specific binding (NSB) 1 mmol L⁻¹ MB327 was added to corresponding binding samples, as it was assumed that this concentration should be sufficient to block specific marker binding to the target almost completely, provided that the *K_d*-value of the marker was ≤ 1 μmol L⁻¹. Unfortunately, as it has been feared, no significant difference between total binding (in absence of competitor) and nonspecific binding (in presence of competitor) could be detected under these conditions, presumably due to the loss of target-bound marker during the washing steps.

Since filtration was not suited for determination of the affinity of [²H₆]MB327 to the nAChR in MS Binding Assays, next, we employed centrifugation for separation of non-bound marker from target-bound marker. Following centrifugation of binding samples, the target-marker complexes are trapped in a pellet, which is only washed on the surface so that bound marker included in the pellet is protected from dissociation. To enable generation of a robust pellet, in accordance with suggestions from literature (Hulme, 1992), a sufficient amount of the *Torpedo* membrane preparation had to be used which resulted in a protein concentration of 0.5–1 mg mL⁻¹ in the assay. For the centrifugation based MS Binding Assays, finally, aliquots of the *Torpedo* membrane preparation were incubated with marker in incubation buffer in reagent tubes for 2 h at 25 °C and subsequently sample tubes were centrifuged for 5 min at 4 °C and 49088g. Afterwards, the supernatant was removed using a Pasteur pipette coupled to vacuum and the remaining pellet washed twice very carefully by addition and subsequent aspiration of 150 μL ice-cold incubation buffer. Next, the bound marker was liberated by addition of 500 μL acetonitrile containing

167 nmol L⁻¹ [²H₁₈]MB327 as internal standard. Subsequently, the sample tubes were placed in an ultrasonic bath for 1 h, vortexed intensely and afterwards centrifuged as before. Finally, the resulting supernatants were transferred – sample by sample – into a 96-well plate, diluted 1:10 in acetonitrile (36 μL sample + 324 μL acetonitrile) in one 96-well plate first and subsequently 1:10 in acetonitrile and 20 mmol L⁻¹ ammonium formate buffer, pH 3.0 in a ratio of 90:10 (36 μL sample + 288 μL acetonitrile + 36 μL buffer) in another 96-well plate before analysis by LC-ESI-MS/MS. A basic scheme for the workflow of the centrifugation based MS Binding Assays is illustrated in Fig. 1.

As for the filtration based binding experiments before, we observed only a negligible loss of intensities for quantification of [²H₆]MB327 by LC-ESI-MS/MS in presence of the matrix (as compared to corresponding solvent standards) resulting from binding samples under these conditions. For nominal marker concentrations of binding samples in the low μmol L⁻¹ range, employing the centrifugation based MS Binding Assays, there was a significant difference between total and nonspecific binding (determined in presence of 1 mmol L⁻¹ MB327), clearly indicating that it was possible to measure specific binding of [²H₆]MB327 towards nAChR. Unfortunately, saturation of specific binding was not seen up to a marker concentration of 20 μmol L⁻¹. In the case of *K_d* > 1 μmol L⁻¹, as was suggested by these results, the concentration of competitor used for NSB determination in these preliminary binding experiments would have been too low for accurate determination of nonspecific binding. To solve this problem, it was clear that the concentration of MB327 would have to be increased distinctly, even though it was not possible to reliably estimate the required concentration to block the targeted binding site exactly since the affinity of MB327 for its binding site was not known. In any case, such high concentrations (> 1 mmol L⁻¹) of MB327 could, however, be assumed to cause solubility problems. Not to mention that, by using mmol L⁻¹ concentrations of native MB327 as competitor for NSB determination, vast amounts of this compound would be consumed. Therefore, we searched for an alternative method for determination of nonspecific binding. Interestingly, it had already been shown (Farach and Martinez-Carrion, 1983) that α-neurotoxin binding to the nAChR was inhibited as a result from exposing aliquots of a nAChR-rich membrane preparation from *Torpedo californica* to a temperature of 60 °C. The authors claimed denaturation of the orthosteric binding sites to be responsible for the loss of respective binding. Based on the

observation that a heat-treatment for 6 min at 60 °C sufficed for heat inactivation of 50% of α -bungarotoxin binding (Saitoh et al., 1979), in our assay, as an attempt to inactivate specific binding sites entirely, we chose to treat the *Torpedo*-nAChR for 1 h at 60 °C. As typically observed for nonspecific binding (Hulme and Trevethick, 2010), its determination based on heat treatment of aliquots of the receptor material and subsequent analysis of the resulting data by linear regression, showed that with increasing marker concentrations (2–100 $\mu\text{mol L}^{-1}$) the increase in NSB was nearly linear. Interestingly, it was found that NSB determination at higher concentrations ($> 20 \mu\text{mol L}^{-1}$) was not as precise as at lower marker concentrations. Therefore, in addition to basing the linear regression on all data points experimentally determined in a concentration range of 2–100 $\mu\text{mol L}^{-1}$, we performed linear regression alternatively only with data points in the range of 2–20 $\mu\text{mol L}^{-1}$ determining NSB at marker concentrations $> 20 \mu\text{mol L}^{-1}$ by extrapolation. Comparing the resulting equations from both calculation models, for six independent NSB determinations, we observed that linear regression based on data points in the range of 2–20 $\mu\text{mol L}^{-1}$ with extrapolation to higher nominal marker concentrations resulted in a more precise NSB determination as compared to linear regression based on all data points in the range of 2–100 $\mu\text{mol L}^{-1}$ (see Supplementary information). As a result from these findings, for all further [$^2\text{H}_6$]MB327 binding experiments, NSB was determined by means of linear regression based on four marker nominal concentration levels in the range of 2–20 $\mu\text{mol L}^{-1}$.

At this stage of our project, basically, it seemed to be possible to achieve characterization of the binding site of MB327 at the *Torpedo*-nAChR with the approach of centrifugation based MS Binding Assays. With the conditions for the binding experiments established so far, also the composition of the matrix of the samples containing the bound marker to be analyzed was defined. Therefore, we validated the developed LC-ESI-MS/MS method for quantification of [$^2\text{H}_6$]MB327 in the matrix resulting from the binding experiments in order to ensure its reliability.

3.3. LC-ESI-MS/MS method validation

For validation of the developed LC-ESI-MS/MS quantification method the FDA's guidance for bioanalytical method validation (FDA, 2001) regarding selectivity, lower limit of quantification (LLOQ), linearity, precision, and accuracy was followed. In summary, validation of the LC-ESI-MS/MS method for quantification of [$^2\text{H}_6$]MB327 in the matrix resulting from the MS Binding Assay showed that the requirements of the CDER guideline of the FDA regarding the above-mentioned parameters are fulfilled (for further detail see Supplementary information).

3.4. Further binding assay development

3.4.1. Characterization of the *Torpedo* membrane preparation by carbachol and PCP binding

Despite the above-mentioned improvements for determination of nonspecific binding, saturation experiments using marker nominal concentrations of 2–100 $\mu\text{mol L}^{-1}$ did still not show saturation of specific binding. As an error-prone marker quantification preventing correct determination of specific binding could be ruled out at this point, we considered the possibility that the batch of *Torpedo* electroplaque organ used for preparation of nAChR-rich membranes might actually not contain enough or not enough intact nAChR for a reliable calculation of saturation isotherms considering the degree of scatter in total as well as nonspecific binding in comparison to the amount of specific [$^2\text{H}_6$]MB327 binding determined. To test this hypothesis, saturation experiments using the agonist carbachol as reporter ligand in MS Binding Assays, applying the same conditions as those previously applied for binding of [$^2\text{H}_6$]MB327, were performed (see Material and methods). These binding experiments should help to clarify, whether

the batch of *Torpedo*-nAChR preparations used for the binding assays contains intact receptor in a sufficient quantity and furthermore also provide an estimate of the density of orthosteric binding sites (and thus the density of nAChRs) in the membrane preparation. The resulting saturation isotherms yielded a K_d of $171 \pm 18 \text{ nmol L}^{-1}$ and a B_{max} value of $611 \pm 30 \text{ pmol mg}^{-1}$ protein ($n = 3$, for further detail see Supplementary information). This K_d is in good agreement with published K_d -values of about 100 nmol L^{-1} for [^3H]carbachol at the nAChR (Boyd and Cohen, 1980; Dunn et al., 1980). The B_{max} determined amounting to $611 \pm 30 \text{ pmol mg}^{-1}$ protein, which should not be affected by the observed marker depletion, gives a valuable estimate of receptor density of the membrane preparation obtained from the *Torpedo* electroplaque organ which should be about 300 pmol mg^{-1} protein, considering that two orthosteric binding sites are present in each receptor. With the binding affinity of the agonist carbachol to nAChR being close to that published from radioligand binding studies, it can be assumed that the *Torpedo* membrane preparation contains intact nAChR in a sufficient amount, for this MS Binding Assays which should hold also true for related MS Binding Assays, as e.g. binding assays addressing the MB327 binding site. Furthermore, these results confirm that the chosen setup for the MS Binding Assays is basically well suited for affinity determination and that the way to determine nonspecific binding (heat denaturation of binding sites) leads to reliable results. As the developed LC method also enables quantification of the allosteric ligand phencyclidine (PCP), we decided to additionally study PCP binding towards nAChRs for our target preparation, as PCP binding in presence of varying concentrations of carbachol has been shown to be sensitive to shifts between different conformational states. In other words, the affinity of PCP is significantly different for different conformational states of the nAChR with the highest affinity towards the receptor in the desensitized state (Eldefrawi et al., 1980; Hamouda et al., 2015). Therefore, MS Binding Assays with PCP as marker, applying the same setup and conditions as those previously applied for binding of [$^2\text{H}_6$]MB327 and carbachol were performed (for experimental detail and a corresponding binding curve see Supplementary information). The results of these binding experiments of PCP towards the nAChR in our membrane preparation clearly showed that PCP binding increases with carbachol concentration in the binding samples indicating a shift to the desensitized state as it has been demonstrated for [^3H]PCP in corresponding radioligand binding experiments (Pedersen et al., 1999). As the nAChR in our membrane preparation appears to be able to change conformational states, the failure to reach saturation of specific [$^2\text{H}_6$]MB327 binding in the concentration range previously examined should not be due to a locked nAChR conformation that does not favor MB327 binding.

3.4.2. [$^2\text{H}_6$]MB327 binding towards the *Torpedo* nAChR

The results of the MS Binding Assays with carbachol and PCP as markers led to the conclusion that the nAChR preparation itself and the established setup for the MS Binding Assays are not the cause for not reaching saturation of specific binding at [$^2\text{H}_6$]MB327 concentrations up to $100 \mu\text{mol L}^{-1}$. Hence, we attempted to identify other factors possibly influencing [$^2\text{H}_6$]MB327 binding towards the nAChR. First, several other incubation buffer compositions e.g. the *torpedo* physiological saline (Hamouda et al., 2015) or a Tris-based binding saline buffer (Arias et al., 2016) and different assay temperatures were tested with regard to their effects on [$^2\text{H}_6$]MB327 binding to the nAChR, but as before, no saturation of specific [$^2\text{H}_6$]MB327 binding at nAChR could be reached.

In addition, the rather high concentration of sucrose present in the binding experiment was considered to possibly affect [$^2\text{H}_6$]MB327 binding towards the nAChR. Though the incubation buffer is devoid of sucrose, the latter is contained in storage buffer I (120 mmol L^{-1} NaCl, 5 mmol L^{-1} KCl, 300 mmol L^{-1} sucrose, 0.5 mmol L^{-1} EDTA, 8.05 mmol L^{-1} Na_2HPO_4 and 1.95 mmol L^{-1} NaH_2PO_4 , pH 7.4) as a cryoprotector (Strauss and Hauser, 1986) and thereby introduced via

the membrane preparation, that is added to establish the final binding samples. Following the procedure published by Niessen et al. (2011) aliquots of the *Torpedo* membrane preparation, stored in storage buffer I, were after thawing directly combined with the other constituents of the final binding samples. In that regard, it has to be mentioned that the centrifugation approach chosen for the [$^2\text{H}_6$]MB327 MS Binding Assays required substantially higher amounts of membrane preparation for the binding sample to enable generation of a robust pellet during centrifugation as compared to binding samples in filtration based radioligand binding assays performed by Niessen et al. (2011), which contained sucrose only in negligible amounts. In our case, addition of aliquots of the *Torpedo* membrane preparation in storage buffer I gave rise to binding samples containing 30 mmol L^{-1} sucrose and $50 \mu\text{mol L}^{-1}$ EDTA, though these components were absent in the incubation buffer. To examine if these components might negatively affect [$^2\text{H}_6$]MB327 binding to the nAChR, the nAChR preparations were washed with incubation buffer prior to their use in the binding experiment. For the washing procedure, the aliquots of the membrane preparation were diluted in incubation buffer, centrifuged, subsequently resuspended in fresh incubation buffer, and stored for 30 min at 4°C . This procedure was repeated five times over a period of 4 h (for experimental detail see Material and methods). Afterwards, the washed aliquots of the membrane preparation were employed in saturation experiments under conditions identical to those before. In contrast to former experiments, now, in absence of sucrose and EDTA specific binding of [$^2\text{H}_6$]MB327 towards nAChR was saturable in the investigated concentration range (up to $120 \mu\text{mol L}^{-1}$) of marker as clearly visible in Fig. 4.

Repeated saturation binding experiments employing washed aliquots of the membrane preparation yielded a K_d of $12.8 \pm 1.0 \mu\text{mol L}^{-1}$ and a B_{max} of $242 \pm 16 \text{ pmol mg}^{-1}$ protein ($n = 3$). Finally, due to the results obtained with these saturation experiments, the assay conditions developed so far, conducting the [$^2\text{H}_6$]MB327 binding experiment in absence of sucrose and EDTA, were considered to be now suitable to characterize MB327 binding towards the nAChR in MS Binding Assays.

After the final conditions for characterization of the MB327 binding site at the nAChR had been fixed, additional [$^2\text{H}_6$]MB327 saturation experiments for determination of its binding affinity towards the nAChR employing the nAChR membrane preparation stored in a modified storage buffer (storage buffer II) were performed. As a logical

consequence from the positive results obtained using washed aliquots of the *Torpedo*-membrane preparation, now, both sucrose and EDTA were omitted from the storage buffer for nAChR membrane preparations, i.e. nAChR membranes were resuspended in a buffer containing 120 mmol L^{-1} NaCl, 5 mmol L^{-1} KCl, 8.05 mmol L^{-1} Na_2HPO_4 and 1.95 mmol L^{-1} NaH_2PO_4 , pH 7.4 (storage buffer II) for storage after preparation. When the nAChR-enriched membrane preparation, stored in the modified storage buffer II, devoid of sucrose and EDTA, was employed in [$^2\text{H}_6$]MB327 saturation experiments as described above (for a representative saturation isotherm see Fig. 5a), a K_d of $15.5 \pm 0.9 \mu\text{mol L}^{-1}$ and a B_{max} of $348 \pm 18 \text{ pmol mg}^{-1}$ protein ($n = 3$) were obtained. Both results are in good agreement with those determined in saturation experiments for which aliquots of the *Torpedo* membrane preparation, washed with incubation buffer, had been used (see above). Regarding quantification of [$^2\text{H}_6$]MB327 in these binding experiments, it had to be considered that the matrix of the binding samples was slightly modified in comparison to the matrix used for validation (i.e. lacking small amounts of sucrose and EDTA being formerly present). Therefore, the validity of the global calibration function determined during validation was examined by investigation of QC samples (for further detail see Material and methods). It is worth mentioning that accuracy and precision were in all cases excellently within the validation criteria (recovery 85–115% and $\text{RSD} \leq 15\%$, respectively), clearly demonstrating reliability of LC-ESI-MS/MS quantification also under these conditions.

Finally, it should be confirmed that the failure in observing saturation of specific binding of [$^2\text{H}_6$]MB327 towards the nAChR, when using *Torpedo* membrane preparation in the original storage buffer (storage buffer I), was indeed due to the presence of sucrose or possibly EDTA. Due to the low concentration of EDTA in the final binding sample, it was more likely that sucrose was responsible for the observed phenomenon. Thus we conducted additional saturation experiments with membrane preparations stored in storage buffer II. In this case sucrose was added to result in a final concentration of 30 mmol L^{-1} in the binding experiment as it had been the case in the binding experiment using the nAChR receptor preparation stored in the original storage buffer (storage buffer I), containing sucrose and EDTA and the mixture allowed to preincubate for a period of 1 h at 4°C . In subsequent saturation experiments with [$^2\text{H}_6$]MB327 performed under standard conditions, no saturation of specific binding up to concentrations of $160 \mu\text{mol L}^{-1}$ [$^2\text{H}_6$]MB327 could be observed which clearly

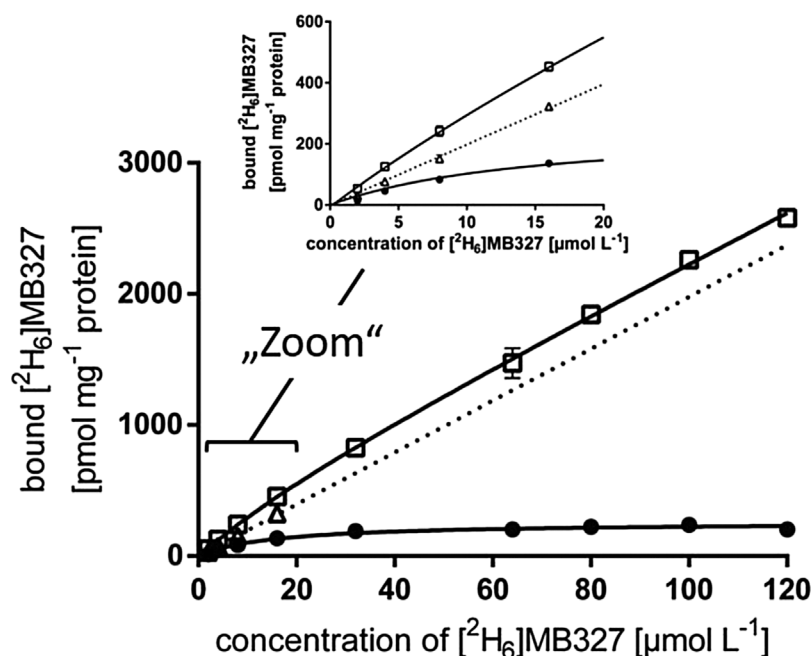


Fig 4. Representative saturation experiment for [$^2\text{H}_6$]MB327 binding towards *Torpedo*-nAChR with total binding (squares) at nominal concentrations from 2 to $120 \mu\text{mol L}^{-1}$ and nonspecific binding (triangles, dashed line) at $2\text{--}16 \mu\text{mol L}^{-1}$ (with extrapolation to higher marker concentrations), shown as means \pm SD ($n = 3$). Specific binding (circles, means) was determined as difference between total and nonspecific binding and yielded a K_d -value of $15.3 \mu\text{mol L}^{-1}$ and a B_{max} of 258 pmol mg^{-1} , in this experiment.

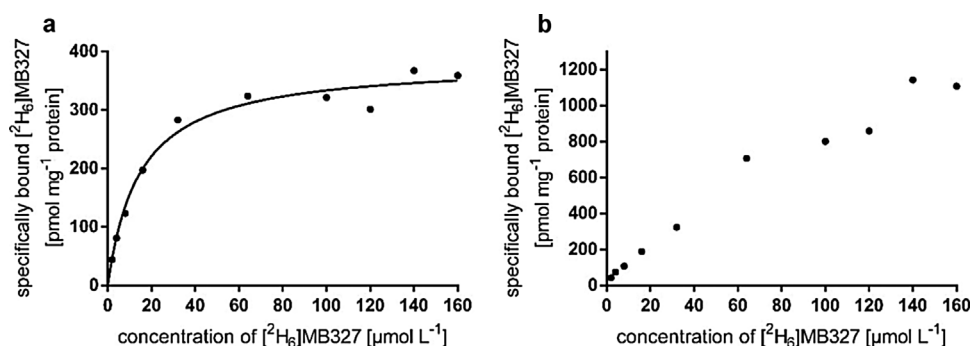


Fig. 5. Representative saturation experiments showing specific [²H₆]MB327 binding (means) towards *Torpedo*-nAChR at marker concentrations from 2 to 160 μmol L⁻¹ without sucrose (a) or in presence of 30 mmol L⁻¹ sucrose (b). For the saturation isotherm shown in (a) a K_d -value of 14.7 μmol L⁻¹ and a B_{max} -value of 382 pmol mg⁻¹ protein was determined.

demonstrates that the presence of sucrose in the given concentration is indeed fatal for [²H₆]MB327 binding (for a representative example see Fig. 5b).

The affinity determined in the developed [²H₆]MB327 saturation experiments ($K_d = 15.5 \pm 0.9 \mu\text{mol L}^{-1}$) seems to be plausible as this concentration is within the range of MB327 concentrations reported to be required for recovery of nAChR function in muscle force experiments (100–200 μmol L⁻¹; Seeger et al., 2012) and for prevention of agonist-induced desensitization in electrophysiological experiments (1 μmol L⁻¹; Niessen et al., 2016), respectively. The comparison of the B_{max} , determined in the above described [²H₆]MB327 binding experiments (348 ± 18 pmol mg⁻¹ protein), with the one determined in carbachol saturation experiments of 611 ± 30 pmol mg⁻¹ protein, shows a ratio of 1:1.8, suggesting a stoichiometry of 1:2 of MB327 binding sites vs carbachol binding sites at the *Torpedo* nAChR. Assuming that the MS Binding Assays performed with carbachol address two (orthosteric) binding sites (Middleton and Cohen, 1991), this indicates that [²H₆]MB327 might bind to a single binding site at the nAChR under the chosen conditions. In this context, it is worth to mention that a concurrent molecular modeling study revealed two potential binding sites for MB327 at the *Torpedo*-nAChR (Wein et al., 2017).

As the ultimate aim with development of MS Binding Assays targeting the MB327 binding site at nAChRs was to determine the affinity of known and newly synthesized test compounds in competitive binding experiments, we tried to exemplify this possibility by assessing the affinity of native MB327 in autocompetition experiments. Besides, this type of experiment should provide an additional affinity measure for MB327 binding towards the nAChR. The autocompetition assays followed the procedure of saturation binding assays, as described above, except that the target was incubated with the marker [²H₆]MB327 at a nominal concentration of 10 μmol L⁻¹ and in addition with MB327 as competitor at concentrations ranging from 100 nmol L⁻¹ to 1 mmol L⁻¹. Nonspecific binding was again determined with aliquots of the *Torpedo* membrane preparation treated for 1 h at 60 °C prior to incubation and for the quantification of bound marker in binding samples, the validated LC-ESI-MS/MS method was used. The data resulting from these competitive binding experiments were used for the construction of competition curves (see Fig. 6) and the calculation of pIC₅₀ values.

The pIC₅₀ determined for MB327 from three competition experiments amounted to 4.39 ± 0.07 (n = 3). With the previously determined K_d for [²H₆]MB327 towards the nAChR ($15.5 \pm 0.9 \mu\text{mol L}^{-1}$) a K_i of $18.3 \pm 2.6 \mu\text{mol L}^{-1}$ (n = 3) could be calculated according to Cheng and Prusoff (Cheng and Prusoff, 1973), demonstrating that the affinities for [²H₆]MB327 obtained from the saturation experiments and those for MB327 from the autocompetition experiments are in excellent agreement. Furthermore, the autocompetition experiments again nicely demonstrate the reliability of heat denaturation for NSB determination as an alternative to the way commonly practiced, i.e. to add another ligand in high excess omitting binding of the reporter ligand to its binding site. In Fig. 6, the

accordance of NSB determination by both approaches is clearly visible, as the amount of bound marker remaining in presence of a 100-fold excess of competitor vs marker (i.e. 1 mmol L⁻¹ MB327 vs 10 μmol L⁻¹ [²H₆]MB327) almost exactly matches the level of nonspecific binding determined by heat denaturation in control experiments.

4. Conclusion

In summary, in the present study, the affinities of [²H₆]MB327 and MB327 towards the MB327 binding site of the nAChR were characterized for the first time. Initially, a sensitive LC-ESI-MS/MS method for detection of [²H₆]MB327 as reporter ligand was developed using [²H₁₈]MB327 as internal standard. Its reliability was demonstrated by validation according to the CDER guidance of the FDA for bioanalytical method validation with respect to selectivity, linearity, lower limit of quantification, accuracy, and precision. In addition to robust quantification of [²H₆]MB327, using the developed HPLC method, quantification of carbachol and PCP was reliably possible, which allowed to employ them as reporter ligands in respective MS Binding Assays as well. Based on the established LC-ESI-MS/MS method MS Binding Assays were developed employing centrifugation for separation of non-bound [²H₆]MB327 from target-bound [²H₆]MB327. For determination of nonspecific binding in MS Binding Assays, it could be shown that heat denaturation represents a suitable method yielding reliable results. Employing the developed centrifugation based MS Binding Assays in saturation experiments for affinity characterization of [²H₆]MB327 binding towards the *Torpedo*-nAChR resulted in a K_d of $15.5 \pm 0.9 \mu\text{mol L}^{-1}$. Autocompetition experiments performed with native MB327 as competitor yielded a K_i of $18.3 \pm 2.6 \mu\text{mol L}^{-1}$ for MB327. The excellent agreement of both affinity measurements determined in MS Binding Assays, as well as the agreement of these

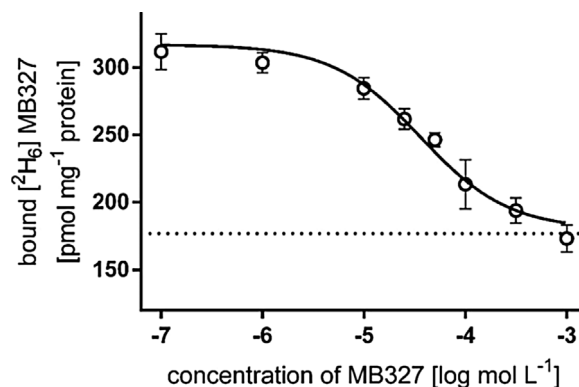


Fig. 6. Representative competition experiment for [²H₆]MB327 binding towards *Torpedo*-nAChR employing native MB327 as competitor in a concentration range of 100 nmol L⁻¹–1 mmol L⁻¹. Total binding of 10 μmol L⁻¹ [²H₆]MB327 is shown as means ± SD. Nonspecific binding, determined in control experiments by heat-denaturation, is shown as dashed line (mean). For this example, a pK_i-value of 4.65 was determined.

affinities with the potencies found in functional assays, indicates that the established MS Binding Assays yield reliable results. Moreover, it demonstrates that they represent a suitable test system for affinity characterization of test compounds towards the binding site of MB327 at the nAChR. Even though the throughput of the developed centrifugation based MS Binding Assays is limited, they provide the first tool for investigation of structure-activity relationships and, hopefully, for identification of new ligands with distinctly higher affinity for the binding site of MB327 at the nAChR as compared to compounds known so far. Such high affinity ligands, when suited as marker, can be expected to allow the setup of filtration based MS Binding Assays that will enable a substantial higher throughput and therefore also extensive screening campaigns in the search for new compounds capable to “resensitize” desensitized nAChR after OPC poisoning with higher potency.

Conflicts of interest

There are no conflicts of interest.

Acknowledgement

The study was funded by the German Ministry of Defense (E/U2AD/CF514/DF561).

Appendix A. Supplementary data

Supplementary data associated with this article can be found, in the online version, at <https://doi.org/10.1016/j.toxlet.2017.11.013>.

References

- Albuquerque, E.X., Pereira, E.F., Alkondon, M., Rogers, S.W., 2009. Mammalian nicotinic acetylcholine receptors: from structure to function. *Physiol. Rev.* 89 (1), 73–120.
- Arias, H.R., Feuerbach, D., Ortells, M.O., 2016. Bupropion and its photoreactive analog (+/-)-SADU-3-72 interact with luminal and non-luminal sites at human $\alpha 4 \beta 2$ nicotinic acetylcholine receptors. *Neurochem. Int.* 100, 67–77.
- Arias, H.R., 2010. Positive and negative modulation of nicotinic receptors. *Adv. Protein Chem. Struct. Biol.* 80, 153–203.
- Arias, H.R., 2011. Allosteric modulation of nicotinic acetylcholine receptors. In: Arias, H.R. (Ed.), *Pharmacology of Nicotinic Acetylcholine Receptors from the Basic and Therapeutic Perspectives*. Research Signpost, Kerala, pp. 151–173.
- Boyd, N.D., Cohen, J.B., 1980. Kinetics of binding of [3H]acetylcholine and [3H]carbamoylcholine to torpedo postsynaptic membranes: slow conformational transitions of the cholinergic receptor. *Biochemistry* 19 (23), 5344–5353.
- Changeux, J.P., Edelstein, S.J., 2005. Allosteric mechanisms of signal transduction. *Science* 308 (5727), 1424–1428.
- Changeux, J.P., 2012. The nicotinic acetylcholine receptor: the founding father of the pentameric ligand-gated ion channel superfamily. *J. Biol. Chem.* 287 (48), 40207–40215.
- Chatzidakis, A., Millar, N.S., 2015. Allosteric modulation of nicotinic acetylcholine receptors. *Biochem. Pharmacol.* 97 (4), 408–417.
- Cheng, Y., Prusoff, W.H., 1973. Relationship between the inhibition constant (K_i) and the concentration of inhibitor which causes 50 percent inhibition (IC_{50}) of an enzymatic reaction. *Biochem. Pharmacol.* 22, 3099–3108.
- Davenport, A.P., Russell, F.D., 1996. Radioligand binding assays: theory and practice. In: Mather, S.J. (Ed.), *Current Directions in Radiopharmaceutical Research and Development*. Kluwer Academic Publishers, Amsterdam, pp. 169–179.
- Dolgin, E., 2013. Syrian gas attack reinforces need for better anti-sarin drugs. *Nat. Med.* 19 (10), 1194–1195.
- Dunn, S.M.J., Blanchard, S.G., Raftery, M.A., 1980. Kinetics of carbamylcholine binding to membrane-bound acetylcholine receptor monitored by fluorescence changes of a covalently bound probe. *Biochemistry* 19 (23), 5645–5652.
- Eldefrawi, M.E., Eldefrawi, A.T., Aronstam, R.S., Maleque, M.A., Warnick, J.E., Albuquerque, E.X., 1980. [3H]phencyclidine: a probe for the ionic channel of the nicotinic receptor. *Proc. Natl. Acad. Sci. U. S. A.* 77 (12), 7458–7462.
- United States Food and Drug Administration (FDA), 2001. Guidance for Industry: Bioanalytical Method Validation. <https://www.fda.gov/downloads/Drugs/Guidance/ucm070107.pdf> (Accessed 10.08.2017).
- Farach, M.C., Martinez-Carrion, M., 1983. A differential scanning calorimetry study of acetylcholine receptor-rich membranes from *Torpedo californica*. *J. Biol. Chem.* 258 (7), 4166–4170.
- Grimm, S.H., Höfner, G., Wanner, K.T., 2015. Development and validation of an LC-ESI-MS/MS method for the triple reuptake inhibitor indatraline enabling its quantification in MS Binding Assays. *Anal. Bioanal. Chem.* 407, 471–485.
- Höfner, G., Wanner, K.T., 2015. MS Binding Assays. In: Kool, J., Niessen, W.M.A. (Eds.), *Analyzing Biomolecular Interactions by Mass Spectrometry*. Wiley-VCH, Weinheim, pp. 165–198.
- Hamouda, A.K., Wang, Z., Stewart, D.S., Jain, A.D., Glennon, R.A., Cohen, J.B., 2015. Desformylflustrabromine (dFBr) and [3H]dFBr-labeled binding sites in a nicotinic acetylcholine receptor. *Mol. Pharmacol.* 88, 1–11.
- Hemström, P., Irgum, K., 2006. Hydrophilic interaction chromatography. *J. Sep. Sci.* 29, 1784–1821.
- Hess, M., Höfner, G., Wanner, K.T., 2011. (S)- and (R)-fluoxetine as native markers in MS Binding Assays addressing the serotonin transporter. *ChemMedChem* 6, 1900–1908.
- Hulme, E.C., Trevethick, M.A., 2010. Ligand binding assays at equilibrium: validation and interpretation. *Br. J. Pharmacol.* 161, 1219–1237.
- Hulme, E.C., 1992. *Receptor Ligand Interactions – A Practical Approach*. IRL Press at Oxford University Press, Oxford.
- Hurst, R., Rollema, H., Bertrand, D., 2013. Nicotinic acetylcholine receptors: from basic science to therapeutics. *Pharmacol. Ther.* 137 (1), 22–54.
- Kalamida, D., Poulas, K., Avramopoulou, V., Fostieri, E., Lagoumintzis, G., Lazaridis, K., Sideri, A., Zouridakis, M., Tzartos, S.J., 2007. Muscle and neuronal nicotinic acetylcholine receptors. Structure, function and pathogenicity. *FEBS J.* 274 (15), 3799–3845.
- Karlin, A., 2002. Emerging structure of the nicotinic acetylcholine receptors. *Nat. Rev. Neurosci.* 3, 102–114.
- Klopman, G., Li, J., Wang, S., Dimayuga, M., 1994. Computer automated log P calculations based on an extended group contribution approach. *J. Chem. Inf. Comput. Sci.* 34 (4), 752–781.
- Marrs, T.C., 1993. Organophosphate poisoning. *Pharmacol. Ther.* 58 (1), 51–66.
- Middleton, R.E., Cohen, J.B., 1991. Mapping of the acetylcholine binding site of the nicotinic acetylcholine receptor: [3H]nicotine as an agonist photoaffinity label. *Biochemistry* 30, 6987–6997.
- Millar, N.S., 2003. Assembly and subunit diversity of nicotinic acetylcholine receptors. *Biochem. Soc. Trans.* 31 (4), 869–874.
- Navedo, M., Nieves, M., Rojas, L., Lasalde-Dominicci, J.A., 2004. Tryptophan substitutions reveal the role of nicotinic acetylcholine receptor R-TM3 domain in channel gating: differences between *Torpedo* and muscle-type AChR. *Biochemistry* 43, 78–84.
- Neiens, P., Höfner, G., Wanner, K.T., 2015. MS Binding Assays for D1 and D5 dopamine receptors. *ChemMedChem* 10, 1924–1931.
- Newmark, J., 2007. Nerve agents. *Neurologist* 13 (1), 20–32.
- Nguyen, H.P., Schug, K.A., 2008. The advantages of ESI-MS detection in conjunction with HILIC mode separations: fundamentals and applications. *J. Sep. Sci.* 31, 1465–1480.
- Niessen, K.V., Tattersall, J.E., Timperley, C.M., Bird, M., Green, C., Seeger, T., Thiermann, H., Worek, F., 2011. Interaction of bispyridinium compounds with the orthosteric binding site of human $\alpha 4 \beta 2$ and *Torpedo californica* nicotinic acetylcholine receptors (nAChRs). *Toxicol. Lett.* 206, 100–104.
- Niessen, K.V., Seeger, T., Tattersall, J.E., Timperley, C.M., Bird, M., Green, C., Thiermann, H., Worek, F., 2013. Affinities of bispyridinium non-oxime compounds to [3H]epibatidine binding sites of *Torpedo californica* nicotinic acetylcholine receptors depend on linker length. *Chem. Biol. Interact.* 206 (3), 545–554.
- Niessen, K.V., Muschik, S., Langguth, F., Rappenglück, S., Seeger, T., Thiermann, H., Worek, F., 2016. Functional analysis of *Torpedo californica* nicotinic acetylcholine receptors in multiple activation states by SSM-based electrophysiology. *Toxicol. Lett.* 247, 1–10.
- Niessen, K.V., Seeger, T., Rappenglück, S., Wein, T., Höfner, G., Wanner, K.T., Thiermann, H., Worek, F., 2017. In vitro pharmacological characterization of the bispyridinium non-oxime compound MB327 and its 2- and 3-regioisomers. *Toxicol. Lett.* same issue.
- Papke, R.L., 2014. Merging old and new perspectives on nicotinic acetylcholine receptors. *Biochem. Pharmacol.* 89 (1), 1–11.
- Pedersen, S.E., Lurtz, M.M., Papineni, R.V.L., 1999. Ligand binding methods for analysis of ion channel structure and function. In: Conn, P.M. (Ed.), *Methods in Enzymology*. Academic Press, pp. 117–135.
- Saitoh, T., Wennogle, L.P., Changeux, J.P., 1979. Factors regulating the susceptibility of the acetylcholine receptor protein to heat inactivation. *FEBS Lett.* 108 (2), 489–494.
- Seeger, T., Eichhorn, M., Lindner, M., Niessen, K.V., Tattersall, J.E., Timperley, C.M., Bird, M., Green, A.C., Thiermann, H., Worek, F., 2012. Restoration of soman-blocked neuromuscular transmission in human and rat muscle by the bispyridinium non-oxime MB327 in vitro. *Toxicology* 294 (2–3), 80–84.
- Smith, P.K., Krohn, R.I., Hermanson, G.T., Mallia, A.K., Gartner, F.H., Provenzano, M.D., Fujimoto, E.K., Goeke, N.M., Olson, B.J., Klenk, D.C., 1985. Measurement of protein using bicinchoninic acid. *Anal. Biochem.* 150 (1), 76–85.
- Snyder, L.R., Kirkland, J.J., Dolan, J.W., 2010. *Introduction to Modern Liquid Chromatography*, third ed. J. Wiley & Sons, New Jersey.
- Strauss, G., Hauser, H., 1986. Stabilization of lipid bilayer vesicles by sucrose during freezing. *Proc. Natl. Acad. Sci. U. S. A.* 83, 2422–2426.
- Tattersall, J.E.H., 1993. Ion channel blockade by oximes and recovery of diaphragm muscle from soman poisoning in vitro. *Br. J. Pharmacol.* 108 (4), 1006–1015.
- Thiermann, H., Seeger, T., Gonder, S., Herkert, N., Antkowiak, B., Zilker, T., Eyer, F., Worek, F., 2010. Assessment of neuromuscular dysfunction during poisoning by organophosphorous compounds. *Chem. Biol. Interact.* 187 (1–3), 265–269.
- Turner, S.R., Chad, J.E., Price, M., Timperley, C.M., Bird, M., Green, A.C., Tattersall, J.E.H., 2011. Protection against nerve agent poisoning by a noncompetitive nicotinic antagonist. *Toxicol. Lett.* 206, 105–111.
- Unger, K.K., Weber, E., 1995. *Handbuch der HPLC, Teil 1, Leitfaden für Anfänger und Praktiker*. GIT Verlag, Darmstadt.
- Unwin, N., 2005. Refined structure of the nicotinic acetylcholine receptor at 4 Å resolution. *J. Mol. Biol.* 346, 967–989.
- Unwin, N., 2013. Nicotinic acetylcholine receptor and the structural basis of neuromuscular transmission: insights from *Torpedo* postsynaptic membranes. *Q. Rev. Biophys.* 46 (4), 283–322.
- Viswanadhan, V.N., Ghose, A.K., Revankar, G.R., Robins, R.K., 1989. Atomic

- physicochemical parameters for three dimensional structure directed quantitative structure-activity relationships. 4. Additional parameters for hydrophobic and dispersive interactions and their application for an automated superposition of certain naturally occurring nucleoside antibiotics. *J. Chem. Inf. Comput. Sci.* 29 (3), 163–172.
- Watson, J.T., Sparkman, O.D., 2007. *Introduction to Mass Spectrometry-instrumentation, Applications and Strategies for Data Interpretation*, fourth ed. Wiley, New York.
- Wein, T., Höfner, G., Rappenglück, S., Sichler, S., Niessen, K.V., Seeger, T., Worek, F., Thiermann, H., Wanner, K.T., 2017. Searching for putative binding sites of the bis-pyridinium compound MB327 in the nicotinic acetylcholine receptor. *Toxicol. Lett.* (same issue).
- Worek, F., Szinicz, L., Eyer, P., Thiermann, H., 2005. Evaluation of oxime efficacy in nerve agent poisoning: development of a kinetic-based dynamic model. *Toxicol. Appl. Pharmacol.* 209 (3), 193–202.
- Worek, F., Thiermann, H., Wille, T., 2016. Oximes in organophosphate poisoning: 60 years of hope and despair. *Chem. Biol. Interact.* 259, 93–98.
- Zepperitz, C., Höfner, G., Wanner, K.T., 2006. MS Binding Assays: Kinetic, saturation, and competitive experiments based on quantification of bound marker as exemplified by the GABA Transporter mGAT1. *ChemMedChem* 1, 208–217.
- de Jong, L.A.A., Uges, D.R.A., Franke, J.P., Bischoff, R., 2005. Receptor ligand binding assays: technologies and applications. *J. Chromatogr. B: Anal. Technol. Biomed. Life Sci.* 829, 1–25.

Supplementary Information

Development of MS Binding Assays targeting the binding site of MB327 at the nicotinic acetylcholine receptor

S. Sichler^a, G. Höfner^a, S. Rappenglück^a, T. Wein^a, K. V. Niessen^b, T. Seeger^b, F. Worek^b, H. Thiermann^b, F.F. Paintner^a, K. T. Wanner^{a*}

^aDepartment of Pharmacy – Center for Drug Research, Ludwig-Maximilians-Universität München, Butenandtstr. 5-13, 81377 Munich, Germany

^bBundeswehr Institute of Pharmacology and Toxicology, Neuherbergstraße 11, 80937 Munich, Germany

* Corresponding author:

K.T. Wanner, Department of Pharmacy – Center for Drug Research

Ludwig-Maximilians-Universität München

Butenandtstr. 5-13, 81377 Munich,

Tel.: +49 (0)89 2180 77249, Fax: +49 (0)89 2180 77247

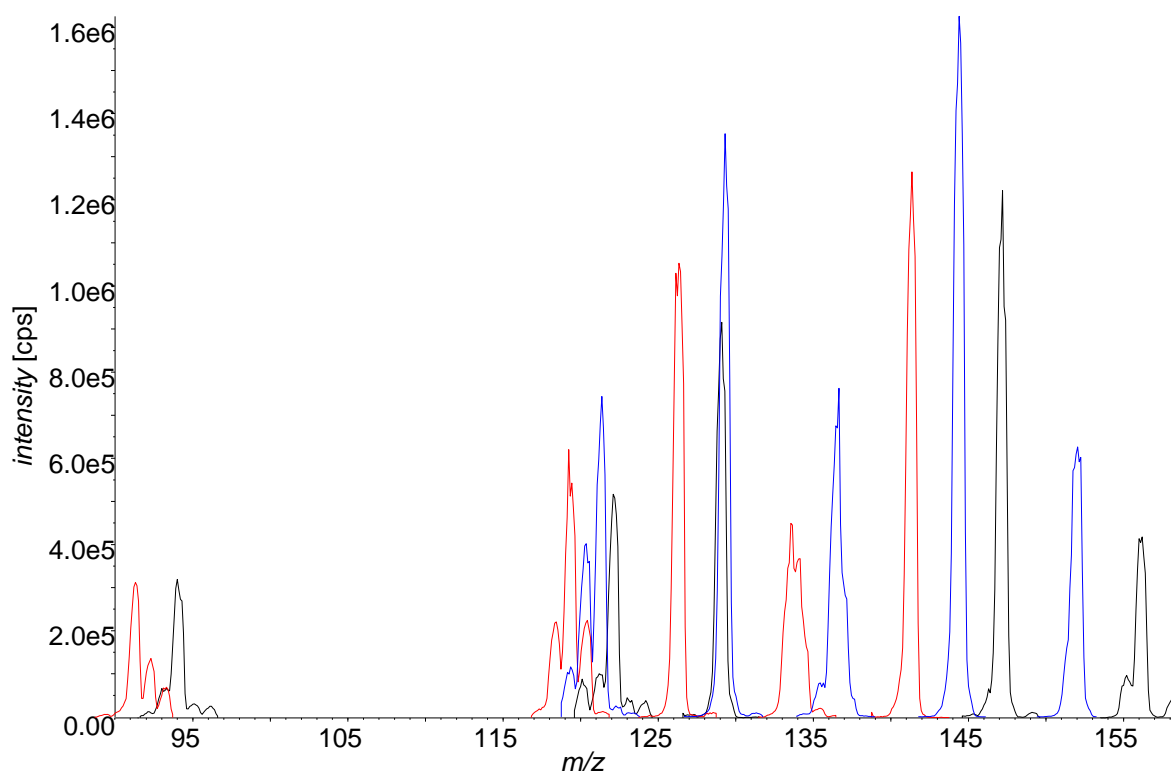
E-Mail: Klaus.Wanner@cup.uni-muenchen.de

Content

Identification of most abundant product ions for MB327, [² H ₆]MB327, and [² H ₁₈]MB327	2
LC-ESI-MS/MS method validation	2
Determination of nonspecific binding by heat denaturation	8
Characterization of the <i>Torpedo</i> membrane preparation by carbachol	9
Modulation of conformational states of nAChR using phencyclidine as reporter ligand	10

Identification of most abundant product ions for MB327, [$^2\text{H}_6$]MB327, and [$^2\text{H}_{18}$]MB327

For identification of suitable mass transitions for MB327 and its deuterated analogues a product scan of the respective precursor ion (m/z 156.2, m/z 159.2 and m/z 165.2 for MB327, [$^2\text{H}_6$]MB327, and [$^2\text{H}_{18}$]MB327, respectively) was performed to identify the most intense product ions (see SI Fig. 1) by direct infusion of respective compounds, employing the Quantitative Optimization Tool of the Analyst v. 1.6.1 software (for experimental detail see Material and Methods).

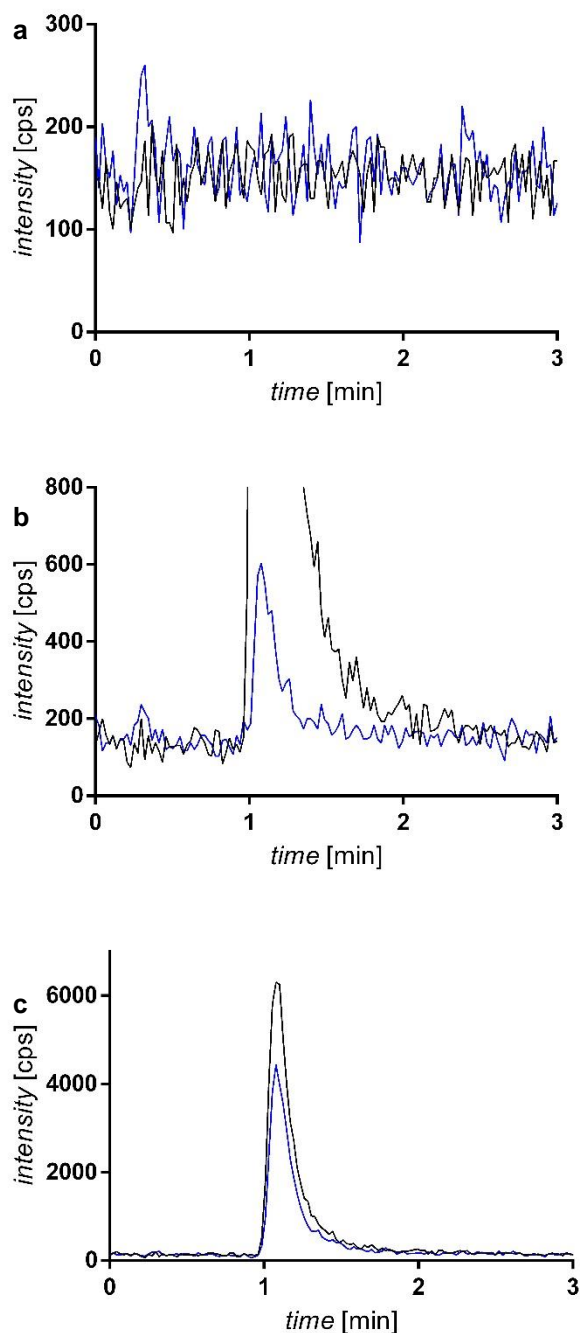


SI Fig. 1. Product ion scans after fragmentation of the respective parent ions of MB327 (m/z 156.2, red), [$^2\text{H}_6$]MB327 (m/z 159.2, blue) and [$^2\text{H}_{18}$]MB327 (m/z 165.2, black).

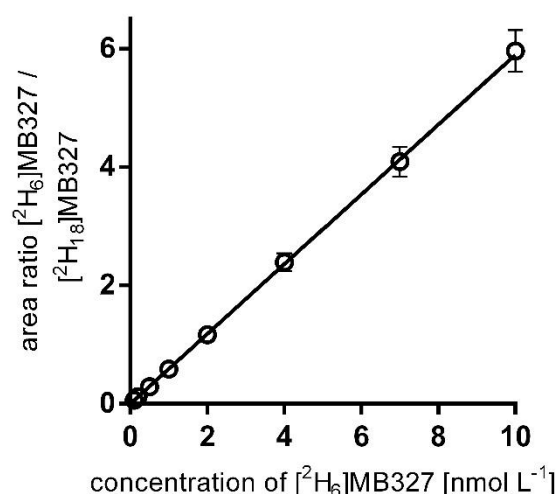
LC-ESI-MS/MS method validation

Validation was based on matrix blanks, zero samples, matrix standards and quality control (QC) samples. Standards as well as QC samples with [$^2\text{H}_6$]MB327 in a range of 100 pmol L⁻¹ to 10 nmol L⁻¹ were prepared in “IS containing blank matrix”, obtained under the conditions of the nAChR binding assays, but without addition of marker. Since the binding assays, as described before, yielded two slightly different matrices with samples for determination of total binding and nonspecific binding (the latter additionally treated for 1 h at 60 °C), both types of matrices were examined. In total 12 validation series, i.e. six sets (each containing matrix blanks, zero samples, calibration standards as well as QC samples) based on total binding matrix and six identical composed sets based on nonspecific binding matrix were investigated. Selectivity was demonstrated by analysis of blank matrix which did not show

any interfering signals for both matrix types at the mass transitions m/z 159.2/144.3 ($[^2\text{H}_6]\text{MB327}$) or m/z 165.2/147.2 ($[^2\text{H}_{18}]\text{MB327}$) (for an example see SI Fig. 2a). Based on the 12 validation series the abovementioned parameters were tested. Linearity was examined based on a global calibration curve that was calculated for all calibration levels (0.1, 0.2, 0.5, 1, 2, 4, 7, 10 nmol L⁻¹) of the 12 validation series. For all standards obtained area ratios (y) of $[^2\text{H}_6]\text{MB327}$ vs. $[^2\text{H}_{18}]\text{MB327}$ were plotted against the corresponding concentration of $[^2\text{H}_6]\text{MB327}$ (x). Linear regression analysis for these data employing a $1/x^2$ weighting yielded the following calibration function: $y = 0.587x - 0.000837$ ($R^2 = 0.9961$, see SI Fig. 3). Representative LC-ESI-MS/MS chromatograms of a 100 pmol L⁻¹ (LLOQ) and a 1 nmol L⁻¹ matrix standard are shown in SI Fig. 2b and c, respectively.



SI Fig. 2. MRM LC-ESI-MS/MS chromatograms of [²H₆]MB327 (blue) and [²H₁₈]MB327 (black) in matrix resulting from binding samples. For quantification the mass transitions m/z 159.2/144.3 and m/z 165.2/147.2 were used for [²H₆]MB327 and [²H₁₈]MB327, respectively. a) matrix blank, b) 100 pmol L⁻¹ [²H₆]MB327 together with 1.67 nmol L⁻¹ [²H₁₈]MB327, c) 1 nmol L⁻¹ [²H₆]MB327 together with 1.67 nmol L⁻¹ [²H₁₈]MB327. All chromatograms were recorded at an API 3200 employing a YMC-Triart Diol-HILIC (50 mm × 2 mm, 3 μm) in combination with acetonitrile and 20 mmol L⁻¹ ammonium formate (pH 3.0, ratio 80 : 20) as mobile phase at a flow rate of 800 μL min⁻¹ at 20 °C. The injection volume was 10 μL in each case.



SI Fig. 3. Global calibration curve ($y = 0.587x - 0.000837$; $R^2 = 0.9961$) for $[^2\text{H}_6]\text{MB327}$ based on 12 validation series (6 validation series for total binding matrix and nonspecific binding matrix, respectively), each consisting of blank and zero samples as well as matrix calibration standards at eight concentration levels (0.1, 0.2, 0.5, 1, 2, 4, 7 and 10 nmol L^{-1}). Area ratios of $[^2\text{H}_6]\text{MB327}$ vs $[^2\text{H}_{18}]\text{MB327}$ (y) for calibration standards as determined with the developed LC-ESI-MS/MS method were plotted against the corresponding concentration of $[^2\text{H}_6]\text{MB327}$ (x). Data points are shown as means \pm SD

For 100 pmol L^{-1} $[^2\text{H}_6]\text{MB327}$ matrix standards (LLOQ), in presence of both matrices, the signal-to-noise ratio was always ≥ 10 (calculated by Analyst v. 1.6.1 software). According to the guideline, QC samples at three different concentration levels (i.e. 0.25, 1 and 8 nmol L^{-1}), each prepared in hexaplicates, were used to evaluate intra- and inter-batch accuracy as well as precision. The requirements for intra-batch accuracy, defined as recovery obtained for QC replicates at each concentration level, were met as the highest deviation of calculated mean concentration from nominal concentration was 10.72% (for the complete set of values using total binding matrix and nonspecific binding matrix see SI Table 1 and SI Table 2, respectively). For calibration standards, the highest deviation was 12.67%. In addition, the requirements of the guideline for intra-batch precision, calculated as relative standard deviation for the same QC replicates used for accuracy determination, were met as the highest RSD within QC replicates at one concentration level was 5.74%. For calibration standards, the highest RSD was 6.69%. Intra-batch accuracy and precision as well as inter-batch accuracy and precision (for respective values see SI Table 3) were determined as described in Material and Methods.

SI Table 1 Validation of [²H₆]MB327 quantification in total binding matrix by LC-ESI-MS/MS with an API 3200 using a YMC-Triart Diol-HILIC (50 mm x 2 mm, 3 μm) and [²H₁₈]MB327 as internal standard. $y = 0.587x - 0.000837$ ($R^2 = 0.9961$) with a $1/x^2$ weighting was used as global calibration curve.

Samples (n)	Intra-series																	
	Series 1			Series 2			Series 3			Series 4			Series 5			Series 6		
	M	Acc	RSD	M	Acc	RSD	M	Acc	RSD	M	Acc	RSD	M	Acc	RSD	M	Acc	RSD
100 pmol L⁻¹ Cal (6)	96.38	96.38	4.34	108.8	108.8	0.98	108.3	108.3	2.59	101.2	101.2	5.12	100.2	100.2	5.31	98.32	98.32	2.55
200 pmol L⁻¹ Cal (6)	190.0	95.13	7.25	207.8	103.8	3.72	200.8	100.3	2.40	183.8	91.90	4.87	204.5	102.3	5.06	205.0	102.4	3.44
500 pmol L⁻¹ Cal (3)	437.0	87.33	1.45	530.3	106.3	1.77	510.0	102.0	1.39	454.0	90.83	0.69	497.0	99.47	2.56	532.3	106.3	2.22
1 nmol L⁻¹ Cal (3)	892.0	89.20	0.81	1103	110.3	1.86	1020	102.0	2.40	922.7	92.27	1.77	1040	104.0	1.36	1080	108.0	0.76
2 nmol L⁻¹ Cal (3)	1843	92.20	1.46	2113	105.7	2.23	2050	102.8	3.03	1797	89.93	1.87	2070	103.7	1.64	2093	104.7	2.74
4 nmol L⁻¹ Cal (3)	3707	92.70	2.91	4307	107.7	2.32	4177	104.3	2.52	3770	94.17	2.21	4187	104.7	6.69	4313	108.0	1.31
7 nmol L⁻¹ Cal (3)	6317	90.23	0.82	7393	105.7	1.18	7427	106.0	2.78	6397	91.40	1.93	7227	103.0	0.79	7383	105.3	1.79
10 nmol L⁻¹ Cal (3)	9343	93.43	3.18	10767	107.7	1.58	10733	107.3	2.67	9347	93.47	0.96	10243	102.4	2.16	10833	108.3	0.87
250 pmol L⁻¹ QC (6)	260.0	103.9	5.18	246.2	103.9	3.85	248.8	99.38	5.74	232.3	92.92	3.78	260.3	104.0	1.84	259.5	103.7	3.80
1 nmol L⁻¹ QC (6)	910.3	91.03	3.93	1047	104.7	2.45	1008	100.8	2.71	892.8	89.28	0.98	1070	107.0	0.54	1018	101.8	2.11
8 nmol L⁻¹ QC (6)	7347	91.83	1.70	8605	107.5	1.45	8218	102.7	1.86	7463	93.30	2.69	8618	107.7	1.48	8122	101.4	1.87

M Mean of calculated concentrations (pmolL⁻¹), *Acc* accuracy (%), *RSD* relative standard deviation (%), *Cal* calibration standard, *QC* quality control sample, *n* number of replicates examined

SI Table 2 Validation of [²H₆]MB327 quantification in nonspecific binding matrix by LC-ESI-MS/MS with an API 3200 using a YMC-Triart Diol-HILIC (50 mm x 2 mm, 3 μm) and [²H₁₈]MB327 as internal standard. $y = 0.587x - 0.000837$ ($R^2 = 0.9961$) with a $1/x^2$ weighting was used as global calibration curve.

Samples (n)	Intra-series																	
	Series 1			Series 2			Series 3			Series 4			Series 5			Series 6		
	M	Acc	RSD	M	Acc	RSD	M	Acc	RSD	M	Acc	RSD	M	Acc	RSD	M	Acc	RSD
100 pmol L⁻¹ Cal (6)	93.37	93.37	6.28	108.8	108.8	1.94	101.7	101.7	3.67	93.63	93.63	1.72	99.78	99.78	4.45	99.22	99.22	4.74
200 pmol L⁻¹ Cal (6)	188.7	94.30	2.59	211.7	106.0	3.77	194.8	97.58	3.76	189.2	94.60	5.05	197.7	98.87	2.96	193.2	96.60	2.75
500 pmol L⁻¹ Cal (3)	461.7	92.30	3.23	514.7	103.0	3.46	493.3	98.53	1.96	442.7	88.53	0.78	518.7	104.0	3.60	503.0	100.8	3.76
1 nmol L⁻¹ Cal (3)	929.0	92.90	3.43	1097	109.7	3.36	1001	100.1	2.25	932.0	93.20	2.05	1040	104.0	2.88	987.7	98.77	1.41
2 nmol L⁻¹ Cal (3)	1833	91.57	2.12	2087	104.7	2.38	2020	101.1	3.07	1883	94.20	1.69	2047	102.2	3.87	2043	102.2	4.15
4 nmol L⁻¹ Cal (3)	3857	96.50	3.36	4350	108.3	3.05	4110	102.7	3.17	3770	94.20	2.86	4157	104.3	4.02	4103	102.7	1.21
7 nmol L⁻¹ Cal (3)	6690	95.53	2.57	7353	105.0	0.78	6927	99.03	3.74	6460	92.27	3.33	7010	100.1	4.92	7073	100.8	1.53
10 nmol L⁻¹ Cal (3)	9543	95.43	1.65	10800	108.0	4.00	10080	100.8	3.81	9673	96.73	0.98	10433	104.3	2.75	10100	101.0	0.81
250 pmol L⁻¹ QC (6)	238.5	95.43	2.52	255.0	102.0	3.95	246.0	98.45	4.43	230.7	92.28	3.86	254.2	102.0	4.63	244.0	97.65	2.98
1 nmol L⁻¹ QC (6)	940.0	94.00	2.25	1035	103.5	4.04	995.2	99.52	2.70	945.6	94.56	3.27	1033	103.3	3.04	988.8	98.88	5.02
8 nmol L⁻¹ QC (6)	7653	95.68	1.20	8393	104.8	1.28	8333	104.2	3.61	7775	97.10	3.12	8175	102.2	2.84	8195	102.5	2.16

M Mean of calculated concentrations (pmolL⁻¹), *Acc* accuracy (%), *RSD* relative standard deviation (%), *Cal* calibration standard, *QC* quality control sample, *n* number of replicates examined

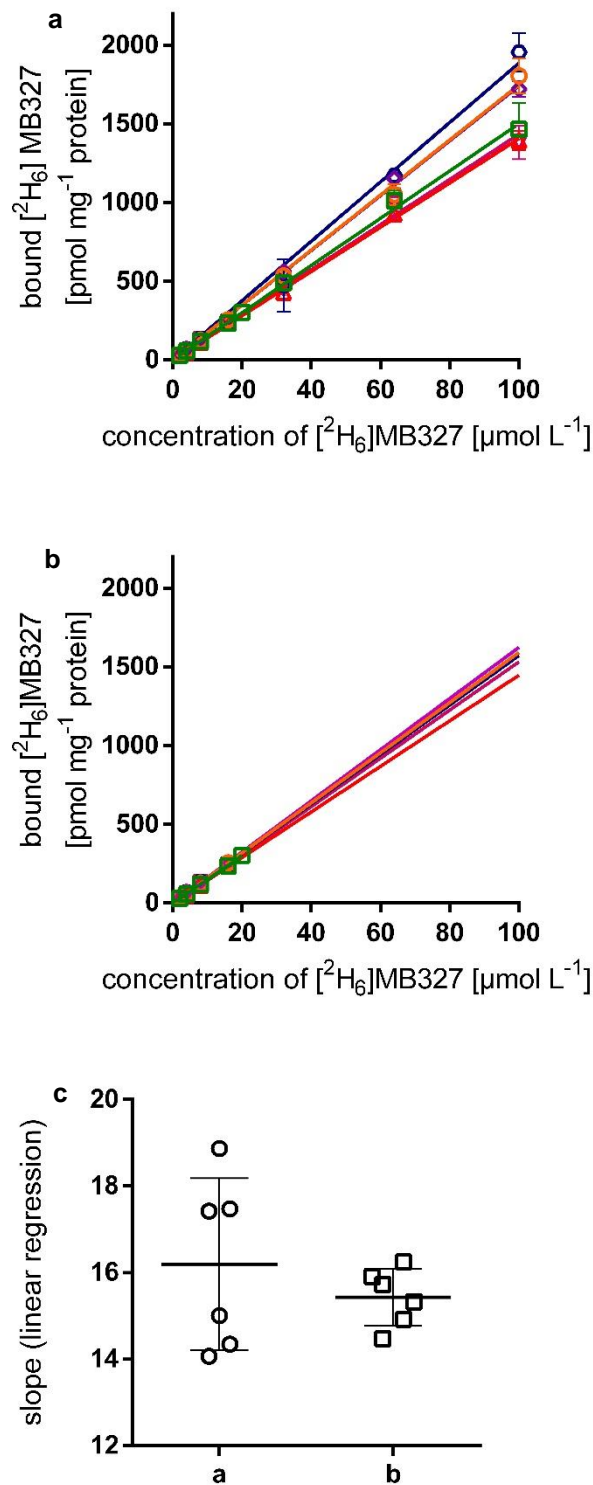
SI Table 3 Inter-series determination of mean, accuracy and precision of the validation of [$^2\text{H}_6$]MB327 quantification in (total and nonspecific) binding matrix by LC-ESI-MS/MS employing [$^2\text{H}_{18}$]MB327 as internal standard. $y = 0.587x - 0.000837$ ($R^2 = 0.9961$) with a $1/x^2$ weighting was used as global calibration curve.

Samples (n)	Inter-series		
	M	Acc	RSD
100 pmol L ⁻¹ Cal (6)	100.8	100.8	5.15
200 pmol L ⁻¹ Cal (6)	197.3	98.65	4.23
500 pmol L ⁻¹ Cal (3)	491.2	98.29	6.65
1 nmol L ⁻¹ Cal (3)	1004	100.4	6.88
2 nmol L ⁻¹ Cal (3)	1990	99.58	5.60
4 nmol L ⁻¹ Cal (3)	4067	102.0	5.42
7 nmol L ⁻¹ Cal (3)	6971	99.54	5.64
10 nmol L ⁻¹ Cal (3)	10158	101.6	5.39
250 pmol L ⁻¹ QC (6)	248.0	99.58	4.12
1 nmol L ⁻¹ QC (6)	990.4	99.04	5.45
8 nmol L ⁻¹ QC (6)	8075	100.9	4.99

M Mean of calculated concentrations (pmol L⁻¹), *Acc* accuracy (%), *RSD* relative standard deviation (%), *Cal* calibration standard, *QC* quality control sample, *n* number of replicates examined

Determination of nonspecific binding by heat denaturation

Nonspecific binding was determined by heat denaturation with eight concentration levels in triplicates over a nominal marker concentration range of 2 – 100 $\mu\text{mol L}^{-1}$ in six independent experiments following two strategies: First, nonspecific binding was determined on the basis of all concentration levels (see SI Fig. 4a). Analysis by means of linear regression (forced through the origin) yielded a slope of 16.2 ± 2.0 ($n = 6$, see SI Fig. 4c). Secondly, only data points in the range of 2 – 20 $\mu\text{mol L}^{-1}$ (five concentration levels) were examined by means of linear regression with extrapolation of NSB at marker concentration $> 20 \mu\text{mol L}^{-1}$ (see SI Fig. 4b). In this case linear regression (forced through the origin) yielded a slope of 15.4 ± 0.7 ($n = 6$, see SI Fig. 4c).

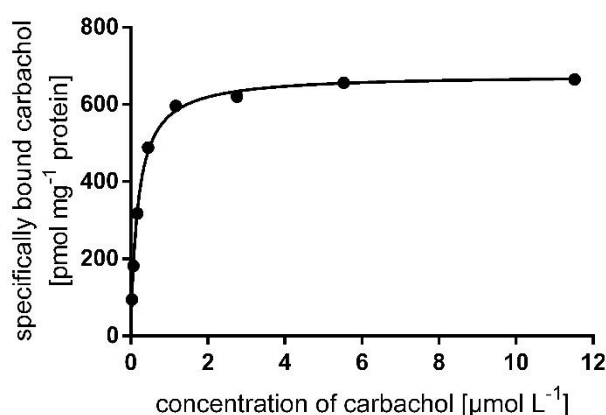


SI Fig. 4. Analysis of nonspecific binding (means \pm SD) with linear regression (a) based on marker concentrations from 2 – 100 $\mu\text{mol L}^{-1}$ or (b) based on marker concentrations from 2 – 20 $\mu\text{mol L}^{-1}$ with extrapolation to higher marker concentrations $> 20 \mu\text{mol L}^{-1}$ ($n = 6$, shown in blue, purple, orange, red, magenta and green). Means \pm SD ($n = 6$) of slopes of respective linear regression analyses in (a, circles) vs (b, squares) are shown SI Fig. 4c.

Characterization of the *Torpedo* membrane preparation by carbachol

Nonspecific binding was determined by heat denaturation, prior to incubation, as for the $[^2\text{H}_6]\text{MB327}$ binding experiments described above. For LC-ESI-MS/MS quantification of carbachol at the mass

transition m/z 148.2/88.0 the same LC-conditions could be employed as for quantification of $[^2\text{H}_6]\text{MB327}$. As an appropriate structural analogue of carbachol serving as internal standard for LC-ESI-MS/MS quantification was not available, quantification was performed by means of external calibration based on data from matrix standards as described in Material and Methods.



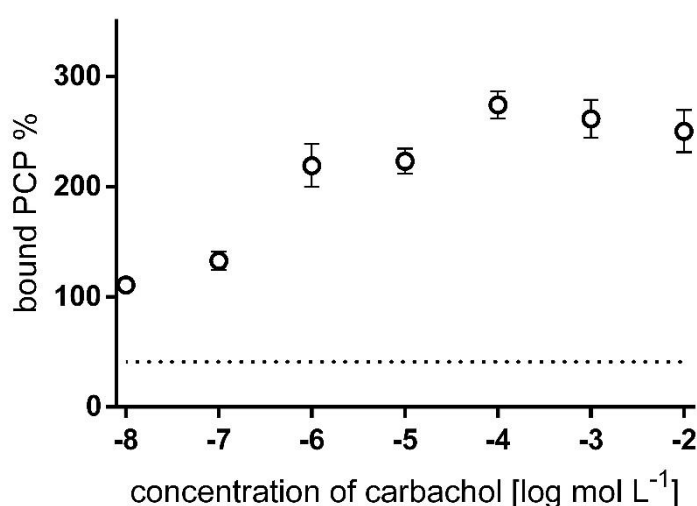
SI Fig. 5. Representative saturation isotherm showing specific carbachol binding (means) towards *Torpedo*-nAChR obtained according to the protocol described in Materials and Methods. In this experiment, a K_d -value of 188 nmol L^{-1} and a B_{max} of 677 pmol mg^{-1} were determined.

Unfortunately, under the employed conditions significant marker depletion was encountered for lower marker concentrations. A reduction of the amount of target material employed in the binding experiment might have allowed to solve this problem, but would have compromised the generation of a sufficiently robust pellet. To counteract the error resulting from ligand depletion (i.e. a distinctly lower concentration of free marker as compared to the nominal marker concentration present in the binding sample) to some extent for the generation of saturation isotherms the calculated free marker concentrations instead of nominal marker concentrations (for data correction see Material and Methods) were used (see SI Fig. 5).

Modulation of conformational states of nAChR using phencyclidine as reporter ligand

MS Binding Assays using carbachol for nAChR modulation and phencyclidine as reporter ligand (see SI Fig. 6) followed the general procedure for centrifugation based binding assays. Total binding of $0.5 \mu\text{mol L}^{-1}$ PCP was measured in presence of carbachol in a concentration range of 10 nmol L^{-1} – 10 mmol L^{-1} . In control experiments, total binding of PCP was determined in absence of carbachol and nonspecific binding was determined by heat treatment of aliquots of the *Torpedo* membrane preparation for 1 h at 60°C prior to incubation. PCP was detected using the LC-method developed for $[^2\text{H}_6]\text{MB327}$ Binding Assays, which was reliably possible also in presence of binding sample matrix, and quantified from integrated peak area (m/z 244.2/159.1) using an external calibration. For the external calibration, blank matrix was obtained from experiments analogous to $[^2\text{H}_6]\text{MB327}$ MS Binding Assays (without

addition of marker) and spiked with PCP at four concentration levels in a range of 0.2 – 5 nmol L⁻¹. Quantification was accepted, if for QC samples, examined at one concentration level throughout quantification of the binding samples, deviation of calculated concentrations from nominal concentrations was not more than 15%, i.e. recovery of QCs was between 85 – 115%.



SI Fig. 6. Modulatory effect of carbachol (10 nmol L⁻¹ – 10 mmol L⁻¹) on the conformation of *Torpedo*-nAChRs recorded by binding of phencyclidine (PCP, *m/z* 244.2/159.1) as reporter ligand. Bound PCP (means ± SD) at a concentration of 0.5 μmol L⁻¹ was quantified from integrated peak area using an external calibration in sample matrix. Binding was normalized to total binding, determined in control experiments in absence of carbachol. Nonspecific binding, determined by heat denaturation, is indicated as dashed line (mean).

3.2 Zweite Publikation

Synthesis of a Series of Structurally Diverse MB327 Derivatives and Their Affinity Characterization at the Nicotinic Acetylcholine Receptor

3.2.1 Zusammenfassung der Ergebnisse

Mit den zuletzt entwickelten MS-Bindungsassays, mit [$^2\text{H}_6$]MB327 als Reporterligand und dem *Torpedo*-nAChR als Target, stand ein robustes und effizientes Testsystem für die Bestimmung der Bindungsaffinitäten von Testverbindungen an die MB327-Bindestelle des Muskeltyp-nAChRs zur Verfügung. Diese etablierten MS-Bindungsassays wurden im Rahmen dieser Studie angewandt, um die Inhibitionskonstanten einer Reihe neu synthetisierter MB327-Derivate an der MB327-Bindestelle zu bestimmen und so erste Struktur-Affinitätsbeziehungen an besagter Bindestelle abzuleiten. Ausgehend von MB327 als Leitstruktur, wurden für diesen Zweck 30 symmetrische Bispyridinium- bzw. N-heteroaromatische, bisquaternäre Salze synthetisiert. Eine zweistufige Reaktion, mit der Synthese der gewünschten N-Heterocyclen im ersten Schritt und anschließender N-Alkylierung mit Propan-1,3-ditriflat bzw. Propan-1,3-diiodid als Alkylans, ermöglichte dabei einen effizienten Zugang zu den Zielverbindungen. Nebst Entwicklung der MB327-Derivate als Testverbindungen wird auch die Synthese der deuterierten MB327-Analoga [$^2\text{H}_6$]MB327 und [$^2\text{H}_{18}$]MB327 dargestellt, die im MS-Bindungsversuch als Reporterligand bzw. Interner Standard eingesetzt wurden. Allen neu synthetisierten Verbindungen wurde eine PTM(Pharmazie und Toxikologie München)-Kennung zugeteilt.

Die Durchführung von MS-Bindungsassays mit [$^2\text{H}_6$]MB327 als Reporterligand am *Torpedo*-nAChR erfolgte wie in der Originalpublikation beschrieben mit einer minimalen Anpassung. Durch Austausch des CaCl_2 -haltigen Lagerungspuffers gegen den CaCl_2 -freien Lagerungspuffer war es möglich durchweg, d.h. ab der Lagerung der extrahierten nAChR-reichen Membranpräparation bis bzw. auch zur Inkubation der Präparation mit dem Reporterliganden im Bindungsexperiment, in einem uniformen Puffersystem zu arbeiten. Ein Vergleich von Sättigungs- und Autokompetitionsexperimenten, durchgeführt nach originären bzw. modifizierten Assayprotokoll d.h. bei Letzterem in Abwesenheit von CaCl_2 , zeigte, dass eine

zuverlässige Bestimmung der Reporterligand-Bindung bzw. von Affinitätskonstanten auch unter modifizierten Versuchsbedingungen gegeben war. Um sicherzustellen, dass sich diese, wenngleich geringfügige Anpassung der Versuchsdurchführung nicht negativ auf die Zuverlässigkeit der Reporterligand-Quantifizierung auswirkt, wurde die LC-MS-Methode erneut validiert. Hier zeigten sich abermals alle Kriterien der Validierungsparameter Selektivität, Linearität, Richtigkeit und Präzision gemäß CDER-Richtlinien der FDA für bioanalytische Methoden erfüllt.

Das modifizierte MS-Bindungsassay wurde schließlich angewandt, um die Bindungsaffinitäten einer Reihe symmetrischer MB327-Derivate an die MB327-Bindestelle des *Torpedo*-nAChR zu bestimmen. Unter den 30 bisquaternären Zielstrukturen zeigte die lipophile 3-Phenyl-4-*tert*-butyl-substituierte Bispyridiniumverbindung PTM0022 die mit Abstand höchste Bindungsaffinität an die MB327-Bindestelle. Die Einführung des zusätzlichen Phenylsubstituenten, jeweils in 3-Position am 4-*tert*-Butyl-substituierten Pyridiniumring, resultierte in einer, im Vergleich zur Leitstruktur, signifikant größeren Affinitätskonstante ($pK_i = 5.16 \pm 0.07$). Durchweg zeigte sich eine Tendenz zu höheren Bindungsaffinitäten für Verbindungen mit lipophilen Substituenten, während die Einführung polarer (z.B. OMe, COOEt, ...) funktioneller Gruppen meist mit einem Verlust an Bindungsaffinität an die MB327-Bindestelle einherging. Interessanterweise fielen die pK_i -Werte dabei stets größer aus, je größer der sterische Anspruch des lipophilen Substituenten war. Wurde die *tert*-Butylgruppe in MB327, in PTM0001 oder in PTM0002 durch eine Isopropylgruppe ersetzt, resultierte dies entsprechend in einem sichtlichen Rückgang der Bindungsaffinität an die MB327-Bindestelle (vgl. PTM0013, PTM0014 und PTM0003). Auch der Austausch der *tert*-Butylgruppe gegen eine Methylgruppe am N-Heteroatom der Bisimidazoliumverbindung PTM0059 reduzierte deren Bindungsaffinität um knapp 0.8 log-Einheiten (vgl. PTM0034). Die geringste Bindungsaffinität an die MB327-Bindestelle zeigte das zwitterionische PTM0028. Mit Einführung einer Carbonsäurefunktion, jeweils in 3-Position an den Pyridiniumeinheiten des MB327-Molekülgerüsts, fiel die Bindungsaffinität um knapp zwei Zehnerpotenzen unter die Bindungsaffinität von MB327 am *Torpedo*-nAChR ($pK_i, \text{PTM0028} = 2.74 \pm 0.13$). Auch der Austausch eines *tert*-Butylsubstituenten gegen eine polare Methoxygruppe in 2-, 3-, oder 4-Position hatte einen deutlichen Verlust an Bindungsaffinität an die MB327-

Bindestelle zur Folge. Überraschenderweise verbesserte sich diese aber deutlich mit der Einführung eines zusätzlichen 4-*tert*-Butyl-Substituenten am Pyridiniumring, wie der Vergleich der Affinitätskonstanten des 3-Methoxy-substituierten PTM0009 und des 4-*tert*-Butyl-3-methoxy-substituierten PTM0016 mit $pK_i = 3.79 \pm 0.09$ bzw. 4.46 ± 0.07 zeigt. Anhand dieser Steigerung des pK_i -Werts um knapp 0.6 log-Einheiten wird auch der positive Effekt des 4-*tert*-Butylmotivs auf die Bindungsaffinität von MB327 und Derivaten an den *Torpedo*-nAChR deutlich. Dass die Einführung polarer Substituenten nicht in jedem Fall zu einer Verschlechterung der Bindungsaffinität an die MB327-Bindestelle führt, zeigt sich anhand der 3-Dimethylamino-substituierten Bispyridiniumverbindung PTM0007, mit einem pK_i -Wert von 4.78 ± 0.05 .

Mithilfe der MS-Bindungsassays mit $[^2\text{H}_6]\text{MB327}$ als Reporterligand war in dieser Studie eine zuverlässige Bestimmung von Affinitätskonstanten mehrerer MB327-Derivate an die MB327-Bindestelle möglich. So konnte mit PTM0022 bereits ein erster nAChR-Ligand mit, im Vergleich zur Leitstruktur, signifikant höherer Affinität an die MB327-Bindestelle identifiziert werden. Schließlich ließen sich anhand der in dieser Studie gewonnenen Bindungsdaten schon erste wichtige Zusammenhänge zwischen Struktur der MB327-Derivate und Affinität an die MB327-Bindestelle ableiten.

3.2.2 Erklärung zum Eigenanteil

Die MS-Bindungsversuche sowie deren Auswertung zur Bestimmung der Bindungsaffinitäten von Testverbindung an die MB327-Bindestelle führte ich eigenständig durch. Alle beschriebenen Synthesen in dieser Studie wurden von Sebastian Rappenglück durchgeführt. Sebastian Rappenglück und ich waren, unterstützt von Georg Höfner, Thomas Wein und Klaus T. Wanner gleichermaßen an der Diskussion der Struktur-Affinitätsbeziehungen sowie am Schreiben des Manuskripts beteiligt. An der Korrektur des Manuskripts wirkten Georg Höfner und Klaus T. Wanner sowie Franz F. Paintner, Karin V. Niessen*, Thomas Seeger*, Franz Worek* und Horst Thiermann* mit.

* Kooperationspartner im Rahmen eines gemeinsamen Forschungsprojekts vom Institut für Pharmakologie und Toxikologie der Sanitätsakademie in München

Synthesis of a Series of Structurally Diverse MB327 Derivatives and Their Affinity Characterization at the Nicotinic Acetylcholine Receptor

Sebastian Rappenglück^{+, [a]} Sonja Sichler^{+, [a]} Georg Höfner^[a] Thomas Wein^[a]
Karin V. Niessen^[b] Thomas Seeger^[b] Franz F. Paintner^[a] Franz Worek^[b] Horst Thiermann^[b]
and Klaus T. Wanner^{*, [a]}

A novel series of 30 symmetric bispyridinium and related *N*-heteroaromatic bisquaternary salts with a propane-1,3-diyl linker was synthesized and characterized for their binding affinity at the **MB327** binding site of nicotinic acetylcholine receptor (nAChR) from *Torpedo californica*. Compounds targeting this binding site are of particular interest for research into new antidotes against organophosphate poisoning, as therapeutically active 4-*tert*-butyl-substituted bispyridinium salt **MB327** was previously identified as a nAChR re-sensitizer. Efficient access to the target compounds was provided by newly developed methods enabling *N*-alkylation of sterically hindered or

electronically deactivated heterocycles exhibiting a wide variety of functional groups. Determination of binding affinities toward the **MB327** binding site at the nAChR, using a recently developed mass spectrometry (MS)-based Binding Assay, revealed that several compounds reached affinities similar to that of **MB327** ($pK_i = 4.73 \pm 0.03$). Notably, the newly prepared lipophilic 4-*tert*-butyl-3-phenyl-substituted bispyridinium salt PTM0022 (**3h**) was found to have significantly higher binding affinity, with a pK_i value of 5.16 ± 0.07 , thus representing considerable progress toward the development of more potent nAChR re-sensitizers.

Introduction

The recent use of sarin as a chemical weapon in Syria as well as the high number of fatal poisonings with organophosphorus pesticides underline the threat emanating from organophosphorus compounds (OPCs) to humanity.^[1–3] Therefore, there is an urgent need for effective medical treatment of OPC intoxications. OPCs inactivate the enzyme acetylcholinesterase (AChE), which results in accumulation of acetylcholine (ACh) in the synaptic cleft of both muscarinic and nicotinic synapses. Whereas overstimulation of muscarinic receptors (mAChRs) can be antagonized by using atropine, administration of anticholinergics to counteract nAChR overstimulation is precluded by their therapeutic limitations.^[4] Thus, ongoing overstimulation by accumulated ACh forces the nAChRs into a desensitized state,^[5,6] which is currently therapeutically inaccessible.^[7] Resulting disturbance of neuromuscular transmission may cause

paralysis of respiratory and other skeletal muscles as the most severe and often lethal consequences of OPC poisoning.

Current medical countermeasures make use of oximes such as obidoxime or pralidoxime to reactivate the inhibited AChE, thus treating cholinergic crisis. However, in many cases oximes have been shown to be ineffective. Rapid dealkylation of the AChE–organophosphonate complex in the case of soman intoxication or very slow reactivation rates of tabun-inhibited AChE for most commonly used oximes are only two of several examples for which the reactivation kinetics of this phenomenon has been well studied.^[8,9] Hundreds of different oximes have been developed and tested over the last decades, without the successful identification of a universal reactivator of AChE.^[10] As a consequence, restoration of nAChR-mediated cholinergic signaling in the event of OPC poisoning remains a highly challenging task, demanding an alternative approach not based exclusively on AChE reactivation.

One very promising strategy might be the direct intervention at the nAChR to recover its activity from desensitization, as recently demonstrated in measurements using a novel electrophysiological (surface electronic event reader, SURFE²R) platform by Niessen et al.^[11] These studies revealed that the 4-*tert*-butyl-substituted bispyridinium compound **MB327** can re-sensitize the desensitized nAChR and restore channel function.^[11,12] As previous investigations have already shown that **MB327** targets the orthosteric binding site with only weak affinity, functional recovery of the nAChR is suggested to be mediated rather by allosteric modulation.^[13,14] In contrast to an

[a] S. Rappenglück,⁺ S. Sichler,⁺ Dr. G. Höfner, Dr. T. Wein, Prof. Dr. F. F. Paintner, Prof. Dr. K. T. Wanner

Department of Pharmacy, Center for Drug Research, Ludwig-Maximilians-Universität München, Butenandtstr. 5–13, 81337 Munich (Germany)
E-mail: klaus.wanner@cup.uni-muenchen.de

[b] K. V. Niessen, Dr. T. Seeger, Prof. Dr. F. Worek, Prof. Dr. H. Thiermann
Bundeswehr Institute of Pharmacology and Toxicology, Neuherbergstr. 11, 80937 Munich (Germany)

[*] These authors contributed equally to this work.

Supporting information and the ORCID identification number(s) for the author(s) of this article can be found under:
<https://doi.org/10.1002/cmdc.201800325>.

oxime-based therapy aiming at reactivation of inhibited AChE, an allosterically mediated re-sensitization of the nAChR has the advantage of restoring nAChR activity, thereby preserving neuromuscular function in any case of organophosphorus nerve agent poisoning.

The therapeutic effect of **MB327** against OPC poisoning has also been demonstrated in several *ex vivo*, *in vitro*, as well as *in vivo* studies. In the case of tabun-poisoned guinea pigs, for example, treatment with **MB327** significantly increased the survival rate relative to the oxime HI-6, both administered together with physostigmine and hyoscine.^[15] Furthermore, Seeger et al. found that **MB327** restores soman-impaired neuromuscular transmission in human and rat respiratory muscle preparations at concentrations of 100–200 μM .^[16] Unfortunately, **MB327** also acts as an AChE inhibitor at slightly higher concentrations ($\text{IC}_{50} \sim 600 \mu\text{M}$) and antagonizes nicotinic currents at concentrations $\geq 100 \mu\text{M}$,^[17,18] possibly leading to adverse effects, if administered *in vivo*.^[19] Therefore, the therapeutic window of **MB327** is too narrow for administration in cases of OPC poisoning, and hence more potent and more selective nAChR re-sensitizers must be developed.

Although **MB327** has been studied extensively in the past few years regarding its potential use in treatment regimens,^[20–22] the targeted binding site at the nAChR was characterized only very recently.^[23] Binding assays using mass spectrometry for marker quantification (MS Binding Assays) that enable the affinity determination for ligands targeting the **MB327** binding site have been established.^[24] Based on these MS Binding Assays, we could characterize the affinity of **MB327** for nAChR with a K_i value of $18.3 \pm 2.6 \mu\text{M}$, which is in line with its potency determined in electrophysiological and pharmacological studies. For our MS Binding Assays, we use the nAChR from *Torpedo californica*, which shows a high degree of homology to the human muscle-type nAChR and represents the most common model system.^[25,26]

In parallel to the development of [$^2\text{H}_6$]**MB327** MS Binding Assays, our research group identified two putative **MB327** binding sites using *in silico* docking studies at the nAChR of *Torpedo marmorata* at 4 Å resolution.^[23] Respective sites are located inside the channel: one in the extracellular and one in the transmembrane domain. The developed MS Binding Assays have allowed the collection of quantitative binding data for the nAChR for the first time. These data are an essential prerequisite for a detailed understanding of the binding interactions at the molecular level and for the development of valid structure–affinity relationships representing a key element in the search for new antidotes against OPC intoxication. Hence, we envisaged the synthesis and affinity characterization of a novel series of structurally different **MB327** analogues, which were expected to be of interest to gain initial insight into structure–affinity relationships. Herein we report the results of this endeavor.

Results and Discussion

Structure of target compounds

With **MB327** as lead structure, we focused on the investigation of symmetrical bispyridinium compounds with distinct structural modifications. The results of how these structural changes affect affinity for the **MB327** binding site should provide information on the molecular interactions important for the binding event. **MB327** is a symmetric bispyridinium diiodide with a *tert*-butyl group at the 4-position of each pyridinium ring and a propyl linker connecting both aromatic rings (Figure 1).

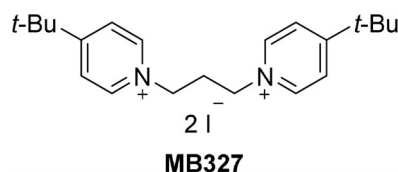


Figure 1. Structure of **MB327**.

Depending on the structural characteristics, the influence of which on the binding affinity should be studied, target compounds were divided into four different types (I–IV), comprising in total 30 structurally related compounds (Figure 2). Compounds of types I and II are bispyridinium salts substituted with either one lipophilic (Me, *i*Pr, *t*Bu) or one hydrophilic (OMe, NMe₂, *N*-methylpyrrolidine) substituent on each pyridinium ring. These moieties were introduced to investigate the influence of the substituent position at the ring system, the steric demand of the functional groups as well as hydrogen bridge interactions between polar moieties and the binding pocket on the binding affinity. Bispyridinium salts of type III were directly delineated from the lead structure **MB327** by introduction of an additional substituent and designed to investigate the resulting affinity. These compounds exhibit a 4-*tert*-butyl group as well as a second functional group (e.g., Ph, CN, OMe, COOEt, Cl) at the 2- or 3-position of the pyridinium ring.

As a consequence, from these compounds, substituent effects can be directly derived by comparing the binding affinity with that of **MB327**, which is devoid of any substituent at the 2- or 3-position. To investigate the importance of π – π interactions with aromatic amino acid side chains of the nAChR during the binding event and to expand the structural diversity amongst the test compounds, pyridine was finally replaced by other heteroaromatic compounds such as isoquinoline, thiazole, or 2-*tert*-butylpyrazine, thus resulting in new target structures of type IV.

Common to all newly synthesized compounds, however, is the propane-1,3-diyl (C3) linker, known from **MB327**. This linker was used for all test compounds, as **MB327** showed a significantly higher re-sensitization potency in SURFE²R-based electrophysiological experiments than structurally analogous compounds with shorter (ethane-1,2-diyl (C2)) or longer (butane-1,4-diyl (C4)) linkers.^[11]

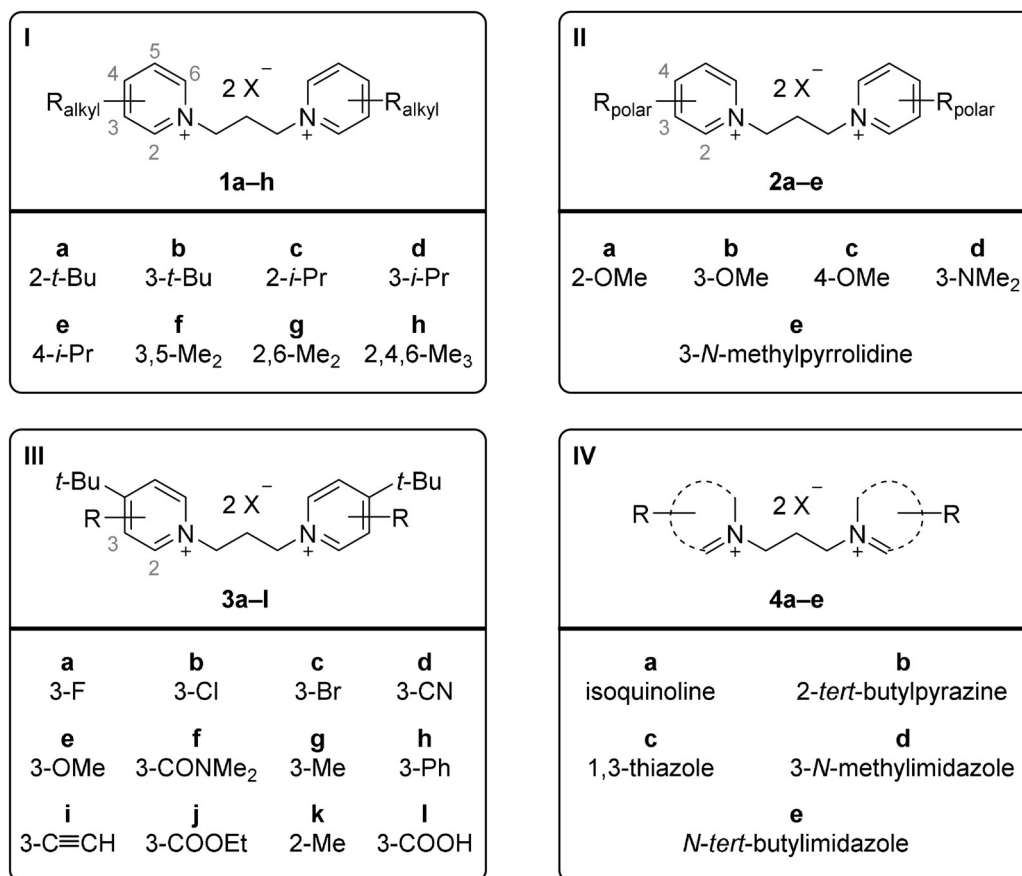


Figure 2. Structures of envisaged target compounds (type I-IV). X = Cl⁻, I⁻, OTf⁻.

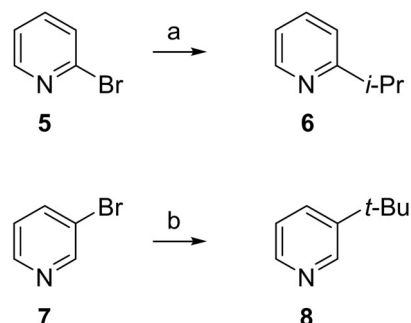
Chemistry

As shown in Figure 2, all target compounds are symmetric bis-pyridinium salts or related from *N*-aromatic-subunit-derived salts with a propane-1,3-diyl linker. As such, these compounds are easily accessible in a two-step reaction sequence. In the first step, the required nitrogen heterocycles are synthesized, which, in the second step, afford the target compounds upon *N*-alkylation. Of the 30 nitrogen heterocycles used in the synthesis of the target compounds, 25 were either commercially available or synthesized according to published procedures,^[27–29] including the 3-substituted 4-*tert*-butylpyridine derivatives, the preparation of which was recently reported by us.^[30] The remaining five pyridine derivatives, namely 4-(*tert*-butyl)-2-methylpyridine (15), 3-*tert*-butylpyridine (8), 2- (6), 3- (11), and 4-isopropylpyridine (13) were prepared as described below.

Preparation of alkyl-substituted pyridine derivatives

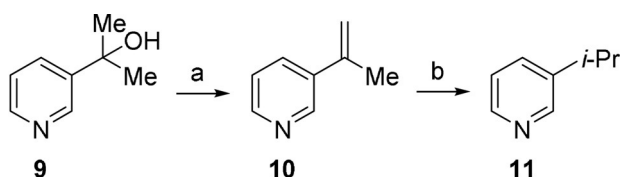
2-Isopropylpyridine (6) as well as 3-*tert*-butylpyridine (8) were prepared from the corresponding bromopyridines 5 and 7 by cuprate-mediated substitution reactions resulting in low to moderate yields of 19 and 43%, respectively, for the target compounds (Scheme 1).^[27] The low yields can be assigned to side reactions that led to pyridine as a byproduct, which, in each of the two cases, was isolated in large amounts. These

side reactions might result from a halogen metal exchange caused by the intermediate isopropyl cuprate and by a β-H elimination of the putative (tBu)₂Cu(III)pyridyl complex.^[31] Interestingly, THF turned out to be far less favorable for substitution with the *tert*-butyl cuprate, affording 8 in only 12% yield (43% in Et₂O). This is likely due to the more reactive cuprate oligomers, present in Et₂O, as compared with the less reactive monomers, predominant in THF, which is a specific feature of cyano cuprates observed by Krause, Gschwind, and co-workers.^[32] Besides, yields were also negatively affected by the remarkably high volatility of compounds 6 and 8.



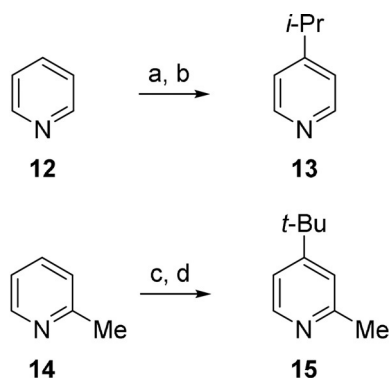
Scheme 1. Synthesis of alkyl pyridines 6 and 8: a) CuCN (4.0 equiv), *i*PrMgCl (8.0 equiv), –78 °C for 2 h → RT for 15 h, THF, 19%; b) CuCN (4.0 equiv), *t*BuMgCl (8.0 equiv), –78 °C for 2 h → RT for 15 h, Et₂O, 43% (12% yield in THF).

As 3-isopropylpyridine (**11**) was found to be inaccessible by cuprate-mediated substitution of **7**, it was synthesized in two steps from tertiary alcohol **9**.^[33] Acid-catalyzed dehydration of **9** and subsequent hydrogenation of the resulting alkene **10** with Pd/C and H₂ afforded **11** in 51 % yield (Scheme 2).^[34]



Scheme 2. Synthesis of **11**: a) conc. AcOH/conc. H₂SO₄ (1:2.7), 150 °C, 30 min; b) Pd/C (5 mol%), H₂, MeOH, 16 h, 51 % over both steps.

The synthesis of 4-isopropylpyridine (**13**) and 4-(*tert*-butyl)-2-methylpyridine (**15**) was accomplished in a two-step reaction starting from **12** and **14**, respectively (Scheme 3). Treatment of **12** with AcCl and of **14** with PhOCOCl followed by addition of the respective organocuprates to the thus formed *N*-acyliminium intermediates provided, after oxidation, compounds **13** and **15** in 33 and 47 % yield, respectively.

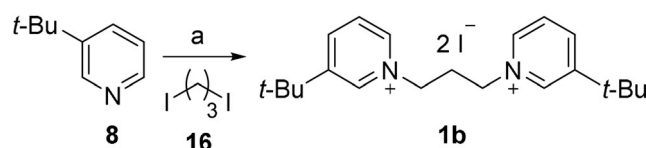


Scheme 3. Synthesis of **13** and **15**: a) AcCl (1.0 equiv), THF, –78 °C, 75 min, then (*i*Pr)₂CuCN(MgCl)₂ (1.1 equiv), 80 min; b) DDQ (1.0 equiv), CH₂Cl₂, RT, 70 min, 33 % over both steps; c) PhOCOCl (1.0 equiv), *t*BuZnBr (1.1 equiv), CuCN (1.1 equiv), LiCl (2.2 equiv), –78 °C for 5 h → RT for 16 h, THF; d) S₈ (1.1 equiv), naphthalene (15 equiv), 200 °C, 20 min, microwave: 300 W, 47 % over both steps.

Preparation of the target compounds

As mentioned above, the synthesis of symmetric bis(pyridinium) salts with a propane-1,3-diyl linker (Figure 2) is commonly accomplished by reaction of 1,3-diiodo- or 1,3-dibromopropane with an excess of the respective pyridine derivatives in DMF or MeCN at 70 °C.^[35–37] However, when these reaction conditions were used for the synthesis of compounds of type I and II, in most cases, only a negligible conversion but substantive decomposition of reactants occurred. This is mainly attributed to the low reactivity of the alkyl halides, especially when sterically hindered 2-substituted pyridine derivatives were used (**6**, **17**, **19**, **20**). Besides, in case of *N*-alkylated **22** and **24**, demethylation reactions by iodide ions also occurred. Notably, even

for the reaction of 1,3-diiodopropane (**16**) with 2.5 equivalents of the pyridine derivative **8**, devoid of any substituents at the 2- and 6-positions and of any electron-withdrawing groups, required 72 h at 70 °C in DMF for full conversion, affording **1b** in 79 % yield (Scheme 4).



Scheme 4. Synthesis of **1b**: 1,3-diiodopropane (**16**, 1.0 equiv), **8** (2.5 equiv), DMF, 70 °C, 72 h, 79 %.

Hence, 1,3-diiodopropane (Scheme 4) did not seem suitable for an efficient preparation of the desired target compounds. This problem could, however, be overcome using the far more reactive propane-1,3-diyl bis(trifluoromethanesulfonate) (**21**). With bistriflate **21**, compounds of type I–III (**1a**, **c–h**, Table 1;

Table 1. Synthesis of bispyridinium compounds of type I (**1a**, **c–h**).

Entry	Starting material R _{alkyl}	No.	T [°C]	t [min]	Product	Yield [%]
1	2- <i>t</i> Bu	17	85	300	1a	73
2	2- <i>i</i> Pr	6	50	5	1c	77
3	3- <i>i</i> Pr	11	50	2	1d	88
4	4- <i>i</i> Pr	13	50	60	1e	81
5	3,5-Me ₂	18	50	1	1f	69
6	2,6-Me ₂	19	70	1	1g	75
7	2,4,6-Me ₃	20	50	15	1h	81

Reagents and conditions: a) pyridine derivatives (2.5 equiv), **21** (1.0 equiv), no solvent, T, t.

2a–e, Table 2; **3a–l**, Table 3) were easily accessible in fair to excellent yields (47–99 %) by alkylation of the corresponding heterocycles. Reactions were performed either at 50 °C in CH₂Cl₂ or, if necessary, at higher temperatures without a solvent. Resulting bis(trifluoromethanesulfonate) salts were finally purified by crystallization without any problems.

In contrast to the above-mentioned alkylation reaction with 1,3-diiodopropane (**16**), the high reactivity of bistriflate **21** allowed short reaction times (1–30 min in most cases) and also gave access to bispyridinium compounds with sterically demanding substituents at the 2-position such as **1a**, **1c**, **1g**, **1h** (Table 1), and **3k** (Table 3).

Despite the high reactivity of bistriflate **21**, a variety of functional groups, that is, alkylarylethers (**2a–c**, **3e**), nitrile (**3d**), halide (**3a–c**), terminal alkyne (**3i**), ester (**3j**), amide (**3f**), and even secondary (**2d**) and tertiary amino substituents (**2e**) were

Table 2. Synthesis of bispyridinium compounds of type II (2a–e).

Entry	Starting material R _{polar}	No.	t [min]	Product	Yield [%]
1	2-OMe	22	1	2a	67
2	3-OMe	23	1	2b	83
3	4-OMe	24	1	2c	84
4	3-NMe ₂	25	10	2d	47
5	3-N-methylpyrrolidine	rac-26	30	2e	72

Reagents and conditions: a) pyridine derivatives (2.5 equiv), 21 (1.0 equiv), 50 °C, t; entry 1–4: no solvent; entry 5: reaction in CH₂Cl₂.

Table 3. Synthesis of bispyridinium compounds of type III (3a–l).

Entry	Starting material R	No.	t [min]	Product	Yield [%]
1	3-F	27 ^[b]	4	3a	85
2	3-Cl	28	30	3b	81
3	3-Br	29	30	3c	99
4	3-CN	30	40	3d	85
5	3-OMe	31	5	3e	83
6	3-CONMe ₂	32	30	3f	77
7	3-Me	33	20	3g	89
8	3-Ph	34	30	3h	99
9	3-C≡CH	35	40	3i	91
10	3-COOEt	36	30	3j	98
11	2-Me	15	30	3k	82
12 ^[a]	3-COOEt	3j	16 h	3l	66

Reagents and conditions: a) pyridine derivatives (2.5 equiv), 21 (1.0 equiv), CH₂Cl₂, 50 °C, t. [a] Compound 3l was synthesized from 3j (1.0 equiv) in 66% yield by basic hydrolysis using aqueous NaOH (0.1 M, 2.5 equiv) in H₂O/MeCN (5:1) at RT for 16 h. [b] 4-(tert-butyl)-3-fluoropyridine was released in situ from the corresponding hydrochloride 27.

well tolerated. Also, the carboxylic acid **3l** (Table 3, entry 12) could be synthesized by basic hydrolysis of the ester function of **3j** with aqueous NaOH. To this end, however, milder conditions had to be used (hydroxide ion concentration of only 0.055 M), to minimize a Zincke–König type cleavage, thus affording **3l** in 66% yield after crystallization.

Although biological evaluation of synthesized bispyridinium salts **1a–h** (Table 1), **2a–e** (Table 2), and **3a–l** (Table 3) using our MS Binding Assays yielded reliable results, the triflate counterion was assumed to cause interference in electrophysiological measurements on the SURFE²R platform.^[38] Thus, we

decided to synthesize compounds of type IV with iodide instead of triflate counterions.

Therefore, compounds **4a–e** were synthesized by reaction of the respective N-heteroaromatics **37–41** with 1,3-diiodopropane (**16**) in MeCN under microwave heating at 90–120 °C. The yields were good to excellent (78–92%, Table 4). Under microwave conditions, higher reaction temperatures could be reached, resulting in distinctly reduced reaction times. Moreover, side reactions appeared to be absent this time.

Table 4. Synthesis of non-bispyridinium compounds of type IV (4a–e).

Table 4. Synthesis of non-bispyridinium compounds of type IV (14-17).						
37-41		4a-e				
Entry	Starting material N _{het.}	No.	T [°C]	t [h]	Product	Yield [%]
1		37	90	3	4a	86
2		38	120	16	4b	78
3		39	120	16	4c	87
4		40	90	1	4d	92
5		41	90	1	4e	82

Reagents and conditions: a) N_{het.} (2.5 equiv), **16** (1.0 equiv), MeCN, T, t, microwave: 150 W.

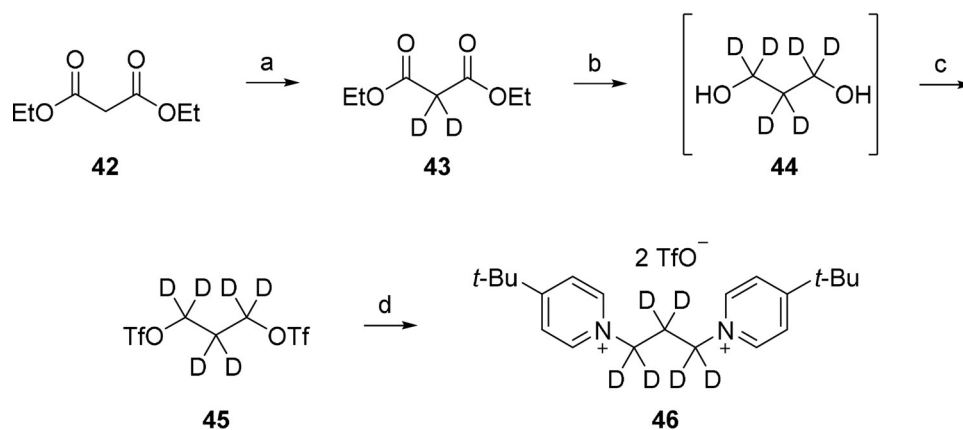
The solubility of compounds of type I–IV in water proved to be sufficient for biological testing and allowed the preparation of solutions with concentrations of at least 2.5 mM. Interestingly, a faster dissolution in water was observed for triflate salts of type I–III relative to iodide salts of type IV.

To evaluate the stability of synthesized target compounds in water, NMR measurements of a random selection of compounds (**1b**, **2a**, **2c**, **3d**, and **3l**) after 12 h incubation in D₂O at room temperature were performed and provided no indications for hydrolysis.

Preparation of deuterated MB327 analogues for MS Binding Assays

For the recently established MS Binding Assays targeting the MB327 binding site at *T. californica* nAChR, deuterated MB327 analogues [²H₆]MB327 (**46**) and [²H₁₈]MB327 (**49**) were required as MS marker and internal standard, respectively. Their synthesis was accomplished as follows.

The deuterium-labeled compound **46** was synthesized in four steps starting from malonic ester **42** in an overall yield of



Scheme 5. Synthesis of $[^2\text{H}_6]\text{MB327}$ (**46**): a) pyridine (6.0 equiv), D_2O (12 equiv), RT, 20 h, 40%, <99.6% D; b) LiAlD_4 (3.0 equiv), Et_2O , 50°C , 5.5 h; c) Tf_2O (2.0 equiv), pyridine (2.0 equiv), CH_2Cl_2 , $-78^\circ\text{C} \rightarrow \text{RT}$, 3 h, 58% over both steps; d) 4-*tert*-butylpyridine (2.5 equiv), CH_2Cl_2 , 50°C , 30 min, 77%, 99% D.

18% and a deuteration degree of $\geq 99\%$ (Scheme 5). At first, **42** was treated with D_2O and pyridine according to Cocker et al., affording the D_2 derivative **43** in 40% yield.^[39] Reduction with LiAlD_4 in Et_2O and subsequent treatment of crude $[\text{D}_6]\text{propanediol}$ **44** with Tf_2O provided the corresponding bis-triflate **45** in 58% yield over both steps. Reaction of **45** with 2.5 equivalents 4-*tert*-butylpyridine finally afforded **46** in a yield of 77%.

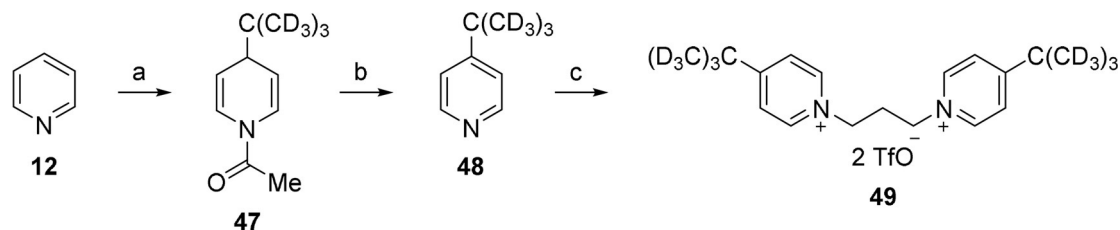
The synthesis of $[^2\text{H}_{18}]\text{MB327}$ (**49**) started from pyridine (**12**) and was performed in three steps, the total yield amounting to 25% and the deuteration degree to $\geq 99\%$ (Scheme 6). In the first step, pyridine (**12**) was treated with AcCl to generate the corresponding *N*-acetylpyridinium ion in situ, which upon trapping with $(t\text{Bu})_2\text{CuCN}(\text{MgCl})_2$, afforded **47** with good regioselectivity (79:21 for C4 isomer). Oxidation of 1,4-dihydropyridine **47** with DDQ led to D_9 -labeled pyridine **48** in 31% yield, which upon reaction of triflate **21** with 2.5 equivalents, provided **49** in 81% yield.

Biological evaluation

All target compounds synthesized in the context of this study were catalogued with a certain PTM number (Pharmacy and Toxicology Munich). Binding affinities toward the **MB327** binding site at *T. californica* nAChR were determined in MS Binding Assays using $[^2\text{H}_6]\text{MB327}$ (**46**) as marker (Table 5).^[24]

With these MS Binding Assays, developed recently in our research group, it was possible to characterize the binding of **MB327** at the nAChR ($\text{p}K_i = 4.75 \pm 0.07$ for **MB327** in auto-com-

petition experiments with $[^2\text{H}_6]\text{MB327}$ (**46**) as marker). According to the corresponding experimental protocol, aliquots of nAChR-enriched membranes, prepared from *T. californica* electropore tissue and frozen in storage buffer (120 mM NaCl, 5 mM KCl, 8.05 mM Na_2HPO_4 , and 1.95 mM NaH_2PO_4 , pH 7.4) were thawed, directly diluted with incubation buffer, and incubated in the presence of the marker (and test compounds if required). Both buffers—storage and incubation buffer—are almost identical in this assay, except that the latter also contains 1 mM CaCl_2 . With the aim to simplify the developed MS Binding Assays, we examined the possibility of using only one buffer for the whole procedure, that is, for the storage of *Torpedo* membrane preparations as well as for incubation in the binding experiments described herein. Because the storage buffer, differing from the incubation buffer by the lack of CaCl_2 , was also identical to the incubation buffer that had been used in $[^3\text{H}]\text{epibatidine}$ binding studies,^[18,38] which were conducted recently for characterization of bispyridinium compounds at the orthosteric binding site of the *T. californica* nAChR, it appeared obvious to choose this buffer for incubation in $[^2\text{H}_6]\text{MB327}$ MS Binding Assays as well. Hence, saturation and auto-competition experiments were conducted exactly as described previously,^[24] but also using the storage buffer for incubation of binding samples. Under these marginally modified conditions, we found a K_d value of $14.2 \pm 1.4 \mu\text{M}$ and a B_{max} value of $263 \pm 30 \text{ pmol}[\text{mg protein}]^{-1}$ ($n=3$) in saturation experiments using $[^2\text{H}_6]\text{MB327}$ (**46**) as marker and a $\text{p}K_i$ of 4.73 ± 0.03 ($K_i = 18.7 \pm 1.2 \mu\text{M}$, $n=3$) for auto-competition experiments using $[^2\text{H}_6]\text{MB327}$ (**46**) as marker and native **MB327**



Scheme 6. Synthesis of $[^2\text{H}_{18}]\text{MB327}$ (**49**): a) AcCl (1.0 equiv), THF, -78°C , 60 min, then $[\text{D}_9]\text{tBuMgCl}$ (2.2 equiv), CuCN (1.1 equiv), THF, -78°C , 1.5 h; b) DDQ (1.0 equiv), CH_2Cl_2 , RT, 1 h, 31% over both steps; c) **21** (0.4 equiv), 50°C , 2.5 h, 81%, 99% D.

Table 5. Structures of synthesized target substances and binding affinities to the **MB327** binding site.

<div style="display: flex; justify-content: space-around; align-items: flex-start;"> <div style="text-align: center;"> Type I: 1a–h </div> <div style="text-align: center;"> Type II: 2a–e </div> </div>				
<div style="display: flex; justify-content: space-around; align-items: flex-start;"> <div style="text-align: center;"> Type III: 3a–l </div> <div style="text-align: center;"> Type IV: 4a–e </div> </div>				
Entry	Compound	R _{alkyl} /R _{polar} /R/N _{het}	pK _i ^[a]	PTM code
1	MB327	4- <i>t</i> Bu	4.73 ± 0.03	
2	1a	2- <i>t</i> Bu	4.43 ± 0.12	0002
3	1b	3- <i>t</i> Bu	4.44 ± 0.10	0001
4	1c	2- <i>i</i> Pr	3.83 ± 0.11*	0003
5	1d	3- <i>i</i> Pr	4.18 ± 0.11	0014
6	1e	4- <i>i</i> Pr	4.27 ± 0.11	0013
7	1f	3,5-Me ₂	3.76 ± 0.14*	0005
8	1g	2,6-Me ₂	3.80 ± 0.04*	0004
9	1h	2,4,6-Me ₃	4.30 ± 0.09	0006
10	2a	2-OMe	3.87 ± 0.13*	0010
11	2b	3-OMe	3.79 ± 0.09*	0009
12	2c	4-OMe	3.97 ± 0.04*	0008
13	2d	3-NMe ₂	4.78 ± 0.05	0007
14	2e	3- <i>N</i> -methylpyrrolidine	3.63 ± 0.13*	0027
15	3a	3-F	4.23 ± 0.05*	0021
16	3b	3-Cl	4.54 ± 0.09	0020
17	3c	3-Br	4.62 ± 0.08	0018
18	3d	3-CN	4.00 ± 0.12*	0019
19	3e	3-OMe	4.46 ± 0.07	0016
20	3f	3-CONMe ₂	4.43 ± 0.10	0024
21	3g	3-Me	4.57 ± 0.08	0017
22	3h	3-Ph	5.16 ± 0.07*	0022
23	3i	3-C≡CH	4.80 ± 0.08	0025
24	3j	3-COOEt	4.50 ± 0.04	0015
25	3k	2-Me	4.31 ± 0.09	0023
26	3l	3-COOH	2.74 ± 0.13*	0028
27	4a	isoquinoline	4.77 ± 0.06	0032
28	4b	2- <i>tert</i> -butylpyrazine	3.56 ± 0.09*	0057
29	4c	1,3-thiazole	4.07 ± 0.13	0033
30	4d	<i>N</i> -methylimidazole	3.55 ± 0.11*	0034
31	4e	<i>N</i> - <i>tert</i> -butylimidazole	4.34 ± 0.13	0059

[a] Data are the mean ± SEM of three independent experiments. Statistically significant pK_i values relative to the binding affinity of **MB327** are indicated by an asterisk (verified by two-sided *t*-test, using a 5% significance level).

as competitor (see the Supporting Information for further details). As there was no significant difference (verified by two-sided *t*-test) between the affinity constants, obtained in experiments with CaCl₂ as opposed to experiments without CaCl₂ in the incubation buffer,^[24] we decided to use the CaCl₂-free storage buffer also as incubation buffer in all binding experiments.

Although this marginal modification of the sample matrix was not expected to affect the quantification of the MS marker, we still decided to again examine the parameters of selectivity, linearity, lower limit of quantification (LLOQ), accuracy, as well as precision of the LC–ESI–MS/MS quantification

method according to the FDA's guidance on bioanalytical method validation.^[40] In short, all requirements of the Center for Drug Evaluation and Research (CDER) guideline of the FDA regarding the above-mentioned parameters were fulfilled (see the Supporting Information for further details), clearly demonstrating the LC–ESI–MS/MS quantification to be robust and reliable also under these binding conditions. This modified protocol for [²H₆]MB327 MS Binding Assays (see the Experimental Section below) was finally used for all further determinations of binding affinities of target compounds.

Initially, the influence of the position of the *tert*-butyl substituent on the binding affinity was investigated by comparing the pK_i value of 2-*tert*-butyl- and 3-*tert*-butyl-substituted compounds **1a** (PTM0002) and **1b** (PTM0001) (type I) with that of 4-*tert*-butyl-substituted **MB327** (Table 5, entries 1–3). Interestingly, the difference between both 2- and 3-regioisomers was negligible, but binding affinity decreased if the *tert*-butyl group was moved from the 4- to the 3- or 2-position. Moreover, reduction of the steric demand of the lipophilic substituent by replacing the *tert*-butyl group in **MB327**, **1a** (PTM0002) and **1b** (PTM0001) with an isopropyl group (**1c–e**, PTM0003, PTM0013, PTM0014, entries 4–6) led to a distinct decrease in binding affinity, except for the 3-substituted compounds, where the difference was less pronounced. A decrease in binding affinity was also observed for the lutidine- (**1f**, **1g**, PTM0005 and PTM0004, entries 7 and 8) and collidine-derived bispyridinium salts (**1h**, PTM0006, entry 9), especially if the 4-position remained unsubstituted (**1f**, PTM0005: 3,5-Me₂, $pK_i = 3.76 \pm 0.14$; **1g**, PTM0004: 2,6-Me₂, $pK_i = 3.80 \pm 0.04$; **1h**, PTM0006: 2,4,6-Me₃, $pK_i = 4.30 \pm 0.09$ relative to **MB327**: $pK_i = 4.73 \pm 0.03$; see Table 5 entries 1 and 7–9).

Comparing the affinities of the bispyridinium salts substituted with lipophilic (type I, Table 5, entries 1–9) with those substituted with polar residues of type II (Table 5, entries 10–14), it becomes clear that replacement of the alkyl substituents with an *N*-methylpyrrolidine moiety at the 3-position (**2e**, PTM0027) or a polar methoxy group (**2a–c**, PTM0008–PTM0010) in the 2-, 3-, or 4-positions has a negative influence on binding affinity. The determined pK_i values range from 3.87 ± 0.13 to 3.97 ± 0.04 and are thus at least about half a log unit lower than those found for the *tert*-butyl-substituted compounds **1a** (PTM0002), **1b** (PTM0001) and **MB327** ($pK_i = 4.43 \pm 0.12$ to 4.73 ± 0.03 , Table 5, entries 1–3). In contrast, the 3-dimethylamino-substituted bispyridinium salt **2d** (PTM0007) showed a higher pK_i value (4.78 ± 0.05 , Table 5, entry 13) than the 3-*tert*-butyl-substituted compound **1b** (PTM0001, $pK_i = 4.44 \pm 0.10$, Table 5, entry 3). In conclusion, the NMe₂ group is suggested as potential substitute for the *tert*-butyl substituent.

The binding affinities of type III compounds exhibiting a F, Cl, Br, CN, OMe, CONMe₂, Me, C≡CH, or COOEt substituent at the 3-position (Table 5, entries 15–21 and 23–25) in addition to the 4-*tert* butyl group in **MB327** varied from 4.00 ± 0.12 in case of 3-CN derivative **3d** (PTM0019, Table 5, entry 18) to 4.80 ± 0.08 for 3-alkyne-substituted **3i** (PTM0025, Table 5, entry 23) without a clear tendency when regarding the nature of the substituent.

However, the results indicate that the 4-*tert*-butyl group in the bispyridinium salts has a beneficial effect on binding affinity. This becomes evident by comparing the pK_i value of 4-*tert*-butyl-substituted **MB327** ($pK_i = 4.73 \pm 0.03$, Table 5, entry 1) with those of 3-methoxy substituted **2b** (PTM0009, $pK_i = 3.79 \pm 0.09$, Table 5, entry 11) and 4-*tert*-butyl-3-methoxy derivative **3e** (PTM0016, $pK_i = 4.46 \pm 0.07$). Apparently, the addition of a *tert*-butyl group at the 4-position increased the binding affinity of the 3-methoxy derivative **2b** (PTM0009) by 0.67 log units from 3.79 ± 0.09 to 4.46 ± 0.07 for **3e** (PTM0016, compare Table 5, entries 11 and 19).

In accordance with the negative effect of polar substituents on binding affinity as discussed above, zwitterionic carboxylic acid **3l** (PTM0028) exhibited the lowest binding affinity of all tested compounds, with a pK_i value of 2.74 ± 0.13 (Table 5, entry 26). The highest binding affinity, on the other hand, was displayed by the lipophilic 3-phenyl-substituted **MB327** analogue **3h** (PTM0022), with a pK_i value of 5.16 ± 0.07 (Table 5, entry 22), which is about half a log unit higher than the pK_i value of **MB327** (Table 5, entry 1) and two and a half orders of magnitude above that found for carboxylic acid **3l** (PTM0028, Table 5, entry 26). The statistical significance of the higher affinity found for the phenyl-substituted derivative **3h** (PTM0022) relative to **MB327** was also verified by two-sided *t*-test (5% significance level). The two additional aromatic phenylpyridinium rings present in **3h** (PTM0022) are likely to be involved in lipophilic interactions with the target, giving rise to increased affinity.

According to the pK_i values found for the non-bispyridinium compounds of type IV (**4a–e**, PTM0032–PTM0034, PTM0057, PTM0059, entries 27–31) none of the heterocyclic systems studied revealed a significantly higher binding affinity than **MB327**. Interestingly, electron-poor 2-*tert*-butylpyrazinium salt **4b** (PTM0057, $pK_i = 3.56 \pm 0.09$, Table 5, entry 28) showed a clearly lower pK_i value than the structurally related but far less electron-deficient 3-*tert*-butylpyridinium salt **1b** (PTM0001, $pK_i = 4.44 \pm 0.10$, Table 5, entry 3). Binding affinity of bisimidazolium salts decreased significantly upon transition from *N*-*tert*-butyl-substituted **4e** (PTM0059, $pK_i = 4.34 \pm 0.13$, Table 5, entry 31) to *N*-methyl-substituted **4d** (PTM0034, $pK_i = 3.55 \pm 0.11$, Table 5, entry 30). This indicates a general beneficial effect of the *tert*-butyl group over smaller groups that had similarly been observed for the bispyridinium salts (compare, for example, **MB327** with **1e** (PTM0013), Table 5, entries 1 and 6). Although being unsubstituted and hence smaller than the *N*-methylimidazole derivative **4d** (PTM0034, Table 5, entry 30), the 1,3-thiazole-derived compound **4c** (PTM0033) still had a reasonable affinity ($pK_i = 4.07 \pm 0.13$, Table 5, entry 29).

Interestingly, bis(isoquinolinium) salt **4a** (PTM0032, $pK_i = 4.77 \pm 0.06$), which is able to undergo more extensive lipophilic interactions, was found to have the highest binding affinity of all non-bispyridinium compounds, being in the same range as the binding affinity of **MB327**. Altogether, the substitution of bispyridinium compounds by the addition of polar but uncharged functional groups generally led to a slight decrease in binding affinity, whereas the addition of a carboxylic acid function decreased binding affinity dramatically (**3l**, PTM0028, Table 5, entry 26). The sole exception is the 3-dimethylamino-substituted bispyridinium compound **2d** (PTM0007, Table 5, entry 13), which shows a slightly increased binding affinity relative to **MB327** (Table 5, entry 1).

Notably, more lipophilic 3-phenyl-4-*tert*-butyl-substituted bispyridinium salt **3h** (PTM0022, $pK_i = 5.16 \pm 0.07$, Table 5, entry 22) revealed the highest binding affinity of all bispyridinium salts tested so far, representing important progress in the development of new nAChR re-sensitizers with improved potency, although its pharmacological effects remain to be determined. Very recently, Wein et al. described the putative binding

site as being composed of two subdomains, one of which is lined with more hydrophilic and the other with more lipophilic residues.^[23] Accordingly, the design of non-symmetric compounds displaying two different polar termini, one with higher and the other with lower polarity, could be a promising strategy for increasing binding affinity.

Conclusions

In summary, a set of 30 symmetric bispyridinium and related salts with a propane-1,3-diyl linker were synthesized and characterized for their binding affinity for the **MB327** binding site at the *T. californica* nAChR. Binding affinities were determined using our recently developed MS Binding Assays and discussed regarding **MB327**'s binding affinity, the most potent nAChR re-sensitizer so far, as reference. To the best of our knowledge, this is the first study to provide quantitative binding data for the **MB327** binding site, which, in turn, should be useful for further developments in the structure- and ligand-based design of nAChR re-sensitizers.

All target compounds were synthesized via N-alkylation of the respective aromatic *N*-heterocycles using either propane-1,3-ditriflate or propane-1,3-diiodide as alkylating agents. Optimized reaction conditions allowed very rapid and clean reactions in the presence of a wide variety of functional groups. Being also well suited for the alkylation of less reactive nitrogen heterocycles, such as sterically hindered 2-*tert*-butylpyridine or electron-deficient 2-*tert*-butylpyrazine, makes both methods highly valuable for organic synthesis.

Regarding structure–affinity relationships, the influence of various lipophilic and hydrophilic functional groups as well as of different heterocycles on the binding affinity of the bisquaternary salts was investigated. Notably, molecular structures allowing additional lipophilic interactions were found to play a vital role in the binding event. In line with this observation, lipophilic 3-phenyl-4-*tert*-butyl-substituted bispyridinium compound **3h** (PTM0022) was found to possess a significantly improved binding affinity relative to **MB327**.

Furthermore, differences in binding affinities were found between polar (OMe, NMe₂, COOEt, etc.) and apolar (C≡CH, Me, *i*Pr, etc.) substituted compounds, generally revealing higher binding affinities for the less polar derivatives. Interestingly, NMe₂ was identified to be the only notable exception, revealing better results than most apolar substituted compounds. As a consequence, the role of hydrogen bridge acceptors on the binding affinity is worthy of more detailed investigation.

Finally, there is compelling evidence that anionic functional groups have a distinct negative influence on the binding process, as the addition of two carboxylic acid functions to the structure of **MB327** resulted in a severe decrease in binding affinity (**3i**, PTM0028). To gain deeper insight into the interaction of bisquaternary salts with the **MB327** binding site at the nAChR, further studies based on structurally more diverse non-symmetric bispyridinium compounds are underway.

Experimental Section

Chemistry

Anhydrous reactions were carried out in vacuum-dried glassware under argon atmosphere. Microwave reactions were performed in sealed glass vials using a CEM Discover SP microwave synthesizer. THF, 1,4-dioxane and CH₂Cl₂ were distilled prior to use under nitrogen atmosphere and dried according to standard procedures.^[41] Et₂O (technical grade) was purified by distillation and dried by holding at reflux for 6 h over sodium without benzophenone under nitrogen atmosphere before being distilled once again prior to use. All other chemicals were used as purchased from commercial sources and solvents were distilled before use. TLC was carried out using plates purchased from Merck (silica gel 60F₂₅₄ on aluminum sheet). Flash chromatography (FC) was performed using Merck silica gel 60 (40–63 μm mesh size) as stationary phase. Melting points were determined with a BÜCHI 510 melting point apparatus and are uncorrected. IR spectroscopy was performed using an FT-IR Spectrometer 1600 and Paragon 1000 (PerkinElmer); oils were measured as film and solid samples as KBr pellets. High-resolution (HR) mass spectrometry was performed on a Finnigan MAT 95 (EI), Finnigan LTQ FT (ESI) and Jeol JMS 700 MStation (FAB). ¹H and ¹³C NMR spectra were recorded with a Bruker BioSpin Avance III HD 400 and 500 MHz (equipped with a Prodigy™ cryoprobe) using TMS as internal standard and integrated with MestReNova (Version 10.0.2), Mestrelab Research S.L. 2015. The purity of the test compounds was determined by means of quantitative NMR using Sigma Aldrich TraceCERT® maleic acid or dimethylsulfone as internal calibrants.^[42, 43] The purity of all tested compounds was >95%. See the Supporting Information for the characterization data of the described compounds.

The following compounds were prepared according to published methods: propane-1,3-diyl bis(trifluoromethanesulfonate) (**21**),^[44, 45] 2-*tert*-butylpyridine (**17**),^[27] 2-(pyridin-3-yl)propan-2-ol (**9**),^[33] *rac*-nicotine (*rac*-**26**),^[28] 1-(*tert*-butyl)-1*H*-imidazole (**41**)^[29] and the 4-*tert*-butyl-substituted pyridine derivatives 4-(*tert*-butyl)-3-methylpyridine (**33**), 4-(*tert*-butyl)-3-methoxypyridine (**31**), 4-(*tert*-butyl)-3-chloropyridine (**28**), 3-bromo-4-(*tert*-butyl)pyridine (**29**), 4-(*tert*-butyl)pyridine-3-carbonitrile (**30**), ethyl 4-(*tert*-butyl)pyridine-3-carboxylate (**36**), 4-(*tert*-butyl)-3-fluoropyridin-1-ium chloride (**27**), 4-(*tert*-butyl)-3-phenylpyridine (**34**), 4-(*tert*-butyl)-*N,N*-dimethylpyridine-3-carboxamide (**32**), and 4-(*tert*-butyl)-3-ethynylpyridine (**35**).^[30]

General procedures

Synthesis of symmetric bispyridinium compounds by N-alkylation with 21 (GP1): **21** (1.0 equiv) was carefully added to a solution of the corresponding pyridine derivative (2.5 equiv) in CH₂Cl₂ (0.8 mL mmol^{−1}) or to the neat pyridine derivative (2.5 equiv) at room temperature. The resulting mixture was stirred at 50 °C for the indicated period and residual CH₂Cl₂ was removed in vacuo if necessary. The residue was finally recrystallized from the given solvent.

Synthesis of symmetric bispyridinium compounds by N-alkylation with 16 (GP2): **16** (1.0 equiv) was added to a solution of the corresponding aromatic nitrogen heterocycle (2.5 equiv) in MeCN (0.8 mL mmol^{−1}) and the resulting mixture was heated at 90 °C (150 W) in a sealed microwave reactor for the indicated period. The solvent was removed in vacuo and the residue was recrystallized from the given solvent.

Synthesis of 2- and 3-alkylpyridines by cuprate-mediated substitution reactions of 2- and 3-bromopyridines (GP3): The corresponding bromopyridine derivative (1.0 equiv) was added dropwise to a suspension of the respective dialkylcuprate (4.0 equiv, prepared according to GP4) in THF or Et₂O at -78°C . The reaction mixture was stirred for 2 h at -78°C before being allowed to stir for additional 15 h at room temperature. The mixture was cooled to 0°C and the reaction was quenched by addition of saturated aqueous NH₄Cl/conc. NH₃ (1:1, 8 mL mmol⁻¹). The mixture was filtrated over Celite® and the residue was alternately washed with Et₂O (3×5 mL mmol⁻¹) and saturated aqueous NaCl (2×5 mL mmol⁻¹). The layers were separated, and the organic phase was washed with saturated aqueous NaCl solution (10 mL mmol⁻¹). The combined aqueous layers were extracted with Et₂O (3×10 mL mmol⁻¹) and the combined organic layers were dried over MgSO₄. The solvent was carefully removed under reduced pressure (40°C bath temperature, 450 mbar) and the resulting crude product was purified in a first step by FC and subsequently by a vacuum distillation (5×10^{-2} mbar at 200°C). The pure alkylpyridine was obtained as a colorless liquid.

Preparation of (iPr)₂CuCN(MgCl)₂, (tBu)₂CuCN(MgCl)₂, and ([D₃]tBu)₂CuCN(MgCl)₂ (GP4): The corresponding Grignard reagent (solution in Et₂O or THF, 2.0 equiv) was added to a suspension of CuCN (1.0 equiv) in Et₂O or THF (2.0–4.5 mL mmol⁻¹) at -78°C and the resulting mixture was stirred for 45 min at -78°C , for 5 min at room temperature and again for 10 min at -78°C .

Preparation of tBuCu(CN)ZnBr·2LiCl: tBuZnBr (0.5 M solution in THF, 11.0 mmol, 22.0 mL, 1.0 equiv) was added to a solution of CuCN (995 mg, 11.0 mmol, 1.0 equiv) and LiCl (933 mg, 22.0 mmol, 2.0 equiv) in THF (50 mL) at -10°C and the resulting 0.15 M cuprate suspension was stirred for 10 min at 0 and -78°C each.

Synthesized compounds

Pyridine derivatives: 3-*tert*-Butylpyridine (**8**, colorless liquid, 43%), 3-isopropylpyridine (**11**, colorless and highly volatile liquid, 51%), 2-isopropylpyridine (**6**, colorless liquid, 20%), 4-isopropylpyridine (**13**, clear and highly volatile liquid, 33%), 4-(*tert*-butyl)-2-methylpyridine (**15**, colorless liquid, 47%).

Compounds of type I (1a–h): 1,1'-(Propane-1,3-diyl)bis[2-(*tert*-butyl)pyridin-1-ium] bis(trifluoromethanesulfonate) (**1a**, colorless solid, 73%), 1,1'-(propane-1,3-diyl)bis[3-(*tert*-butyl)pyridin-1-ium] diiodide (**1b**, yellow crystals, 79%), 1,1'-(propane-1,3-diyl)bis(2-isopropylpyridin-1-ium) bis(trifluoromethanesulfonate) (**1c**, colorless solid, 77%), 1,1'-(propane-1,3-diyl)bis(3-isopropylpyridin-1-ium) bis(trifluoromethanesulfonate) (**1d**, colorless solid, 88%), 1,1'-(propane-1,3-diyl)bis(4-isopropylpyridin-1-ium) bis(trifluoromethanesulfonate) (**1e**, colorless solid, 81%), 1,1'-(propane-1,3-diyl)bis(3,5-dimethylpyridin-1-ium) bis(trifluoromethanesulfonate) (**1f**, colorless solid, 69%), 1,1'-(propane-1,3-diyl)bis(2,6-dimethylpyridin-1-ium) bis(trifluoromethanesulfonate) (**1g**, colorless solid, 75%), 1,1'-(propane-1,3-diyl)bis(2,4,6-trimethylpyridin-1-ium) bis(trifluoromethanesulfonate) (**1h**, colorless solid, 81%).

Compounds of type II (2a–e): 1,1'-(Propane-1,3-diyl)bis(2-methoxy-pyridin-1-ium) bis(trifluoromethanesulfonate) (**2a**, colorless solid, 67%), 1,1'-(propane-1,3-diyl)bis(3-methoxypyridin-1-ium) bis(trifluoro-methanesulfonate) (**2b**, colorless solid, 83%), 1,1'-(propane-1,3-diyl)bis(4-methoxypyridin-1-ium) bis(trifluoromethanesulfonate) (**2c**, colorless solid, 84%), 1,1'-(propane-1,3-diyl)bis[3-(dimethylamino)pyridin-1-ium] bis-(trifluoromethanesulfonate) (**2d**, yellowish solid, 47%), *rac*-{1,1'-(propane-1,3-diyl)bis[3-(1-methylpyrrolidin-2-

yl)pyridin-1-ium]} bis(trifluoromethane-sulfonate) (**2e**, yellowish solid, 72%).

Compounds of type III (3a–l): 1,1'-(Propane-1,3-diyl)bis[4-(*tert*-butyl)-3-fluoropyridin-1-ium] bis(trifluoromethanesulfonate) (**3a**, colorless solid, 85%), 1,1'-(propane-1,3-diyl)bis[4-(*tert*-butyl)-3-chloropyridin-1-ium] bis-(trifluoromethanesulfonate) (**3b**, colorless solid, 81%), 1,1'-(propane-1,3-diyl)bis[3-bromo-4-(*tert*-butyl)pyridin-1-ium] bis(trifluoromethanesulfonate) (**3c**, colorless solid, 99%), 1,1'-(propane-1,3-diyl)bis[4-(*tert*-butyl)-3-cyanopyridin-1-ium] bis(trifluoromethanesulfonate) (**3d**, slightly beige solid, 85%), 1,1'-(propane-1,3-diyl)bis[4-(*tert*-butyl)-3-methoxypyridin-1-ium] bis(trifluoromethanesulfonate) (**3e**, colorless solid, 83%), 1,1'-(propane-1,3-diyl)-bis[4-(*tert*-butyl)-3-(dimethylcarbamoyl)-pyridin-1-ium] bis-(trifluoromethanesulfonate) (**3f**, colorless solid, 77%), 1,1'-(propane-1,3-diyl)bis[4-(*tert*-butyl)-3-methylpyridin-1-ium] bis(trifluoromethanesulfonate) (**3g**, colorless solid, 89%), 1,1'-(propane-1,3-diyl)bis[4-(*tert*-butyl)-3-phenylpyridin-1-ium] bis(trifluoromethanesulfonate) (**3h**, colorless solid, 99%), 1,1'-(propane-1,3-diyl)bis[4-(*tert*-butyl)-3-ethynylpyridin-1-ium] bis-(trifluoromethanesulfonate) (**3i**, colorless solid, 91%), 1,1'-(propane-1,3-diyl)bis[4-(*tert*-butyl)-3-(ethoxycarbonyl)pyridin-1-ium] bis(trifluoro-methanesulfonate) (**3j**, colorless solid, 98%), 1,1'-(propane-1,3-diyl)bis[4-(*tert*-butyl)-2-methylpyridin-1-ium] bis(trifluoromethanesulfonate) (**3k**, colorless solid, 82%), 4-(*tert*-butyl)-1-[3-[4-(*tert*-butyl)-3-carboxypyridin-1-ium-1-yl]propyl]-pyridin-1-ium-3-carboxylate trifluoromethanesulfonate (**3l**, colorless solid, 66%).

Compounds of type IV (4a–e): 2,2'-(Propane-1,3-diyl)bis(isoquinolin-2-ium) diiodide (**4a**, yellow solid, 86%), 1,1'-(propane-1,3-diyl)-bis[3-(*tert*-butyl)pyrazin-1-ium] diiodide (**4b**, yellow powder, 78%), 3,3'-(propane-1,3-diyl)bis(thiazol-3-ium) diiodide (**4c**, beige solid, 87%), 3,3'-(propane-1,3-diyl)bis(1-methyl-1*H*-imidazol-3-ium) diiodide (**4d**, colorless solid, 92%), 3,3'-(propane-1,3-diyl)bis[1-(*tert*-butyl)-1*H*-imidazol-3-ium] diiodide (**4e**, colorless solid, 82%).

Deuterated compounds: 4-(2-[²H₃]Methyl[1,1,1,3,3,3-²H₆]propan-2-yl)pyridine (**48**, colorless liquid, 31%), 1,1'-(propane-1,3-diyl)bis[4-(2-[²H₃]methyl[1,1,1,3,3,3-²H₆]propan-2-yl)pyridin-1-ium] bis(trifluoro-methanesulfonate) (**49**, colorless solid, 81%), diethyl [²H₅]malonate (**43**, colorless liquid, 40%), [²H₆]propane-1,3-diol (**44**) and [²H₆]propane-1,3-diyl bis(trifluoromethanesulfonate) (**45**, grayish and turbid oil, 58%), 1,1'-(²H₆]propane-1,3-diyl)bis[4-(*tert*-butyl)-pyridin-1-ium] bis(trifluoromethane-sulfonate) (**46**, colorless solid, 77%).

Biological evaluation

General procedure for [²H₆]MB327 MS Binding Assays: Membranes from frozen *Torpedo californica* electroplaque tissue were prepared as previously reported and stored in storage buffer (120 mM NaCl, 5 mM KCl, 8.05 mM Na₂HPO₄, 1.95 mM NaH₂PO₄, pH 7.4).^[24] Total protein concentration was determined by the bicinchoninic acid method using bovine serum albumin as standard.^[46] All binding experiments were performed as described previously,^[24] but in absence of CaCl₂ during incubation. For saturation and competition experiments, aliquots of the membrane preparation (60–120 µg protein per sample) were incubated with [²H₆]MB327 (**46**) as marker (saturation: 2–160 µM, competition: 10 µM) in triplicates in storage buffer in a total volume of 125 µL for 2 h at 25°C . In competition experiments the concentrations of the competitors ranged from 100 nM to 1 mM. After incubation, binding samples were processed exactly as previously described.^[22] In saturation experiments, the maximum density of binding sites (*B*_{max}) and the equilibrium dissociation constant (*K*_d) were deter-

mined from saturation isotherms calculated for specific binding using the “one-site—specific binding” regression tool (Prism ver. 5.0, GraphPad Software, La Jolla, CA, USA). Competition curves were analyzed with the “one-site-fit K_i ” regression tool fixing top and bottom level of the sigmoidal competition curves to total binding (in absence of competitor, $n=3$) and nonspecific binding (determined by heat denaturation, $n=3$). For statistical comparisons, data were examined by means of a t -test (two-sided, $\alpha=0.05$). If not stated otherwise, results are given as means \pm SEM.

Validation of the LC-ESI-MS/MS quantification method: In accordance with the FDA’s guidance for bioanalytical method validation selectivity, lower limit of quantification (LLOQ), linearity, precision, and accuracy were investigated exactly in the same way as described for marker quantification in binding samples resulting from incubation in presence of 1 mM CaCl_2 .^[24]

Supporting Information

Synthetic procedures and analytical characterization of all compounds as well as details of the improved MS Binding Assay protocol and validation data can be found in the Supporting Information.

Acknowledgements

This study was funded by the German Ministry of Defense (E/U2AD/CF514/DF561).

Conflict of interest

The authors declare no conflict of interest.

Keywords: bispyridinium • drug design • MS Binding Assays • nitrogen heterocycles • re-sensitizers

- [1] D. Gunnell, M. Eddleston, M. R. Phillips, F. Konradsen, *BMC Public Health* **2007**, *7*, 357–372.
- [2] E. Dolgin, *Nat. Med.* **2013**, *19*, 1194–1195.
- [3] J. Newmark, *Neurologist* **2007**, *13*, 20–32.
- [4] R. D. Sheridan, A. P. Smith, S. R. Turner, J. E. H. Tattersall, *J. R. Soc. Med.* **2005**, *98*, 114–115.
- [5] R. Giniatullin, A. Nistri, J. L. Yakel, *Trends Neurosci.* **2005**, *28*, 371–378.
- [6] R. L. Papke, *Biochem. Pharmacol.* **2014**, *89*, 1–11.
- [7] H. Thiermann, T. Seeger, S. Gonder, N. Herkert, B. Antkowiak, T. Zilker, F. Eyer, F. Worek, *Chem.-Biol. Interact.* **2010**, *187*, 265–269.
- [8] F. Worek, N. Aurbek, M. Koller, C. Becker, P. Eyer, H. Thiermann, *Biochem. Pharmacol.* **2007**, *73*, 1807–1817.
- [9] F. Worek, H. Thiermann, L. Szincicz, P. Eyer, *Biochem. Pharmacol.* **2004**, *68*, 2237–2248.
- [10] F. Worek, H. Thiermann, T. Wille, *Chem.-Biol. Interact.* **2016**, *259*, 93–98.
- [11] K. V. Niessen, S. Muschik, F. Langguth, S. Rappenglück, T. Seeger, H. Thiermann, F. Worek, *Toxicol. Lett.* **2016**, *247*, 1–10.
- [12] D. K. Williams, J. Wang, R. L. Papke, *Biochem. Pharmacol.* **2011**, *82*, 915–930.
- [13] K. V. Niessen, T. Seeger, J. E. H. Tattersall, C. M. Timperley, M. Bird, C. Green, H. Thiermann, F. Worek, *Chem.-Biol. Interact.* **2013**, *206*, 545–554.
- [14] J. E. H. Tattersall, *Br. J. Pharmacol.* **1993**, *108*, 1006–1015.
- [15] S. R. Turner, J. E. Chad, M. Price, C. M. Timperley, M. Bird, A. C. Green, J. E. H. Tattersall, *Toxicol. Lett.* **2011**, *206*, 105–111.
- [16] T. Seeger, M. Eichhorn, M. Lindner, K. V. Niessen, J. E. H. Tattersall, C. M. Timperley, M. Bird, A. C. Green, H. Thiermann, F. Worek, *Toxicology* **2012**, *294*, 80–84.
- [17] C. Scheffel, K. V. Niessen, S. Rappenglück, K. T. Wanner, H. Thiermann, F. Worek, T. Seeger, *Toxicol. Lett.* **2018**, *293*, 157–166.
- [18] K. V. Niessen, J. E. H. Tattersall, C. M. Timperley, M. Bird, C. Green, T. Seeger, H. Thiermann, F. Worek, *Toxicol. Lett.* **2011**, *206*, 100–104.
- [19] M. E. Price, C. J. Docx, H. Rice, S. J. Fairhall, S. J. C. Poole, M. Bird, L. Whaley, D. P. Flint, A. C. Green, C. M. Timperley, J. E. H. Tattersall, *Toxicol. Lett.* **2016**, *244*, 154–160.
- [20] K. Schoene, J. Steinhanses, H. Oldiges, *Biochem. Pharmacol.* **1976**, *25*, 1955–1958.
- [21] A. Ring, B. Oddvar Strom, S. R. Turner, C. M. Timperley, M. Bird, A. C. Green, J. E. Chad, F. Worek, J. E. H. Tattersall, *PLoS ONE* **2015**, *10*, e0135811.
- [22] C. M. Timperley, M. Bird, C. Green, M. E. Price, J. E. Chad, S. R. Turner, J. E. H. Tattersall, *MedChemComm* **2012**, *3*, 352–356.
- [23] T. Wein, G. Höfner, S. Rappenglück, S. Sichler, K. V. Niessen, T. Seeger, F. Worek, H. Thiermann, K. T. Wanner, *Toxicol. Lett.* **2018**, *293*, 184–189.
- [24] S. Sichler, G. Höfner, S. Rappenglück, T. Wein, K. V. Niessen, T. Seeger, F. Worek, H. Thiermann, F. F. Paintner, K. T. Wanner, *Toxicol. Lett.* **2018**, *293*, 172–183.
- [25] N. S. Millar, *Biochem. Soc. Trans.* **2003**, *31*, 869–874.
- [26] M. Navedo, M. Nieves, L. Rojas, J. A. Lasalde-Dominicci, *Biochemistry* **2004**, *43*, 78–84.
- [27] T. W. Bell, L. Y. Hu, S. V. Patel, *J. Org. Chem.* **1987**, *52*, 3847–3850.
- [28] E. R. Bowman, H. McKennis, Jr., B. R. Martin, *Synth. Commun.* **1982**, *12*, 871–879.
- [29] C. H. Leung, A. R. Chianese, B. R. Garrett, C. S. Letko, R. H. Crabtree, *Inorg. Synth.* **2010**, *35*, 84–87.
- [30] S. Rappenglück, K. V. Niessen, T. Seeger, F. Worek, H. Thiermann, K. T. Wanner, *Synthesis* **2017**, *49*, 4055–4064.
- [31] N. Yoshikai, E. Nakamura, *Chem. Rev.* **2012**, *112*, 2339–2372.
- [32] W. Henze, A. Vyater, N. Krause, R. M. Gschwind, *J. Am. Chem. Soc.* **2005**, *127*, 17335–17342.
- [33] J. Epszajn, A. Bieniek, *J. Chem. Soc. Perkin Trans. 1* **1985**, 213–219.
- [34] H. C. Brown, W. A. Murphey, *J. Am. Chem. Soc.* **1951**, *73*, 3308–3312.
- [35] K. Musilek, M. Komloova, V. Zavadova, O. Holas, M. Hrabanova, M. Pohanka, V. Dohnal, F. Nachon, M. Dolezal, K. Kuca, Y.-S. Jung, *Bioorg. Med. Chem.* **2010**, *20*, 1763–1766.
- [36] K. Musilek, J. Roder, M. Komloova, O. Holas, M. Hrabanova, M. Pohanka, V. Dohnal, V. Opletalova, K. Kuca, Y.-S. Jung, *Bioorg. Med. Chem.* **2011**, *21*, 150–154.
- [37] C. M. Timperley, M. Bird, S. C. Heard, S. Notman, R. W. Read, J. E. H. Tattersall, S. R. Turner, *J. Fluorine Chem.* **2005**, *126*, 1160–1165.
- [38] K. V. Niessen, T. Seeger, S. Rappenglück, T. Wein, G. Höfner, K. T. Wanner, H. Thiermann, F. Worek, *Toxicol. Lett.* **2018**, *293*, 190–197.
- [39] W. Cocker, N. W. A. Geraghty, T. B. H. McMurry, P. V. R. Shannon, *J. Chem. Soc. Perkin Trans. 1* **1984**, 2245–2254.
- [40] *Bioanalytical Method Validation, Guidance for Industry*, United States Food and Drug Administration (FDA), **2001**: <https://www.fda.gov/downloads/Drugs/Guidance/ucm070107.pdf> (accessed August 10, 2017).
- [41] D. D. Perrin, W. L. F. Armarego, *Purification of Laboratory Chemicals*, Pergamon, New York, **1988**.
- [42] M. Cushman, G. I. Georg, U. Holzgrabe, S. Wang, *J. Med. Chem.* **2014**, *57*, 9219.
- [43] G. F. Pauli, S.-N. Chen, C. Simmler, D. C. Lankin, T. Gödecke, B. U. Jaki, J. B. Friesen, J. B. McAlpine, J. G. Napolitano, *J. Med. Chem.* **2014**, *57*, 9220–9231.
- [44] M. J. Corr, K. F. Gibson, A. R. Kennedy, J. A. Murphy, *J. Am. Chem. Soc.* **2009**, *131*, 9174–9175.
- [45] E. Lindner, G. Von Au, H. J. Eberle, *Chem. Ber.* **1981**, *114*, 810–813.
- [46] P. K. Smith, R. I. Krohn, G. T. Hermanson, A. K. Mallia, F. H. Gartner, M. D. Provenzano, E. K. Fujimoto, N. M. Goeke, B. J. Olson, D. C. Klenk, *Anal. Biochem.* **1985**, *150*, 76–85.

Manuscript received: May 14, 2018

Revised manuscript received: June 28, 2018

Accepted manuscript online: July 5, 2018

Version of record online: August 1, 2018

Supporting Information

Synthesis of a Series of Structurally Diverse MB327 Derivatives and Their Affinity Characterization at the Nicotinic Acetylcholine Receptor

Sebastian Rappenglück^{+, [a]} Sonja Sichler^{+, [a]} Georg Höfner,^[a] Thomas Wein,^[a]
Karin V. Niessen,^[b] Thomas Seeger,^[b] Franz F. Paintner,^[a] Franz Worek,^[b] Horst Thiermann,^[b]
and Klaus T. Wanner^{*, [a]}

cmdc_201800325_sm_miscellaneous_information.pdf

Content

- 1 Syntheses and Analytical Data
- 2 Characterization of [$^2\text{H}_6$]MB327's affinity towards the *Torpedo*-nAChR employing an improved MS Binding Assay protocol
- 3 Validation of the developed LC-ESI-MS/MS quantification method

1 Syntheses and Analytical Data

3-*tert*-Butylpyridine (8)

According to GP3, with **7** (319 mg, 2.00 mmol, 197 μ L, 1.0 eq.) and (*t*-Bu)₂CuCN(MgCl)₂ (4 eq.), which was prepared according to GP4 with *t*-BuMgCl (2.0 M solution in Et₂O, 16.0 mmol, 8.00 mL, 8.0 eq.) and CuCN (724 mg, 8.00 mmol, 4.0 eq.) in Et₂O (35 mL). FC (SiO₂, *n*-pentane/Et₂O = 7:1) and subsequent vacuum distillation yielded pure 3-*tert*-butylpyridine (**8**, 115 mg, 43%) as a colorless liquid.

R_f =0.26 (Et₂O/*n*-pentane 1:1); ¹H NMR (500 MHz, CDCl₃): δ =1.35 (s, 9 H, CH₃), 7.22 (ddd, J =8.0/4.7/0.9 Hz, 1 H, NCHCHCH), 7.68 (ddd, J =8.0/2.5/1.6 Hz, 1 H, NCHCHCH), 8.43 (dd, J =4.7/1.6 Hz, 1 H, NCHCHCH), 8.67 ppm (dd, J =2.5/0.8 Hz, 1 H, NCHC(C(CH₃)₃)); ¹³C NMR (125 MHz, CDCl₃): δ =30.99 (CH₃), 33.61 (C(CH₃)₃), 122.95 (NCHCHCH), 132.85 (NCHCHCH), 145.86 (CC(CH₃)₃), 146.90 (NCHCHCH), 147.45 ppm NCHC(C(CH₃)₃); IR (film): $\tilde{\nu}$ =3088, 3033, 2964, 2904, 2870, 2716, 1904, 1870, 1715, 1589, 1572, 1481, 1462, 1414, 1396, 1369, 1335, 1273, 1242, 1204, 1184, 1125, 1104, 1041, 1021, 948, 926, 841, 808, 714, 624 cm⁻¹; HRMS-ESI m/z [$M+H$]⁺ calcd for C₉H₁₄N: 136.1121, found: 136.1120.

The analytical data were consistent with those previously reported.¹

3-Isopropylpyridine (11)

A solution of **9** (0.71 g, 5.2 mmol, 1.0 eq.) in conc. H₂SO₄ (2.2 mL) and conc. AcOH (3.7 mL) was heated to reflux at 150 °C for 30 min. The solution was allowed to cool to room temperature, poured into H₂O (100 mL) and adjusted to pH 9 by addition of K₂CO₃. The mixture was extracted with CH₂Cl₂ (3 x 40 mL), the combined organic layers were dried over MgSO₄ and the solvent was carefully removed under reduced pressure (40 °C bath temperature, 400 mbar). The resulting liquid was dissolved in MeOH (10 mL), treated with Pd/C (10% Pd, 0.27 g, 0.25 mmol, 0.05 eq.) and the suspension was stirred for 16 h under H₂ atmosphere (normal pressure) at room temperature. The mixture was diluted with CH₂Cl₂ (40 mL), H₂O (30 mL) and saturated aqueous NaCl (30 mL) and the layers were separated. The aqueous phase was extracted with CH₂Cl₂ (2 x 30 mL), the combined organic layers were dried over

[1] T. Fujii, T. Hiraga, S. Yoshifuji, M. Ohba, K. Yoshida, *Chem. Pharm. Bull.* **1978**, 26 (10), 3233–3237.

MgSO₄ and the solvent was carefully removed under reduced pressure. The resulting brownish oil was purified by FC (SiO₂, *n*-pentane/Et₂O = 3:1) to yield **11** (323 mg, 51%) as a clear, colorless and highly volatile liquid.

*R*_f=0.18 (*n*-pentane/Et₂O 3:1); ¹H NMR (500 MHz, CDCl₃): δ=1.28 (dd, *J*=6.9/0.7 Hz, 6 H, CH₃), 2.94 (hept, *J*=6.9 Hz, 1 H, CH(CH₃)₂), 7.19–7.24 (m, 1 H, NCHCH), 7.51–7.56 (m, 1 H, NCHCHCH), 8.41–8.45 (m, 1 H, NCHCH), 8.48–8.51 ppm (m, 1 H, NCHC(CH(CH₃)₂)); ¹³C NMR (125 MHz, CDCl₃): δ=23.68 (CH₃), 31.78 (CH(CH₃)₂), 123.31 (NCHCH), 133.65 (NCHCHCH), 143.66 (NCHC(CH(CH₃)₂)), 147.35 (NCHCH), 148.68 ppm (NCHC(CH(CH₃)₂)); IR (film): $\tilde{\nu}$ =3027, 2962, 2927, 2872, 1575, 1478, 1423, 1385, 1365, 1310, 1192, 1145, 1126, 1102, 1064, 1036, 1023, 925, 807, 759, 715 cm⁻¹. HRMS-EI *m/z* [*M*]⁺ calcd for C₈H₁₁N: 121.0886, found: 121.0886.

2-Isopropylpyridine (**6**)

According to GP3, with **5** (1.39 g, 861 μL, 8.82 mmol, 1.00 eq.) and (*i*-Pr)₂CuCN(MgCl)₂ (4 eq.), which was prepared according to GP4 with *i*-PrMgCl (2.0 M solution in THF, 70.6 mmol, 35.3 mL, 8.00 eq.) and CuCN (3.19 g, 35.3 mmol, 4.00 eq.) in THF (70 mL). For reaction quenching and aqueous workup half of the volumes indicated in GP3 were used. FC (SiO₂, *n*-pentane/Et₂O = 7:1) and subsequent vacuum distillation yielded pure 2-isopropylpyridine (**6**, 216 mg, 20%) as a colorless liquid.

*R*_f=0.44 (*n*-pentane/Et₂O 1:1); ¹H NMR (400 MHz, CDCl₃): δ=1.31 (d, *J*=6.9 Hz, 6 H, C(CH₃)₂), 3.06 (sept., *J*=6.9 Hz, 1 H, CH(CH₃)₂), 7.09 (ddd, *J*=7.5/4.9/1.1 Hz, 1 H, NCHCH), 7.17 (dt, *J*=7.9/0.8 Hz, 1 H, CHCCH(CH₃)₂), 7.60 (td, *J*=7.7/1.9 Hz, 1 H, NCHCHCH), 8.54 ppm (ddd, *J*=4.9/1.8/0.9 Hz, 1 H, NCHCH); ¹³C NMR (100 MHz, CDCl₃): δ=22.58 (CH₃), 36.36 (CH(CH₃)₂), 120.62 (CHCCH(CH₃)₂), 120.98 (NCHCH), 136.35 (NCHCHCH), 149.06 (NCHCH), 167.33 ppm (NCCH(CH₃)₂); IR (film): $\tilde{\nu}$ =3066, 3007, 2964, 2930, 2870, 2341, 1591, 1570, 1476, 1433, 1379, 1361, 1335, 1287, 1216, 1149, 1103, 1059, 1044, 991, 958, 923, 893, 784, 747, 668 cm⁻¹; HRMS-EI *m/z* [*M*]⁺ calcd for C₈H₁₁N: 121.0886, found: 121.0897.

The analytical data were consistent with those previously reported.^{2,3}

4-Isopropylpyridine (**13**)

Acetylchloride (0.79 g, 10 mmol, 0.72 mL, 1.0 eq.) was added to a solution of **12** (0.79 g, 10 mmol, 0.81 mL, 1.0 eq.) in THF (18 mL) at $-78\text{ }^{\circ}\text{C}$ and the resulting suspension was stirred for 1 h before $(i\text{-Pr})_2\text{CuCN}(\text{MgCl})_2$ (1.1 eq.), prepared according to GP4 with $i\text{-PrMgCl}$ (1.95 M solution in Et_2O , 22 mmol, 11 mL, 2.2 eq.) and CuCN (1.0 g, 11 mmol, 1.1 eq.) in THF (50 mL), was added via transfer cannula. The reaction was stirred for an additional 2.5 h at $-78\text{ }^{\circ}\text{C}$ and quenched by addition of saturated aqueous $\text{NH}_4\text{Cl}/\text{conc. NH}_3$ (1:1, 20 mL). The mixture was diluted with H_2O (20 mL) and the aqueous phase was extracted with Et_2O (3 x 50 mL). The combined organic layers were washed with saturated aqueous NaCl (30 mL) and dried over MgSO_4 . The solvent was removed under reduced pressure and the crude dihydropyridine was purified by FC (Al_2O_3 -neutral, activity III, $n\text{-pentane}/\text{Et}_2\text{O} = 9:1$). The resulting colorless oil was dissolved in CH_2Cl_2 (30 mL) and treated with DDQ (2.3 g, 10 mmol, 1.0 eq.). The reaction was stirred for 70 min at room temperature prior to being diluted with CH_2Cl_2 (30 mL). The mixture was extracted with 2 M HCL (3 x 30 mL) and the combined aqueous layers were washed with Et_2O (30 mL). The aqueous phase was neutralized by addition of K_2CO_3 and adjusted to pH 12 by adding 1 M NaOH. The aqueous mixture was extracted with Et_2O (3 x 30 mL) and the combined organic layers were washed with saturated aqueous NaCl (50 mL). The combined organic layers were dried over MgSO_4 and the solvent was carefully removed under reduced pressure (780 mbar, $40\text{ }^{\circ}\text{C}$). The residue was purified by FC (SiO_2 , $n\text{-pentane}/\text{Et}_2\text{O} = 5:1 \rightarrow 1:1$) followed by vacuum distillation ($120\text{ }^{\circ}\text{C}$, 40 mbar) to obtain **13** (0.41 g, 33%) as a clear and highly volatile liquid.

$R_f=0.25$ ($n\text{-pentane}/\text{Et}_2\text{O}$ 1:1); $^1\text{H NMR}$ (500 MHz, CDCl_3): $\delta=1.26$ (d, $J=6.9$ Hz, 6 H, $\text{CH}(\text{CH}_3)_2$), 2.88 (sept., $J=6.9$ Hz, 1 H, $\text{CH}(\text{CH}_3)_2$), 7.11–7.16 (m, 2 H, NCHCH), 8.47–8.52 ppm (m, 2 H, NCH); $^{13}\text{C NMR}$ (125 MHz, CDCl_3): $\delta=23.10$ ($\text{CH}(\text{CH}_3)_2$), 33.55 ($\text{CH}(\text{CH}_3)_2$), 121.96 (NCHCH), 149.79 (NCH), 157.45 ppm (NCHCHC); IR (film): $\tilde{\nu}=3070, 3025, 2965, 2929, 2891, 2873, 2342, 1935, 1686, 1599, 1556, 1493$,

[2] E. Pasquinet, P. Rocca, F. Marsais, A. Godard, G. Queguiner, *Tetrahedron* **1998**, *54* (30), 8771–8782.

[3] M. R. Friedfeld, G. W. Margulieux, B. A. Schaefer, P. J. Chirik, *J. Am. Chem. Soc.* **2014**, *136* (38), 13178–13181.

1464, 1413, 1385, 1365, 1309, 1239, 1220, 1145, 1090, 1070, 1054, 993, 923, 893, 819, 783, 750 cm⁻¹; HRMS-El m/z [M]⁺ calcd for C₈H₁₁N: 121.0886, found: 121.0899.

The analytical data were consistent with those previously reported.⁴

4-(*tert*-Butyl)-2-methylpyridine (**15**)

Phenyl chloroformate (1.59 g, 10.0 mmol, 1.28 mL, 1.0 eq) was added to a solution of **14** (950 mg, 10.0 mmol, 1.00 mL, 1.0 eq.) in THF (18 mL) at –78 °C and the resulting suspension was stirred for 1 h before *t*-BuCu(CN)ZnBr·2LiCl (0.15 M suspension in THF, 11.0 mmol, 72.0 mL, 1.1 eq.) was added via transfer cannula. The mixture was stirred for additional 5 h at –78 °C and for 16 h at room temperature. The reaction was quenched by addition of saturated aqueous NH₄Cl/conc. NH₃ (1:1, 20 mL) and extracted with Et₂O (3 x 50 mL). The combined organic layers were washed with saturated aqueous NaCl (100 mL) and dried over MgSO₄. The solvent was removed under reduced pressure and the crude dihydropyridine was purified by FC (SiO₂, *n*-pentane/Et₂O = 12:1). Sulfur (353 mg, 11.0 mmol, 1.1 eq.) and naphthalene (19.3 g, 150 mmol, 15 eq.) were added and the reaction mixture was stirred at 200 °C for 20 min under microwave conditions (300 W). The reaction was allowed to cool to room temperature and the solid residue was dissolved in Et₂O (70 mL). The organic phase was washed with 1 M NaOH (2 x 40 mL) and the combined aqueous layers were extracted with Et₂O (40 mL). The combined organic layers were extracted with 2 M HCl (3 x 40 mL) and the combined acidic aqueous layers were washed with Et₂O (50 mL). The acidic aqueous phase was neutralized by addition of K₂CO₃ and extracted with CH₂Cl₂ (3 x 40 mL). The combined organic layers were dried over MgSO₄ and the solvent was removed under reduced pressure. The residue was purified by FC (SiO₂, *n*-pentane/Et₂O = 2:1) to yield **15** (701 mg, 47%) as a colorless liquid.

R_f =0.11 (*n*-pentane/Et₂O 2:1); ¹H NMR (500 MHz, CDCl₃): δ =1.30 (s, 9 H, C(CH₃)₃), 2.54 (s, 3 H, CCH₃), 7.06–7.10 (m, 1 H, NCHCH), 7.12–7.15 (m, 1 H, NC(CH₃)CH), 8.39 ppm (d, J =5.3 Hz, 1 H, NCHCH); ¹³C NMR (125 MHz, CDCl₃): δ =24.61 (CCH₃), 30.54 (C(CH₃)₃), 34.54 (C(CH₃)₃), 117.86 (NCHCH), 120.14 (NC(CH₃)CH), 148.94 (NCHCH), 158.08 (NCCH₃), 160.22 ppm (CC(CH₃)₃); IR (film): $\tilde{\nu}$ =3069, 3012, 2964, 2870, 1600, 1549, 1480, 1459, 1395, 1363, 1299, 1284, 1221, 1201, 1118, 1039, 997,

[4] A. R. Katritzky, H. Beltrami, M. P. Sammes, *J. Chem. Soc., Perkin Trans. 1* **1980**, (11), 2480–2484.

896, 879, 832, 742, 711, 613 cm^{-1} ; HRMS-EI m/z [M] $^{+}$ calcd for $\text{C}_{10}\text{H}_{15}\text{N}$: 149.1204, found: 149.1197.

1,1'-(Propane-1,3-diyl)bis[2-(*tert*-butyl)pyridin-1-ium] bis(trifluoromethanesulfonate) (1a)

According to GP1, with **17** (402 mg, 2.97 mmol, 2.5 eq.) and **21** (410 mg, 1.21 mmol, 1.0 eq.) at 85 °C without CH_2Cl_2 as solvent. Reaction time: 5 h. Recrystallization from EtOH (1 mL) yielded **1a** (537 mg, 73%) as a colorless solid.

mp: 165 °C; ^1H NMR (500 MHz, $[\text{D}_6]\text{DMSO}$): δ =1.60 (s, 18 H, CH_3), 2.55–2.57 (m, 2 H, NCH_2CH_2), 4.94–5.07 (m, 4 H, NCH_2), 8.07–8.15 (m, 2 H, NCHCH), 8.15–8.21 (m, 2 H, $\text{CHCC}(\text{CH}_3)_3$), 8.50–8.59 (m, 2 H, NCHCHCH), 9.08–9.17 ppm (m, 2 H, NCH); ^{13}C NMR (125 MHz, $[\text{D}_6]\text{DMSO}$): δ =29.51 ($\text{C}(\text{CH}_3)_3$), 34.71 (NCH_2CH_2), 37.27 ($\text{C}(\text{CH}_3)_3$), 54.70 (NCH_2), 120.50 (q, J =322.3 Hz, CF_3), 125.90 (NCHCH), 126.95 ($\text{CHCC}(\text{CH}_3)_3$), 146.06 (NCHCHCH), 148.18 (NCH), 163.45 ppm ($\text{CC}(\text{CH}_3)_3$); IR (KBr): $\tilde{\nu}$ =3162, 3086, 3066, 3049, 2988, 2285, 1628, 1576, 1510, 1487, 1453, 1438, 1409, 1375, 1261, 1226, 1158, 1031, 1081, 1031, 935, 901, 872, 848, 838, 819, 784, 757, 706, 639, 573, 545, 517, 466 cm^{-1} ; HRMS-ESI m/z [$M\text{-OTf}$] $^{+}$ calcd for $\text{C}_{22}\text{H}_{32}\text{F}_3\text{N}_2\text{O}_3\text{S}$: 461.2080, found: 461.2076.

1,1'-(Propane-1,3-diyl)bis[3-(*tert*-butyl)pyridin-1-ium] diiodide (1b)

16 (395 mg, 1.32 mmol, 153 μL , 1.0 eq.) was added to a solution of **8** (393 mg, 2.91 mmol, 2.2 eq.) in DMF (2.4 mL) and the resulting mixture was stirred for 72 h at 70 °C under the exclusion of light. The solvent was removed under reduced pressure and the residue was recrystallized from DMF/Acetone (1:10, 11 mL) to afford **1b** (592 mg, 79%) as yellow crystals.

mp: 243 °C; ^1H NMR (500 MHz, $[\text{D}_6]\text{DMSO}$): δ =1.39 (s, 18 H, $\text{C}(\text{CH}_3)_3$), 2.71 (quin., J =7.3 Hz, 2 H, NCH_2CH_2), 4.77 (t, J =7.1 Hz, 4 H, NCH_2), 8.13–8.20 (m, 2 H, NCHCH), 8.70–8.76 (m, 2 H, NCHCHCH), 8.94–8.98 (m, 2 H, NCHCH), 9.06 ppm (s, 2 H, $\text{NCHC}(\text{C}(\text{CH}_3)_3)$); ^{13}C NMR (125 MHz, $[\text{D}_6]\text{DMSO}$): δ =29.91 ($\text{C}(\text{CH}_3)_3$), 31.85 (NCH_2CH_2), 34.51 ($\text{C}(\text{CH}_3)_3$), 57.54 (NCH_2), 127.54 (NCHCH), 142.03 ($\text{NCHC}(\text{C}(\text{CH}_3)_3)$), 142.24 (NCHCH), 143.13 (NCHCHCH), 150.93 ppm ($\text{CC}(\text{CH}_3)_3$);

IR (KBr): $\tilde{\nu}$ =3429, 3142, 3063, 3036, 3019, 2985, 2961, 2866, 2009, 1968, 1933, 1794, 1628, 1508, 1479, 1462, 1449, 1400, 1374, 1365, 1353, 1325, 1282, 1248, 1222, 1195, 1180, 1148, 1064, 1043, 903, 893, 821, 750, 688 cm^{-1} ; HRMS-ESI m/z [$M-I$]⁺ calcd for $\text{C}_{21}\text{H}_{32}\text{IN}_2$: 439.1605, found: 439.1601.

1,1'-(Propane-1,3-diyl)bis(2-isopropylpyridin-1-ium) bis(trifluoromethanesulfonate) (1c)

According to GP1, with **6** (410 mg, 3.38 mmol, 2.5 eq.) and **21** (460 mg, 1.35 mmol, 1.0 eq.) without CH_2Cl_2 as solvent. Reaction time: 5 min. Recrystallization from EtOH (1.5 mL) afforded **1c** (604 mg, 77%) as a colorless solid.

mp: 164–165°C; ^1H NMR (500 MHz, $[\text{D}_6]\text{DMSO}$): δ =1.39 (d, 6.9 Hz, 12 H, CH_3), 2.35–2.46 (m, 2 H, NCH_2CH_2), 3.64 (sept., J =6.6 Hz, 2 H, $\text{CH}(\text{CH}_3)_2$), 4.74–4.84 (m, 4 H, NCH_2CH_2), 7.99–8.05 (m, 2 H, NCHCH), 8.18–8.24 (m, 2 H, $\text{CHCCH}(\text{CH}_3)_2$), 8.53–8.60 (m, 2 H, NCHCHCH), 8.92–8.98 ppm (m, 2 H, NCHCH); ^{13}C NMR (125 MHz, $[\text{D}_6]\text{DMSO}$): δ =21.99 (CH_3), 29.29 ($\text{CH}(\text{CH}_3)_2$), 32.10 (NCH_2CH_2), 53.80 (NCH_2), 120.52 (q, J =322.3 Hz, CF_3), 125.50 (NCHCH), 126.32 ($\text{CHCCH}(\text{CH}_3)_2$), 145.43 (NCHCH), 145.79 (NCHCHCH), 163.59 ppm ($\text{CCH}(\text{CH}_3)_2$); IR (KBr): $\tilde{\nu}$ =3154, 3087, 2987, 2951, 2884, 2343, 2361, 1631, 1581, 1511, 1481, 1465, 1450, 1397, 1376, 1363, 1272, 1259, 1224, 1162, 1149, 1103, 1090, 1057, 1029, 943, 892, 788, 766, 755, 747, 637, 572, 517, 484, 465 cm^{-1} ; HRMS-ESI m/z [$M-\text{OTf}$]⁺ calcd for $\text{C}_{20}\text{H}_{28}\text{F}_3\text{N}_2\text{O}_3\text{S}$: 433.1767, found: 433.1762.

1,1'-(Propane-1,3-diyl)bis(3-isopropylpyridin-1-ium) bis(trifluoromethanesulfonate) (1d)

According to GP1, with **11** (225 mg, 1.86 mmol, 2.5 eq.) and **21** (253 mg, 0.743 mmol, 1.0 eq.) without CH_2Cl_2 as solvent. Reaction time: 2 min. Precipitation from *i*-PrOH (2 mL) by addition of Et_2O (7 mL) afforded **1d** (382 mg, 88%) as a colorless solid.

mp: 123°C; ^1H NMR (500 MHz, CDCl_3): δ =1.38 (d, J =6.9 Hz, 12 H, CH_3), 2.92–3.01 (m, 2 H, NCH_2CH_2), 3.21 (hept, J =6.5 Hz, 2 H, $\text{CH}(\text{CH}_3)_2$), 4.95–5.03 (m, 4 H, NCH_2), 7.90 (dd, J =7.9/6.2 Hz, 2 H, NCHCH), 8.24 (d, J =8.1 Hz, 2 H, NCHCHCH), 9.23–9.30 (m, 2 H, NCHCH), 9.35 ppm (s, 2 H, $\text{NCHC}(\text{CH}(\text{CH}_3)_2)$); ^{13}C NMR (125 MHz, CDCl_3): δ =22.89 (CH_3), 32.21 ($\text{CH}(\text{CH}_3)_2$), 34.99 (NCH_2CH_2), 57.74 (NCH_2CH_2), 120.55 (q, J =319.3 Hz, CF_3), 128.02 (NCHCH), 142.89 (NCHCH), 143.31

(NCHCHCH), 144.15 (NCHC(CH(CH₃)₂)), 150.98 ppm (C(CH(CH₃)₂)); IR (KBr): $\tilde{\nu}$ =3064, 2969, 2932, 2881, 1637, 1515, 1480, 1470, 1394, 1370, 1336, 1273, 1225, 1161, 1105, 1064, 1028, 824, 742, 756, 699, 692 cm⁻¹; HRMS-FAB m/z [M -OTf]⁺ calcd for C₂₀H₂₈F₃N₂O₃S: 433.1767, found: 433.1782.

1,1'-(Propane-1,3-diyl)bis(4-isopropylpyridin-1-ium) bis(trifluoromethanesulfonate) (1e)

According to GP1, with **13** (350 mg, 2.89 mmol, 2.5 eq.) and **21** (393 mg, 1.16 mmol, 1.0 eq.) without CH₂Cl₂ as solvent. Reaction time: 1 h. Precipitation from *i*-PrOH (2 mL) by addition of Et₂O (7 mL) afforded **1e** (549 mg, 81%) as a colorless solid.

mp: 86–87°C; ¹H NMR (500 MHz, CDCl₃): δ =1.35 (d, J =6.9 Hz, 12 H, CH₃), 2.84–2.94 (m, 2 H, NCH₂CH₂), 3.17 (sept., J =6.8 Hz, 2 H, CH(CH₃)₂), 4.88–4.97 (m, 4 H, NCH₂), 7.80 (d, J =6.7 Hz, 4 H, NCHCH), 9.24 ppm (d, J =6.8 Hz, 4 H, NCH); ¹³C NMR (125 MHz, CDCl₃): δ =22.40 (CH₃), 34.39 (NCH₂CH₂), 34.64 (CH(CH₃)₂), 56.99 (NCH₂), 120.55 (q, J =319.9 Hz, CF₃), 126.52 (NCHCH), 144.88 (NCH), 169.28 ppm (NCHCHC); IR (KBr): $\tilde{\nu}$ =3132, 3078, 2981, 2940, 2880, 2296, 1960, 1644, 1572, 1516, 1473, 1390, 1371, 1341, 1264, 1223, 1184, 1165, 1081, 1056, 1031, 974, 892, 853, 824, 756, 637, 594, 573, 517 cm⁻¹; HRMS-FAB m/z [M]⁺ calcd for C₂₁H₂₈F₆N₂O₆S₂: 582.1293, found: 582.1290.

1,1'-(Propane-1,3-diyl)bis(3,5-dimethylpyridin-1-ium) bis(trifluoromethanesulfonate) (1f)

According to GP1, with **18** (1.30 g, 12.0 mmol, 1.38 mL, 2.5 eq.) and **21** (1.63 g, 4.80 mmol, 1.0 eq.) without CH₂Cl₂ as solvent. Reaction time: 1 min. Recrystallization from EtOH (2 mL) afforded **1f** (1.83 g, 69%) as a colorless solid.

mp: 110°C; ¹H NMR (500 MHz, [D₆]DMSO): δ =2.46 (s, 12 H, CH₃), 2.64 (quin., J =6.9 Hz, 2 H, NCH₂CH₂), 4.59 (t, J =6.9 Hz, 4 H, NCH₂), 8.34 (s, 2 H, (CH₃)CCHC(CH₃)), 8.77 ppm (s, 4 H, NCH); ¹³C NMR (125 MHz, [D₆]DMSO): δ =17.61 (CH₃), 31.03 (NCH₂CH₂), 57.30 (NCH₂), 120.51 (q, J =322.3 Hz, CF₃), 137.91 ((CH₃)C), 141.56 (NCH), 146.41 ppm (CH₃)CCHC(CH₃)); IR (KBr): $\tilde{\nu}$ =3061, 2957, 2360, 2341, 1637, 1611, 1509, 1484, 1468, 1445, 1387, 1309, 1277, 1251, 1224, 1196, 1163, 1144, 1068, 1028, 953, 936, 878, 756, 697, 637, 573, 518 cm⁻¹; HRMS-ESI m/z [M -OTf]⁺ calcd for C₁₈H₂₄F₃N₂O₃S: 405.1454, found: 405.1449.

1,1'-(Propane-1,3-diyl)bis(2,6-dimethylpyridin-1-ium) bis(trifluoromethanesulfonate) (1g)

According to GP1, with **19** (137 mg, 1.26 mmol, 149 μ L, 2.5 eq.) and **21** (171 mg, 503 μ mol, 1.0 eq.) without CH₂Cl₂ as solvent at 70 °C. Reaction time: 1 min. Recrystallization from EtOH (4 mL) afforded **1g** (210 mg, 75%) as a colorless solid.

mp: 221 °C; ¹H NMR (500 MHz, [D₆]DMSO): δ =2.34–2.42 (m, 2 H, NCH₂CH₂), 2.92 (s, 12 H, CH₃), 4.73–4.80 (m, 4 H, NCH₂CH₂), 7.91 (d, J =7.9 Hz, 4 H, NC(CH₃)CH), 8.35 ppm (t, J =7.9 Hz, 2 H, C(CH₃)CHCH); ¹³C NMR (125 MHz, [D₆]DMSO): δ =20.74 (CH₃), 24.86 (NCH₂CH₂), 48.97 (NCH₂), 120.5 (q, J =322.3 Hz, CF₃), 127.55 (C(CH₃)CH), 144.44 (C(CH₃)CHCH), 155.70 ppm (NC(CH₃)); IR (KBr): $\tilde{\nu}$ =3095, 3072, 3040, 1627, 1589, 1495, 1477, 1453, 1414, 1388, 1329, 1258, 1225, 1158, 1058, 1030, 902, 802, 754, 638, 572, 517, 487 cm⁻¹; HRMS-ESI m/z [M -OTf]⁺ calcd for C₁₈H₂₄F₃N₂O₃S: 405.1454, found: 405.1451.

1,1'-(Propane-1,3-diyl)bis(2,4,6-trimethylpyridin-1-ium) bis(trifluoromethanesulfonate) (1h)

According to GP1, with **20** (1.23 g, 10.0 mmol, 1.34 mL, 3.2 eq.) and **21** (1.07 g, 3.15 mmol, 1.0 eq.) without CH₂Cl₂ as solvent. Reaction time: 15 min. Recrystallization from EtOH (5.5 mL) afforded **1h** (1.48 g, 81%) as a colorless solid.

mp: 146 °C; ¹H NMR (500 MHz, [D₆]DMSO): δ =2.32 (quin., J =11.5 Hz, 2 H, NCH₂CH₂), 2.49 (s, 6 H, NC(CH₃)CHC(CH₃)), 2.84 (s, 12 H, NC(CH₃)), 4.61–4.72 (m, 4 H, NCH₂CH₂), 7.76 ppm (s, 4 H, NC(CH₃)CH); ¹³C NMR (125 MHz, [D₆]DMSO): δ =20.62 (NC(CH₃)), 20.81 (NC(CH₃)CHC(CH₃)), 25.23 (NCH₂CH₂), 48.41 (NCH₂), 120.65 (q, J =322.3 Hz, CF₃), 128.04 (NC(CH₃)CH), 154.57 (NC(CH₃)), 157.38 ppm (NC(CH₃)CHC); IR (KBr): $\tilde{\nu}$ =3574, 4379, 3070, 2981, 1642, 1575, 1508, 1482, 1444, 1419, 1388, 1321, 1256, 1225, 1195, 1146, 1059, 1031, 872, 804, 756, 717, 638, 573, 553, 517 cm⁻¹; HRMS-FAB m/z [M -OTf]⁺ calcd for C₂₀H₂₈F₃N₂O₃S: 433.1767, found: 433.1770.

1,1'-(Propane-1,3-diyl)bis(2-methoxypyridin-1-ium) bis(trifluoromethanesulfonate) (2a)

According to GP1, with **22** (918 mg, 8.25 mmol, 863 μ L, 3.8 eq) and **21** (731 mg, 2.15 mmol, 1.0 eq.) without CH_2Cl_2 as solvent. Reaction time: 1 min. Recrystallization from EtOH (5 mL) afforded **2a** (746 mg, 67%) as a colorless solid.

mp: 153–154°C; ^1H NMR (500 MHz, $[\text{D}_6]\text{DMSO}$): δ =2.37 (quin., J =7.3 Hz, 2 H, NCH_2CH_2), 4.25 (s, 6 H, CH_3), 4.49 (t, J =7.3 Hz, 4 H, NCH_2), 7.60–7.65 (m, 2 H, NCHCH), 7.80 (d, J =8.9 Hz, 2 H, OCCH), 8.53–8.59 (m, 2 H, OCCHCH), 8.67 ppm (dd, J =6.4/1.6 Hz, 2 H, NCH); ^{13}C NMR (125 MHz, $[\text{D}_6]\text{DMSO}$): δ =28.13 (NCH_2CH_2), 51.46 (NCH_2), 60.01 (CH_3), 112.37 (OCCH), 117.29 (NCHCH), 121.13 (q, J =322.3 Hz, CF_3), 143.33 (NCH), 148.62 (OCCHCH), 160.56 ppm (NCO); IR (KBr): $\tilde{\nu}$ =3166, 3098, 3066, 2365, 2345, 2296, 1639, 1586, 1521, 1477, 1441, 1397, 1356, 1330, 1266, 1224, 1158, 1077, 1048, 1030, 1006, 866, 824, 781, 753, 637, 604, 573, 517, 479 cm^{-1} ; HRMS-ESI m/z [$M\text{-OTf}$] $^+$ calcd for $\text{C}_{16}\text{H}_{20}\text{F}_3\text{N}_2\text{O}_5\text{S}$: 409.1040, found: 409.1036.

1,1'-(Propane-1,3-diyl)bis(3-methoxypyridin-1-ium) bis(trifluoromethanesulfonate) (2b)

According to GP1, with **23** (791 mg, 7.03 mmol, 730 μ L, 2.6 eq.) and **21** (929 mg, 2.73 mmol, 1.0 eq.) without CH_2Cl_2 as solvent. Reaction time: 1 min. Recrystallization from EtOH (2 mL) afforded **2b** (1.27 g, 83%) as a colorless solid.

mp: 101°C; ^1H NMR (500 MHz, $[\text{D}_6]\text{DMSO}$): δ =2.66 (quin., J =6.7 Hz, 2 H, NCH_2CH_2), 4.02 (s, 6 H, CH_3), 4.65 (t, J =6.9 Hz, 4 H, NCH_2), 8.13 (dd, J =8.8/5.9 Hz, 2 H, NCHCH), 8.29 (dd, J =8.8/2.4 Hz, 2 H, OCCHCH), 8.68 (d, J =5.9 Hz, 2 H, NCHCH), 8.88–8.92 ppm (m, 1 H, NCHCOCH_3); ^{13}C NMR (125 MHz, $[\text{D}_6]\text{DMSO}$): δ =31.29 (NCH_2CH_2), 57.23 (CH_3), 57.67 (NCH_2), 120.50 (q, J =322.5 Hz, CF_3), 128.42 (NCHCH), 130.33 (OCCHCH), 132.82 (NCHCO), 137.08 (NCHCH), 157.94 ppm (OCCH); IR (KBr): $\tilde{\nu}$ =3087, 2993, 2965, 2857, 1638, 1627, 1589, 1508, 1480, 1465, 1451, 1341, 1296, 1267, 1226, 1188, 1165, 1096, 1043, 1031, 1013, 919, 907, 800, 766, 754, 687, 682, 642, 636, 573, 517 cm^{-1} ; HRMS-ESI m/z [$M\text{-OTf}$] $^+$ calcd for $\text{C}_{16}\text{H}_{20}\text{F}_3\text{N}_2\text{O}_5\text{S}$: 409.1040, found: 409.1036.

1,1'-(Propane-1,3-diyl)bis(4-methoxypyridin-1-ium) bis(trifluoromethanesulfonate) (2c)

According to GP1, with **24** (791 mg, 6.25 mmol, 654 μ L, 2.5 eq) and **21** (851 mg, 2.50 mmol, 1.0 eq.) without CH_2Cl_2 as solvent. Reaction time: 1 min. Recrystallization from EtOH (5 mL) afforded **2c** (1.17 g, 84%) as a colorless solid.

mp: 153°C; ^1H NMR (500 MHz, D_2O): δ =2.52–2.71 (m, 2 H, NCH_2CH_2), 4.01–4.14 (m, 6 H, CH_3), 4.46–4.59 (m, 2 H, NCH_2), 7.40–7.49 (m, 4 H, NCHCH), 8.52–8.60 ppm (m, 4 H, NCH); ^{13}C NMR (125 MHz, D_2O): δ =30.83 (NCH_2CH_2), 55.75 (NCH_2), 57.35 (CH_3), 113.37 (NCHCH), 119.19 (q, J =317.2 Hz, CF_3), 144.97 (NCH), 171.28 ppm (OCCH); IR (KBr): $\tilde{\nu}$ =3150, 3070, 3017, 2968, 2373, 2313, 1647, 1575, 1529, 1493, 1464, 1445, 1376, 1328, 1317, 1280, 1254, 1226, 1215, 1193, 1158, 1067, 1030, 1005, 851, 788, 757, 741, 661, 637, 573, 518 cm^{-1} ; HRMS-ESI m/z [$M\text{-OTf}$] $^+$ calcd for $\text{C}_{16}\text{H}_{20}\text{F}_3\text{N}_2\text{O}_5\text{S}$: 409.1040, found: 409.1036.

1,1'-(Propane-1,3-diyl)bis[3-(dimethylamino)pyridin-1-ium] bis(trifluoromethanesulfonate) (2d)

According to GP1, with **25** (1.16 g, 9.53 mmol, 2.5 eq.) and **21** (1.29 g, 3.80 mmol, 1.0 eq.) without CH_2Cl_2 as solvent. Reaction time: 10 min. Recrystallization from EtOH (2 mL) afforded **2d** (1.04 g, 47%) as a yellowish solid.

mp: 155°C; ^1H NMR (500 MHz, $[\text{D}_6]\text{DMSO}$): δ = 2.66 (quin., J =7.2 Hz, 2 H, NCH_2CH_2), 3.08 (s, 12 H, $\text{N}(\text{CH}_3)_2$), 4.60 (t, J =7.1 Hz, 4 H, NCH_2), 7.79 (dd, J =8.9/2.4 Hz, 2 H, NCHCHCH), 7.84 (dd, J =9.0/5.6 Hz, 2 H, NCHCH), 8.20 (d, J =5.6 Hz, 1 H, NCHCH), 8.27–8.29 ppm (m, 2 H, $\text{NCHCN}(\text{CH}_3)_2$); ^{13}C NMR (125 MHz, $[\text{D}_6]\text{DMSO}$): δ =31.48 (NCH_2CH_2), 57.99 (NCH_2), 120.62 (q, J =322.9 Hz, CF_3), 125.53 (NCHCHCH), 127.41 (2 C, NCHCH , $\text{NCHCN}(\text{CH}_3)_2$), 130.31 (NCHCH), 148.17 ppm ($\text{NCHCN}(\text{CH}_3)_2$); IR (KBr): $\tilde{\nu}$ =3094, 2929, 2839, 1624, 1587, 1529, 1448, 1389, 1349, 1265, 1225, 1204, 1159, 1068, 1028, 864, 802, 756, 741, 683, 636, 573, 517 cm^{-1} ; HRMS-ESI m/z [$M\text{-OTf}$] $^+$ calcd for $\text{C}_{18}\text{H}_{26}\text{F}_3\text{N}_4\text{O}_3\text{S}$: 435.1672, found: 435.1668.

***rac*-{1,1'-(Propane-1,3-diyl)bis[3-(1-methylpyrrolidin-2-yl)pyridin-1-ium]} bis-(trifluoromethanesulfonate) (2e)**

According to GP1, with ***rac*-26** (324 mg, 2.00 mmol, 0.318 mL, 2.5 eq.) and **21** (272 mg, 800 μ mol, 1.0 eq.) in CH₂Cl₂ (1.6 mL). Reaction time: 30 min. Recrystallization from EtOAc/hexanes (1 mL, 1:1) afforded **2e** (380 mg, 72%) as a slightly yellowish solid.

mp: 120°C; ¹H NMR (500 MHz, [D₆]DMSO): δ =1.60–1.70 (m, 2 H, NCHCHH), 1.83–2.01 (m, 4 H, CH₃NCH₂CH₂), 2.22 (s, 6 H, NCH₃), 2.34–2.51 (m, 4 H, NCHCHH, CH₃NCHH), 2.92–3.02 (m, 2 H, NCH₂CH₂CH₂N), 3.27 (ddd, J =9.5/7.6/2.4 Hz, 2 H, CH₃NCHH), 3.52 (t, J =8.1 Hz, 2 H, NCHCH₂), 4.92–5.03 (m, 4 H, NCH₂CH₂CH₂N), 7.93 (dd, J =8.0/6.1 Hz, 2 H, NCHCH), 8.47–8.53 (m, 2 H, NCHCHCH), 9.24–9.30 (m, 2 H, NCHCH), 9.31 ppm (s, 2 H, NCHCCHNCH₃); ¹³C NMR (125 MHz, [D₆]DMSO): δ =23.25 (CH₃NCH₂CH₂), 34.78 (NCH₂CH₂CH₂N), 35.77 (NCHCH₂), 40.32 (NCH₃), 56.73 (CH₃NCH₂), 57.74 (NCH₂CH₂CH₂N), 66.79 (NCHCH₂), 120.57 (q, J =319.5 Hz, CF₃), 128.24 (NCHCH), 143.69 (NCHCCHNCH₃), 144.06 (NCHCHCH), 144.53 (NCHCH), 147.88 ppm (NCHCCHNCH₃); IR (KBr): $\tilde{\nu}$ =3061, 2959, 2881, 2848, 2792, 1636, 1505, 1483, 1468, 1318, 1276, 1258, 1225, 1156, 1090, 1048, 1029, 820, 755, 693, 638, 572, 517 cm⁻¹; HRMS-FAB m/z [M +H]⁺ calcd for C₂₅H₃₅F₆N₄O₆S₂: 665.1897, found: 665.1920.

1,1'-(Propane-1,3-diyl)bis[4-(*tert*-butyl)-3-fluoropyridin-1-ium] bis(trifluoromethanesulfonate) (3a)

27 (440 mg, 2.32 mmol, 2.5 eq.) was dissolved in H₂O (10 mL) and the solution was neutralized by the addition of K₂CO₃. The aqueous phase was extracted with CH₂Cl₂ (3 x 20 mL), dried over MgSO₄ and the solvent was carefully removed under reduced pressure (40 °C, 600 mbar). The resulting clear liquid was dissolved in CH₂Cl₂ (1 mL) and treated according to GP1 with **21** (316 mg, 0.928 mmol, 1.0 eq.). Reaction time: 4 min. Recrystallization from EtOAc/MeOH (7.7 mL, 11:1) afforded **3a** (512 mg, 85%) as a colorless solid.

mp: 206–207°C; ¹H NMR (500 MHz, [D₆]DMSO): δ =1.40–1.47 (m, 18 H, C(CH₃)₃), 2.65 (quin. J =7.2 Hz, 2 H, NCH₂CH₂), 4.65 (t, J =7.1 Hz, 4 H, NCH₂CH₂), 8.19 (dd, J =8.0/6.6 Hz, 2 H, NCHCH), 8.91 (dd, J =6.5/1.4 Hz, 2 H, NCHCH), 9.35 ppm (dd, J =6.6/1.2 Hz, 2 H, NCHCF); ¹³C NMR (125 MHz, [D₆]DMSO): δ =28.15 (d, J =2.8 Hz,

C(CH₃)₃), 30.70 (NCH₂CH₂), 35.60 (d, *J*=3.0 Hz, C(CH₃)₃), 56.90 (NCH₂CH₂), 120.50 (q, *J*=322.3 Hz, CF₃), 126.59 (d, *J*=5.8 Hz, NCHCH), 134.80 (d, *J*=42.5 Hz, NCHCF), 141.60 (d, *J*=3.5 Hz, NCHCH), 155.50 (d, *J*=9.4 Hz, CC(CH₃)₃), 158.56 ppm (d, *J*=254.0 Hz, CF); IR (KBr): $\tilde{\nu}$ =3060, 2973, 2881, 1651, 1513, 1486, 1462, 1371, 1285, 1260, 1225, 1167, 1100, 1031, 988, 953, 920, 847, 832, 802, 756, 728, 617, 638, 617 cm⁻¹; HRMS-FAB *m/z* [*M*-OTf]⁺ calcd for C₂₂H₃₀F₅N₂O₃S: 497.1892, found: 497.1917.

1,1'-(Propane-1,3-diyl)bis[4-(*tert*-butyl)-3-chloropyridin-1-ium] bis(trifluoromethanesulfonate) (3b)

According to GP1, with **28** (272 mg, 1.60 mmol, 2.5 eq.) and **21** (218 mg, 0.641 mmol, 1.0 eq.) in CH₂Cl₂ (1.3 mL). Reaction time: 30 min. Recrystallization from EtOAc (4.5 mL) afforded **3b** (353 mg, 81%) as a colorless solid.

mp: 178°C; ¹H NMR (500 MHz, CDCl₃): δ =1.54 (s, 18 H, C(CH₃)₃), 2.88–2.98 (m, 2 H, NCH₂CH₂), 4.94–5.02 (m, 4 H, NCH₂), 7.97 (d, *J*=6.6 Hz, 2 H, NCHCH), 9.22 (dd, *J*=6.6/1.5 Hz, 2 H, NCHCH), 9.35 ppm (d, *J*=1.5 Hz, 2 H, NCHCCl); ¹³C NMR (125 MHz, CDCl₃): δ =28.00 (C(CH₃)₃), 34.06 (NCH₂CH₂), 38.20 (C(CH₃)₃), 57.02 (NCH₂CH₂), 120.45 (q, *J*=319.4 Hz, CF₃), 126.71 (NCHCH), 135.79 (NCHCCl), 143.04 (NCHCH), 145.47 (NCHCCl), 167.42 ppm (CC(CH₃)₃); IR (KBr): $\tilde{\nu}$ =3121, 3045, 2974, 2881, 1638, 1496, 1453, 1368, 1282, 1224, 1197, 1163, 1084, 1030, 924, 895, 847, 790, 755, 705, 637 cm⁻¹; HRMS-FAB *m/z* [*M*-OTf]⁺ calcd for C₂₂H₃₀Cl₂F₃N₂O₃S: 529.1301, found: 529.1331.

1,1'-(Propane-1,3-diyl)bis[3-bromo-4-(*tert*-butyl)pyridin-1-ium] bis(trifluoromethanesulfonate) (3c)

According to GP1, with **29** (281 mg, 1.31 mmol, 2.5 eq.) and **21** (179 mg, 0.525 mmol, 1.0 eq.) in CH₂Cl₂ (1 mL). Reaction time: 30 min. Recrystallization from EtOH/Et₂O/*n*-pentane (1:1:2.5, 9 mL) afforded **3c** (402 mg, 99%) as a colorless solid.

mp: 169–170°C; ¹H NMR (500 MHz, CDCl₃): δ =1.57 (s, 18 H, C(CH₃)₃), 2.88–2.97 (m, 2 H, NCH₂CH₂), 4.93–4.99 (m, 4 H, NCH₂), 7.97 (d, *J*=6.6 Hz, 2 H, NCHCH), 9.28 (d, *J*=6.6 Hz, 2 H, NCHCH), 9.50 ppm (s, 2 H, NCHCBr); ¹³C NMR (125 MHz, CDCl₃): δ =28.06 (C(CH₃)₃), 34.26 (NCH₂CH₂), 38.81 (C(CH₃)₃), 56.77 (NCH₂CH₂), 120.47 (q, *J*=319.4 Hz, CF₃), 123.41 (NCHCBr), 126.69 (NCHCH), 143.28 (NCHCH), 148.16 (NCHCBr), 168.90 ppm (CC(CH₃)₃); IR (KBr): $\tilde{\nu}$ =3120, 3040, 2978, 1635,

1559, 1541, 1489, 1455, 1368, 1279, 1257, 1224, 1196, 1160, 1133, 1079, 1030, 935, 907, 846, 785, 755 cm^{-1} ; HRMS-FAB m/z $[M-\text{OTf}]^+$ calcd for $\text{C}_{22}\text{H}_{30}\text{Br}_2\text{F}_3\text{N}_2\text{O}_3\text{S}$: 617.0290, found: 617.0294.

1,1'-(Propane-1,3-diyl)bis[4-(*tert*-butyl)-3-cyanopyridin-1-ium] bis(trifluoromethanesulfonate) (3d)

According to GP1, with **30** (705 mg, 4.40 mmol, 2.5 eq.) and **21** (599 mg, 1.76 mmol, 1.0 eq.) in CH_2Cl_2 (3.5 mL). Reaction time: 40 min. Recrystallization from EtOAc (4 mL) afforded **3d** (991 mg, 85%) as a slightly beige solid.

mp: 172°C; ^1H NMR (500 MHz, $[\text{D}_6]\text{DMSO}$): δ =1.55 (s, 18 H, $\text{C}(\text{CH}_3)_3$), 2.67 (quin., J =7.1 Hz, 2 H, NCH_2CH_2), 4.68 (t, J =7.1 Hz, 4 H, NCH_2), 8.36 (d, J =6.7 Hz, 2 H, NCHCH), 9.22 (dd J =6.8/1.5 Hz, 2 H, NCHCH), 9.74 ppm (d, J =1.3 Hz, 2 H, NCHCCN); ^{13}C NMR (125 MHz, $[\text{D}_6]\text{DMSO}$): δ =28.33 ($\text{C}(\text{CH}_3)_3$), 30.41 (NCH_2CH_2), 37.08 ($\text{C}(\text{CH}_3)_3$), 57.02 (NCH_2CH_2), 110.77 (NCHCCN), 114.84 (CN), 120.49 (q, J =322.3 Hz, CF_3), 126.12 (NCHCH), 147.73 (NCHCH), 150.61 (NCHCCN), 170.63 ppm ($\text{CC}(\text{CH}_3)_3$); IR (KBr): $\tilde{\nu}$ =3150, 3115, 3058, 2987, 2970, 2942, 1642, 1557, 1499, 1483, 1463, 1373, 1285, 1251, 1226, 1166, 1098, 1030, 1006, 939, 856, 830, 806, 759, 638 cm^{-1} ; HRMS-FAB m/z $[M-\text{OTf}]^+$ calcd for $\text{C}_{24}\text{H}_{30}\text{F}_3\text{N}_4\text{O}_3\text{S}$: 511.1985, found: 511.1968.

1,1'-(Propane-1,3-diyl)bis[4-(*tert*-butyl)-3-methoxypyridin-1-ium] bis(trifluoromethanesulfonate) (3e)

According to GP1, with **31** (254 mg, 1.54 mmol, 2.5 eq.) and **21** (210 mg, 0.617 mmol, 1.0 eq.) without CH_2Cl_2 as solvent. Reaction time: 5 min. The residue was dissolved in *i*-PrOH (1 mL) and precipitated by the addition of $\text{Et}_2\text{O}/n$ -pentane (2:3, 15 mL) to afford **3e** (342 mg, 83%) as a colorless solid.

mp: 104°C; ^1H NMR (500 MHz, CDCl_3): δ =1.41 (s, 18 H, $\text{C}(\text{CH}_3)_3$), 2.92–3.00 (m, 2 H, NCH_2CH_2), 4.14 (s, 6H, OCH_3), 4.88–4.93 (m, 4 H, NCH_2), 7.73 (d, J =6.3 Hz, 2 H, NCHCH), 8.94–8.97 (m, 2 H, NCHCH), 9.01–9.04 ppm (m, 2 H, NCHCOCH_3); ^{13}C NMR (125 MHz, CDCl_3): δ =28.08 ($\text{C}(\text{CH}_3)_3$), 34.92 (NCH_2CH_2), 36.74 ($\text{C}(\text{CH}_3)_3$), 57.11 (NCH_2CH_2), 57.88 (OCH_3), 119.27 (q, J =319.2 Hz, CF_3), 125.17 (NCHCH), 128.10 (NCHCOCH_3), 137.88 (NCHCH), 157.99 (NCHCOCH_3)*, 158.07 ppm ($\text{CC}(\text{CH}_3)_3$)*; IR (KBr): $\tilde{\nu}$ =3566, 3493, 3063, 2970, 1635, 1570, 1559, 1513, 1477,

1454, 1366, 1345, 1325, 1316, 1285, 1257, 1225, 1199, 1165, 1097, 1043, 1034, 1028, 891, 845, 798, 757 cm^{-1} ; HRMS-FAB m/z $[M\text{-OTf}]^+$ calcd for $\text{C}_{24}\text{H}_{36}\text{F}_3\text{N}_2\text{O}_5\text{S}$: 521.2292, found: 521.2281.

1,1'-(Propane-1,3-diyl)bis[4-(*tert*-butyl)-3-(dimethylcarbamoyl)pyridin-1-ium] bis-(trifluoromethanesulfonate) (3f)

According to GP1, with **32** (299 mg, 1.45 mmol, 2.5 eq.) and **21** (197 mg, 0.580 mmol, 1.0 eq.) in CH_2Cl_2 (1.2 mL). Reaction time: 30 min. Recrystallization from EtOAc (12 mL) afforded **3f** (335 mg, 77%) as a colorless solid.

mp: 199–201°C; ^1H NMR (500 MHz, $[\text{D}_6]\text{DMSO}$): δ =1.40 (s, 18 H, $\text{C}(\text{CH}_3)_3$), 2.62 (quin., J =7.1 Hz, 2 H, NCH_2CH_2), 2.87 (m, 6 H, NCH_3), 3.05 (d, J =1.6 Hz, 6 H, NCH_3), 4.56–4.68 (m, 4 H, NCH_2CH_2), 8.33 (dd, J =6.6/2.0 Hz, 2 H, NCHCH), 8.95–9.01 ppm (m, 4 H, NCHCH , NCHCCO); ^{13}C NMR (125 MHz, $[\text{D}_6]\text{DMSO}$): δ =29.96 ($\text{C}(\text{CH}_3)_3$), 31.60 (NCH_2CH_2), 34.97 (NCH_3), 38.22 ($\text{C}(\text{CH}_3)_3$), 40.32 (NCH_3), 57.32 (NCH_2NCH_2), 121.13 (q, J =322.4 Hz, CF_3), 128.02 (NCHCH), 135.17 (NCHCCO), 143.05 (NCHCCO), 144.61 (NCHCH), 165.74 (CO), 166.30 ppm ($\text{CC}(\text{CH}_3)_3$); IR (KBr): $\tilde{\nu}$ =3047, 2972, 1646, 1559, 1495, 1457, 1403, 1369, 1261, 1225, 1158, 1117, 1087, 1060, 1031, 962, 852, 756, 660, 639, 574, 557, 518 cm^{-1} ; HRMS-FAB m/z $[M\text{-OTf}]^+$ calcd for $\text{C}_{28}\text{H}_{42}\text{F}_3\text{N}_4\text{O}_5\text{S}$: 603.2823, found: 603.2843.

1,1'-(Propane-1,3-diyl)bis[4-(*tert*-butyl)-3-methylpyridin-1-ium] bis(trifluoromethanesulfonate) (3g)

According to GP1, with **33** (279 mg, 1.87 mmol, 2.5 eq.) and **21** (254 mg, 0.748 mmol, 1.0 eq.) in CH_2Cl_2 (1 mL). Reaction time: 20 min. Recrystallization from EtOAc/hexanes (1.1:1, 3.8 mL) afforded **3g** (425 mg, 89%) as a colorless solid.

mp: 90°C; ^1H NMR (500 MHz, CDCl_3): δ =1.47 (s, 18 H, $\text{C}(\text{CH}_3)_3$), 2.73 (s, 6 H, CHCCH_3), 2.85–2.92 (m, 2 H, NCH_2CH_2), 4.82–4.87 (m, 4 H, NCH_2), 7.85 (d, J =6.6 Hz, 2 H, NCHCH), 9.05–9.09 ppm (m, 4 H, NCH); ^{13}C NMR (125 MHz, CDCl_3): δ =20.26 (CHCCH_3), 29.25 ($\text{C}(\text{CH}_3)_3$), 34.60 (NCH_2CH_2), 37.69 ($\text{C}(\text{CH}_3)_3$), 56.44 (NCH_2CH_2), 120.57 (q, J =319.4 Hz, CF_3), 125.44 (NCHCH), 138.78 ($\text{CHC}(\text{CH}_3)$), 141.91 (NCH)*, 145.94 (NCH)*, 168.72 ppm ($\text{CC}(\text{CH}_3)_3$); IR (KBr): $\tilde{\nu}$ =3066, 2972, 1644, 1508, 1479, 1387, 1368, 1282, 1256, 1224, 1155, 1099,

1028, 969, 935, 850, 805, 755 cm^{-1} ; HRMS-FAB m/z $[M-\text{OTf}]^+$ calcd for $\text{C}_{24}\text{H}_{36}\text{F}_3\text{N}_2\text{O}_3\text{S}$: 489.2393, found: 489.2399.

1,1'-(Propane-1,3-diyl)bis[4-(*tert*-butyl)-3-phenylpyridin-1-ium] bis(trifluoromethanesulfonate) (3h)

According to GP1, with **34** (444 mg, 2.10 mmol, 2.5 eq.) and **21** (286 mg, 0.84 mmol, 1.0 eq.) in CH_2Cl_2 (1.7 mL). Reaction time: 30 min. Recrystallization from EtOAc/Et₂O (1:5, 12 mL) afforded **3h** (620 mg, 99 %) as a colorless solid.

mp: 178–179°C; ^1H NMR (500 MHz, $[\text{D}_6]\text{DMSO}$): δ =1.25 (s, 18 H, $\text{C}(\text{CH}_3)_3$), 2.86–2.95 (m, 2 H, NCH_2CH_2), 4.82–4.90 (m, 2 H, NCH_2CH_2), 7.29–7.34 (m, 4 H, NCHCCCH), 7.45–7.55 (m, 6 H, NCHCCCHCH , NCHCCCHCHCH), 8.06 (d, J =6.8 Hz, 2 H, NCHCH), 8.74 (d, J =1.7 Hz, 2 H, NCHCCCH), 9.15 ppm (dd, J =6.8/1.8 Hz, 2 H, NCHCH); ^{13}C NMR (125 MHz, $[\text{D}_6]\text{DMSO}$): δ =31.38 ($\text{C}(\text{CH}_3)_3$), 34.22 (NCH_2CH_2), 38.98 ($\text{C}(\text{CH}_3)_3$), 57.07 (NCH_2CH_2), 120.98 (q, J =320.1 Hz, CF_3), 127.14 (NCHCH), 128.67 (NCHCCCHCH), 129.77 (NCHCCCHCHCH), 130.18 (NCHCCCH), 136.09 (NCHCCCH), 142.95 (NCHCH), 143.24 (NCHCCCH), 146.27 (NCHCCCH), 169.28 ppm ($\text{CC}(\text{CH}_3)_3$); IR (KBr): $\tilde{\nu}$ =3057, 2972, 2876, 1636, 1507, 1488, 1473, 1445, 1368, 1257, 1224, 1156, 1102, 1030, 851, 765, 755, 707, 638, 572, 517 cm^{-1} ; HRMS-FAB m/z $[M-\text{OTf}]^+$ calcd for $\text{C}_{44}\text{H}_{40}\text{F}_3\text{N}_2\text{O}_3\text{S}$: 613.2706, found: 613.2718.

1,1'-(Propane-1,3-diyl)bis[4-(*tert*-butyl)-3-ethynylpyridin-1-ium] bis(trifluoromethanesulfonate) (3i)

According to GP1, with **35** (259 mg, 1.63 mmol, 2.5 eq.) and **21** (225 mg, 0.661 mmol, 1.0 eq.) in CH_2Cl_2 (1.3 mL). Reaction time: 40 min. Recrystallization from EtOAc/hexanes (2.3:1, 4 mL) afforded **3i** (392 mg, 91%) as a colorless solid.

mp: 161°C; ^1H NMR (500 MHz, $[\text{D}_6]\text{DMSO}$): δ =1.56 (s, 18 H, $\text{C}(\text{CH}_3)_3$), 2.86–2.96 (m, 2 H, NCH_2CH_2), 3.95 (s, 2 H, CCH), 4.88–5.00 (m, 4 H, NCH_2CH_2), 7.92 (d, J =6.6 Hz, 2 H, NCHCH), 9.23 (dd, J =6.6/1.4 Hz, 2 H, NCHCH), 9.34 ppm (d, J =1.3 Hz, 2 H, NCHCCCH); ^{13}C NMR (125 MHz, $[\text{D}_6]\text{DMSO}$): δ =28.39 ($\text{C}(\text{CH}_3)_3$), 34.25 (NCH_2CH_2), 37.87 ($\text{C}(\text{CH}_3)_3$), 56.92 (NCH_2NCH_2), 92.75 (NCHCCCH), 120.52 (q, J =319.5 Hz, CF_3), 123.35 (NCHCCCH), 125.56 (NCHCH), 143.77 (NCHCH), 149.42 (NCHCCCH), 171.65 ppm ($\text{CC}(\text{CH}_3)_3$); IR (KBr): $\tilde{\nu}$ =3308, 3234, 3062, 2969, 2108, 1637, 1497, 1460,

1368, 1294, 1262, 1225, 1160, 1098, 1034, 1028, 936, 842, 757, 638, 573, 517 cm⁻¹; HRMS-FAB *m/z* [*M*-OTf]⁺ calcd for C₂₆H₃₂F₃N₂O₃S: 509.2080, found: 509.2105.

1,1'-(Propane-1,3-diyl)bis[4-(*tert*-butyl)-3-(ethoxycarbonyl)pyridin-1-ium] bis-(trifluoromethanesulfonate) (3j)

According to GP1, with **36** (477 mg, 2.30 mmol, 2.5 eq.) and **21** (313 mg, 0.920 mmol, 1.0 eq.) in CH₂Cl₂ (1.8 mL). Reaction time: 30 min. Recrystallization from EtOAc (1.5 mL) afforded **3j** (677 mg, 98%) as a colorless solid.

mp: 157°C; ¹H NMR (500 MHz, CDCl₃): δ=1.45 (t, *J*=7.2 Hz, 6 H, CH₂CH₃), 1.48 (s, 18 H, C(CH₃)₃), 2.88–2.97 (m, 2 H, NCH₂CH₂), 4.49 (q, *J*=7.2 Hz, 4 H, CH₂CH₃), 4.92–5.00 (m, 4 H, NCH₂CH₂), 8.02 (d, *J*=6.7 Hz, 2 H, NCHCH), 9.36 (dd, *J*=6.7/1.6 Hz, 2 H, NCHCH), 9.43 ppm (d, *J*=1.5 Hz, 2 H, NCHCCO); ¹³C NMR (125 MHz, CDCl₃): δ=13.64 (CH₂CH₃), 29.98 (C(CH₃)₃), 34.75 (NCH₂CH₂), 38.18 (C(CH₃)₃), 56.88 (NCH₂CH₂), 64.22 (CH₂CH₃), 120.51 (q, *J*=319.4 Hz, CF₃), 127.01 (NCHCH), 134.40 (NCHCCO), 144.84 (NCHCCO), 145.08 (NCHCH), 164.34 (CH₃CH₂OCO), 169.01 ppm (CC(CH₃)₃); IR (KBr): $\tilde{\nu}$ =3100, 3052, 2983, 1735, 1641, 1559, 1499, 1466, 1372, 1317, 1258, 1226, 1194, 1156, 1136, 1091, 1031, 1009, 936, 855, 782, 755, 712, 695, 638, 607, 573, 553, 517 cm⁻¹; HRMS-FAB *m/z* [*M*-OTf]⁺ calcd for C₂₈H₄₀F₃N₂O₇S: 605.2503, found: 605.2480.

1,1'-(Propane-1,3-diyl)bis[4-(*tert*-butyl)-2-methylpyridin-1-ium] bis(trifluoromethanesulfonate) (3k)

According to GP1, with **15** (547 mg, 3.67 mmol, 2.5 eq.) and **21** (499 mg, 1.47 mmol, 1.0 eq.) in CH₂Cl₂ (3 mL). Reaction time: 30 min. Recrystallization from EtOAc/hexanes (2:1, 3 mL) afforded **3k** (773 mg, 82%) as a colorless solid.

mp: 115–116°C; ¹H NMR (500 MHz, [D₆]DMSO): δ=1.38 (s, 18 H, C(CH₃)₃), 2.59–2.69 (m, 2 H, NCH₂CH₂), 3.02 (s, 6 H, CH₃), 4.86–4.96 (m, 4 H, NCH₂CH₂), 7.71 (d, *J*=2.2 Hz, 2 H, CH₃CCH), 7.73 (dd, *J*=6.7/2.3 Hz, 1 H, NCHCH), 9.14 ppm (d, *J*=6.7 Hz, 2 H, NCHCH); ¹³C NMR (125 MHz, [D₆]DMSO): δ=20.76 (CH₃), 29.86 (C(CH₃)₃), 30.65 (NCH₂CH₂), 36.38 (C(CH₃)₃), 53.41 (NCH₂CH₂), 120.54 (q, *J*=320.1 Hz, CF₃), 123.46 (NCHCH), 127.00 (CH₃CCH), 145.26 (NCHCH), 154.93 (NCCH₃), 171.24 ppm (CC(CH₃)₃); IR (KBr): $\tilde{\nu}$ =3062, 2974, 2879, 1641, 1567, 1517, 1469, 1373, 1259, 1224,

1156, 1108, 1030, 919, 851, 755, 637, 573, 517 cm^{-1} ; HRMS-FAB m/z [$M\text{-OTf}$] $^{+}$ calcd for $\text{C}_{24}\text{H}_{36}\text{F}_3\text{N}_2\text{O}_3\text{S}$: 489.239, found: 489.2381.

4-(*tert*-Butyl)-1-{3-[4-(*tert*-butyl)-3-carboxypyridin-1-ium-1-yl]propyl}pyridin-1-ium-3-carboxylate trifluoromethanesulfonate (3l**)**

Aqueous NaOH (0.1 M solution, 16.6 mL, 1.66 mmol, 2.5 eq.) was added to a solution of **3j** (500 mg, 0.662 mmol, 1.0 eq.) in $\text{H}_2\text{O}/\text{MeCN}$ (5:1, 30 mL) and the resulting solution was stirred for 16 h at room temperature. The reaction mixture was washed with Et_2O (3 x 50 mL) and the water was removed under reduced pressure. The residue was dissolved in H_2O (20 mL) and the pH was adjusted to 2 by the addition of 5 % aqueous TfOH. The aqueous phase was washed with CH_2Cl_2 (3 x 50 mL) and the water was removed under reduced pressure. The solid residue was dissolved in EtOH/MeOH (1:1, 40 mL) and insoluble components were removed by filtration. The solvent was removed under reduced pressure and the residue was purified by crystallization from EtOH/MeOH (2.4:1, 29 mL) to yield **3l** (242 mg, 66%) as a colorless solid.

mp (decomposition): 209°C; ^1H NMR (500 MHz, $[\text{D}_4]\text{MeOH}$): δ =1.55 (s, 18 H, $\text{C}(\text{CH}_3)_3$), 2.70 (quin. J =7.6 Hz, 2 H, NCH_2CH_2), 4.67–4.73 (m, 4 H, NCH_2CH_2), 8.17 (d, J =6.7 Hz, 2 H, NCHCH), 8.80 (dd, J =6.7/1.7 Hz, 2 H, NCHCH), 8.89 ppm (d, J =1.6 Hz, 2 H, NCHCCO); ^{13}C NMR (125 MHz, $[\text{D}_4]\text{MeOH}$): δ =30.41 ($\text{C}(\text{CH}_3)_3$), 33.03 (NCH_2CH_2), 39.02 ($\text{C}(\text{CH}_3)_3$), 58.41 (NCH_2NCH_2), 121.82 (q, J =318.5 Hz, CF_3), 128.33 (NCHCH), 139.98 (NCHCCO), 144.34 (NCHCH , NCHCCO), 168.13 ($\text{CC}(\text{CH}_3)_3$), 170.12 ppm (COO); IR (KBr): $\tilde{\nu}$ =3111, 3055, 2977, 2478, 1709, 1638, 1556, 1499, 1476, 1374, 1252, 1224, 1201, 1164, 1093, 1070, 1030, 933, 856, 809, 785, 774, 756, 712, 680, 639, 560, 517, 500 cm^{-1} ; HRMS-FAB m/z [$M\text{+H}$] $^{+}$ calcd for $\text{C}_{24}\text{H}_{32}\text{F}_3\text{N}_2\text{O}_7\text{S}$: 549.1877, found: 549.1907.

2,2'-(Propane-1,3-diyl)bis(isoquinolin-2-ium) diiodide (4a**)**

According to GP2, with **37** (680 mg, 5.00 mmol, 624 μL , 2.5 eq.) and **16** (592 mg, 2.00 mmol, 230 μL , 1.0 eq.) in MeCN (4 mL). Reaction time: 3 h. Recrystallization from MeOH (30 mL) afforded **4a** (950 mg, 86%) as a yellow solid.

mp (decomposition): 260°C; ^1H NMR (500 MHz, $[\text{D}_6]\text{DMSO}$): δ =2.88 (quin., J =7.2 Hz, 2 H, NCH_2CH_2), 4.91 (t, J =7.2 Hz, 4 H, NCH_2CH_2), 8.08–8.13 (m, 2 H, NCHCCHCH),

8.27–8.32 (m, 2 H, NCHCHCCHCH), 8.36–8.39 (m, 2 H, NCHCHCCH), 8.47–8.52 (m, 2 H, NCHCCH), 8.63–8.67 (m, 2 H, NCHCH), 8.81–8.85 (m, 2 H, NCHCH), 10.13 ppm (s, 2 H, NCHCCH); ^{13}C NMR (125 MHz, $[\text{D}_6]\text{DMSO}$): δ =31.72 (NCH₂CH₂), 58.05 (NCH₂CH₂), 126.46 (NCHCH), 127.72 (NCHCCH), 127.75 (NCHCHCCH), 130.91 (NCHCCH), 131.76 (NCHCCHCH), 135.38 (NCHCH), 137.56 (NCHCHCCHCH, NCHCHCCH), 150.89 ppm (NCHCCH); IR (KBr): $\tilde{\nu}$ =3011, 2937, 2022, 1943, 1855, 1804, 1643, 1607, 1580, 1516, 1477, 1426, 1402, 1394, 1370, 1356, 1282, 1234, 1217, 1202, 1185, 1168, 1131, 1103, 1071, 1017, 982, 931, 880, 840, 832, 777, 759, 745, 646, 628, 532, 519, 474 cm⁻¹; HRMS-FAB m/z $[M-I]^+$ calcd for C₂₁H₂₀IN₂: 427.0666, found: 427.0670.

1,1'-(Propane-1,3-diyl)bis[3-(*tert*-butyl)pyrazin-1-ium] diiodide (**4b**)

According to GP2, with **38** (460 mg, 3.28 mmol, 2.5 eq.) and **16** (388 mg, 1.31 mmol, 150 μL , 1.0 eq.) in MeCN (2.6 mL). Reaction time: 16 h at 120 °C. Recrystallization from MeOH (60 mL), dissolution of the yellow crystals in H₂O (70 mL) and subsequent lyophilization afforded **4b** (578 mg, 78%) as a yellow powder.

mp: 273 °C; ^1H NMR (500 MHz, $[\text{D}_6]\text{DMSO}$): δ =1.44 (s, 18 H, C(CH₃)₃), 2.73–2.85 (m, 2 H, NCH₂CH₂), 4.81 (t, J =6.8 Hz, 4 H, NCH₂), 9.08 (s, 2 H, CH₂NCHCHN), 9.26 (s, 2 H, NCHC(C(CH₃)₃)), 9.55 ppm (s, 2 H, CH₂NCHCHN); ^{13}C NMR (125 MHz, $[\text{D}_6]\text{DMSO}$): δ =28.86 (C(CH₃)₃), 30.56 (NCH₂CH₂), 37.68 (C(CH₃)₃), 57.99 (NCH₂), 132.69–135.01 (CH₂NCHCHN, NCHC(C(CH₃)₃)), 149.42 (CH₂NCHCHN), 170.30 ppm (NCHC(C(CH₃)₃)); IR (KBr): $\tilde{\nu}$ =3109, 3009, 2965, 2869, 1619, 1552, 1484, 1457, 1367, 1296, 1253, 1190, 1160, 1134, 1020, 863, 811, 760, 744, 643, 623, 461 cm⁻¹; HRMS-ESI m/z $[M-I]^+$ calcd for C₁₉H₃₀IN₄: 441.1510, found: 441.1514.

3,3'-(Propane-1,3-diyl)bis(thiazol-3-ium) diiodide (**4c**)

According to GP2, with **39** (426 mg, 5.00 mmol, 355 μL , 2.5 eq.) and **16** (592 mg, 2.00 mmol, 230 μL , 1.0 eq.) in MeCN (4 mL). Reaction time: 16 h at 120 °C. Recrystallization from MeOH (22 mL) afforded **4c** (806 mg, 87%) as a beige solid.

mp: 218 °C; ^1H NMR (400 MHz, $[\text{D}_6]\text{DMSO}$): δ =2.60 (quin., J =7.2 Hz, 2 H, NCH₂CH₂), 4.65 (t, J =7.2 Hz, 4 H, NCH₂CH₂), 8.40 (dd, J =3.7/2.4 Hz, 2 H, CH₂NCHCH), 8.59 (dd, J =3.7/1.3 Hz, 2 H, CH₂NCHCH), 10.21 ppm (dd, J =2.3/1.4 Hz, 2 H, NCHS); ^{13}C NMR (100 MHz, $[\text{D}_6]\text{DMSO}$): δ =30.33 (NCH₂CH₂), 51.87 (NCH₂CH₂), 127.59

(CH₂NCHCH), 137.47 (CH₂NCHCH), 160.32 ppm (NCHS); IR (KBr): $\tilde{\nu}$ =3028, 2951, 1622, 1546, 1448, 1418, 1348, 1321, 1259, 1195, 1160, 1087, 1060, 970, 955, 908, 825, 742, 699, 677, 638, 620, 601, 589, 569, 556 cm⁻¹; HRMS-FAB m/z [$M-I$]⁺ calcd for C₉H₁₂IN₂S₂: 338.9481, found: 338.9493.

3,3'-(Propane-1,3-diyl)bis(1-methyl-1*H*-imidazol-3-ium) diiodide (4d)

According to GP2, with **40** (411 mg, 5.00 mmol, 399 μ L, 2.5 eq.) and **16** (592 mg, 2.00 mmol, 230 μ L, 1.0 eq.) in MeCN (4 mL). Reaction time: 1 h. Recrystallization from EtOH (2 mL) afforded **4d** (845 mg, 92%) as a colorless solid.

mp: 226°C; ¹H NMR (500 MHz, CD₃CN): δ =1.65 (s, 18 H, C(CH₃)₃), 2.62 (quin., J =6.8 Hz, 2 H, NCH₂CH₂), 4.38 (t, J =7.1 Hz, 4 H, NCH₂), 7.57 (s, 2 H, CH₂NCHCHN), 7.64 (s, 2 H, CH₂NCHCHN), 9.26 ppm (s, 2 H, NCHN); ¹³C NMR (125 MHz, CD₃CN): δ =29.91 (C(CH₃)₃), 31.08 (NCH₂CH₂), 47.53 (NCH₂), 61.35 (C(CH₃)₃), 121.03 (CH₂NCHCHN), 123.78 (CH₂NCHCHN), 135.75 ppm (NCHN); IR (KBr): $\tilde{\nu}$ =3133, 3075, 2969, 2874, 1617, 1552, 1457, 1408, 1376, 1312, 1295, 1239, 1208, 1136, 1118, 1098, 1049, 1001, 944, 892, 826, 787, 751, 654, 629, 616 cm⁻¹; HRMS-ESI m/z [$M-I$]⁺ calcd for C₁₇H₃₀IN₄: 417.1510, found: 417.1515.

3,3'-(Propane-1,3-diyl)bis[1-(*tert*-butyl)-1*H*-imidazol-3-ium] diiodide (4e)

According to GP2, with **41** (404 mg, 3.25 mmol, 2.5 eq.) and **16** (385 mg, 1.30 mmol, 150 μ L, 1.0 eq.) in MeCN (2.6 mL). Reaction time: 1 h. Recrystallization from EtOH (30 mL) afforded **4e** (581 mg, 82%) as a colorless solid.

mp: 226°C; ¹H NMR (500 MHz, CD₃CN): δ =1.65 (s, 18 H, C(CH₃)₃), 2.62 (quin., J =6.8 Hz, 2 H, NCH₂CH₂), 4.38 (t, J =7.1 Hz, 4 H, NCH₂), 7.57 (s, 2 H, CH₂NCHCHN), 7.64 (s, 2 H, CH₂NCHCHN), 9.26 ppm (s, 2 H, NCHN); ¹³C NMR (125 MHz, CD₃CN): δ =29.91 (C(CH₃)₃), 31.08 (NCH₂CH₂), 47.53 (NCH₂), 61.35 (C(CH₃)₃), 121.03 (CH₂NCHCHN), 123.78 (CH₂NCHCHN), 135.75 ppm (NCHN); IR (KBr): $\tilde{\nu}$ =3133, 3075, 2969, 2874, 1617, 1552, 1457, 1408, 1376, 1312, 1295, 1239, 1208, 1136, 1118, 1098, 1049, 1001, 944, 892, 826, 787, 751, 654, 629, 616 cm⁻¹; HRMS-ESI m/z [$M-I$]⁺ calcd for C₁₇H₃₀IN₄: 417.1510, found: 417.1515.

4-(2-[²H₃]Methyl[1,1,1,3,3,3-²H₆]propan-2-yl)pyridine (48)

Acetyl chloride (0.22 g, 2.8 mmol, 0.20 mL, 1.0 eq.) was added to a solution of **12** (0.22 g, 2.8 mmol, 0.23 mL, 1.0 eq.) in THF (5 mL) at $-78\text{ }^{\circ}\text{C}$ and the resulting suspension was stirred for 1 h before $(d_9\text{-}t\text{-Bu})_2\text{CuCN}(\text{MgCl})_2$ (1.1 eq.), prepared according to GP4 with $d_9\text{-}t\text{-BuMgCl}^*$ (0.67 M solution in THF, 6.2 mmol, 9.2 mL, 2.2 eq.) and CuCN (0.28 g, 3.1 mmol, 1.1 eq.) in THF (8 mL), was added via transfer cannula. The reaction was stirred for an additional 1 h at $-78\text{ }^{\circ}\text{C}$ and quenched by addition of saturated aqueous $\text{NH}_4\text{Cl}/\text{conc. NH}_3$ (1:1, 10 mL). The mixture was extracted with CH_2Cl_2 (3 x 30 mL), the combined organic layers were washed with saturated aqueous NaCl (30 mL) and dried over MgSO_4 . The solvent was removed under reduced pressure and the crude dihydropyridine was purified by FC (Al_2O_3 -neutral, activity III, $n\text{-pentane}/\text{Et}_2\text{O} = 9:1$). The resulting colorless oil was dissolved in CH_2Cl_2 (10 mL) and treated with DDQ (0.64 g, 2.8 mmol, 1.0 eq.). The reaction was stirred for 60 min at room temperature prior to being diluted with CH_2Cl_2 (20 mL). The mixture was extracted with 2 M HCl (3 x 20 mL) and the combined aqueous layers were washed with Et_2O (30 mL). The aqueous phase was neutralized by addition of K_2CO_3 and adjusted to pH 10 by adding 1 M NaOH. The aqueous mixture was extracted with Et_2O (3 x 30 mL) and the combined organic layers were dried over MgSO_4 . The solvent was carefully removed under reduced pressure (200 mbar, $40\text{ }^{\circ}\text{C}$). The residue was purified by FC (SiO_2 , $n\text{-pentane}/\text{Et}_2\text{O} = 5:1 \rightarrow 1:1$) and subsequently by vacuum distillation ($5\cdot 10^{-2}$ mbar, $200\text{ }^{\circ}\text{C}$) to yield pure **48** (126 mg, 31%, 99% D) as a colorless liquid.

$R_f=0.37$ ($n\text{-pentane}/\text{Et}_2\text{O}$ 1:1); $^1\text{H NMR}$ (500 MHz, CD_2Cl_2): $\delta=7.09\text{--}7.45$ (m, 2 H, NCHCH), 8.26–8.66 ppm (m, 2 H, NCH); $^{13}\text{C NMR}$ (125 MHz, CD_2Cl_2): $\delta=29.55$ (sept., $J=19.6$ Hz, $\text{C}(\text{CD}_3)_3$), 34.24 ($\text{C}(\text{CD}_3)_3$), 121.08 (NCHCH), 150.02 (NCH) 160.24 ppm (NCHCHC); IR (film): $\tilde{\nu}=3078, 3025, 2982, 2934, 2361, 2336, 2219, 2152, 2119, 2077, 2050, 1934, 1597, 1552, 1492, 1407, 1331, 1294, 1257, 1225, 1172, 1062, 1037, 995, 840, 801, 780, 757, 738\text{ cm}^{-1}$; HRMS-EI m/z [M] $^+$ calcd for $\text{C}_9\text{H}_4\text{D}_9\text{N}$: 144.1607, found: 144.1607.

*Prepared from $d_9\text{-}t\text{-BuCl}$ with magnesium turnings in THF.

1,1'-(Propane-1,3-diyl)bis[4-(2-[$^2\text{H}_3$]methyl[1,1,1,3,3,3- $^2\text{H}_6$]propan-2-yl)pyridin-1-ium] bis(trifluoromethanesulfonate) (49**)**

According to GP1, with **48** (75 mg, 0.52 mmol, 2.5 eq.) and **21** (71 mg, 0.21 mmol, 1.0 eq.) without CH₂Cl₂ as solvent. Reaction time: 2.5 h. Recrystallization from *i*-PrOH/Et₂O (1:3.5, 9 mL) afforded **49** (106 mg, 81%, 99% D) as a colorless solid.

mp: 146°C; ¹H NMR (400 MHz, CDCl₃): δ=2.81–2.97 (m, 2 H, NCH₂CH₂), 4.86–5.01 (m, 4 H, NCH₂), 7.91 (d, *J*=6.9 Hz, 4 H, NCHCH), 9.27 ppm (d, *J*=7.0 Hz, 4 H, NCH); ¹³C NMR (100 MHz, CDCl₃): δ=28.88 (m, C(CD₃)₃), 34.56 (NCH₂CH₂), 36.10 (C(CD₃)₃), 56.79 (NCH₂), 120.54 (q, *J*=319.7 Hz, CF₃), 125.50 (NCHCH), 144.68 (NCH), 171.93 ppm (NCHCHC); IR (KBr): $\tilde{\nu}$ =3135, 3066, 2365, 2221, 1646, 1570, 1517, 1465, 1286, 1261, 1225, 1167, 1149, 1059, 1029, 860, 811, 757, 638, 573, 559, 518 cm⁻¹; HRMS-ESI *m/z* [*M*]⁺ calcd for C₂₂H₁₄D₁₈F₃N₂O₃S: 479.3210, found: 479.3212.

Diethyl [²H₂]malonate (**43**)

12 (5.0 g, 5.0 mL, 63 mmol, 3.2 eq.) was added to a solution of **42** (3.2 g, 3.0 mL, 20 mmol, 1.0 eq.) in D₂O (2.3 g, 2.1 mL, 0.12 mol, 5.9 eq.) and the resulting mixture was stirred for 20 h at room temperature. **12** and D₂O were removed by vacuum distillation and the procedure was repeated for further three times using identical amounts of **12** and D₂O. To remove residual pyridine, D₂O (10 mL) was added to the oily residue and removed by distillation. The resulting oil was purified by vacuum distillation (bath temp.: 100 °C, boiling point: 80 °C) to afford **43** (1.3 g, 40%, > 99.5% D) as a colorless liquid.

*R*_f=0.74 (*n*-pentane/EtOAc 5:1); ¹H NMR (500 MHz, CD₂Cl₂): δ=1.26 (t, *J*=7.1 Hz, 6 H, CH₂CH₃), 4.17 ppm (q, *J*=7.1 Hz, 4 H, CH₂CH₃); ¹³C NMR (125 MHz, CD₂Cl₂): δ=14.26 (CH₂CH₃), 41.60 (quin., *J*=20.0 Hz, CD₂), 61.79 (CH₂CH₃), 166.98 ppm (CO); IR (film): $\tilde{\nu}$ =2985, 2940, 2908, 1733, 1467, 1447, 1391, 1368, 1272, 1155, 1087, 1045, 1026, 912, 865, 812, 756 cm⁻¹; HRMS-EI *m/z* [*M*]⁺ calcd for C₇H₁₀D₂O₄: 162.0856, found: 162.0848.

The analytical data were consistent with those previously reported.⁵

[²H₆]Propane-1,3-diol (**44**) and [²H₆]propane-1,3-diyl bis(trifluoromethanesulfonate) (**45**)

[5] J. S. Dickschat, C. A. Citron, N. L. Brock, R. Riclea, H. Kuhz, *Eur. J. Org. Chem.* **2011**, 3339–3346.

A solution of **43** (1.50 g, 1.40 mL, 9.22 mmol, 1.0 eq.) in Et₂O (3 mL) was dropwise added to a suspension of LiAlD₄ (98% D, 1.19 g, 27.7 mmol, 3.0 eq.) in Et₂O (38 mL) at 0 °C and the resulting suspension was stirred for 5.5 h at 50 °C and for another 72 h at room temperature. The reaction was quenched by addition of 1 M NaOH (18.4 mL, 18.4 mmol, 2.0 eq.) at 0 °C and the mixture was filtrated. The solid residue was washed with Et₂O (20 mL) and repeatedly extracted with THF (4 x 30 mL). The filtrates were combined, and the solvent was removed under reduced pressure to yield the crude corresponding diol **44** (732 mg) as a yellowish and turbid oil. A mixture of **44** (732 mg, 8.92 mmol, 1.0 eq.) and **12** (1.41 g, 1.44 mL, 17.8 mmol, 2.0 eq.) in CH₂Cl₂ (4.4 mL) was added to a solution of Tf₂O (5.14 g, 3.06 mL, 17.8 mmol, 2.0 eq.) in CH₂Cl₂ (22 mL) at –78 °C and the reaction was stirred for 3 h at room temperature. The mixture was washed with D₂O (3 x 10 mL) and the organic phase was dried over MgSO₄. The solvent was removed under reduced pressure and the residue was purified by flash column chromatography (SiO₂, CH₂Cl₂) to afford **45** (1.86 g, 58%) as a grayish and turbid oil.

$R_f=0.88$ (SiO₂, CH₂Cl₂); ¹³C NMR (125 MHz, CDCl₃): $\delta=28.35$ (quin., $J=20.0$ Hz, OCD₂CD₂), 70.62 (quin., $J=23.7$ Hz, OCD₂CD₂), 118.56 ppm (q, $J=319.6$ Hz, CF₃); IR (film): $\tilde{\nu}=1415, 1252, 1207, 1147, 1083, 1062, 960, 833, 741\text{cm}^{-1}$.

1,1'-([²H₆]Propane-1,3-diyl)bis[4-(*tert*-butyl)pyridin-1-ium] bis(trifluoromethanesulfonate) (46**)**

According to GP1, with 4-*tert*-butylpyridine (1.82 g, 13.4 mmol, 1.97 mL, 2.5 eq.) and **45** (1.86 g, 5.38 mmol, 1.0 eq.) in CH₂Cl₂ (11 mL). Reaction time: 30 min. Recrystallization from EtOAc afforded **46** (2.54 g, 77%, > 99% D) as a colorless solid.

mp: 144°C; ¹H NMR (400 MHz, [D₆]DMSO): $\delta=1.39$ (s, 18 H, C(CH₃)₃), 8.23 (d, $J=7.1$ Hz, 4 H, NCHCH), 8.95 ppm (d, $J=7.1$ Hz, 4 H, NCHCH); ¹³C NMR (100 MHz, [D₆]DMSO): $\delta=22.58$ (NCD₂CD₂), 30.00 (C(CH₃)₃), 36.78 (C(CH₃)₃), 56.12–56.84 (m, NCD₂CD₂), 121.14 (q, $J=322.3$ Hz, CF₃), 125.54 (NCHCH), 144.74 (NCHCH), 170.66 ppm (CC(CH₃)₃); IR (KBr): $\tilde{\nu}=3134, 3077, 3057, 2970, 2913, 2877, 2361, 2341, 1646, 1564, 1515, 1466, 1373, 1287, 1256, 1226, 1147, 1114, 1094, 1069, 1029, 846, 829, 756, 667, 639, 601, 573, 561, 518\text{ cm}^{-1}$; HRMS-ESI m/z : [$M\text{-TfO}$]⁺ calcd for C₂₂H₂₆D₂O₃N₂F₃S: 467.2457, found: 467.2454.

2 Characterization of [$^2\text{H}_6$]MB327's affinity towards the *Torpedo*-nAChR employing a improved [$^2\text{H}_6$]MB327 MS Binding Assay protocol

To test the possibility of a uniform buffer system from storage of *Torpedo* membranes to incubation, [$^2\text{H}_6$]MB327 MS Binding Assays were conducted in incubation buffer devoid of CaCl_2 (= storage buffer). Corresponding binding experiments yielded a K_d of $14.2 \pm 1.4 \mu\text{mol L}^{-1}$ and a B_{max} of $263 \pm 30 \text{ pmol} [\text{mg protein}]^{-1}$ for saturation experiments ($n = 3$, for a representative saturation isotherm see Fig. 1a) and a K_i of $18.7 \pm 1.2 \mu\text{mol L}^{-1}$ for autocompetition experiments using native MB327 as competitor ($n = 3$, for a representative saturation isotherm see Fig. 1b). Specific binding was defined as the difference between total binding and nonspecific binding. In all [$^2\text{H}_6$]MB327 binding experiments, total ligand binding never exceeded 10% of the nominal concentration of the marker, so marker depletion was negligible.

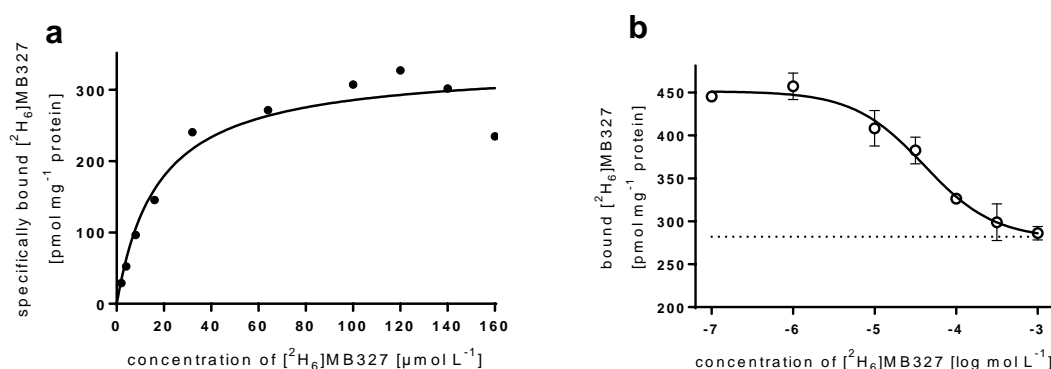


Fig. 1: Representative saturation and autocompetition binding experiments for [$^2\text{H}_6$]MB327 binding towards *Torpedo*-nAChR in absence of $1 \text{ mmol L}^{-1} \text{ CaCl}_2$. a) Specific binding is shown at marker concentrations from $2 - 160 \mu\text{mol L}^{-1}$ yielding a K_d of $17.5 \mu\text{mol L}^{-1}$ and B_{max} of $335 \text{ pmol} [\text{mg protein}]^{-1}$ in this example. b) Total binding, shown as mean \pm SD with [$^2\text{H}_6$]MB327 employed in a nominal concentration of $10 \mu\text{mol L}^{-1}$ and MB327 as competitor yielded a pK_i of 4.61 in this case. Nonspecific binding, determined in control experiments by heat-denaturation ($n = 3$) is shown as dashed line.

3 Validation of the developed LC-ESI-MS/MS quantification method

With final changes to the [$^2\text{H}_6$]MB327 MS Binding Assay protocol the LC-ESI-MS/MS quantification method was validated again exactly as previously published.⁶ For each validation series “IS containing blank matrix” from either nonspecific or total binding samples was spiked with marker to generate a set of matrix standards (Cal, 0.1, 0.2, 0.5, 1, 2, 4, 7, 10 nmol L⁻¹) as well as quality control samples (QCs, 0.25, 1, 8 nmol L⁻¹). Selectivity was demonstrated by analysis of blank matrix which did not show any interfering signals for both matrix types at the mass transitions m/z 159.2/144.3 ([$^2\text{H}_6$]MB327) or m/z 165.2/147.2 ([$^2\text{H}_{18}$]MB327). For 100 pmol L⁻¹ [$^2\text{H}_6$]MB327 matrix standards (LLOQ), in presence of both matrix types, the signal-to-noise ratio was always ≥ 13 (calculated by Analyst v. 1.6.1 software). For generation of a global calibration curve obtained area ratios (y) of [$^2\text{H}_6$]MB327 vs [$^2\text{H}_{18}$]MB327 were plotted against the concentration of [$^2\text{H}_6$]MB327 (x) in calibration standards. Linear regression analysis for these data employing a $1/x^2$ weighting yielded the following calibration function: $y = 0.562x - 0.00346$ ($R^2 = 0.9989$). Calibration standards and QCs were examined with respect to accuracy and precision within one validation series following the CDER guideline of the FDA for bioanalytical method validation in total binding matrix (for respective values see Table 1) and nonspecific binding matrix (for respective values see Table 2). Accuracy and precision were also determined inter-batch as recovery and relative standard deviation, respectively, for QC samples as well as matrix standards at all concentration levels over all validation series (for respective values see Table 3).

[6] S. Sichler, G. Höfner, S. Rappenglück, T. Wein, K. V. Niessen, T. Seeger, F. Worek, H. Thiermann, F. F. Paintner, K. T. Wanner, *Toxicol. Lett.* **2017**, ahead of print.

Table 1: Validation of [²H₆]MB327 quantification in total binding matrix by LC-ESI-MS/MS with an API 3200 using a YMC-Triart Diol-HILIC (50 mm x 2 mm, 3 µm) and [²H₁₈]MB327 as internal standard. $y = 0.562x - 0.00346$ ($R^2 = 0.9989$) with a $1/x^2$ weighting was used as global calibration curve.

Samples (n)	Intra-series																	
	Series 1			Series 2			Series 3			Series 4			Series 5			Series 6		
	M	Acc	RSD	M	Acc	RSD	M	Acc	RSD	M	Acc	RSD	M	Acc	RSD	M	Acc	RSD
100 pmol L⁻¹ Cal (6)	100.0	100.0	4.94	96.52	96.52	4.32	105.3	105.3	3.32	96.97	96.97	5.00	107.5	107.5	4.08	107.4	107.4	4.49
200 pmol L⁻¹ Cal (6)	199.17	99.58	1.60	191.2	95.62	2.38	205.0	102.5	2.49	193.8	96.72	2.85	199.7	99.87	4.55	206.2	103.2	3.88
500 pmol L⁻¹ Cal (3)	506.00	101.2	3.84	481.7	96.33	2.21	506.7	101.0	0.81	487.7	97.67	3.25	504.3	100.9	3.84	534.3	107.0	3.50
1 nmol L⁻¹ Cal (3)	1020	102.0	2.77	992.7	99.27	1.80	963.7	96.37	4.75	972.0	97.20	1.52	1047	104.7	2.25	1093	109.3	1.14
2 nmol L⁻¹ Cal (3)	2037	101.8	2.35	1913	95.60	2.70	1907	95.43	0.92	1937	96.77	1.79	1957	97.83	0.90	2103	105.0	1.35
4 nmol L⁻¹ Cal (3)	4107	102.8	5.42	4123	103.0	2.10	3943	98.53	1.89	3963	98.90	2.56	4030	100.9	3.10	4243	106.0	2.31
7 nmol L⁻¹ Cal (3)	6910	98.77	0.51	6743	96.30	1.50	7063	101.0	1.62	6963	99.37	1.28	6820	97.47	1.98	7453	106.7	2.21
10 nmol L⁻¹ Cal (3)	10053	100.5	1.75	10533	105.3	0.90	10467	104.7	1.19	10133	101.3	1.23	9833	98.33	2.48	10833	108.3	1.74
250 pmol L⁻¹ QC (6)	249.0	99.52	2.42	231.5	92.72	4.99	245.7	98.47	4.77	240.0	96.02	1.24	253.7	101.4	2.08	259.7	103.8	3.85
1 nmol L⁻¹ QC (6)	988.8	98.88	2.69	947.0	94.70	1.70	960.8	96.08	1.74	962.5	96.25	0.99	980.2	98.02	4.28	1062	106.2	3.46
8 nmol L⁻¹ QC (6)	7828	97.87	1.56	8045	100.5	3.36	7845	97.97	2.73	7892	98.62	1.86	7775	97.13	2.50	8247	103.0	2.51

M Mean of calculated concentrations (pmol L⁻¹), *Acc* accuracy (%), *RSD* relative standard deviation (%), *Cal* calibration standard, *QC* quality control sample, *n* number of replicates examined

Table 2: Validation of [²H₆]MB327 quantification in nonspecific binding matrix by LC-ESI-MS/MS with an API 3200 using a YMC-Triart Diol-HILIC (50 mm x 2 mm, 3 μm) and [²H₁₈]MB327 as internal standard. $y = 0.562x - 0.00346$ ($R^2 = 0.9989$) with a $1/x^2$ weighting was used as global calibration curve.

Samples (n)	Intra-series																	
	Series 1			Series 2			Series 3			Series 4			Series 5			Series 6		
	M	Acc	RSD	M	Acc	RSD	M	Acc	RSD	M	Acc	RSD	M	Acc	RSD	M	Acc	RSD
100 pmol L⁻¹ Cal (6)	103.4	103.4	6.50	94.53	94.53	3.75	102.8	102.8	5.57	91.28	91.28	5.15	110.0	110.0	3.82	107.2	107.2	3.30
200 pmol L⁻¹ Cal (6)	206.3	102.9	3.18	189.8	94.93	3.48	200.0	99.88	3.28	188.0	94.08	2.02	204.3	102.2	5.33	213.2	106.7	2.46
500 pmol L⁻¹ Cal (3)	481.3	96.27	1.40	456.7	91.30	2.15	483.0	96.67	0.77	475.0	95.00	1.13	486.0	97.07	2.27	519.7	103.9	3.51
1 nmol L⁻¹ Cal (3)	1010	101.0	2.19	948.7	94.87	2.46	941.7	94.17	2.56	952.3	95.23	2.32	983.7	98.37	2.73	1067	106.7	1.77
2 nmol L⁻¹ Cal (3)	1963	98.17	1.82	1813	90.63	2.20	1900	95.03	2.82	1953	97.73	4.19	1883	94.23	2.34	2050	102.8	2.58
4 nmol L⁻¹ Cal (3)	3963	99.17	0.42	3870	96.57	2.88	3817	95.27	3.51	3877	96.87	0.52	3803	95.13	2.80	4223	106.0	2.04
7 nmol L⁻¹ Cal (3)	6890	98.43	0.75	6647	94.90	0.98	6707	95.67	4.84	6737	96.20	1.15	6713	95.93	2.58	7173	102.3	1.22
10 nmol L⁻¹ Cal (3)	9990	99.90	2.39	9937	99.37	0.58	10067	100.7	0.94	9903	99.03	4.55	9650	96.50	5.40	10400	104.0	2.08
250 pmol L⁻¹ QC (6)	255.3	102.3	3.12	230.2	92.12	2.64	241.5	96.63	4.70	241.8	96.78	4.97	255.3	102.2	1.19	243.0	106.6	2.82
1 nmol L⁻¹ QC (6)	1020	101.9	2.24	932.5	93.25	2.47	978.7	97.87	2.45	968.3	96.83	4.11	978.7	97.87	3.53	1047	104.7	2.11
8 nmol L⁻¹ QC (6)	7948	99.28	4.17	7848	98.13	2.99	7935	99.05	2.39	7917	99.02	3.51	7722	96.63	2.58	8397	105.0	2.80

M Mean of calculated concentrations (pmol L⁻¹), *Acc* accuracy (%), *RSD* relative standard deviation (%), *Cal* calibration standard, *QC* quality control sample, *n* number of replicates examined

Table 3: Inter-series determination of mean, accuracy and precision of the validation of [²H₆]MB327 quantification in (total and nonspecific) binding matrix by LC-ESI-MS/MS employing [²H₁₈]MB327 as internal standard. $y = 0.562x - 0.00346$ ($R^2 = 0.9989$) with a $1/x^2$ weighting was used as global calibration curve.

Samples (n)	Inter-series		
	M	Acc	RSD
100 pmol L ⁻¹ Cal (6)	101.9	101.9	5.62
200 pmol L ⁻¹ Cal (6)	199.7	99.84	3.71
500 pmol L ⁻¹ Cal (3)	493.5	98.69	4.14
1 nmol L ⁻¹ Cal (3)	999.3	99.93	4.71
2 nmol L ⁻¹ Cal (3)	1951	97.59	3.93
4 nmol L ⁻¹ Cal (3)	3997	99.93	3.67
7 nmol L ⁻¹ Cal (3)	6902	98.59	3.30
10 nmol L ⁻¹ Cal (3)	10150	101.5	3.21
250 pmol L ⁻¹ QC (6)	245.6	99.04	4.26
1 nmol L ⁻¹ QC (6)	985.4	98.54	3.77
8 nmol L ⁻¹ QC (6)	7950	99.35	2.35

M Mean of calculated concentrations (pmol L⁻¹), *Acc* accuracy (%), *RSD* relative standard deviation (%), *Cal* calibration standard, *QC* quality control sample, *n* number of replicates examined

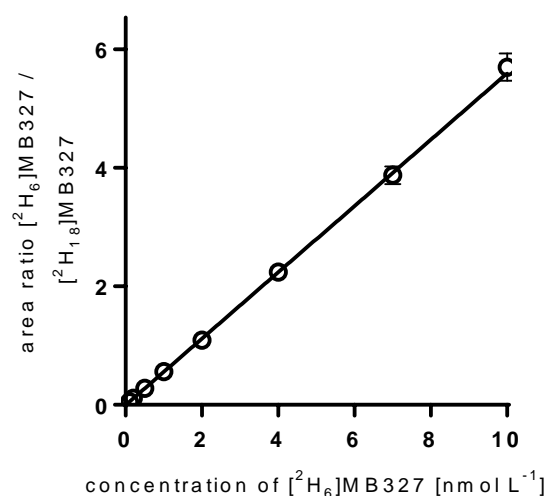


Fig. 2: Global calibration curve ($y = 0.562x - 0.00346$, $R^2 = 0.9989$) for [²H₆]MB327 based on 12 validation series (6 validation series for total binding matrix and nonspecific binding matrix, respectively), each consisting of blank and zero samples as well as matrix calibration standards at eight concentration levels (0.1, 0.2, 0.5, 1, 2, 4, 7 and 10 nmol L⁻¹). Area ratios of [²H₆]MB327 vs [²H₁₈]MB327 (*y*) for calibration standards as determined with the developed LC-ESI-MS/MS method were plotted against the corresponding concentration of [²H₆]MB327 (*x*). Data points are shown as means \pm SD.

3.3 Drittes Manuskript

Synthesis of a Series of Non-Symmetric Bispyridinium and Related Compounds and Their Affinity Characterization at the Nicotinic Acetylcholine Receptor

3.3.1 Zusammenfassung der Ergebnisse

Die Untersuchung einer Reihe symmetrischer, bisquaternärer MB327-Derivate in MS-Bindungsstudien mit [$^2\text{H}_6$]MB327 als Reporterligand ermöglichte zuletzt den Aufbau erster Struktur-Affinitätsbeziehungen an der MB327-Bindestelle des nikotinischen Acetylcholinrezeptors (nAChR). Im Rahmen von Docking-Studien durch Wein⁹² an einem 3D-Strukturmodell des nAChR aus *Torpedo marmorata* gelang unterdessen die Identifikation zweier putativer MB327-Bindestellen, die asymmetrisch, mit polaren Resten zur Interaktion mit MB327 auf der einen und lipophilen Seitenketten auf der anderen Seite, aufgebaut sind. Vor dem Hintergrund dieser Ergebnisse wurden 26 neue Zielstrukturen mit einem 4-*tert*-Butyl- bzw. 3-Methoxy-substituierten Pyridiniumring auf der einen Seite und verschiedenen aromatischen Motiven mit polaren und lipophilen Substituenten auf der gegenüberliegenden Seite, entwickelt. Als weitere Referenzverbindung nebst MB327 wurde PTM0029, mit einem 4-*tert*-Butyl-substituierten Pyridiniumring auf der einen und einer nicht-substituierten Pyridiniumeinheit auf der anderen Seite, synthetisiert. Für die zweistufige Synthese der neuen Zielstrukturen war zunächst eine Isolierung der monoalkylierten Spezies nötig, welche in einem zweiten Schritt mit dem zweiten Heterocyclus bzw. Aromaten umgesetzt werden konnte. Für alle neu synthetisierten Testverbindungen wurden, analog zur biologischen Evaluation der symmetrischen MB327-Derivate, Bindungsaffinitäten bezüglich der MB327-Bindestelle in MS-Bindungsassays mit [$^2\text{H}_6$]MB327 als Reporterligand und dem nAChR aus *Torpedo californica* als Target bestimmt.

Die Einführung mehrerer polarer Gruppen (z.B. COOEt, NMe₂) am nicht-substituierten Pyridiniumring von PTM0029 zeigte einen positiven Effekt auf die Bindungsaffinität (vgl. PTM0030, PTM0050, PTM0056). Insbesondere PTM0030 und PTM0056, jeweils mit einer Dimethylamino-Gruppe in 3- bzw. 4-Position, adressierten die MB327-Bindestelle mit im Vergleich zur Leitstruktur sichtlich erhöhter Affinität ($pK_i = 4.92 \pm 0.09$ bzw. 4.90 ± 0.06). Dagegen wirkte sich die Einführung einer 3-Methoxy-Gruppe

am nicht-substituierten Pyridiniumring von PTM0029 bzw. der Austausch eines der 4-*tert*-Butyl- gegen einen 3-Methoxysubstituenten im MB327-Molekülgerüst nachteilig auf die Bindungsaffinität an die MB327-Bindestelle aus, wie der Vergleich der pK_i -Werte von PTM0029 und PTM0040 bzw. MB327 und PTM0040 zeigt. Dieser Affinitätsverlust konnte, in Analogie zu Bindungsdaten der symmetrischen MB327-Derivate, durch Kombination mit einer 4-*tert*-Butyl-Gruppe als Zweitsubstituent am Pyridiniumring kompensiert werden. Die Bispyridiniumverbindung PTM0038 mit 4-*tert*-Butylsubstituenten auf der einen und 4-*tert*-Butyl-3-methoxysubstitution auf der anderen Seite adressierte die MB327-Bindestelle sogar mit einer höheren Bindungsaffinität als die Leitstruktur und mit der höchsten Affinität innerhalb der Reihe getesteter Verbindungen ($pK_i, \text{PTM0038} = 4.97 \pm 0.02$). So zeigt sich auch hier, wie zuvor bei Testung der symmetrischen MB327-Derivate beobachtet, der Affinitätsverstärkenden Effekt des *tert*-Butylsubstituenten in 4-Position auf die Bindung am *Torpedo*-nAChR. Nebst 4-*tert*-Butylgruppe scheint es sich beim kationischen Stickstoff-Heteroatom der Pyridiniumeinheit um ein weiteres, wichtiges Strukturmotiv in Bezug auf die Bindung an der MB327-Bindestelle zu handeln. Der Austausch des Stickstoff-Heteroatoms gegen ein Kohlenstoffatom geht, wie der Vergleich der pK_i -Werte von MB327 und PTM0060 zeigt, mit einer deutlichen Verschlechterung der Bindungsaffinität an die MB327-Bindestelle, um knapp 0.4 log-Einheiten, einher. Fehlen an einer Pyridiniumeinheit sowohl die positive Ladung des N-Heteroatoms als auch der 4-*tert*-Butylsubstituent, geht die Bindungsaffinität der entsprechenden Verbindung (PTM0036, $pK_i = 3.65 \pm 0.12$) im Vergleich zur Leitstruktur sogar um über eine Zehnerpotenz zurück. Die besonders hohe Affinität von PTM0054, mit einer 4-*tert*-Butyl-Pyridiniumeinheit auf der einen und einer Isoquinolinium-Einheit auf der anderen Seite weist darauf hin, dass π -Wechselwirkungen vermutlich ebenfalls eine wichtige Rolle für die Bindung von MB327 und Derivaten an der MB327-Bindestelle spielen.

Mit der Synthese von 26 neuen Zielstrukturen konnte in dieser Studie der Testverbindungs-Pool für MS-Bindungsexperimente um einige strukturell-diverse MB327-Derivate erweitert werden. Die biologische Testung lieferte erneut wertvolle Daten, mit denen bereits entwickelte Struktur-Affinitätsbeziehungen an der MB327-Bindestelle weiter ausgebaut werden konnten.

3.3.2 Erklärung zum Eigenanteil

Die MS-Bindungsversuche sowie deren Auswertung zur Bestimmung der Bindungsaffinitäten von Testverbindung an die MB327-Bindestelle führte ich eigenständig durch. Alle Testverbindungen wurden von Sebastian Rappenglück synthetisiert. Sebastian Rappenglück und ich waren, unterstützt von Georg Höfner, Thomas Wein und Klaus T. Wanner, gleichermaßen an der Diskussion der Struktur-Affinitätsbeziehungen sowie am Schreiben des Manuskripts beteiligt. An der Korrektur des Manuskripts wirkten Georg Höfner und Klaus T. Wanner sowie Franz F. Paintner, Karin V. Niessen*, Thomas Seeger*, Franz Worek* und Horst Thiermann* mit.

* Kooperationspartner im Rahmen eines gemeinsamen Forschungsprojekts vom Institut für Pharmakologie und Toxikologie der Sanitätsakademie in München

CHEM MED CHEM

CHEMISTRY ENABLING DRUG DISCOVERY

Accepted Article

Title: Synthesis of a Series of Non-Symmetric Bispyridinium and Related Compounds and Their Affinity Characterization at the Nicotinic Acetylcholine Receptor

Authors: Klaus Theodor Wanner, Sebastian Rappenglück, Sonja Sichler, Georg Höfner, Thomas Wein, Karin V. Niessen, Thomas Seeger, Franz F. Paintner, Franz Worek, and Horst Thiermann

This manuscript has been accepted after peer review and appears as an Accepted Article online prior to editing, proofing, and formal publication of the final Version of Record (VoR). This work is currently citable by using the Digital Object Identifier (DOI) given below. The VoR will be published online in Early View as soon as possible and may be different to this Accepted Article as a result of editing. Readers should obtain the VoR from the journal website shown below when it is published to ensure accuracy of information. The authors are responsible for the content of this Accepted Article.

To be cited as: *ChemMedChem* 10.1002/cmdc.201800539

Link to VoR: <http://dx.doi.org/10.1002/cmdc.201800539>

WILEY-VCH

www.chemmedchem.org

A Journal of



Synthesis of a Series of Non-Symmetric Bispyridinium and Related Compounds and Their Affinity Characterization at the Nicotinic Acetylcholine Receptor

Sebastian Rappenglück,^[a] Sonja Sichler,^[a] Georg Höfner,^[a] Thomas Wein,^[a] Karin V. Niessen,^[b] Thomas Seeger,^[b] Franz F. Paintner,^[a] Franz Worek,^[b] Horst Thiermann,^[b] and Klaus T. Wanner^{*,[a]}

⁺ These authors contributed equally as first authors

[a] S. Rappenglück, S. Sichler, Dr. G. Höfner, Dr. T. Wein, Prof. Dr. F. F. Paintner, Prof. Dr. K. T. Wanner ORCID:0000-0003-4399-1425
Department of Pharmacy – Center for Drug Research
Ludwig-Maximilians-Universität München
Butenandtstr. 5-13, 81377 Munich, Germany
E-mail: klaus.wanner@cup.uni-muenchen.de

[b] K.V. Niessen, Dr. T. Seeger, Prof. Dr. F. Worek, Prof. Dr. H. Thiermann
Bundeswehr Institute of Pharmacology and Toxicology
Neuherbergstr. 11, 80937 Munich, Germany

Supporting information for this article is given via a link at the end of the document

Abstract: The current standard therapy to counteract organophosphate intoxications is not effective in equal measure against all types of organophosphorus compounds (OPCs) as the outcome of oxime induced reactivation of inactivated acetylcholinesterase (AChE) strongly depends on the particular OPC. In case the reactivation is insufficient, acetylcholine concentrations that rise to pathophysiological levels force the nicotinic acetylcholine receptor (nAChR) into a desensitized state and hence a functionally inactive state. In consequence, neurotransmission is irreversibly disrupted at the neuromuscular junction. Previous electrophysiological studies identified the symmetric bispyridinium compound 1,1'-(propane-1,3-diyl)bis[4-(tert-butyl)pyridin-1-ium] diiodide (**MB327**) as re-sensitizer of the desensitized nAChR. **MB327** is thereby capable of restoring the functional activity. Very recently, *in silico* modeling studies suggested non-symmetric derivatives of **MB327** as potential re-sensitizers with enhanced binding affinity and thus with possibly enhanced efficacy. In this study, 26 novel non-symmetric bispyridinium compounds and related derivatives were synthesized. For the synthesis of the highly polar target compounds in sufficient quantities, newly developed and highly efficient two-step procedures were employed. Compounds were characterized in terms of their binding affinity toward the MB327 binding site at the nAChR using recently developed mass spectrometry (MS) Binding Assays. Regarding structure-affinity relationships at the MB327 binding site, the presence of two quaternary aromatic nitrogen centers as well as of pyridinium systems with a *tert*-butyl group in 4-position or a NMe₂ group in 3- or 4-position appeared to be beneficial for high binding affinities.

Organophosphorus compounds (OPCs) have been investigated for plant protection since the early 20th century. In the 1930s and 1940s nerve agents like tabun, sarin, and soman were found which possess increased toxicity against humans. Since then, such chemicals have been repeatedly used in warfare as well as in terrorist attacks.^[1–3] OPCs still cause high numbers of annual fatalities, mostly due to pesticide self-poisoning.^[4, 5] Hence, there is an urgent need for an effective medical treatment to counteract OPC intoxications. Unfortunately, the currently available antidotal treatment is not effective against all types of OPCs.

OPCs inactivate the enzyme acetylcholinesterase (AChE), which leads to accumulation of acetylcholine (ACh) in the synaptic cleft and effects subsequently an overstimulation of muscarinic and nicotinic acetylcholine receptors (mAChRs and nAChRs, respectively). The current standard drug therapy for OPC poisoning includes administration of atropine and an oxime reactivator of AChE such as obidoxime or pralidoxime. As a competitive antagonist of mAChRs, atropine selectively counteracts overstimulation of this receptor. In contrast, an analogous application of nAChR antagonists to treat nAChR overstimulation is not feasible as their therapeutic window is too small and patients would need artificial ventilation.^[6] Here oxime reactivators of AChE as part of the treatment regimen come into play. These compounds help to regain mAChR as well as nAChR function as they restore AChE activity and thus reduce the ACh overload in the synaptic cleft. However, as indicated before, oxime reactivators of AChE do not show equipotent activity against all types of OPCs. For example, in case of soman poisoning, the enzyme-organophosphate complex undergoes a rapid dealkylation reaction (so-called “aging”) which prevents any subsequent restoration of AChE activity.^[7] If ACh cannot be removed, progressive overstimulation forces the nAChR into a desensitized state thereby disrupting nAChR-mediated

Introduction

FULL PAPER

cholinergic signalling.^[8] In conclusion, there is an urgent need for a novel therapeutic approach enabling direct restoration of nAChR function rather than the indirect way via AChE promoted removal of the neurotransmitter ACh from the synaptic cleft.

The bispyridinium salt **MB327** (Figure 1), which is the most potent representative of a class of analogous compounds, was shown to be capable of recovering muscle function even after soman poisoning.^[9] Since **MB327** does not reactivate AChE, restoration of cholinergic transmission was assumed to be mediated by a direct intervention at the nAChR. Further examination of the effect of **MB327** and of structural analogues on the nAChR by Niessen et al., employing electrophysiological measurements on a SURFE²R (surface electronic event reader) platform, corroborated this hypothesis and demonstrated the capability of **MB327** to reconstitute nAChR function after agonist-induced desensitization as well as to prevent desensitization when co-applied with the agonist carbamoylcholine.^[10]

MB327, however, needs to be applied at high concentration (100 – 200 $\mu\text{mol L}^{-1}$) to achieve muscle force recovery in vitro.^[9] This low potency of **MB327** is in line with a low binding affinity toward the nAChR (**MB327**: $pK_i = 4.73 \pm 0.03$), which was determined by MS Binding Assays previously developed by us.^[11] We were planning to develop compounds with increased affinity to the MB327 binding site. Assuming that an increase in affinity is paralleled by intrinsic activity, these compounds should display also a higher potency as nAChR re-sensitizers, hence, being more effective antidotes for the treatment of OPC poisoning. Since **MB327** is the most potent nAChR re-sensitizer known so far, it appeared to be a well suited starting point for this endeavor.

First attempts to create nAChR re-sensitizers with increased potency were previously published by us.^[12] We reported on the synthesis of 30 novel symmetric bispyridinium and related salts structurally analogous to **MB327** and their binding affinities toward the MB327 binding site. The most affine compound, lipophilic 3-phenyl-4-*tert*-butyl substituted bispyridinium salt **PTM0022** (Figure 1), showed a pK_i value significantly higher than that of **MB327**.^[12] Furthermore, the study provided vital information on the influence of various functional groups and structural motives on binding affinity. Later on, using the 3D structure of the nAChR of *Torpedo marmorata* published by Unwin et al.^[13] in silico docking studies revealed two putative binding sites for **MB327**.^[14] Both sites are located inside the channel, one in the extracellular domain between the γ and α subunits and the other between the β and δ subunits in the transmembrane region. These putative sites were found to be non-symmetrical with regard to their polarity, i.e. one of the two pyridinium rings is embedded in a more hydrophilic and the other in a more lipophilic environment. This finding suggests that a non-

symmetric substitution of the two pyridinium rings with hydrophilic and lipophilic residues might lead to compounds with improved affinities towards the MB327 binding site. However, in order to gain more information on the effect of selective substitutions on binding affinity, we aimed at novel non-symmetric bisquaternary compounds with a wide variety of different residues. More precisely, we focused on structures with either two lipophilic, two hydrophilic, or one lipophilic and one hydrophilic substituted N-aromatic subunit. As lead structure, **MB327** instead of the recently developed **PTM0022** was chosen as so far only for **MB327**, but not for **PTM0022**, the therapeutic efficacy has been verified. In particular, evaluation of non-symmetric compounds in terms of their binding affinity toward the **MB327** binding site was anticipated to provide a more comprehensive and detailed insight in individual, regio, and functional group dependent ligand–target interactions. In this paper, we report on the results of this study.

Results and Discussion

Structure of Target Compounds

For the synthesis of the envisaged non-symmetric bisquaternary target compounds (Figures 2 and 3), symmetric bispyridinium salt **MB327** (Figure 1) served as a starting point.

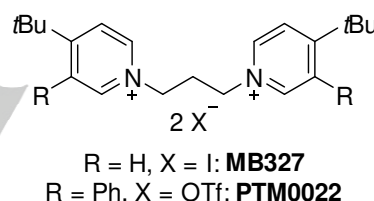


Figure 1. Structures of **MB327** and **PTM0022**.

Taking into account the results from the aforementioned in silico modeling studies at the *Torpedo*-nAChR,^[14] one of the two 4-*tert*-butylpyridinium rings of **MB327** should be replaced by different N-heterocycles or pyridine rings substituted either with lipophilic or hydrophilic functional groups at varying ring positions (**1 a–l**, **2 a–e** and **3 a–e**, Figures 2 and 3). To allow a straightforward analysis of the effect of newly introduced pyridine ring substituents and N-heterocycles on the binding affinity for the putative MB327 binding site, pyridinium salt **1 a** being devoid of one of the two *tert*-butyl residues of **MB327** should be synthesized as reference compound.

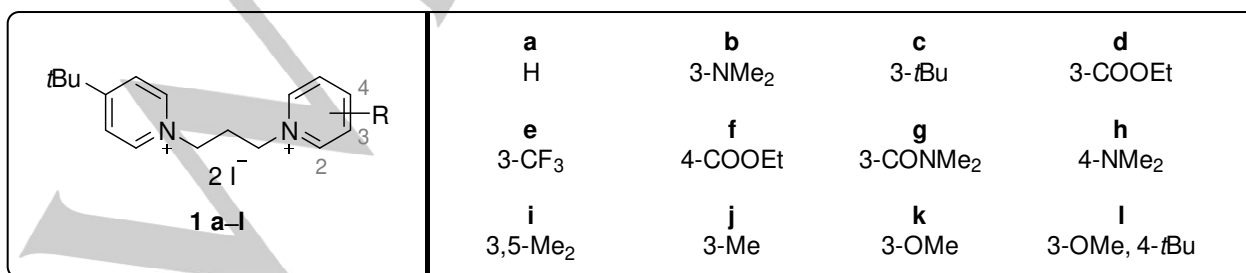


Figure 2. Structures of envisaged target compounds **1 a–l**.

FULL PAPER

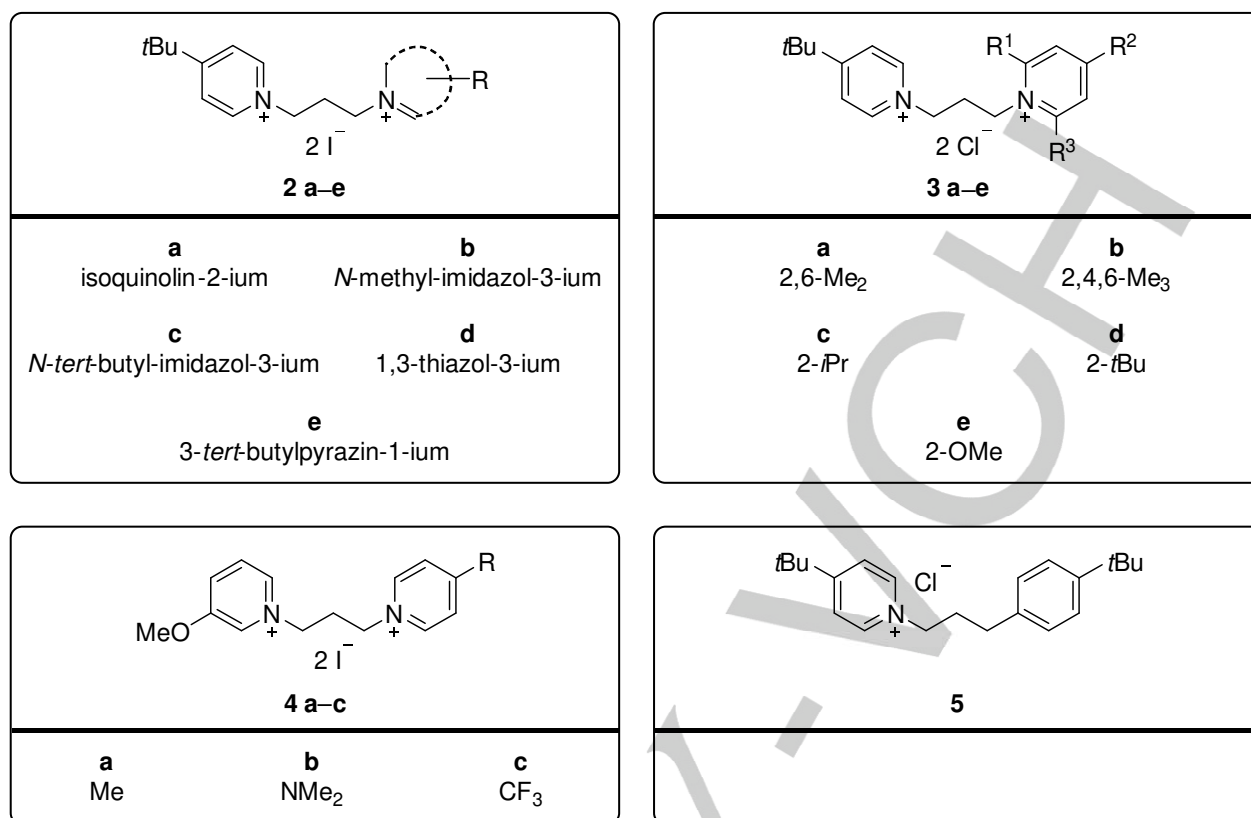


Figure 3. Structures of envisaged target compounds **2 a–e**, **3 a–e**, **4 a–c** and **5**.

Moreover, analysis of the MB327 binding site suggested^[14] that non-symmetric bispyridinium compounds combining a 3-methoxypyridinium motive (**4 a–c**) with a second pyridinium ring exhibiting either an electron donating (**4 b**: 4-NMe₂), withdrawing (**4 c**: 4-CF₃), or neutral (**4 a**: 4-Me) substituent, might also have reasonable binding affinities (Figure 3). Finally, to expand the pool of target compounds beyond highly polar bisquaternary species, one of both 4-*tert*-butylpyridinium rings of **MB327** should be replaced by a 4-*tert*-butylphenyl unit to afford mono-cationic species **5**. Being structurally closely related to **MB327**, the biological characterization of compound **5** should allow to estimate the effect of the second positively charged pyridine ring in **MB327** on binding affinity.

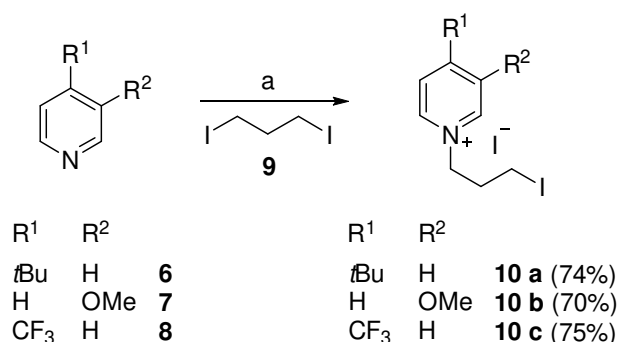
Chemistry

Depending on the substitution pattern of the aromatic nitrogen heterocycles present in the envisaged bispyridinium and related salts, target compounds were synthesized via two straightforward routes allowing the synthesis of reasonable quantities sufficient for use in biological testing.

Compounds **1 a–l** (Figure 2), **2 a–e** (Figure 3) and **4 a–c** (Figure 3) being devoid of any ring substituents adjacent to the quaternary nitrogen atom of the aromatic heterocycles were synthesized in two steps. First, 4-*tert*-butylpyridine (**6**), 3-methoxypyridine (**7**) or 4-trifluoromethylpyridine (**8**) were subjected to a N-alkylation with 4.0 equivalents 1,3-diiodopropane (**9**) at 90 °C for 1–16 h under microwave irradiation to yield *N*-(3-iodopropyl)pyridinium salts **10 a–c** (Scheme 1). Using diiodide **9** in excess reduced the formation of undesired bispyridinium species and allowed the formation of the monoalkylation products

10 a–c in 70–75% yield after purification by flash column chromatography.

In the next step, the second nitrogen heterocycle was introduced to afford target compounds **1 a–l**, **2 a–e** and **4 a–c** (Table 1). For that purpose, *N*-(3-iodopropyl)pyridinium iodides **10 a–c** were subjected to microwave assisted reactions with the corresponding nitrogen heteroaromatics **7** and **11–27**.



Scheme 1. Synthesis of *N*-(3-iodopropyl)pyridinium iodides **10 a–c**. Reagents and conditions: a) **9** (4.0 equiv), MeCN, microwave: 150 W, 90 °C, 1 h (**10 a** and **b**) or 16 h (**10 c**).

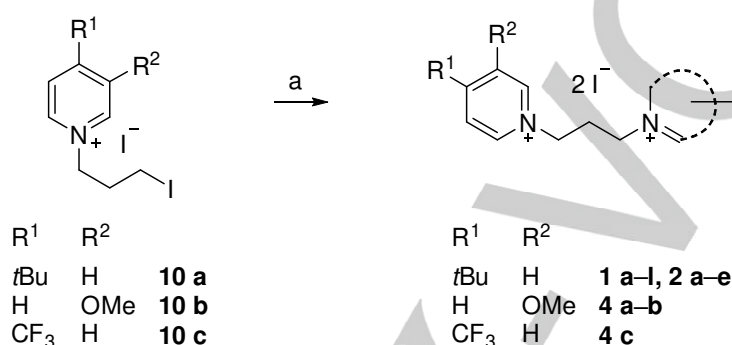
Subsequent purification by RP-MPLC (C18, MeOH/H₂O) or crystallization was found most effective to isolate bispyridinium compounds **1 a–l** (Table 1, entries 1–12) and **4 a–c** (Table 1, entries 18–20) as well as mixed pyridinium-azaheterocyclic salts

FULL PAPER

2 a–e (Table 1, entries 13–17) in pure form in moderate to excellent yields of 51–99%. The employed synthetic conditions were well tolerated by various synthetically important functional groups, i.e. alkylarylethers (**1 k**, **1 l**, **4 c**), secondary amines (**1 b**, **1 h**, **4 b**), ethyl esters (**1 d**, **1 f**), an amide (**1 g**), and a trifluoromethyl residue (**1 e**). In case of 2-*tert*-butylpyrazine (**26**, Table 1, entry 17), alkylation occurred selectively in 4-position of the heterocycle due to the sterically demanding *tert*-butyl substituent. In general, reaction temperature and reaction time for complete consumption of the starting material depended strongly

on the nature of the employed nitrogen heterocycles. Thus, the reaction temperature ranged from 1 h at 90 °C in case of more basic methylimidazole **23** ($pK_{BH^+} = 7.1$, Table 1, entry 14)^[15] up to 16 h at 120 °C for less basic thiazole **25** ($pK_{BH^+} = 2.5$, Table 1, entry 16),^[16, 17] for example. Notably, no side reactions affecting the functional groups of the target compounds or the integrity of the pyridinium system were observed as for example O-demethylation or Zincke-König-type pyridinium ring cleavage reactions.

Table 1. Synthesis of non-symmetric bispyridinium and related diiodides **1 a–l**, **2 a–e** and **4 a–c**.



Entry	Starting materials			T [°C]	t [h]	Product	Yield [%]
	10	N-heterocycle	No.				
1	a		11	90	1	1 a	52
2	a		12	90	1	1 b	51
3	a		13	90	1	1 c	94
4	a		14	90	3	1 d	82
5	a		15	90	16	1 e	61
6	a		16	90	3	1 f	73
7	a		17	90	3	1 g	87

FULL PAPER

8	a	18	90	1	1 h	95
9	a	19	90	1	1 i	87
10	a	20	90	1	1 j	86
11	a	7	90	1	1 k	78
12	a	21	90	1	1 l	85
13	a	22	90	1	2 a	96
14	a	23	90	1	2 b	80
15	a	24	90	1	2 c	99
16	a	25	120	16	2 d	89
17	a	26	120	16	2 e	87
18	b	27	90	1	4 a	83
19	b	18	90	1	4 b	70
20	c	7	90	1	4 c	62

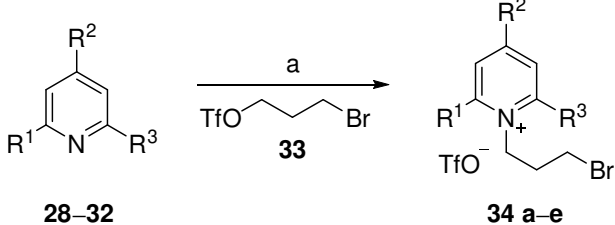
Reagents and conditions: a) pyridinium iodides **10 a–c** (1.0 equiv), N-heterocycles (1.2 equiv), MeCN, *T*, *t*, microwave: 150 W.

FULL PAPER

The synthesis of envisaged bispyridinium salts **3 a–e** (Figure 3) exhibiting substituents adjacent to one of the two pyridinium nitrogen atoms proved to be challenging, since the reactivity of the alkyl iodide function of *N*-(3-iodopropyl)pyridinium salts **10 a, b** and **c** as well as of 1,3-diiodopropane (**9**) was too low for the alkylation reaction of sterically hindered pyridine rings such as 2,6-lutidine (**28**, Table 2, entry 1) or 2-*tert*-butylpyridine (**31**, Table 2, entry 4). For that reason, we developed an alternative approach that allows the straightforward N-alkylation of sterically hindered heterocycles and gives efficient access to the desired target compounds within two steps.

First, sterically hindered pyridine derivatives **28–32** were subjected to a reaction with the highly reactive bromopropyltriflate **33** providing the corresponding *N*-(3-bromopropyl)pyridinium salts **34 a–e** in 67–96% yield after purification by flash column chromatography (Table 2).

Table 2. Synthesis of *N*-(3-bromopropyl)pyridinium triflates **34 a–e**.

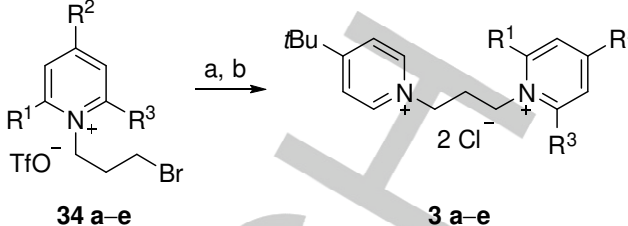


Entry	Starting material		<i>T</i> [°C]	<i>T</i> [h]	Product	Yield [%]
	R ¹ /R ² /R ³	No.				
1	Me/H/Me	28	RT	16	34 a	83
2	Me/Me/Me	29	RT	16	34 b	81
3	<i>i</i> -Pr/H/H	30	50	3	34 c	78
4	<i>t</i> -Bu/H/H	31	85	1.5	34 d	67
5	OMe/H/H	32	RT	16	34 e	96

Reagents and conditions: a) pyridine derivatives (1.0 equiv), **33** (1.2 equiv), CH₂Cl₂, *T*, *t*.

In the second step, **34 a–e** were treated with 1.2 equivalents of 4-*tert*-butylpyridine (**6**) for 3 h at 90 °C under microwave heating (Table 3). The markedly different reactivities of the two electrophilic centres present in biselectrophile **33** allowed both, the smooth alkylation of sterically demanding N-heterocycles in the first step (Table 2) by the triflate function as well as a facile subsequent substitution of the iodide function by 4-*tert*-butylpyridine (**6**) in the second step (Table 3). Subsequent treatment without prior isolation of the formed mixed triflate/bromide salts with a chloride loaded anion exchange resin finally afforded bispyridinium dichlorides **3 a–d** in 78–94% yield after purification by RP-MPLC (Table 3). However, treatment of **34 e** with 1.2 equivalents 4-*tert*-butylpyridine (**6**) and subsequent ion exchange reaction did not lead to the desired bispyridinium salt **3 e** (Table 3, entry 5). Instead, pyridiniumpropylpyridone **3 f** (scheme 2) was obtained amongst various side products in 21% yield. As compound **3 f** is an interesting monocationic species with a polar pyridone subunit, it was worth to be included for biological testing.

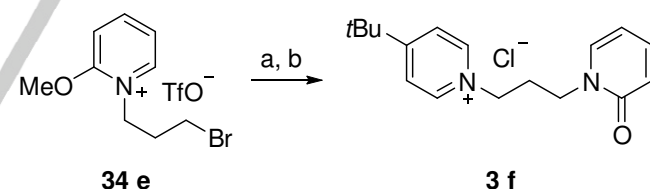
Table 3. Synthesis of bispyridinium dichlorides **3 a–d** exhibiting alkyl substituents in 2-position.



Entry	34	Product		Yield [%]
		R ¹ /R ² /R ³	No.	
1	a	Me/H/Me	3 a	78
2	b	Me/Me/Me	3 b	85
3	c	H/H/ <i>i</i> Pr	3 c	94
4	d	H/H/ <i>t</i> Bu	3 d	90
5	e	H/H/OMe	3 e	---

Reagents and conditions: a) pyridinium bromides **34 a–e** (1.0 equiv), 4-*tert*-butylpyridine (**6**, 1.2 equiv), MeCN, 90 °C, 3 h, microwave: 150 W; b) Amberlite® IRA-410 Cl[−]-form, H₂O, RT, 16 h.

Hence, an attempt to improve the formation of **3 f** was undertaken. Since pyridiniumpropylpyridone **3 f** was assumed to be mainly formed by O-demethylation of **34 e** effected by 4-*tert*-butylpyridine (**6**), the reaction was repeated, but this time employing 3.0 equivalents of 4-*tert*-butylpyridine (**6**) instead of 1.2 (Scheme 2). That way, indeed, complete O-demethylation occurred and compound **3 f** could be obtained in 90% yield after ion exchange and purification by RP-MPLC.

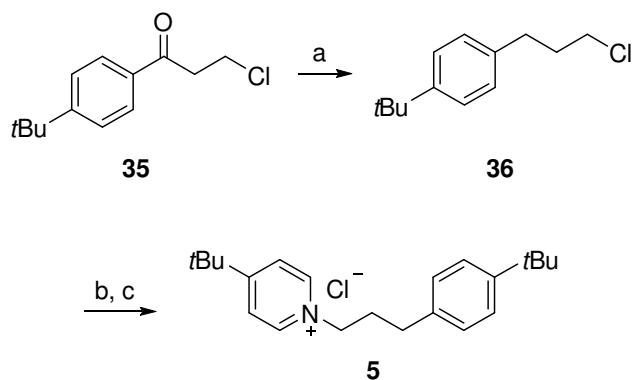


Scheme 2. Synthesis of pyridiniumpropylpyridone **3 f**. Reagents and conditions: a) **6** (3.0 equiv), MeCN, 90 °C, 3 h, microwave: 150 W; b) Amberlite® IRA-410 Cl[−]-form, H₂O, RT, 16 h, 90% over both steps.

Finally, the synthesis of the mono cationic **MB327** analogue **5** could be accomplished in two steps starting from chloropropanone **35** (Scheme 3).^[18–29] Reduction of the keto function with Et₃SiH in TFA at 75 °C under microwave irradiation following a procedure adapted from Perlmutter et al. led to chloropropyl benzene **36** in 90% yield.^[21] Subsequent treatment of **36** with 4-*tert*-butylpyridine in the presence of stoichiometric amounts of NaI (16 h, 90 °C) and ion exchange reaction with Amberlite® IRA-410 in its chloride form provided target compound **5** in 81% yield.

Altogether, with **1 a–l**, **2 a–e**, **3 a–d**, **3 f**, **4 a–c** and **5**, a set of 26 non-symmetric salts featuring a broad variety of lipophilic and hydrophilic substituents could be made available for biological characterization in MS Binding Assays.

FULL PAPER



Scheme 3. Synthesis of mono-cationic **MB327** analogue **5**. *Reagents and conditions:* a) Et_3SiH (4.0 equiv), TFA, 75 °C, 15 h, microwave: 100 W, 90%; b) NaI (1.1 equiv), **6** (1.2 equiv), MeCN, 90 °C, 16 h, microwave: 150 W; c) Amberlite® IRA-410 Cl^- -form, H_2O , RT, 16 h, 90% over both steps.

Biological evaluation

All target compounds synthesized in the context of this study were catalogued with a certain PTM number (Pharmacy and Toxicology Munich). Binding affinities toward the nAChR were determined in MS Binding Assays using $[^2\text{H}_6]\text{MB327}$ as marker and nAChR-enriched membranes prepared from *Torpedo californica* electroplaque tissue as target (Table 4).^[12] In the following, binding data for compounds are given and discussed with respect to the substitution pattern using bispyridinium salt **1 a** as reference compound. This compound is characterized by the presence of a 4-*tert*-butylpyridinium and an unsubstituted pyridinium unit. The latter will be referred to as blank pyridine when it comes to the substitution at this part of **1 a**. For reference compound **1 a** (PTM0029), the pK_i value for the binding toward the MB327 binding site amounts to 4.52 ± 0.06 (Table 4, entry 2). Hence omitting one *tert*-butyl residue from **MB327** ($pK_i = 4.73 \pm 0.03$), the most prototypic re-sensitizer of desensitized nAChR, caused a slight decrease in binding affinity.

In case of the new target compounds, binding affinities ranged from $pK_i = 3.65 \pm 0.12$, found for pyridin-2(1*H*)-one derivative **3 f** (PTM0036, Table 4, entry 23), up to $pK_i = 4.97 \pm 0.02$ for **1 i** with a 3-methoxy and a 4-*tert*-butyl substituent at the second pyridinium ring (PTM0038, Table 4, entry 13).

As compared to symmetric 4-*tert*-butyl substituted **MB327** (Table 4, $pK_i = 4.73 \pm 0.03$, entry 1), non-symmetric compounds **3 d** (PTM0047, $pK_i = 4.54 \pm 0.05$, Table 4, entry 22) and **1 c** (PTM0049, $pK_i = 4.50 \pm 0.02$, Table 4, entry 4) with a *tert*-butyl substituent at one of the two pyridinium groups in 2- or 3-position have a somewhat lower binding affinity. Interestingly, the pK_i values of **3 d** and **1 c** are similar to that of reference compound **1 a** (PTM0029). This indicates that a *tert*-butyl substituent in 2- or 3-position of blank pyridine is rather ineffective at increasing binding affinity toward the MB327 binding site. Similar binding affinities as determined for **3 d** and **1 c** or parent compound **1 a**, respectively, were also found at the blank pyridine 3-CONMe₂, 3,5-Me₂, 3-Me or 2-*i*Pr substituted compounds **1 g** (PTM0053, Table 4, entry 8), **1 i** (PTM0035, Table 4, entry 10), **1 j** (PTM0037, Table 4, entry 11), and **3 c** (PTM0048, Table 4, entry 21), showing pK_i values from 4.39 ± 0.08 to 4.62 ± 0.08 . Distinctly reduced binding affinities compared to parent compound **1 a**, however, were found for pyridinium salts exhibiting a 3-CF₃ (**1 e**, PTM0051,

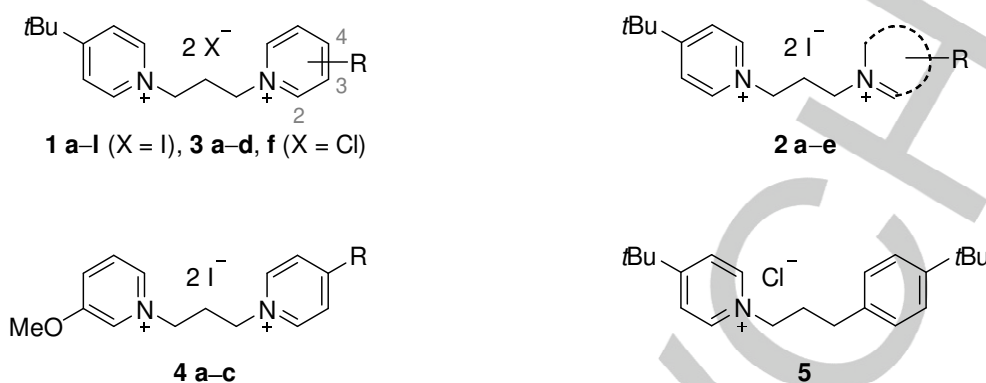
Table 4, entry 6), 4-COOEt (**1 f**, PTM0052, Table 4, entry 7), or 3-OMe (**1 k**, PTM0040, Table 4, entry 12) group at the blank pyridine with pK_i values ranging from 4.14 ± 0.10 for **1 e** (PTM0051) up to 4.35 ± 0.08 for **1 k** (PTM0040). For compounds displaying a 3-(ethoxycarbonyl)unit (**1 d**, PTM0050: $pK_i = 4.84 \pm 0.03$, Table 4, entry 5) or two methyl groups in 2,6-position (**3 a**, PTM0046: $pK_i = 4.82 \pm 0.04$, Table 4, entry 19) at blank pyridine, binding affinities were increased. In fact, pK_i values were about 0.3 log units higher as compared to reference compound **1 a** (PTM0029, Table 4, entry 2).

The binding affinities of these compounds are at least as high as the one of the currently most potent nAChR re-sensitizer **MB327** ($pK_i = 4.73 \pm 0.03$, Table 4, entry 1). Promising results were further obtained for compounds in which the blank pyridinium subunit of **1 a** is replaced by a 2,4,6-collidinium (**3 b**, PTM0041, $pK_i = 4.89 \pm 0.04$, Table 4, entry 20) or 3- and 4-dimethylamino pyridinium moiety (**1 b**, PTM0030, $pK_i = 4.92 \pm 0.09$, Table 4, entry 3; **1 h**, PTM0056, $pK_i = 4.90 \pm 0.06$, Table 4, entry 9), showing pK_i values about 0.4 log units higher as the respective pK_i value of the unsubstituted reference **1 a** (PTM0029, Table 4, entry 2). Notably, the increased binding affinity of dimethylamino substituted compounds is in accordance with recently published structure-affinity relationships found for symmetric bispyridinium compounds. The dimethylamino group was identified as potential substitute for the lipophilic 4-*tert*-butyl substituent since it enhances binding affinity as well.^[12] Although 3-methoxy substituted **1 k** (PTM0040, $pK_i = 4.35 \pm 0.08$, Table 4, entry 12) showed a reduced binding affinity compared to unsubstituted **1 a** (PTM0029, $pK_i = 4.52 \pm 0.06$, Table 4, entry 2), the pK_i value for the bifunctional compound **1 i** (PTM0038, Table 4, entry 13), with an additional 4-*tert*-butyl group next to the 3-methoxy moiety, increased significantly (determined by a two-sided t-test, $\alpha = 0.05$) about 0.6 log units (**1 i**, PTM0038: $pK_i = 4.97 \pm 0.02$) as compared to the pK_i value of compound **1 a** (PTM0029). With a pK_i value even 0.24 log units above the respective value of **MB327**, **1 i** (PTM0038) showed the highest affinity toward the MB327 binding site of all compounds synthesized in this study. This result underlines not only the positive effect of the *tert*-butyl group at the 4-position of the pyridinium ring, but also demonstrates the possibility to improve binding affinity toward the MB327 binding site by a synergistic effect of two functional groups, in this case with an additional 3-methoxy moiety, even if the latter alone has a rather negative effect.

Binding affinities of compounds with a 3-methoxypyridinium motive (**4 a–c**, PTM0042, PTM0043, PTM0044, Table 4, entries 24–26) were distributed within a small range from $pK_i = 4.40 \pm 0.06$ for 4-Me derivative **4 a** (PTM0042) to $pK_i = 4.64 \pm 0.09$ for 4-NMe₂ substituted **4 b** (PTM0043). In line with the results obtained for 4-*tert*-butylpyridinium compounds **1 a–i** (PTM0029, PTM0030, PTM0035, PTM0037, PTM0038, PTM0040, PTM0049–0053, PTM0056), the highest binding affinity was found for NMe₂ substituted **4 b** (PTM0043).

Nevertheless, the 4-*tert*-butylpyridinium analogue **1 h** displays a clearly higher binding affinity (PTM0056, $pK_i = 4.90 \pm 0.06$, Table 4, entry 9) than the 3-methoxypyridinium salt **4 b** (PTM0043, $pK_i = 4.64 \pm 0.09$, Table 4, entry 25). Hence, the 4-*tert*-butylpyridinium motive still appears to be better suited as a subunit for the development of new bisquaternary N-aromatic re-sensitizers with high potency.

FULL PAPER

Table 4. Structures of synthesized non-symmetric target compounds and binding affinities to the MB327 binding site, determined in MS Binding Assays as previously described.^[12]

Entry	Compound	R/N _{net}	pK _i ^[a]	PTM code
1	MB327	4- <i>t</i> Bu	4.73 ± 0.03	
2	1 a	H	4.52 ± 0.06	0029
3	1 b	3-NMe ₂	4.92 ± 0.09	0030
4	1 c	3- <i>t</i> Bu	4.50 ± 0.02	0049
5	1 d	3-COOEt	4.84 ± 0.03	0050
6	1 e	3-CF ₃	4.14 ± 0.10	0051
7	1 f	4-COOEt	4.26 ± 0.03	0052
8	1 g	3-CONMe ₂	4.62 ± 0.08	0053
9	1 h	4-NMe ₂	4.90 ± 0.06	0056
10	1 i	3,5-Me ₂	4.48 ± 0.04	0035
11	1 j	3-Me	4.50 ± 0.09	0037
12	1 k	3-OMe	4.35 ± 0.08	0040
13	1 l	3-OMe, 4- <i>t</i> Bu	4.97 ± 0.02	0038
14	2 a	isoquinolin-2-ium	4.90 ± 0.06	0054
15	2 b	<i>N</i> -methyl-imidazol-3-ium	4.70 ± 0.04	0031
16	2 c	<i>N</i> - <i>tert</i> -butyl-imidazol-3-ium	4.40 ± 0.06	0058
17	2 d	1,3-thiazol-3-ium	4.30 ± 0.11	0039
18	2 e	3- <i>tert</i> -butylpyrazin-1-ium	4.33 ± 0.12	0055
19	3 a	2,6-Me ₂	4.82 ± 0.04	0046
20	3 b	2,4,6-Me ₃	4.89 ± 0.04	0041
21	3 c	2- <i>i</i> Pr	4.39 ± 0.08	0048
22	3 d	2- <i>t</i> Bu	4.54 ± 0.05	0047
23	3 f	pyridin-2(1 <i>H</i>)-one	3.65 ± 0.12	0036
24	4 a	4-Me	4.40 ± 0.06	0042
25	4 b	4-NMe ₂	4.64 ± 0.09	0043
26	4 c	4-CF ₃	4.52 ± 0.10	0044
27	5	---	4.34 ± 0.04	0060

[a] Data are given as mean ± SEM of three independent experiments.

FULL PAPER

Next, analogues of the bispyridinium salts in which one of the two pyridinium rings was replaced by a nitrogen containing heteroaromatic were studied (**2 a–e**, PTM0031, PTM0039, PTM0054, PTM0055, PTM0058, Table 4, entries 14–18). Interestingly, N-methylimidazolium derivative **2 b** (PTM0031, $pK_i = 4.70 \pm 0.04$, Table 4, entry 15) showed a higher binding affinity than its *tert*-butyl imidazolium analogue **2 c** (PTM0058, $pK_i = 4.40 \pm 0.06$, Table 4, entry 16). Also 3-*tert*-butylpyrazinium salt **2 e** (PTM0055, $pK_i = 4.33 \pm 0.12$, Table 4, entry 18) exhibited a reduced binding affinity as compared to its 3-*tert*-butylpyridinium analogue **1 c** (PTM0049, $pK_i = 4.50 \pm 0.02$, Table 4, entry 4).

According to these results, *tert*-butyl groups do not have a beneficial effect on binding affinity of N-aromatic bisquaternary species toward the MB327 binding site in general, but only in 4-position of bispyridinium systems as observed for **MB327** or **1 i** (PTM0038). A relatively low binding affinity was also determined for 1,3-thiazolium derivative **2 d** (PTM0039, $pK_i = 4.30 \pm 0.11$, Table 4, entry 17). Notably, isoquinolinium species **2 a** (PTM0054, $pK_i = 4.90 \pm 0.06$, Table 4, entry 14) revealed one of the highest binding affinities of all tested target compounds, suggesting extended π -systems to be important for binding.

To further expand the scope of structure-affinity relationships, we studied the mono-cationic **MB327** analogue **5** (PTM0060, $pK_i = 4.34 \pm 0.04$, Table 4, entry 27), in which one 4-*tert*-butyl pyridinium ring of **MB327** has been replaced by an uncharged 4-*tert*-butylphenyl ring. Apparently, due to the missing quaternary nitrogen atom, **5** (PTM0060) showed a lower binding affinity compared to biscationic **MB327** ($pK_i = 4.73 \pm 0.03$, Table 4, entry 1). In consequence, pyridinium systems or quaternary aromatic nitrogen centers which are able to undergo additional ionic, ion-dipole or cation- π interactions appear to be important parts of compounds targeting the MB327 binding site that cannot be replaced by a sole lipophilic moiety like a phenyl residue.

Finally, the lowest binding affinity of all tested compounds was found for pyridiniumpropylpyridone **3 f** (PTM0036, $pK_i = 3.65 \pm 0.12$, Table 4, entry 23). This result seems to be, again, in accordance with the structure-affinity relationships discussed so far, since the pyridone subunit of **3 f** (PTM0036) misses a cationic center as well as a functional group that contributes to positive target interactions, such as a *tert*-butyl group in 4-position or a NMe₂ group in 3- or 4-position.

Conclusion

In conclusion, 26 novel non-symmetric bispyridinium and related salts with a 4-*tert*-butylpyridinium or 3-methoxypyridinium motive were synthesized and characterized with respect to their binding affinity toward the MB327 binding site at the *Torpedo*-nAChR.

All target compounds were prepared from aromatic N-heterocyclic precursors in two consecutive alkylation reactions. By the combination of microwave synthesis with RP-MPLC purification a very efficient and reliable access to a broad variety of highly polar bisquaternary compounds in practical quantities was achieved. The synthetic value of our method is particularly demonstrated by the fact that even less nucleophilic N-heterocycles, such as 2-*tert*-butylpyrazine or 1,3-thiazole, underwent a smooth alkylation reaction and that a broad variety of functional groups (e.g., COOEt, CONMe₂, OMe, NMe₂ or CF₃) was tolerated.

Binding affinities were determined in MS Binding Assays with [²H₆]**MB327** as marker. Altogether, it was found that biscationic

compounds exhibiting a 4-*tert*-butylpyridinium motive on one side and an isoquinolinium (**2 a**, PTM0054), 3-dimethylamino (**1 b**, PTM0030), 4-dimethylamino- (**1 h**, PTM0056) or 3-methoxy-4-*tert*-butylpyridinium (**1 i**, PTM0038) motive on the opposite side display improved binding affinities as compared to that of the unsubstituted analogue **1 a** (PTM0029) possessing pK_i values in the same range as **MB327**. In contrast, a distinctly lower binding affinity was found for mono-cationic compounds, i.e. without a second quaternary nitrogen atom such as **5** (PTM0060) or **3 f** (PTM0036).

Although none of the synthesized compounds showed a binding affinity much higher than lipophilic substituents carrying **MB327**, the results shed light on the importance of extended π -systems as well as of ionic, ion-dipole and cation- π interactions for binding toward the MB327 binding site. Interestingly, polar NMe₂-group was identified as fully adequate isoster of the *tert*-butyl group in terms of binding affinity. Regarding the fit into the MB327 binding pocket, non-symmetric compounds presented in this study obviously do not yet exhibit the specific substitution pattern required for favorable interactions with amino acid side chains of the nAChR. Especially the polar site of the putative binding pocket is assumed to be rich in aspartate, threonine, or tyrosine side chains^[14] which are usually strongly hydrogen bonded by surrounding water molecules. Clearly this removal of the hydration shell requires ligands that exactly match the substitution in the binding pocket, otherwise, binding energy will not be gained, but lost. The information on the influence of polar and lipophilic substituents, ionic interactions as well as extended π -systems on binding affinity gathered in this as well as in the previous study will certainly be of great value for a more rational optimization of the lead structure **MB327**.^[12] Further in-depth studies on binding interactions at the MB327 binding site and studies associated with the development of new re-sensitizers targeting the nAChR are under way.

Experimental Section

General Methods

Anhydrous reactions were carried out in vacuum-dried glassware under argon atmosphere. Microwave reactions were performed in sealed glass vials using a CEM Discover SP microwave synthesizer. THF, Et₂O, 1,4-dioxane and CH₂Cl₂ were distilled prior to use under nitrogen atmosphere and dried according to standard procedures.^[22] All other chemicals were used as purchased from commercial sources and solvents were distilled before use. TLC was carried out using plates purchased from Merck (silica gel 60 F₂₅₄ on aluminum sheet). Medium pressure liquid chromatography (MPLC) was carried out using a Büchi preparative chromatography system with YMC-Triart Prep C18-S (reversed phase, 20 μ m mesh size) or YMC SIL-HG (normal phase, 20 μ m mesh size) silica gel as stationary phase. Flash column chromatography (FC) was performed using Merck silica gel 60 (40–63 μ m mesh size) as stationary phase. Melting points were determined with a BÜCHI 510 melting point apparatus and are uncorrected. IR spectroscopy was performed using an FT-IR Spectrometer 1600 and Paragon 1000 (PerkinElmer); oils were measured as film and solid samples as KBr pellets. High-resolution (HR) mass spectrometry was performed on a Finnigan MAT 95 (EI), Finnigan LTQ FT (ESI) and Jeol JMS 700 MStation (FAB). ¹H and ¹³C NMR spectra were recorded with a Bruker BioSpin Avance III HD 400 and 500 MHz (equipped with a Prodigy™ cryo probe) using TMS as internal standard and integrated with MestReNova (Version 10.0.2), Mestrelab Research S.L. 2015. The purity of the test compounds was determined by means of quantitative NMR using Sigma Aldrich TraceCERT® maleic acid or dimethylsulfone as

FULL PAPER

internal calibrants.^[23, 24] The purity of all tested compounds was > 95%. See the Supporting Information for the characterization data of the described compounds.

The following compounds were prepared according to literature: 3-Bromopropyl trifluoromethanesulfonate (**33**),^[25, 26] 2-*tert*-butylpyridine (**31**),^[27] 4-(*tert*-butyl)-3-methoxypyridine (**21**),^[28] 2-isopropylpyridine (**30**),^[12] 3-*tert*-butylpyridine (**13**),^[12] 1-(*tert*-butyl)-1*H*-imidazole (**24**),^[29] 1-[4-(*tert*-Butyl)phenyl]-3-chloropropan-1-one (**35**).^[18, 19]

General Procedures

Synthesis of *N*-(3-bromopropyl)pyridinium salts (GP1): **A**) The corresponding pyridine derivative (1.0 equiv) was added to a solution of 3-bromopropyl trifluoromethanesulfonate (**33**, 1.25 equiv) in CH₂Cl₂ and the resulting mixture was stirred for the indicated period at room temperature and/or 50 °C. The solvent was removed in vacuo and the crude product was purified by FC. **B**) 3-Bromopropyl trifluoromethanesulfonate (**33**, 1.25 equiv) was added dropwise to the corresponding pyridine derivative (1.0 equiv) and the resulting mixture was stirred at given reaction conditions. The mixture was allowed to cool to room temperature and the crude product was purified by crystallization from EtOAc.

Synthesis of non-symmetric diiodide target compounds by a substitution reaction of *N*-(3-iodopropyl)pyridinium salts with *N*-heterocycles (GP2): The corresponding pyridine derivative (1.2 equiv) was added to a solution of the respective *N*-(3-iodopropyl)pyridinium salt (1.0 equiv) in MeCN (2 mL mmol⁻¹) and the resulting reaction mixture was stirred at 90 or 120 °C for 1, 3 or 16 h under microwave conditions (150 W). The solvent was removed under reduced pressure and the crude product was purified by RP-MPLC. The resulting highly viscous liquid was dissolved in H₂O bidest. (8 mL mmol⁻¹) and lyophilized to obtain the corresponding salt as a solid. In case of hygroscopic products, the purified material was treated repeatedly with EtOAc (3 x 10 mL mmol⁻¹) and the solvent was removed under reduced pressure. If mentioned, the crude product was purified by crystallization instead of RP-MPLC.

Synthesis of non-symmetric dichloride target compounds by a substitution reaction of *N*-(3-bromopropyl)pyridinium salts with 4-*tert*-butylpyridine (GP3): 4-*tert*-Butylpyridine (**6**) was added to a suspension/solution of the corresponding *N*-(3-bromopropyl)pyridinium salt (1.0 equiv, prepared according to GP1) in MeCN (2 mL mmol⁻¹) and the resulting mixture was stirred for 3 h at 90 °C under microwave conditions (150 W). The solvent was removed under reduced pressure and the residue was dissolved in H₂O bidest. (40 mL mmol⁻¹). Amberlite® IRA-410 Cl⁻ form ion exchange resin (20 g mmol⁻¹, 50 meq mmol⁻¹) was added to the aqueous solution and the resulting suspension was vigorously stirred for 16 h at room temperature. The resin was removed by filtration, washed with H₂O bidest. (65 mL mmol⁻¹) and the solvent was removed under reduced pressure. The crude product was purified by RP-MPLC and the resulting highly viscous liquid was dissolved in H₂O bidest. (8 mL mmol⁻¹) and lyophilized to obtain the corresponding salt as a solid. In case of hygroscopic products, the purified material was treated repeatedly with EtOAc (3 x 10 mL mmol⁻¹) and the solvent was removed under reduced pressure. If mentioned, the crude product was purified by crystallization instead of RP-MPLC.

Synthesized compounds

***N*-Alkylpyridinium salts:** 4-(*tert*-Butyl)-1-(3-iodopropyl)pyridin-1-ium iodide (**10 a**, yellow solid, 74%), 1-(3-iodopropyl)-3-methoxypyridin-1-ium iodide (**10 b**, yellow solid, 70%), 1-(3-iodopropyl)-4-(trifluoromethyl)pyridin-1-ium iodide (**10 c**, yellow solid, 75%), 1-(3-bromopropyl)-2,6-dimethylpyridin-1-ium trifluoromethanesulfonate (**34 a**, colorless solid, 83%), 1-(3-bromopropyl)-2,4,6-trimethylpyridin-1-ium trifluoromethanesulfonate (**34 b**, colorless solid, 81%), 1-(3-bromopropyl)-2-isopropylpyridin-1-ium trifluoromethanesulfonate (**34 c**, colorless solid, 78%), 1-(3-bromopropyl)-2-(*tert*-butyl)pyridin-1-ium trifluoromethane-

sulfonate (**34 d**, colorless solid, 67%), 1-(3-bromopropyl)-2-methoxypyridin-1-ium trifluoromethanesulfonate (**34 e**, colorless solid, 96%).

Compounds 1 a–l: 4-(*tert*-Butyl)-1-[3-(pyridin-1-ium-1-yl)propyl]pyridin-1-ium diiodide (**1 a**, colorless hygroscopic solid, 52%), 1-[3-[4-(*tert*-butyl)pyridin-1-ium-1-yl]propyl]-3-(dimethylamino)-pyridin-1-ium diiodide (**1 b**, yellow hygroscopic solid, 51%), 3-(*tert*-butyl)-1-[3-[4-(*tert*-butyl)pyridin-1-ium-1-yl]propyl]pyridin-1-ium diiodide (**1 c**, yellow solid, 94%), 1-[3-[4-(*tert*-butyl)pyridin-1-ium-1-yl]propyl]-3-(ethoxycarbonyl)-pyridin-1-ium diiodide (**1 d**, yellow solid, 82%), 1-[3-[4-(*tert*-butyl)pyridin-1-ium-1-yl]propyl]-3-(trifluoromethyl)-pyridin-1-ium diiodide (**1 e**, yellow solid, 61%), 4-(*tert*-butyl)-1-[3-[4-(ethoxycarbonyl)pyridin-1-ium-1-yl]propyl]-pyridin-1-ium diiodide (**1 f**, orange solid, 73%), 1-[3-[4-(*tert*-butyl)pyridin-1-ium-1-yl]propyl]-3-(dimethylcarbamoyl)-pyridin-1-ium diiodide (**1 g**, yellow solid, 87%), 4-(*tert*-butyl)-1-[3-[4-(dimethylamino)pyridin-1-ium-1-yl]propyl]-pyridin-1-ium diiodide (**1 h**, yellow solid, 95%), 1-[3-[4-(*tert*-butyl)pyridin-1-ium-1-yl]propyl]-3,5-dimethylpyridin-1-ium diiodide (**1 i**, yellow solid, 87%), 1-[3-[4-(*tert*-butyl)pyridin-1-ium-1-yl]propyl]-3-methylpyridin-1-ium diiodide (**1 j**, yellow solid, 86%), 1-[3-[4-(*tert*-butyl)pyridin-1-ium-1-yl]propyl]-3-methoxypyridin-1-ium diiodide (**1 k**, yellow solid, 78%), 4-(*tert*-butyl)-1-[3-[4-(*tert*-butyl)pyridin-1-ium-1-yl]propyl]-3-methoxypyridin-1-ium diiodide (**1 l**, as a yellow solid, 85%).

Compounds 2 a–e: 2-[3-[4-(*tert*-Butyl)pyridin-1-ium-1-yl]propyl]isoquinolin-2-ium diiodide (**2 a**, yellow solid, 96%), 4-(*tert*-butyl)-1-[3-[1-methyl-1*H*-imidazol-3-ium-3-yl]propyl]pyridin-1-ium diiodide (**2 b**, slightly yellowish solid, 80%), 4-(*tert*-butyl)-1-[3-[1-(*tert*-butyl)-1*H*-imidazol-3-ium-3-yl]propyl]-pyridin-1-ium diiodide (**2 c**, yellow solid, 99%), 3-[3-[4-(*tert*-butyl)pyridin-1-ium-1-yl]propyl]thiazol-3-ium diiodide (**2 d**, yellow solid, 89%), 3-(*tert*-butyl)-1-[3-[4-(*tert*-butyl)pyridin-1-ium-1-yl]propyl]pyrazin-1-ium diiodide (**2 e**, yellow solid, 87%).

Compounds 3 a–f: 1-[3-[4-(*tert*-Butyl)pyridin-1-ium-1-yl]propyl]-2,6-dimethylpyridin-1-ium dichloride (**3 a**, colorless solid, 78%), 1-[3-[4-(*tert*-butyl)pyridin-1-ium-1-yl]propyl]-2,4,6-trimethylpyridin-1-ium dichloride (**3 b**, colorless solid, 85%), 1-[3-[4-(*tert*-butyl)pyridin-1-ium-1-yl]propyl]-2-isopropylpyridin-1-ium dichloride (**3 c**, colorless solid, 94%), 2-(*tert*-butyl)-1-[3-[4-(*tert*-butyl)pyridin-1-ium-1-yl]propyl]pyridin-1-ium dichloride (**3 d**, slightly hygroscopic and colorless solid, 90%), 4-(*tert*-butyl)-1-[3-(2-oxopyridin-1(2*H*)-yl)propyl]pyridin-1-ium chloride (**3 f**, colorless and moderately hygroscopic solid, 90%).

Compounds 4 a–c: 3-Methoxy-1-[3-(4-methylpyridin-1-ium-1-yl)propyl]pyridin-1-ium diiodide (**4 a**, yellow solid, 83%), 1-[3-[4-(dimethylamino)pyridin-1-ium-1-yl]propyl]-3-methoxypyridin-1-ium diiodide (**4 b**, yellow solid, 70%), 3-methoxy-1-[3-[4-(trifluoromethyl)pyridin-1-ium-1-yl]propyl]pyridin-1-ium diiodide (**4 c**, yellow solid, 62%).

Compound 5: 1-(*tert*-Butyl)-4-(3-chloropropyl)benzene (**36**, colorless liquid, 90%), 4-(*tert*-butyl)-1-[3-[4-(*tert*-butyl)phenyl]propyl]pyridin-1-ium chloride (**5**, colorless and less hygroscopic solid, 90%).

Biological Evaluation – MS Binding Assays

MS Binding Assays were performed with [³H]MB327 as marker and nAChR-enriched membranes, prepared from *Torpedo californica* electroplaque tissue, as previously described.^[11, 12]

Supporting Information

Synthetic procedures and analytical characterization of all compounds can be found within the supporting information.

FULL PAPER

Acknowledgements

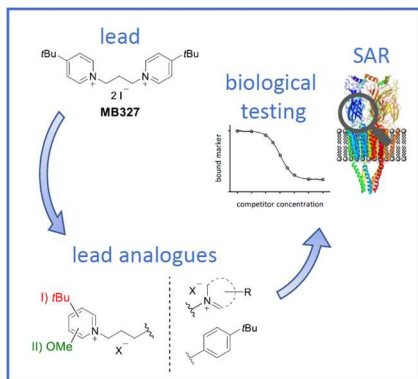
This study was funded by the German Ministry of Defense (E/U2AD/CF514/DF561).

Keywords: Re-sensitizer • MS Binding Assay • Bispyridinium • Drug design • Microwave chemistry

- [1] E. Dolgin, *Nat. Med.* **2013**, *19*, 1194–1195.
- [2] J. Newmark, *Neurologist*. **2007**, *13*, 20–32.
- [3] F. R. Sidell, J. Borak, *Ann. Emerg. Med.* **1992**, *21*, 865–871.
- [4] F. Worek, H. Thiermann, T. Wille, *Chem. Biol. Interact.* **2016**, *259*, 93–98.
- [5] D. Gunnell, M. Eddleston, M. R. Phillips, F. Konradsen, *BMC Public Health*. **2007**, *7*:357.
- [6] R. D. Sheridan, A. P. Smith, S. R. Turner, J. E. H. Tattersall, *J. R. Soc. Med.* **2005**, *98* (3), 114–115.
- [7] F. Worek, L. Szinicz, P. Eyer, H. Thiermann, *Toxicol. Appl. Pharmacol.* **2005**, *209*, 193–202.
- [8] R. A. Maselli, C. Leung, *Muscle & Nerve* **1993**, *16*, 548–553.
- [9] T. Seeger, M. Eichhorn, M. Lindner, K. V. Niessen, J. E. H. Tattersall, C. M. Timperley, M. Bird, A. C. Green, H. Thiermann, F. Worek, *Toxicology* **2012**, *294*, 80–84.
- [10] K. V. Niessen, S. Muschik, F. Langguth, S. Rappenglück, T. Seeger, H. Thiermann, F. Worek, *Toxicol. Lett.* **2016**, *247*, 1–10.
- [11] S. Sichler, G. Höfner, S. Rappenglück, T. Wein, K. V. Niessen, T. Seeger, F. Worek, H. Thiermann, F. F. Paintner, K. T. Wanner, *Toxicol. Lett.* **2018**, *293*, 172–183.
- [12] S. Rappenglück, S. Sichler, G. Höfner, T. Wein, K. V. Niessen, T. Seeger, F. Worek, H. Thiermann, K. T. Wanner, *ChemMedChem* **2018**, in press.
- [13] N. Unwin, *J. Mol. Biol.* **2005**, *346*, 967–989.
- [14] T. Wein, G. Höfner, S. Rappenglück, S. Sichler, K. V. Niessen, T. Seeger, F. Worek, H. Thiermann, K. T. Wanner, *Toxicol. Lett.* **2018**, *293*, 184–189.
- [15] L. Cecchi, F. D. Sarlo, F. Machetti, *Eur. J. Org. Chem.* **2006**, 4852–4860.
- [16] F. Tao, S. L. Bernasek, *J. Am. Chem. Soc.* **2007**, *129*, 4815–4823.
- [17] C. Ögretir, S. Demirayak, N. F. Tay, M. Duran, *J. Chem. Eng. Data* **2008**, *53*, 422–426.
- [18] C. Gronnier, S. Kramer, Y. Odabachian, F. Gagosz, *J. Am. Chem. Soc.* **2012**, *134*, 828–831.
- [19] A. Gomtsyan, E. K. Bayburt, R. G. Schmidt, C. S. Surowy, P. Honore, K. C. Marsh, S. M. Hannick, H. A. McDonald, J. M. Wetter, J. P. Sullivan, M. F. Jarvis, C. R. Faltynek, C.-H. Lee, *J. Med. Chem.* **2008**, *51*, 392–395.
- [20] M. S. Gowda, S. S. Pande, R. A. Ramakrishna, K. R. Prabhu, *Org. Biomol. Chem.* **2011**, *9*, 5365–5368.
- [21] J. I. Perlmutter, L. T. Forbes, D. J. Krysan, K. Ebsworth-Mojica, J. M. Colquhoun, J. L. Wang, P. M. Dunman, D. P. Flaherty, *J. Med. Chem.* **2014**, *57*, 8540–8562.
- [22] D. D. Perrin, W. L. F. Armarego, *Purification of Laboratory Chemicals*, Pergamon, New York, **1988**.
- [23] M. Cushman, G. I. Georg, U. Holzgrabe, S. Wang, *J. Med. Chem.* **2016**, *57*, 9219.
- [24] G. F. Pauli, S.-N. Chen, C. Simmler, D. C. Lankin, T. Gödecke, B. U. Jaki, J. B. Friesen, J. B. McAlpine, J. G. Napolitano, *J. Med. Chem.* **2014**, *57*, 9220–9231.
- [25] C. L. Huglshofer, K. T. Mellem, A. G. Myers, *Org. Lett.* **2013**, *15*, 3134–3137.
- [26] M. Sajadi, F. Berndt, C. Richter, M. Gerecke, R. Mahrwald, N. P. Ernsting, *J. Phys. Chem. Lett.* **2014**, *5*, 1845–1849.
- [27] T. W. Bell, L. Y. Hu, S. V. Patel, *J. Org. Chem.* **1987**, *52*, 3847–3850.
- [28] S. Rappenglück, K. V. Niessen, T. Seeger, F. Worek, H. Thiermann, K. T. Wanner, *Synthesis* **2017**, *49*, 4055–4064.
- [29] C. H. Leung, A. R. Chianese, B. R. Garrett, C. S. Letko, R. H. Crabtree, *Inorg. Synth.* **2010**, *35*, 84–87.

FULL PAPER

Entry for the Table of Contents



Advancing toward new nAChR re-sensitizers!

Based on in silico modeling results, a series of 26 non-symmetric analogues of bispyridinium lead compound MB327 was synthesized and characterized in terms of binding affinity at the nicotinic acetylcholine receptor (nAChR) using our recently developed MS Binding Assays. We developed new structure-affinity relationships, providing a comprehensive groundwork for the design of novel nAChR re-sensitizers.

Experimental Procedures and Analytical Data of Synthesized Compounds

4-(*tert*-Butyl)-1-(3-iodopropyl)pyridin-1-ium iodide (**10 a**)

9 (11.8 g, 40.0 mmol, 4.59 mL, 4.0 eq.) was added to a solution of **6** (1.35 g, 10.0 mmol, 1.46 mL, 1.0 eq.) in MeCN (20 mL) and the resulting mixture was stirred for 1 h at 90 °C under microwave conditions (150 W). The reaction mixture was allowed to cool to room temperature and the crude product was precipitated by addition of Et₂O (120 mL). Subsequent purification by FC (first purification: SiO₂, CH₂Cl₂ → CH₂Cl₂/MeOH = 9:1; second purification: SiO₂, CH₂Cl₂/MeOH = 9:1) afforded **10 a** (3.19 g, 74%) as a yellow solid.

*R*_f=0.25–0.50 (CH₂Cl₂/MeOH 9:1); mp: 154–155°C; ¹H NMR (500 MHz, CD₃OD): δ=1.45 (s, 9 H, C(CH₃)₃), 2.53 (quin., *J*=6.9 Hz, 2 H, NCH₂CH₂), 3.27 (t, *J*=6.8 Hz, 2 H, CH₂I), 4.69 (t, *J*=7.2 Hz, 2 H, NCH₂), 8.13–8.17 (m, 2 H, NCHCH), 8.86–8.90 ppm (m, 2 H, NCHCH); ¹³C NMR (125 MHz, CD₃OD): δ=-0.56 (CH₂I), 30.24 (C(CH₃)₃), 35.46 (NCH₂CH₂), 37.67 (CC(CH₃)₃), 62.27 (NCH₂), 126.80 (NCHCH), 145.44 (NCHCH), 173.14 ppm (CC(CH₃)₃); IR (KBr): $\tilde{\nu}$ =3073, 3016, 2965, 2866, 1991, 1636, 1557, 1511, 1460, 1438, 1373, 1330, 1306, 1271, 1239, 1228, 1190, 1111, 991, 926, 881, 866, 847, 789, 735, 577 cm⁻¹; HRMS-ESI *m/z* [*M*-I]⁺ calcd for C₁₂H₁₉IN: 304.0557, found: 304.0563.

1-(3-iodopropyl)-3-methoxy-pyridin-1-ium iodide (**10 b**)

9 (12.5 g, 42.4 mmol, 4.87 mL, 4.0 eq.) was added to a solution of **7** (1.19 g, 10.6 mmol, 1.10 mL, 1.0 eq.) in MeCN (21 mL) and the resulting mixture was stirred for 1 h at 90 °C under microwave conditions (150 W). The reaction mixture was allowed to cool to room temperature and the crude product was precipitated by adding successively Et₂O (80 mL), EtOAc (20 mL), MeOH (20 mL) and again Et₂O (100 mL). Subsequent purification by FC (SiO₂, CH₂Cl₂/MeOH = 9:1) and lyophilization of the resulting highly viscous liquid in H₂O bidest. (5 mL) afforded **10 b** (3.02 g, 70%) as a yellow solid.

*R*_f=0.20 (CH₂Cl₂/MeOH 9:1); mp: 97°C; ¹H NMR (500 MHz, CD₃OD): δ=2.56 (quin., *J*=7.0 Hz, 2 H, CH₂I), 3.27 (t, *J*=6.9 Hz, 2 H, CH₂CH₂I), 4.08 (s, 3 H, OCH₃), 4.72 (t, *J*=7.2 Hz, 2 H, NCH₂), 8.02 (dd, *J*=8.8/6.0 Hz, 1 H, NCHCHCH), 8.20 (ddd,

$J=8.8/2.6/0.7$ Hz, 1 H, NCHCH), 8.62 (d, $J=5.9$ Hz, 1 H, NCHCH), 8.80–8.83 ppm (m, 1 H, NCHCOCH₃); ¹³C NMR (125 MHz, CD₃OD): $\delta=-0.76$ (CH₂l), 35.59 (CH₂CH₂l), 58.24 (OCH₃), 63.52 (NCH₂), 129.92 (NCHCHCH), 132.08 (NCHCH), 133.86 (NCHCOCH₃), 138.34 (NCHCH), 160.64 ppm (COCH₃); IR (KBr): $\tilde{\nu}=3130, 3082, 3044, 3023, 2983, 2958, 2933, 2842, 1997, 1622, 1594, 1505, 1478, 1446, 1431, 1423, 1356, 1328, 1289, 1269, 1217, 1197, 1171, 1150, 1127, 1098, 1039, 997, 950, 893, 863, 854, 807, 765, 715, 670, 561, 503$ cm⁻¹; HRMS-ESI m/z [$M-I$]⁺ calcd for C₉H₁₃INO: 278.0036, found: 278.0033.

1-(3-Iodopropyl)-4-(trifluoromethyl)pyridin-1-ium iodide (**10 c**)

9 (4.14 g, 14.0 mmol, 1.61 mL, 4.0 eq.) was added to a solution of **8** (515 mg, 3.50 mmol, 400 μ L, 1.0 eq) in MeCN (7 mL) and the resulting mixture was stirred for 16 h at 90 °C under microwave conditions (150 W). The solvent was removed under reduced pressure and the residue was purified by FC (SiO₂, CH₂Cl₂/MeOH = 9:1) yielding **10 c** (1.16 g, 75%) as a yellow solid.

$R_f=0.1-0.4$ (CH₂Cl₂/MeOH 9:1); mp: 88–90°C; ¹H NMR (500 MHz, CD₃CN): $\delta=2.55$ (quin., $J=7.1$ Hz, 2 H, CH₂CH₂l), 3.27 (t, $J=7.0$ Hz, 2 H, CH₂l), 4.81 (t, $J=7.3$ Hz, 2 H, NCH₂), 8.36–8.40 (m, 2 H, NCHCH), 9.18 ppm (d, $J=6.5$ Hz, 2 H, NCHCH); ¹³C NMR (125 MHz, CD₃CN): $\delta=-0.22$ (CH₂l), 35.03 (CH₂CH₂l), 63.51 (t, $J=3.4$ Hz, NCH₂), 122.08 (q, $J=275.2$ Hz, CF₃), 126.27 (q, $J=3.2$ Hz, NCHCH), 145.50 (q, $J=36.5$ Hz, CCF₃), 147.90 ppm (t, $J=8.9$ Hz, NCH); IR (KBr): $\tilde{\nu}=3113, 3040, 3010, 2951, 2856, 1649, 1582, 1463, 1425, 1324, 1288, 1188, 1155, 1124, 1108, 1080, 1048, 968, 852, 766, 745, 733, 658, 643$ cm⁻¹; HRMS-ESI m/z [$M-I$]⁺ calcd for C₉H₁₀F₃IN: 315.9805, found: 315.9802.

1-(3-Bromopropyl)-2,6-dimethylpyridin-1-ium trifluoromethanesulfonate (**34 a**)

According to GP1A, with **33** (678 mg, 2.50 mmol, 1.25 eq.) and **28** (214 mg, 2.00 mmol, 232 μ L, 1.0 eq.) in CH₂Cl₂ (5 mL). Reaction time: 16 h at room temperature and 1 h at 50 °C. Purification by FC (SiO₂, CH₂Cl₂/MeOH = 9:1) afforded **34 a** (628 mg, 83%) as a colorless solid.

$R_f=0.1-0.3$ (CH₂Cl₂/MeOH 9:1); mp: 76°C; ¹H NMR (500 MHz, CD₃CN): $\delta=2.31-2.41$ (m, 2 H, NCH₂CH₂), 2.83 (s, 6 H, CH₃), 3.66 (t, $J=6.2$ Hz, 2 H, CH₂Br), 4.51–4.59 (m, 2 H, NCH₂), 7.71 (d, $J=7.9$ Hz, 2 H, NC(CH₃)CH), 8.19 ppm (t, $J=7.9$ Hz, 1 H,

CHCHCH); ^{13}C NMR (125 MHz, CD_3CN): δ =21.72 (CH_3), 30.65 (CH_2Br), 31.16 ($\text{CH}_2\text{CH}_2\text{Br}$), 52.87 (NCH_2), 122.15 (q, J =320.7 Hz, CF_3), 129.24 ($\text{NC}(\text{CH}_3)\text{CH}$), 145.70 (CHCHCH), 156.93 ppm (CCH_3); IR (KBr): $\tilde{\nu}$ =3073, 3026, 2983, 2952, 1626, 1591, 1495, 1461, 1413, 1388, 1371, 1264, 1226, 1174, 1157, 1031, 990, 900, 854, 820, 806, 766, 755, 691, 638, 572, 560, 517 cm^{-1} ; HRMS-ESI m/z [$M\text{-TfO}$] $^+$ calcd for $\text{C}_{10}\text{H}_{15}\text{BrN}$: 228.0382, found: 228.0383.

1-(3-Bromopropyl)-2,4,6-trimethylpyridin-1-ium trifluoromethanesulfonate (34 b)

According to GP1A, with **33** (576 mg, 2.13 mmol, 1.25 eq.) and **29** (206 mg, 1.70 mmol, 225 μL , 1.0 eq.) in CH_2Cl_2 (5 mL). Reaction time: 16 h at room temperature and 1 h at 50 $^\circ\text{C}$. Purification by FC (SiO_2 , $\text{CH}_2\text{Cl}_2/\text{MeOH}$ = 9:1) afforded **34 b** (538 mg, 81%) as a colorless solid.

R_f =0.1–0.33 ($\text{CH}_2\text{Cl}_2/\text{MeOH}$ 9:1); mp: 53 $^\circ\text{C}$; ^1H NMR (500 MHz, CD_3CN): δ =2.29–2.37 (m, 2 H, NCH_2CH_2), 2.49 (s, 3 H, $\text{NC}(\text{CH}_3)\text{CHCCH}_3$), 2.76 (s, 6 H, NCCH_3), 3.64 (t, J =6.2 Hz, 2 H, CH_2Br), 4.44–4.51 (m, 2 H, NCH_2), 7.54 ppm (s, 2 H, CH); ^{13}C NMR (125 MHz, CD_3CN): δ =21.43 (NCCH_3), 21.59 $\text{NC}(\text{CH}_3)\text{CHCCH}_3$, 30.68 (CH_2Br), 31.31 (NCH_2CH_2), 52.12 (NCH_2), 122.21 (q, J =320.8 Hz, CF_3), 129.67 (CH), 155.56 (NCCH_3), 159.43 ppm (NCCH_3); IR (KBr): $\tilde{\nu}$ =3071, 3006, 2981, 2923, 1644, 1583, 1508, 1483, 1471, 1456, 1421, 1380, 1327, 1259, 1159, 1030, 1071, 1030, 990, 922, 871, 843, 764, 755, 718, 638, 571, 517 cm^{-1} ; HRMS-ESI m/z [$M\text{-TfO}$] $^+$ calcd for $\text{C}_{11}\text{H}_{17}\text{BrN}$: 242.0539, found: 242.0538.

1-(3-Bromopropyl)-2-isopropylpyridin-1-ium trifluoromethanesulfonate (34 c)

According to GP1B, with **33** (643 mg, 2.37 mmol, 1.25 eq.) and **30** (230 mg, 1.90 mmol, 1.0 eq.) at 50 $^\circ\text{C}$. Reaction time: 3 h. Crystallization from EtOAc (1 mL) by dropwise addition of Et_2O (3.5 mL) afforded **34 c** (584 mg, 78%) as a colorless solid.

mp: 93 $^\circ\text{C}$; ^1H NMR (400 MHz, CD_3CN): δ =1.41 (s, 6 H, $\text{CH}(\text{CH}_3)_2$), 2.42–2.50 (m, 2 H, CH_2Br), 3.47–3.60 (m, 3 H, $\text{CH}_2\text{CH}_2\text{Br}$, $\text{CH}(\text{CH}_3)_2$), 4.62–4.67 (m, 2 H, NCH_2), 7.82 (ddd, J =7.6/6.5/1.4 Hz, 1 H, NCHCH), 7.98–8.03 (m, 1 H, NCHCHCHCH), 8.39–8.46 (m, 1 H, NCHCHCH), 8.58 ppm (dd, J =6.3/1.1 Hz, 1 H, NCH); ^{13}C NMR (100 MHz, CD_3CN): δ =22.51 ($\text{CH}(\text{CH}_3)_2$), 30.03 ($\text{CH}_2\text{CH}_2\text{Br}$), 31.12 ($\text{CH}(\text{CH}_3)_2$), 34.37 (CH_2Br), 57.40 (NCH_2), 119.38–124.86 (m, CF_3), 126.81 (NCHCH), 127.82 (NCHCHCHCH), 146.42 (NCH), 147.05 (NCHCHCH), 165.41 ppm ($\text{NC}(\text{CH}(\text{CH}_3)_2)$); IR (KBr): $\tilde{\nu}$ =3155,

3097, 3058, 2988, 1632, 1579, 1516, 1479, 1454, 1431, 1396, 1366, 1279, 1255, 1237, 1225, 1164, 984, 895, 854, 812, 795, 769, 756, 640, 572, 555, 538, 517, 469 cm⁻¹; HRMS-ESI m/z [M -TfO]⁺ calcd for C₁₁H₁₇BrN: 242.0539, found: 242.0539.

1-(3-Bromopropyl)-2-(*tert*-butyl)pyridin-1-ium trifluoromethanesulfonate (34 d)

According to GP1B, with **33** (551 mg, 2.03 mmol, 1.25 eq.) and **31** (220 mg, 1.63 mmol, 1.0 eq.) at 85 °C. Reaction time: 1.5 h. Recrystallization from EtOAc (4 mL) afforded **34 d** (441 mg, 67%) as a colorless solid.

mp: 102°C; ¹H NMR (400 MHz, CD₃CN): δ=1.61 (s, 9 H, C(CH₃)₃), 2.49–2.58 (m, 2 H, CH₂CH₂Br), 3.66 (t, J =6.3 Hz, 2 H, CH₂Br), 4.80–4.88 (m, 2 H, NCH₂), 7.89 (ddd, J =7.7/6.4/1.5 Hz, 1 H, NCHCH), 8.10 (dd, J =8.4/1.3 Hz, 1 H, NCHCHCHCH), 8.40 (ddd, J =8.5/7.6/1.6 Hz, 1 H, NCHCHCHCH), 8.62–8.66 ppm (m, 1 H, NH); ¹³C NMR (100 MHz, CD₃CN): δ=30.16 (CH₂Br), 30.55 (C(CH₃)₃), 35.48 (CH₂CH₂Br), 38.66 (C(CH₃)₃), 58.37 (NCH₂), 117.10–127.03 (m, CF₃), 127.27 (NCHCH), 128.66 (NCHCHCHCH), 147.08 (NCHCHCH), 148.71 (NCH), 165.59 ppm (CC(CH₃)₃); IR (KBr): $\tilde{\nu}$ =3150, 3084, 3063, 2995, 1625, 1577, 1509, 1481, 1444, 1432, 1379, 1260, 1224, 1189, 1160, 1030, 980, 835, 805, 788, 770, 756, 640, 573, 556, 547, 517, 473 cm⁻¹; HRMS-ESI m/z [M -TfO]⁺ calcd for C₁₂H₁₉BrN: 256.0695, found: 256.0673.

1-(3-Bromopropyl)-2-methoxypyridin-1-ium trifluoromethanesulfonate (34 e)

According to GP1A, with **33** (650 mg, 2.40 mmol, 1.25 eq.) and **32** (214 mg, 1.92 mmol, 200 μL, 1.0 eq.) in CH₂Cl₂ (4.8 mL). Reaction time: 16 h at room temperature. Purification by FC (SiO₂, CH₂Cl₂/MeOH = 9:1) afforded **34 e** (702 mg, 96%) as a colorless solid.

R_f =0.15–0.33 (CH₂Cl₂/MeOH 9:1); mp: 74°C; ¹H NMR (400 MHz, CD₃OD): δ=2.42–2.50 (m, 2 H, NCH₂CH₂), 3.53 (t, J =6.3 Hz, 2 H, CH₂Br), 4.34 (s, 3 H, CH₃), 4.62 (t, J =7.1 Hz, 2 H, NCH₂), 7.55 (ddd, J =7.5/6.4/1.2 Hz, 1 H, NCHCH), 7.72 (d, J =8.9 Hz, 1 H, CH₃OCCH), 8.50 (ddd, J =9.1/7.4/1.8 Hz, 1 H, NCHCHCH), 8.57 ppm (dd, J =6.4/1.7 Hz, 1 H, NCH); ¹³C NMR (125 MHz, CD₃OD): δ=29.77 (CH₂Br), 32.64 (NCH₂CH₂), 54.67 (NCH₂), 60.12 (CH₃), 112.80 (CH₃OCCH), 120.21 (NCHCH), 121.82 (q, J =318.5 Hz, CF₃), 144.25 (NCH), 149.61 (NCHCHCH), 162.20 (CH₃OC) ppm; IR (KBr): $\tilde{\nu}$ =3093, 3063, 1638, 1587, 1521, 1477, 1462, 1441, 1373, 1350, 1316,

1263, 1226, 1158, 1032, 1011, 841, 756, 797, 787, 756, 747, 640, 573, 552, 518, 474 cm^{-1} ; HRMS-ESI m/z [$M\text{-TfO}$] $^{+}$ calcd for $\text{C}_9\text{H}_{13}\text{BrNO}$: 230.0175, found: 230.0180.

4-(*tert*-Butyl)-1-[3-(pyridin-1-ium-1-yl)propyl]pyridin-1-ium diiodide (1 a)

According to GP2, with **10 a** (647 mg, 1.50 mmol, 1.0 eq.) and **11** (237 mg, 3.00 mmol, 2.0 eq.) in MeCN (3 mL) at 90 °C. Reaction time: 1 h. Recrystallization from *i*PrOH/MeCN (6:1, 4 mL) under argon atmosphere afforded **1 a** (398 mg, 52%) as a colorless hygroscopic solid.

mp: 171 °C; ^1H NMR (400 MHz, $[\text{D}_6]\text{DMSO}$): δ =1.38 (s, 9 H, $\text{C}(\text{CH}_3)_3$), 2.66 (quin., J =7.5 Hz, 2 H, NCH_2CH_2), 4.68 (t, J =7.3 Hz, 2 H, $\text{CH}_2\text{NCHCHCC}(\text{CH}_3)_3$), 4.74 (t, J =7.3 Hz, 2 H, $\text{CH}_2\text{NCHCHCH}$), 8.19–8.25 (m, 4 H, $\text{NCHCHCC}(\text{CH}_3)_3$, NCHCHCH), 8.63–8.69 (m, 1 H, NCHCHCH), 8.96–9.00 (m, 2 H, $\text{NCHCHCC}(\text{CH}_3)_3$), 9.08–9.12 ppm (m, 2 H, NCHCHCH); ^{13}C NMR (125 MHz, $[\text{D}_6]\text{DMSO}$): δ =30.02 ($\text{C}(\text{CH}_3)_3$), 31.97 (NCH_2CH_2), 36.80 ($\text{C}(\text{CH}_3)_3$), 57.08 ($\text{CH}_2\text{NCHCHCC}(\text{CH}_3)_3$), 58.12 ($\text{CH}_2\text{NCHCHCH}$), 125.62 ($\text{NCHCHCC}(\text{CH}_3)_3$), 128.68 (NCHCHCH), 144.75 ($\text{NCHCHCC}(\text{CH}_3)_3$), 145.42 (NCHCHCH), 146.35 (NCHCHCH), 170.63 ppm ($\text{CC}(\text{CH}_3)_3$); IR (KBr): $\tilde{\nu}$ =3483, 3417, 3126, 3041, 3013, 2963, 2865, 1644, 1637, 1605, 1580, 1569, 1518, 1503, 1489, 1471, 1447, 1374, 1366, 1350, 1280, 1201, 1187, 1177, 1156, 1119, 884, 860, 853, 817, 807, 766, 758, 737, 679, 604, 573, cm^{-1} ; HRMS-FAB m/z [$M\text{-I}$] $^{+}$ calcd for $\text{C}_{17}\text{H}_{24}\text{IN}_2$: 383.0979, found: 383.0985.

1-{3-[4-(*tert*-Butyl)pyridin-1-ium-1-yl]propyl}-3-(dimethylamino)pyridin-1-ium diiodide (1 b)

According to GP2, with **10 a** (604 mg, 1.40 mmol, 1.0 eq.) and **12** (349 mg, 2.80 mmol, 2.0 eq.) in MeCN (3 mL) at 90 °C. Reaction time: 1 h. Recrystallization from MeCN (1.5 mL) under argon atmosphere afforded **1 b** (395 mg, 51%) as a yellow hygroscopic solid.

^1H NMR (500 MHz, $[\text{D}_6]\text{DMSO}$): δ =1.37 (s, 9 H, $\text{C}(\text{CH}_3)_3$), 2.66 (quin., J =7.1 Hz, 2 H, NCH_2CH_2), 3.09 (s, 6 H, NCH_3), 4.62–4.70 (m, 4 H, NCH_2), 7.79 (dd, J =8.8/2.5 Hz, 1 H, $\text{CHCN}(\text{CH}_3)_2$), 7.85 (dd, J =9.0/5.6 Hz, 1 H, NCHCHCH), 8.22–8.19 (m, 2 H, $\text{NCHCHCC}(\text{CH}_3)_3$), 8.22–8.24 (m, 1 H, NCHCHCH), 8.33–8.38 (m, 1 H, $\text{NCHCN}(\text{CH}_3)_2$), 8.96–9.01 ppm (m, 2 H, $\text{NCHCHCC}(\text{CH}_3)_3$); ^{13}C NMR (125 MHz, $[\text{D}_6]\text{DMSO}$): δ =30.00 ($\text{C}(\text{CH}_3)_3$), 32.00 (NCH_2CH_2), 36.79 ($\text{C}(\text{CH}_3)_3$), 40.10 ($\text{N}(\text{CH}_3)_2$),

57.28 (CH₂NCHCHCC(CH₃)₃), 58.31 (CH₂NCHCHCH), 125.56 (NCHCHCC(CH₃)₃), 126.08 (CHCN(CH₃)₂), 127.95 (NCHCN(CH₃)₂, NCHCHCH), 130.85 (NCHCHCH), 144.73 (NCHCHCC(CH₃)₃), 148.69 (NCHCN(CH₃)₂), 170.61 ppm (CC(CH₃)₃); IR (KBr): $\tilde{\nu}$ =3037, 3008, 2963, 1638, 1617, 1581, 1524, 1466, 1385, 1351, 1274, 1239, 1194, 1157, 1115, 1029, 855, 817, 805, 776, 677, 573 cm⁻¹; HRMS-FAB m/z [$M-I$]⁺ calcd for C₁₉H₂₉IN₃: 426.1401, found: 426.1391.

3-(*tert*-Butyl)-1-{3-[4-(*tert*-butyl)pyridin-1-ium-1-yl]propyl}pyridin-1-ium diiodide (1 c)

According to GP2, with **10 a** (604 mg, 1.40 mmol, 1.0 eq.) and **13** (227 mg, 1.68 mmol, 1.2 eq.) in MeCN (2.2 mL) at 90 °C. Reaction time: 1 h. Purification by RP-MPLC (C18, MeOH/H₂O = 30:70) afforded **1 c** (743 mg, 94%) as a yellow solid.

RP-MPLC: t_R =975 s (C18, MeOH/H₂O 30:70); mp: 221°C; ¹H NMR (500 MHz, CD₃CN): δ =1.39 (s, 9 H, NCHCHC(C(CH₃)₃)), 1.44 (s, 9 H, NCHC(C(CH₃)₃)), 2.78 (quin, J =8.2 Hz, 2 H, NCH₂CH₂), 4.82–4.88 (m, 2 H, CH₂NCHCHC(C(CH₃)₃)), 4.88–4.94 (m, 2 H, CH₂NCHC(C(CH₃)₃)), 7.95–8.01 (m, 1 H, NCHCHCH), 8.06 (d, J =6.1 Hz, 2 H, NCHCHC(C(CH₃)₃)), 8.54 (d, J =8.0 Hz, 1 H, NCHCHCH), 8.89 (d, J =5.6 Hz, 1 H, NCHCHCH), 9.02 (d, J =6.2 Hz, 2 H, NCHCHC(C(CH₃)₃)), 9.24 ppm (s, 1 H, NCHC(C(CH₃)₃)); ¹³C NMR (125 MHz, CD₃CN): δ =30.10 (NCHCHC(C(CH₃)₃)), 30.78 (NCHC(C(CH₃)₃)), 34.08 (NCH₂CH₂), 35.94 (NCHC(C(CH₃)₃)), 37.45 (NCHCHC(C(CH₃)₃)), 57.50 (CH₂NCHCHC(C(CH₃)₃)), 58.47 (CH₂NCHC(C(CH₃)₃)), 126.64 (NCHCHC(C(CH₃)₃)), 128.84 (NCHCHCH), 142.97 (NCHCHCH), 143.75 (NCHC(C(CH₃)₃)), 144.43 (NCHCHCH), 145.03 (NCHCHC(C(CH₃)₃)), 153.39 (NCHC(C(CH₃)₃)), 172.69 ppm (NCHCHC(C(CH₃)₃)); IR (KBr): $\tilde{\nu}$ =3417, 2994, 2962, 2867, 1643, 1565, 1510, 1469, 1445, 1398, 1372, 1345, 1278, 1231, 1205, 1184, 1150, 1116, 1077, 1053, 1029, 993, 935, 915, 868, 853, 840, 810, 766, 738, 714, 687, 578, 567 cm⁻¹; HRMS-FAB m/z [$M-I$]⁺ calcd for C₂₁H₃₂IN₂: 439.1605, found: 439.1625.

1-{3-[4-(*tert*-Butyl)pyridin-1-ium-1-yl]propyl}-3-(ethoxycarbonyl)pyridin-1-ium diiodide (1 d)

According to GP2, with **10 a** (476 mg, 1.10 mmol, 1.0 eq.) and **14** (202 mg, 1.32 mmol, 183 μ L, 1.2 eq.) in MeCN (2.2 mL) at 90 °C. Reaction time: 3 h. Purification by RP-MPLC (C18, MeOH/H₂O = 15:85) afforded **1 d** (528 mg, 82%) as a yellow solid.

RP-MPLC: t_R =1500 s (C18, MeOH/H₂O 15:85); mp: 174°C; ¹H NMR (500 MHz, CD₃CN): δ =1.39 (s, 9 H, C(CH₃)₃), 1.43 (t, J =7.0 Hz, 3 H, OCH₂CH₃), 2.74–2.83 (m, 2 H, NCH₂CH₂), 4.48 (q, J =6.9 Hz, 2 H, OCH₂CH₃), 4.84 (t, J =7.6 Hz, 2 H, CH₂NCHCHC(C(CH₃)₃)), 4.99 (t, J =7.7 Hz, 2 H, CH₂NCHCHCH), 8.06 (d, J =5.7 Hz, 2 H, NCHCHC(C(CH₃)₃)), 8.21 (t, J =6.9 Hz, 1 H, NCHCHCH), 8.93–9.01 (m, 3 H, NCHCHC(C(CH₃)₃), NCHCHCH), 9.33 (d, J =5.7 Hz, 1 H, NCHCHCH), 9.60 ppm (s, 1 H, NCHCCO); ¹³C NMR (125 MHz, CD₃CN): δ =14.55 (OCH₂CH₃), 30.10 (C(CH₃)₃), 33.57 (NCH₂CH₂), 37.46 (C(CH₃)₃), 57.42 (CH₂NCHCHC(C(CH₃)₃)), 59.00 (CH₂NCHCHCH), 64.23 (OCH₂CH₃), 126.68 (NCHCHC(C(CH₃)₃)), 129.96 (NCHCHCH), 132.52 (NCHCCO), 145.04 (NCHCHC(C(CH₃)₃)), 146.98 (NCHCHCH, NCHCCO), 147.05 (NCHCHCH), 148.78 (CCO), 172.77 ppm (CC(CH₃)₃); IR (KBr): $\tilde{\nu}$ =3044, 2967, 1736, 1639, 1587, 1563, 1514, 1487, 1473, 1424, 1389, 1367, 1321, 1293, 1229, 1193, 1182, 1162, 1115, 1010, 858, 834, 745, 677, 577 cm⁻¹; HRMS-FAB m/z [$M-I$]⁺ calcd for C₂₀H₂₈IN₂O₂: 455.1190, found: 455.1199.

1-{3-[4-(*tert*-Butyl)pyridin-1-ium-1-yl]propyl}-3-(trifluoromethyl)pyridin-1-ium diiodide (**1 e**)

According to GP2, with **10 a** (474 mg, 1.10 mmol, 1.0 eq.) and **15** (194 mg, 1.32 mmol, 152 μ L, 1.2 eq.) in MeCN (2.2 mL) at 90 °C. Reaction time: 16 h. Recrystallization from EtOH (5 mL) afforded **1 e** (390 mg, 61%) as a yellow solid.

mp: 194°C; ¹H NMR (400 MHz, CD₃CN): δ =1.39 (s, 9 H, C(CH₃)₃), 2.79–2.88 (m, 2 H, NCH₂CH₂), 4.84–4.89 (m, 2 H, CH₂NCHCHC(C(CH₃)₃)), 5.02–5.07 (m, 2 H, CH₂NCHCCF₃), 8.04–8.09 (m, 2 H, NCHCHC(C(CH₃)₃)), 8.29–8.35 (m, 1 H, NCHCHCH), 8.84 (d, J =8.3 Hz, 1 H, NCHCHCH), 8.98–9.03 (m, 2 H, NCHCHC(C(CH₃)₃)), 9.46 (d, J =6.2 Hz, 1 H, NCHCHCH), 9.75 ppm (s, 1 H, NCHCCF₃); ¹³C NMR (125 MHz, CD₃CN): δ =30.10 (C(CH₃)₃), 33.59 (NCH₂CH₂), 37.46 (C(CH₃)₃), 57.34 (CH₂NCHCHC(C(CH₃)₃)), 59.19 (CH₂NCHCCF₃), 122.55 (q, J =273.0 Hz, CF₃), 126.71 (NCHCHC(C(CH₃)₃)), 130.71 (NCHCHCH), 131.53 (q, J =36.4 Hz, CCF₃), 144.16–144.54 (m, NCHCCF₃, NCHCHCH), 145.04 (NCHCHC(C(CH₃)₃)), 149.61 (NCHCHCH), 172.74 ppm (CC(CH₃)₃); IR (KBr): $\tilde{\nu}$ =3010, 2967, 1640, 1593, 1562, 1513, 1468, 1373, 1333, 1275, 1228, 1142, 1114, 1096, 896, 851, 776, 735, 682, 575, cm⁻¹; HRMS-FAB m/z [$M-I$]⁺ calcd for C₁₈H₂₃F₃IN₂: 451.0853, found: 451.0850.

4-(*tert*-Butyl)-1-{3-[4-(ethoxycarbonyl)pyridin-1-ium-1-yl]propyl}pyridin-1-ium diiodide (1 f)

According to GP2, with **10 a** (474 mg, 1.10 mmol, 1.0 eq.) and **16** (204 mg, 1.32 mmol, 202 μ L, 1.2 eq.) in MeCN (2.2 mL) at 90 °C. Reaction time: 3 h. Purification by RP-MPLC (C18, MeOH/H₂O = 10:90) afforded **1 f** (465 mg, 73%) as an orange solid.

RP-MPLC: t_R =2100 s (C18, MeOH/H₂O 10:90); mp: 162°C; ¹H NMR (400 MHz, CD₃CN): δ =1.38–1.43 (m, 12 H, C(CH₃)₃, OCH₂CH₃), 2.76–2.86 (m, 2 H, NCH₂CH₂), 4.47 (q, J =7.1 Hz, 2 H, OCH₂CH₃), 4.84–4.90 (m, 2 H, CH₂NCHCHC(C(CH₃)₃)), 4.98–5.04 (m, 2 H, CH₂NCHCHCCO), 8.04–8.08 (m, 2 H, NCHCHC(C(CH₃)₃)), 8.48 (d, J =6.7 Hz, 2 H, NCHCHCCO), 9.01–9.05 (m, 2 H, NCHCHC(C(CH₃)₃)), 9.36 ppm (d, J =6.9 Hz, 2 H, NCHCHCCO); ¹³C NMR (100 MHz, CD₃CN): δ =14.32 (OCH₂CH₃), 30.10 (C(CH₃)₃), 33.64 (NCH₂CH₂), 37.46 (C(CH₃)₃), 57.37 (CH₂NCHCHC(C(CH₃)₃)), 58.94 (CH₂NCHCHCCO), 64.52 (OCH₂CH₃), 126.67 (NCHCHC(C(CH₃)₃)), 128.85 (NCHCHCCO), 145.05 (NCHCHC(C(CH₃)₃)), 146.57 (NCHCHCCO), 147.34 (NCHCHCCO), 162.93 (NCHCHCCO), 172.72 ppm (CC(CH₃)₃); IR (KBr): $\tilde{\nu}$ =3121, 3007, 2967, 2949, 2870, 1731, 1645, 1572, 1518, 1464, 1394, 1371, 1328, 1296, 1214, 1198, 1182, 1129, 1114, 1048, 1018, 875, 857, 847, 807, 765, 686, 660, 574, 538, 506 cm⁻¹; HRMS-FAB m/z [$M-I$]⁺ calcd for C₂₀H₂₈IN₂O₂: 455.1190, found: 455.1186.

1-{3-[4-(*tert*-Butyl)pyridin-1-ium-1-yl]propyl}-3-(dimethylcarbamoyl)pyridin-1-ium diiodide (1 g)

According to GP2, with **10 a** (474 mg, 1.10 mmol, 1.0 eq.) and **17** (198 mg, 1.32 mmol, 1.2 eq.) in MeCN (2.2 mL) at 90 °C. Reaction time: 3 h. Purification by RP-MPLC (C18, MeOH/H₂O = 15:85) afforded **1 g** (554 mg, 87%) as a yellow solid.

RP-MPLC: t_R =950 s (C18, MeOH/H₂O 15:85); mp: 70°C; ¹H NMR (500 MHz, CD₃CN): δ =1.38 (s, 9 H, C(CH₃)₃), 2.66 (quin. J =7.2 Hz, 2 H, NCH₂CH₂), 2.99 (s, 3 H, NCH₃), 3.05 (s, 3 H, NCH₃), 4.69 (t, J =7.3 Hz, 2 H, CH₂NCHCCO), 4.74 (t, J =7.3 Hz, 2 H, CH₂NCHCHC(C(CH₃)₃)), 8.23 (d, J =6.9 Hz, 2 H, NCHCHC(C(CH₃)₃)), 8.27 (dd, J =7.8/6.3 Hz, 1 H, NCHCHCH), 8.72 (d, J =8.0 Hz, 1 H, NCHCHCH), 8.99 (d, J =6.9 Hz, 2 H, NCHCHC(C(CH₃)₃)), 9.16 (d, J =6.1 Hz, 1 H, NCHCHCH), 9.30 ppm (s, 1 H, NCHCCO); ¹³C NMR (125 MHz, CD₃CN): δ =30.01 (C(CH₃)₃), 31.92 (NCH₂CH₂), 35.60 (NCH₃), 36.80 (C(CH₃)₃), 39.50 (NCH₃), 57.06 (CH₂NCHCCO), 58.36 (CH₂NCHCHC(C(CH₃)₃)), 125.61 (NCHCHC(C(CH₃)₃)), 128.63 (NCHCHCH), 136.50

(CCO), 144.22 (NCHCHCH)*, 144.23 (NCHCCO)*, 144.76 (NCHCHC(C(CH₃)₃)), 145.95 (NCHCHCH), 164.40 (CO), 170.63 ppm (C(C(CH₃)₃)); IR (KBr): $\tilde{\nu}$ =3010, 2963, 1642, 1561, 1512, 1492, 1465, 1399, 1372, 1267, 1229, 1192, 1158, 1113, 1058, 846, 738, 681, 652, 570 cm⁻¹; HRMS-FAB m/z [$M-I$]⁺ calcd for C₂₀H₂₉IN₃O: 454.1350, found: 454.1341.

4-(*tert*-Butyl)-1-{3-[4-(dimethylamino)pyridin-1-ium-1-yl]propyl}pyridin-1-ium diiodide (1 h)

According to GP2, with **10 a** (431 mg, 1.00 mmol, 1.0 eq.) and **18** (134 mg, 1.10 mmol, 1.2 eq.) in MeCN (2 mL) at 90 °C. Reaction time: 1 h. Purification by RP-MPLC (C18, MeOH/H₂O = 15:85) afforded **1 h** (525 mg, 95%) as a yellow solid.

RP-MPLC: t_R =1200 s (C18, MeOH/H₂O 15:85); mp: 261°C; ¹H NMR (400 MHz, CD₃CN): δ =1.39 (s, 9 H, C(CH₃)₃), 2.54–2.64 (m, 2 H, NCH₂CH₂), 3.18 (s, 6 H, N(CH₃)₂), 4.36–4.42 (m, 2 H, CH₂NCHCHC(N(CH₃)₂)), 4.71–4.78 (m, 2 H, CH₂NCHCHC(C(CH₃)₃)), 6.85–6.92 (m, 2 H, NCHCHC(N(CH₃)₂)), 8.01–8.07 (m, 2 H, NCHCHC(C(CH₃)₃)), 8.23–8.29 (m, 2 H, NCHCHC(N(CH₃)₂)), 8.92–8.98 ppm (m, 1 H, NCHCHC(C(CH₃)₃)); ¹³C NMR (100 MHz, CD₃CN): δ =30.11 (C(CH₃)₃), 33.26 (NCH₂CH₂), 37.43 (C(CH₃)₃), 40.82 (N(CH₃)₂), 54.66 (CH₂NCHCHC(N(CH₃)₂)), 57.83 (CH₂NCHCHC(C(CH₃)₃)), 108.94 (NCHCHC(N(CH₃)₂)), 126.60 (NCHCHC(C(CH₃)₃)), 142.89 (NCHCHC(N(CH₃)₂)), 145.00 (NCHCHC(C(CH₃)₃)), 157.54 (NCHCHC(N(CH₃)₂)), 172.55 ppm (NCHCHC(C(CH₃)₃)); IR (KBr): $\tilde{\nu}$ =3013, 2962, 1652, 1575, 1536, 1518, 1469, 1454, 1427, 1404, 1373, 1352, 1279, 1232, 1211, 1200, 1187, 1119, 1067, 1036, 946, 858, 834, 808, 743, 578, 529, 507 cm⁻¹; HRMS-ESI m/z [$M-I$]⁺ calcd for C₁₉H₂₉IN₃: 426.1401, found: 426.1405.

1-{3-[4-(*tert*-Butyl)pyridin-1-ium-1-yl]propyl}-3,5-dimethylpyridin-1-ium diiodide (1 i)

According to GP2, with **10 a** (431 mg, 1.00 mmol, 1.0 eq.) and **19** (130 mg, 1.20 mmol, 140 μ L, 1.2 eq.) in MeCN (2 mL) at 90 °C. Reaction time: 1 h. Purification by RP-MPLC (C18, MeOH/H₂O = 10:90 → 15:85) afforded **1 i** (467 mg, 87%) as a yellow solid.

RP-MPLC: t_R =470 s (MeOH/H₂O 15:85); mp: 177°C; ¹H NMR (500 MHz, [D₆]DMSO): δ =1.38 (s, 9 H, C(CH₃)₃), 2.47 (s, 6 H, CH₃CH₃), 2.66 (quin., J =7.2 Hz, 2 H, NCH₂CH₂), 4.63 (t, J =7.2 Hz, 2 H, CH₂NCHCCH₃), 4.68 (t, J =7.3 Hz, 2 H,

$\text{CH}_2\text{NCHCHCC}(\text{CH}_3)_3$, 8.20–8.25 (m, 2 H, $\text{NCHCHCC}(\text{CH}_3)_3$), 8.35 (br. s, 1 H, $\text{CH}_3\text{CCHCCH}_3$), 8.84 (br. s, 2 H, NCHCCH_3), 8.97–9.01 ppm (m, 2 H, $\text{NCHCHCC}(\text{CH}_3)_3$); ^{13}C NMR (125 MHz, $[\text{D}_6]\text{DMSO}$): δ =17.63 (CHCCH_3), 29.38 ($\text{C}(\text{CH}_3)_3$), 31.08 (NCH_2CH_2), 36.17 ($\text{C}(\text{CH}_3)_3$), 56.50 ($\text{CH}_2\text{NCHCHCC}(\text{CH}_3)_3$), 57.19 ($\text{CH}_2\text{NCHCCH}_3$), 124.95 ($\text{NCHCHCC}(\text{CH}_3)_3$), 137.80 (CHCCH_3), 141.56 (NCHCCH_3), 144.11 ($\text{NCHCHCC}(\text{CH}_3)_3$), 146.36 ($\text{CH}_3\text{CCHCCH}_3$), 170.01 ppm ($\text{CC}(\text{CH}_3)_3$); IR (KBr): $\tilde{\nu}$ =3128, 3032, 3010, 2966, 2932, 2868, 1639, 1606, 1565, 1510, 1498, 1469, 1444, 1402, 1375, 1361, 1348, 1302, 1276, 1263, 1229, 1211, 1190, 1114, 1052, 1027, 910, 900, 849, 840, 821, 767, 675, 564, 552 cm^{-1} ; HRMS-FAB m/z $[\text{M-I}]^+$ calcd for $\text{C}_{19}\text{H}_{28}\text{IN}_2$: 411.1292, found: 411.1322.

1-{3-[4-(*tert*-Butyl)pyridin-1-ium-1-yl]propyl}-3-methylpyridin-1-ium diiodide (1 j)

According to GP2, with **10 a** (431 mg, 1.00 mmol, 1.0 eq.) and **20** (112 mg, 1.20 mmol, 117 μL , 1.2 eq.) in MeCN (2 mL) at 90 °C. Reaction time: 1 h. Purification by RP-MPLC (C18, MeOH/ H_2O = 10:90) afforded **1 j** (450 mg, 86%) as a yellow solid.

RP-MPLC: t_{R} =900 s (MeOH/ H_2O 10:90); mp: 159°C; ^1H NMR (500 MHz, $[\text{D}_6]\text{DMSO}$): δ =1.38 (s, 9 H, $\text{C}(\text{CH}_3)_3$), 2.52 (s, 3 H, CH_3), 2.66 (quin., J =7.1 Hz, 2 H, NCH_2CH_2), 4.68 (t, J =7.1 Hz, 4 H, NCH_2), 8.10 (dd, J =7.9/6.2 Hz, 1 H, NCHCHCH), 8.23 (d, J =7.0 Hz, 2 H, $\text{CHCC}(\text{CH}_3)_3$), 8.49 (d, J =7.8 Hz, 1 H, NCHCHCH), 8.92 (d, J =6.0 Hz, 1 H, NCHCHCH), 8.99 (d, J =7.0 Hz, 2 H, $\text{NCHCHCC}(\text{CH}_3)_3$), 9.02 ppm (s, 1 H, NCHCCH_3); ^{13}C NMR (125 MHz, $[\text{D}_6]\text{DMSO}$): δ =17.79 (CHCCH_3), 29.38 ($\text{C}(\text{CH}_3)_3$), 31.21 (NCH_2CH_2), 36.17 ($\text{C}(\text{CH}_3)_3$), 56.46 (NCH_2), 57.31 (NCH_2), 124.97 ($\text{CHCC}(\text{CH}_3)_3$), 127.33 (NCHCHCH), 138.61 (CHCCH_3), 142.01 (NCHCHCH), 144.11 ($\text{NCHCHCC}(\text{CH}_3)_3$), 144.24 (NCHCCH_3), 145.96 (NCHCHCH), 170.00 ppm ($\text{CC}(\text{CH}_3)_3$); IR (KBr): $\tilde{\nu}$ =3511, 3430, 3080, 3042, 3005, 2966, 2867, 1638, 1590, 1562, 1508, 1471, 1456, 1420, 1373, 1353, 1275, 1250, 1231, 1205, 1193, 1163, 1114, 1083, 1047, 1032, 994, 929, 913, 864, 853, 808, 776, 679, 580, 5442 cm^{-1} ; HRMS-FAB m/z $[\text{M-I}]^+$ calcd for $\text{C}_{18}\text{H}_{26}\text{IN}_2$: 397.1135, found: 397.1164.

1-{3-[4-(*tert*-Butyl)pyridin-1-ium-1-yl]propyl}-3-methoxypyridin-1-ium diiodide (1 k)

According to GP2, with **10 a** (438 mg, 1.02 mmol, 1.0 eq.) and **7** (137 mg, 1.22 mmol, 127 μL , 1.2 eq.) in MeCN (2 mL) at 90 °C. Reaction time: 1 h. Purification by RP-MPLC (C18, MeOH/ H_2O = 10:90) afforded **1 k** (430 mg, 78%) as a yellow solid.

RP-MPLC: t_R =1300 s (MeOH/H₂O 10:90); mp: 117°C; ¹H NMR (500 MHz, [D₆]DMSO): δ =1.38 (s, 9 H, C(CH₃)₃), 2.66 (quin., J =7.0 Hz, 2 H, NCH₂CH₂), 4.03 (s, 3 H, OCH₃), 4.66 (t, J =7.4 Hz, 2 H, CH₂NCHCHC(C(CH₃)₃)), 4.71 (t, J =7.1 Hz, 2 H, CH₂NCHCOCH₃), 8.13 (dd, J =8.8/5.9 Hz, 1 H, NCHCHCH), 8.22 (d, J =6.9 Hz, 2 H, NCHCHC(C(CH₃)₃)), 8.28 (dd, J =8.7/2.3 Hz, 1 H, NCHCHCH), 8.93–8.96 (m, 1 H, NCHCOCH₃), 8.98 ppm (d, J =6.9 Hz, 2 H, NCHCHC(C(CH₃)₃)); ¹³C NMR (125 MHz, [D₆]DMSO): δ =30.01 (C(CH₃)₃), 31.91 (NCH₂CH₂), 36.80 (C(CH₃)₃), 57.07 (CH₂NCHCHC(C(CH₃)₃)), 57.98 (OCH₃), 58.36 (CH₂NCHCOCH₃), 125.59 (NCHCHC(C(CH₃)₃)), 129.04 (NCHCHCH), 131.07 (NCHCHCH), 133.33 (NCHCOCH₃), 137.76 (NCHCHCH), 144.75 (NCHCHC(C(CH₃)₃)), 158.51 (NCHCOCH₃), 170.64 ppm (C(C(CH₃)₃)); IR (KBr): $\tilde{\nu}$ =3013, 2966, 1639, 1585, 1567, 1512, 1468, 1373, 1339, 1296, 1233, 1192, 1164, 1116, 1045, 1008, 933, 906, 848, 817, 778, 743, 570 cm⁻¹; HRMS-FAB m/z [M -Cl]⁺ calcd for C₁₈H₂₆IN₂O: 413.1084, found: 413.1082.

4-(*tert*-Butyl)-1-{3-[4-(*tert*-butyl)pyridin-1-ium-1-yl]propyl}-3-methoxypyridin-1-ium diiodide (**1 I**)

According to GP2, with **10 a** (431 mg, 1.00 mmol, 1.0 eq.) and **21** (198 mg, 1.20 mmol, 1.2 eq.) in MeCN (2 mL) at 90 °C. Reaction time: 1 h. Purification by RP-MPLC (C18, MeOH/H₂O = 30:70) afforded **1 I** (508 mg, 85%) as a yellow solid.

RP-MPLC: t_R =1300 s (MeOH/H₂O 30:70); mp: 209°C; ¹H NMR (500 MHz, [D₆]DMSO): δ =1.38 (s, 9 H, CHC(C(CH₃)₃)CH), 1.40 (s, 9 H, CH₃OCC(C(CH₃)₃)), 2.68 (quin., J =7.3 Hz, 2 H, NCH₂CH₂), 4.09 (s, 3 H, OCH₃), 4.70 (dt, J =10.5/7.4 Hz, 4 H, NCH₂), 7.96 (d, J =6.3 Hz, 1 H, CH₃OCC(C(CH₃)₃)CH), 8.24 (d, J =7.0 Hz, 2 H, CHC(C(CH₃)₃)CH), 8.66–8.70 (m, 1 H, NCHCHC(C(CH₃)₃)COCH₃), 8.80–8.83 (m, 1 H, NCHCOCH₃), 9.01 ppm (d, J =7.0 Hz, 2 H, NCHCHC(C(CH₃)₃)CH); ¹³C NMR (125 MHz, [D₆]DMSO): δ =28.38 (CHC(C(CH₃)₃)CH), 30.02 (CH₃OCC(C(CH₃)₃)), 31.96 (NCH₂CH₂), 36.58 (CH₃OCC(C(CH₃)₃)), 36.81 (CHC(C(CH₃)₃)CH), 57.13 (CH₂NCHCOCH₃), 57.59 (CH₂NCHCHC(C(CH₃)₃)CH), 58.27 (OCH₃), 125.52 (NCHCHC(C(CH₃)₃)COCH₃), 125.61 (NCHCHC(C(CH₃)₃)CH), 129.43 (NCHCOCH₃), 138.15 (CH₃OCC(C(CH₃)₃)CHCH), 144.74 (NCHCHC(C(CH₃)₃)CH), 156.10 (CH₃OCC(C(CH₃)₃)), 157.09 (CH₃OC), 170.64 ppm (NCHCHC(C(CH₃)₃)CH); IR (KBr): $\tilde{\nu}$ =3119, 3015, 2965, 2869, 1642, 1563, 1507, 1477, 1459, 1441, 1396, 1367, 1360, 1343, 1312, 1278, 1230, 1194, 1116, 1098, 1065, 1049, 1027, 973, 957, 889,

871, 854, 819, 740, 700, 677, 630, 573, 559, 530 cm^{-1} ; HRMS-FAB m/z $[M-I]^+$ calcd for $\text{C}_{22}\text{H}_{34}\text{I}\text{N}_2\text{O}$: 469.1710, found: 469.1692.

2-{3-[4-(*tert*-Butyl)pyridin-1-ium-1-yl]propyl}isoquinolin-2-ium diiodide (2 a)

According to GP2, with **10 a** (474 mg, 1.10 mmol, 1.0 eq.) and **22** (170 mg, 1.32 mmol, 1.2 eq.) in MeCN (2.2 mL) at 90 °C. Reaction time: 1 h. Purification by RP-MPLC (C18, MeOH/ H_2O = 50:50) afforded **2 a** (591 mg, 96%) as a yellow solid.

RP-MPLC: t_R =460 s (C18, MeOH/ H_2O 50:50); mp: 173°C; ^1H NMR (400 MHz, CD_3CN): δ =1.37 (s, 9 H, $\text{C}(\text{CH}_3)_3$), 2.84–2.95 (m, 2 H, NCH_2CH_2), 4.86–4.93 (m, 2 H, $\text{CH}_2\text{NCHCHC}(\text{C}(\text{CH}_3)_3)$), 4.99–5.07 (m, 2 H, CH_2NCHCC), 8.02–8.09 (m, 3 H, $\text{NCHCHC}(\text{C}(\text{CH}_3)_3)$, NCHCCHCH), 8.18–8.27 (m, 2 H, NCHCCHCHCH), 8.28 (d, J =8.0 Hz, 1 H, NCHCCCH), 8.45 (d, J =6.8 Hz, 1 H, NCHCHCC), 8.52 (d, J =8.9 Hz, 1 H, NCHCCH), 8.78 (dd, J =6.8/1.4 Hz, 1 H, NCHCHCC), 9.03 (d, J =7.1 Hz, 2 H, $\text{NCHCHC}(\text{C}(\text{CH}_3)_3)$), 10.30 ppm (s, 1 H, NCHCC); ^{13}C NMR (100 MHz, CD_3CN): δ =30.10 ($\text{C}(\text{CH}_3)_3$), 33.40 (NCH_2CH_2), 37.44 ($\text{C}(\text{CH}_3)_3$), 57.69 ($\text{CH}_2\text{NCHCHC}(\text{C}(\text{CH}_3)_3)$), 58.38 (CH_2NCHCC), 126.66 ($\text{NCHCHC}(\text{C}(\text{CH}_3)_3)$), 127.58 (NCHCHCC), 128.40 (NCHCCCH), 128.88 (NCHCCH), 131.40 (NCHCCH), 132.60 (NCHCCHCH), 135.68 (NCHCHCC), 138.43 (NCHCCHCHCH), 138.90 (NCHCHCC), 145.06 ($\text{NCHCHC}(\text{C}(\text{CH}_3)_3)$), 150.95 (NCHCCH), 172.65 ppm ($\text{C}(\text{C}(\text{CH}_3)_3)$); IR (KBr): $\tilde{\nu}$ =3007, 2965, 2866, 1720, 1642, 1608, 1581, 1568, 1514, 1460, 1399, 1364, 1286, 1277, 1223, 1200, 1182, 1160, 1117, 1066, 1021, 996, 980, 926, 906, 877, 847, 838, 767, 755, 641, 628, 572, 527, 475 cm^{-1} ; HRMS-FAB m/z $[M-I]^+$ calcd for $\text{C}_{21}\text{H}_{26}\text{I}\text{N}_2$: 433.1135, found: 433.1129.

4-(*tert*-Butyl)-1-[3-(1-methyl-1*H*-imidazol-3-ium-3-yl)propyl]pyridin-1-ium diiodide (2 b)

According to GP2, with **10 a** (647 mg, 1.50 mmol, 1.0 eq.) and **23** (246 mg, 3.00 mmol, 1.2 eq.) in MeCN (3 mL) at 90 °C. Reaction time: 1 h. Recrystallization from EtOAc/Aceton/MeCN (2/7/1.3 mL) afforded **2 b** (614 mg, 80%) as a slightly yellowish solid.

mp: 148°C; ^1H NMR (500 MHz, CD_3CN): δ =1.39 (s, 9 H, $\text{C}(\text{CH}_3)_3$), 2.57–2.65 (m, 2 H, NCH_2CH_2), 3.88 (s, 3 H, NCH_3), 4.42 (t, J =7.2 Hz, 2 H, NCHNCH_2), 4.71–4.77 (m, 2 H, $\text{CH}_2\text{NCHCHCC}(\text{CH}_3)_3$), 7.38 (t, J =1.8 Hz, 1 H, CH_3NCHCH), 7.61 (t, J =1.8 Hz, 1 H,

CH₃NCHCH), 8.03–8.07 (m, 2 H, NCHCHCC(CH₃)₃), 8.94–8.98 (m, 2 H, NCHCHCC(CH₃)₃), 9.00 ppm (br. s, 1 H, NCHN); ¹³C NMR (125 MHz, CD₃CN): δ=30.11 (C(CH₃)₃), 32.36 (NCH₂CH₂), 37.28 (NCH₃), 37.43 (C(CH₃)₃), 47.09 (NCHNCH₂), 57.88 (CH₂NCHCHCC(CH₃)₃), 123.53 (CH₃NCHCH), 124.84 (CH₃NCHCH), 126.61 (NCHCHCC(CH₃)₃), 137.63 (NCHN), 145.08 (NCHCHCC(CH₃)₃), 172.57 ppm (CC(CH₃)₃); IR (KBr): $\tilde{\nu}$ =3138, 3056, 2966, 2870, 1639, 1575, 1562, 1512, 1466, 1369, 1352, 1327, 1275, 1197, 1169, 1113, 843, 830, 777, 766, 637, 620, 572 cm⁻¹; HRMS-FAB *m/z* [*M*-I]⁺ calcd for C₁₆H₂₅IN₃: 386.1088, found: 386.1107.

4-(*tert*-Butyl)-1-{3-[1-(*tert*-butyl)-1*H*-imidazol-3-ium-3-yl]propyl}pyridin-1-ium diiodide (**2 c**)

According to GP2, with **10 a** (474 mg, 1.10 mmol, 1.0 eq.) and **24** (164 mg, 1.32 mmol, 1.2 eq.) in MeCN (2.2 mL) at 90 °C. Reaction time: 1 h. Purification by RP-MPLC (C18, MeOH/H₂O = 15:85) afforded **2 c** (603 mg, 99%) as a yellow solid.

RP-MPLC: *t_R*=1300 s (C18, MeOH/H₂O 15:85); mp: 151 °C; ¹H NMR (400 MHz, CD₃CN): δ=1.39 (s, 9 H, NCHCHC(C(CH₃)₃)), 1.65 (s, 9 H, NC(CH₃)₃), 2.63–2.72 (m, 2 H, NCH₂CH₂), 4.41–4.47 (m, 2 H, CH₂NCHN), 4.72–4.78 (m, 2 H, CH₂NCHCHC(C(CH₃)₃)), 7.57 (t, *J*=2.0 Hz, 1 H, CH₂NCHCHN), 7.65 (t, *J*=1.9 Hz, 1 H, CH₂NCHCHN), 8.03–8.07 (m, 2 H, NCHCHC(C(CH₃)₃)), 8.94–8.98 (m, 2 H, NCHCHC(C(CH₃)₃)), 9.28 ppm (t, *J*=1.7 Hz, 1 H, NCHN); ¹³C NMR (100 MHz, CD₃CN): δ=29.89 (NC(CH₃)₃), 30.12 (NCHCHC(C(CH₃)₃)), 32.32 (NCH₂CH₂), 37.43 (NCHCHC(C(CH₃)₃)), 47.13 (CH₂NCHN), 58.08 (CH₂NCHCHC(C(CH₃)₃)), 61.36 (NC(CH₃)₃), 121.07 (CH₂NCHCHN), 123.78 (CH₂NCHCHN), 126.63 (NCHCHC(C(CH₃)₃)), 135.76 (NCHN), 145.06 (NCHCHC(C(CH₃)₃)), 172.55 ppm (C(C(CH₃)₃)); IR (KBr): $\tilde{\nu}$ =3427, 3374, 3118, 3071, 2961, 2868, 2004, 1733, 1638, 1552, 1513, 1483, 1467, 1451, 1425, 1407, 1373, 1359, 1348, 1310, 1280, 1241, 1207, 1134, 1120, 1113, 1084, 1056, 1035, 982, 937, 850, 817, 780, 742, 690, 657, 629, 570, 537 cm⁻¹; HRMS-ESI *m/z* [*M*-I]⁺ calcd for C₁₉H₃₁IN₃: 428.1557, found: 428.1562.

3-{3-[4-(*tert*-Butyl)pyridin-1-ium-1-yl]propyl}thiazol-3-ium diiodide (**2 d**)

According to GP2, with **10 a** (474 mg, 1.10 mmol, 1.0 eq.) and **25** (198 mg, 1.20 mmol, 1.2 eq.) in MeCN (2.2 mL) at 120 °C. Reaction time: 16 h. Purification by RP-MPLC (C18, MeOH/H₂O = 10:90) afforded **2 d** (504 mg, 89%) as a yellow solid.

RP-MPLC: t_R = 850 s (MeOH/H₂O 10:90); mp: 180°C; ¹H NMR (500 MHz, [D₆]DMSO): δ =1.38 (s, 9 H, C(CH₃)₃), 2.62 (quin., J =7.2 Hz, 2 H, NCH₂CH₂), 4.66 (dt, J =10.1/7.3 Hz, 4 H, NCH₂), 8.22 (d, J =7.0 Hz, 2 H, NCHCHC(C(CH₃)₃)), 8.39 (dd, J =3.7/2.4 Hz, 1 H, NCHCHS), 8.59 (dd, J =3.7/1.3 Hz, 1 H, NCHCHS), 8.98 (d, J =7.0 Hz, 2 H, NCHCHC(C(CH₃)₃)), 10.19–10.22 ppm (m, 1 H, NCHS); ¹³C NMR (125 MHz, [D₆]DMSO): δ =30.02 (C(CH₃)₃), 31.08 (NCH₂CH₂), 36.80 (C(CH₃)₃), 51.94 (CH₂NCHS), 57.14 (CH₂NCHCHC(C(CH₃)₃)), 125.60 (NCHCHC(C(CH₃)₃)), 127.56 (NCHCHS), 137.47 (NCHCHS), 144.74 (NCHCHC(C(CH₃)₃)), 160.35 (NCHS), 170.60 ppm (C(C(CH₃)₃)); IR (KBr): $\tilde{\nu}$ =3099, 3047, 3010, 2966, 2952, 2904, 2872, 1644, 1566, 1545, 1516, 1475, 1455, 1421, 1399, 1371, 1341, 1333, 1290, 1278, 1257, 1206, 1182, 1164, 1154, 1116, 1085, 1049, 915, 873, 853, 841, 815, 741, 734, 614, 604, 574, 552, 523 cm⁻¹; HRMS-FAB m/z [$M-I$]⁺ calcd for C₁₅H₂₂IN₂S: 389.0543, found: 389.0565.

3-(*tert*-Butyl)-1-{3-[4-(*tert*-butyl)pyridin-1-ium-1-yl]propyl}pyrazin-1-ium diiodide (2 e)

According to GP2, with **10 a** (474 mg, 1.10 mmol, 1.0 eq.) and **26** (185 mg, 1.32 mmol, 1.2 eq.) in MeCN (2.2 mL) at 120 °C. Reaction time: 16 h. Recrystallization from EtOH (18 mL) afforded **2 e** (539 mg, 87%) as a yellow solid.

mp: 240°C; ¹H NMR (400 MHz, [D₆]DMSO): δ =0.67 (s, 9 H, NC(C(CH₃)₃)), 0.74 (s, 9 H, NCHCHC(C(CH₃)₃)), 2.05–2.16 (m, 2 H, NCH₂CH₂), 4.08–4.13 (m, 2 H, CH₂NCHCHC(C(CH₃)₃)), 4.17–4.23 (m, 2 H, CH₂NCHCHN), 7.37–7.43 (m, 2 H, NCHCHC(C(CH₃)₃)), 8.22–8.28 (m, 3 H, NCHCHC(C(CH₃)₃), CH₂NCHCHN), 8.54 (s, 1 H, NCHC(C(CH₃)₃)), 8.64 ppm (q, J =3.2/2.7 Hz, 1 H, CH₂NCHCHN); ¹³C NMR (100 MHz, [D₆]DMSO): δ =29.77 (NCHCHC(C(CH₃)₃)), 30.26 (NC(C(CH₃)₃)), 33.27 (NCH₂CH₂), 37.75 (NCHCHC(C(CH₃)₃)), 39.48 (NC(C(CH₃)₃)), 58.15 (CH₂NCHCHC(C(CH₃)₃)), 59.97–60.18 (m, CH₂NCHCHN), 126.96 (NCHCHC(C(CH₃)₃)), 135.07–135.57 (m, NCHC(C(CH₃)₃), CH₂NCHCHN), 145.51 (NCHCHC(C(CH₃)₃)), 151.20 ((CH₂NCHCHN), 173.40 (NCHCHC(C(CH₃)₃)), 173.72 ppm (NCHC(C(CH₃)₃)); IR (KBr): $\tilde{\nu}$ =3420, 3004, 2966, 2869, 1644, 1567, 1517, 1483, 1459, 1367, 1298, 1277, 1262, 1193, 1166, 1137, 1115, 1076, 1022, 992, 920, 864, 847, 822, 806, 765, 745, 634, 568 cm⁻¹; HRMS-FAB m/z [$M-I$]⁺ calcd for C₂₀H₃₁IN₃: 440.1557, found: 440.1576.

1-{3-[4-(*tert*-Butyl)pyridin-1-ium-1-yl]propyl}-2,6-dimethylpyridin-1-ium dichloride (3 a)

According to GP3, with **6** (203 mg, 1.50 mmol, 220 μ L, 1.2 eq.) and **34 a** (473 mg, 1.25 mmol, 1.0 eq.) in MeCN (2.5 mL). Purification by RP-MPLC (C18, MeOH/H₂O = 10:90) afforded **3 a** (347 mg, 78%) as a colorless solid.

RP-MPLC: t_R =700 s (MeOH/H₂O 10:90); mp: 238°C; ¹H NMR (400 MHz, CD₃CN): δ =1.39 (s, 9 H, C(CH₃)₃), 2.56–2.66 (m, 2 H, NCH₂CH₂), 3.00 (s, 6 H, NCCH₃), 4.77–4.85 (m, 2 H, CH₃CNCH₂), 5.17–5.25 (m, 2 H, CH₂NCHCHC(C(CH₃)₃)), 7.71 (d, J =7.9 Hz, 2 H, NC(CH₃)CH), 8.04 (d, J =7.1 Hz, 2 H, NCHCH), 8.17 (t, J =7.9 Hz, 1 H, NC(CH₃)CHCH), 9.69 ppm (d, J =7.0 Hz, 2 H, NCHCH); ¹³C NMR (100 MHz, CD₃CN): δ =22.41 (NCCH₃), 30.13 (C(CH₃)₃), 30.75 (NCH₂CH₂), 37.35 (C(CH₃)₃), 50.98 (CH₃CNCH₂), 57.15 (CH₂NCHCHC(C(CH₃)₃)), 126.23 (NCHCH), 129.05 (CHC(CH₃)N), 145.57 (CHCHC(CH₃)N), 145.86 (NCHCH), 157.45 (NCCH₃), 172.22 ppm (CC(CH₃)₃); IR (KBr): $\tilde{\nu}$ =3120, 3023, 2966, 1642, 1625, 1586, 1562, 1517, 1495, 1464, 1374, 1275, 1237, 1191, 1114, 1057, 1035, 856, 840, 801, 585 cm⁻¹; HRMS-FAB m/z [M -Cl]⁺ calcd for C₁₉H₂₈ClN₂: 319.1936, found: 319.1941.

1-{3-[4-(*tert*-Butyl)pyridin-1-ium-1-yl]propyl}-2,4,6-trimethylpyridin-1-ium dichloride (3 b)

According to GP3, with **6** (202 mg, 1.50 mmol, 219 μ L, 1.2 eq.) and **34 b** (489 mg, 1.25 mmol, 1.0 eq.) in MeCN (2.5 mL). Purification by RP-MPLC (C18, MeOH/H₂O = 10:90) afforded **3 b** (384 mg, 85%) as a colorless solid.

RP-MPLC: t_R =670 s (MeOH/H₂O 10:90); mp: 230°C; ¹H NMR (500 MHz, CD₃CN): δ =1.38 (s, 9 H, C(CH₃)₃), 2.47 (s, 3 H, NC(CH₃)CHCCH₃), 2.58 (quin., J =8.2 Hz, 2 H, NCH₂CH₂), 2.93 (s, 6 H, NCCH₃), 4.70–4.77 (m, 2 H, CH₂NCCH₃), 5.15–5.22 (m, 2 H, CHNCH₂), 7.54 (s, 2 H, CH₃CCH), 8.04 (d, J =6.8 Hz, 2 H, NCHCH), 9.68 ppm (d, J =6.9 Hz, 2 H, NCHCH); ¹³C NMR (125 MHz, CD₃CN): δ =21.57 (NC(CH₃)CHCCH₃), 22.10 (NCCH₃), 30.13 (C(CH₃)₃), 30.90 (NCH₂CH₂), 50.21 (CH₂NCCH₃), 57.19 (CHNCH₂), 126.21 (NCHCH), 129.50 (CHCCH₃), 145.86 (NCHCH), 156.07 (NCCH₃), 159.22 (NC(CH₃)CHCCH₃), 172.17 ppm (CC(CH₃)₃); IR (KBr): $\tilde{\nu}$ =3013, 2964, 2869, 1639, 1574, 1516, 1468, 1418, 1374, 1354, 1318, 1275, 1240, 1195, 1149, 1118, 1061, 1034, 877, 745, 586, 562 cm⁻¹; HRMS-FAB m/z [M -Cl]⁺ calcd for C₂₀H₃₀ClN₂: 333.2092, found: 333.2094.

1-{3-[4-(*tert*-Butyl)pyridin-1-ium-1-yl]propyl}-2-isopropylpyridin-1-ium dichloride (3 c)

According to GP3, with **6** (230 mg, 1.70 mmol, 249 μ L, 1.2 eq.) and **34 c** (555 mg, 1.42 mmol, 1.0 eq.) in MeCN (2.8 mL). Purification by RP-MPLC (C18, MeOH/H₂O = 15:85) afforded **3 c** (497 mg, 94%) as a colorless solid.

RP-MPLC: t_R =675 s (MeOH/H₂O 15:85); mp: 102°C; ¹H NMR (400 MHz, CD₃CN): δ =1.38 (s, 9 H, C(CH₃)₃), 1.40 (d, J =6.7 Hz, 6 H, (CH(CH₃)₂), 2.68–2.77 (m, 2 H, NCH₂CH₂), 3.98 (hept, J =7.6/7.1 Hz, 1 H, CH(CH₃)₂), 4.97–5.06 (m, 2 H, CH₂NC(CH(CH₃)₂)), 5.13–5.22 (m, 2 H, CH₂NCHCHC(C(CH₃)₃)), 7.84 (ddd, J =7.7/6.4/1.5 Hz, 1 H, NCHCHCH), 7.98 (dd, J =8.3/1.2 Hz, 1 H, NCHCHCHCH), 8.02–8.06 (m, 2 H, NCHCHC(C(CH₃)₃)), 8.36–8.42 (m, 1 H, NCHCHCH), 9.55 (d, J =6.1 Hz, 2 H, NCHCHC(C(CH₃)₃)), 9.71 ppm (d, J =6.3 Hz, 1 H, NCHCHCH); ¹³C NMR (100 MHz, CD₃CN): δ =22.73 (CH(CH₃)₂), 30.12 (C(CH₃)₃), 30.94 (CH(CH₃)₂), 34.72 (NCH₂CH₂), 37.32 (C(CH₃)₃), 55.06 (CH₂NC(CH(CH₃)₂)), 57.59 (CH₂NCHCHC(C(CH₃)₃)), 126.31 (NCHCHC(C(CH₃)₃)), 126.57 (NCHCHCH), 127.35 (NCHCHCHCH), 145.60 (NCHCHC(C(CH₃)₃)), 146.65 (NCHCHCH), 147.18 (NCHCHCH), 165.64 (C(CH(CH₃)₂)), 172.11 ppm (C(C(CH₃)₃)); IR (KBr): $\tilde{\nu}$ =3441, 3374, 3023, 2968, 2871, 1641, 1576, 1515, 1476, 1454, 1388, 1372, 1361, 1279, 1247, 1198, 1173, 1162, 1119, 1092, 1065, 1042, 986, 934, 893, 866, 835, 793, 751, 608, 581, 567, 539, 480 cm⁻¹; HRMS-ESI m/z [M-Cl]⁺ calcd for C₂₀H₃₀ClN₂: 333.2092, found: 333.2092.

2-(*tert*-Butyl)-1-{3-[4-(*tert*-butyl)pyridin-1-ium-1-yl]propyl}pyridin-1-ium dichloride (3 d)

According to GP3, with **6** (252 mg, 1.86 mmol, 273 μ L, 1.2 eq.) and **34 d** (630 mg, 1.55 mmol, 1.0 eq.) in MeCN (3.1 mL). Purification by RP-MPLC (C18, MeOH/H₂O = 15:85) afforded **3 d** (537 mg, 90%) as a slightly hygroscopic and colorless solid.

RP-MPLC: t_R =800 s (MeOH/H₂O 10:90); mp: 83°C; ¹H NMR (400 MHz, CD₃CN): δ =1.38 (s, 9 H, NCHCHC(C(CH₃)₃)), 1.63 (s, 9 H, NC(C(CH₃)₃)), 2.76–2.86 (m, 2 H, NCH₂CH₂), 5.08–5.15 (m, 4 H, NCH₂), 7.91 (ddd, J =7.7/6.3/1.5 Hz, 1 H, NCHCHCH), 8.02–8.08 (m, 3 H, NCHCHC(C(CH₃)₃), NCHCHCHCH), 8.37 (ddd, J =8.5/7.6/1.6 Hz, 1 H, NCHCHCH), 9.55–9.60 (m, 2 H, NCHCHC(C(CH₃)₃)),

10.07 ppm (dd, $J=6.4/1.5$ Hz, 1 H, NCHCHCH); ^{13}C NMR (100 MHz, CD_3CN): $\delta=30.12$ (NCHCHC(C(CH₃)₃)), 30.64 (NC(C(CH₃)₃)), 35.91 (NCH₂CH₂), 37.35 (NCHCHC(C(CH₃)₃)), 38.60 (NC(C(CH₃)₃)), 56.08 (CH₂NC(C(CH₃)₃))* , 57.44 (CH₂NCHCHC(C(CH₃)₃))* , 126.27 (NCHCHC(C(CH₃)₃)), 127.10 (NCHCHCH), 128.13 (NCHCHCHCH), 145.73 (NCHCHC(C(CH₃)₃)), 146.88 (NCHCHCH), 150.11 (NCHCHCH), 165.47 (NC(C(CH₃)₃)), 172.28 ppm (NCHCHC(C(CH₃)₃)); IR (KBr): $\tilde{\nu}=2968, 1640, 1624, 1572, 1512, 1468, 1373, 1276, 1253, 1189, 1167, 1115, 1049, 932, 851, 786, 578, 547$ cm⁻¹; HRMS-ESI m/z [M-Cl]⁺ calcd for C₂₁H₃₂ClN₂: 347.2249, found: 347.2248.

4-(*tert*-Butyl)-1-[3-(2-oxopyridin-1(2*H*)-yl)propyl]pyridin-1-ium chloride (**3 f**)

6 (483 mg, 3.57 mmol, 524 μL , 3.0 eq.) was added to a suspension of **34 e** (453 mg, 1.19 mmol, 1.0 eq.) in MeCN (2.4 mL) and the resulting mixture was stirred at 90 °C for 16 h under microwave conditions (150 W). The solvent was removed under reduced pressure and the residue was dissolved in H₂O bidest. (50 mL). Amberlite® IRA-410 Cl-form ion exchange resin (29.0 g, 60.0 meq) was added to the aqueous solution and the resulting suspension was vigorously stirred for 72 h at room temperature. The resin was removed by filtration, washed with H₂O bidest. (100 mL) and the solvent was removed under reduced pressure. The crude product was purified by RP-MPLC (C18, MeOH/H₂O = 15:85), dissolved in H₂O bidest. (10 mL) and lyophilized. Due to its very high hygroscopicity, the purified material was treated repeatedly with EtOAc (3 x 10 mL) and the solvent was removed under reduced pressure affording **3 f** (330 mg, 90%) as a colorless and moderately hygroscopic solid.

RP-MPLC: $t_R=850$ s (MeOH/H₂O 15:85); mp: 183°C; ^1H NMR (500 MHz, [D₆]DMSO): $\delta=1.36$ (s, 9 H, C(CH₃)₃), 2.34 (quin., $J=7.0$ Hz, 2 H, NCH₂CH₂), 3.98 (t, $J=6.9$ Hz, 2 H, OCNCH₂CH₂), 4.63 (t, $J=7.2$ Hz, 2 H, CH₂NCHCHCC(CH₃)₃), 6.23 (td, $J=6.7/1.4$ Hz, 1 H, OCCHCHCH), 6.33–6.38 (m, 1 H, OCCH), 7.40 (ddd, $J=8.9/6.6/2.1$ Hz, 1 H, OCCHCH), 7.71 (dd, $J=6.8/2.0$ Hz, 1 H, OCNCH), 8.16 (d, $J=7.0$ Hz, 2 H, NCHCHCC(CH₃)₃), 9.05 ppm (d, $J=6.8$ Hz, 2 H, NCHCHCC(CH₃)₃); ^{13}C NMR (125 MHz, [D₆]DMSO): $\delta=30.00$ (C(CH₃)₃), 30.69 (NCH₂CH₂), 36.69 (NCHCHCC(CH₃)₃), 45.83 (OCNCH₂), 58.05 (CH₂NCHCHCC(CH₃)₃), 106.13 (OCCHCHCH), 120.05 (OCCH), 125.34 (NCHCHCC(CH₃)₃), 139.39 (NCHCHCH), 140.52 (OCCHCH), 144.72 (NCHCHCC(CH₃)₃), 161.96 (CO), 170.29 ppm (CC(CH₃)₃); IR (KBr): $\tilde{\nu}=3124, 3048, 2971, 1656, 1575, 1541, 1515, 1466, 1375, 1352, 1276, 1191,$

1169, 1153, 1116, 1063, 893, 852, 776, 737, 572 cm⁻¹; HRMS-FAB *m/z* [M-Cl]⁺ calcd for C₁₇H₂₃N₂O: 271.1805, found: 271.1810.

3-Methoxy-1-[3-(4-methylpyridin-1-ium-1-yl)propyl]pyridin-1-ium diiodide (4 a)

According to GP2, with **10 b** (405 mg, 1.00 mmol, 1.0 eq.) and **27** (112 mg, 1.20 mmol, 117 μ L, 1.2 eq.) in MeCN (2.2 mL) at 90 °C. Reaction time: 1 h. Purification by RP-MPLC (C18, MeOH/H₂O = 10:90) afforded **4 a** (415 mg, 83%) as a yellow solid.

RP-MPLC: *t_R*=600 s (MeOH/H₂O 10:90); mp: 147°C; ¹H NMR (400 MHz, CD₃CN): δ =2.63 (s, 3 H, CCH₃), 2.74–2.85 (m, 2 H, NCH₂CH₂), 4.07 (s, 3 H, OCH₃), 4.80–4.86 (m, 2 H, CH₃CCHCHNCH₂), 4.87–4.93 (m, 2 H, CH₂NCHCOCH₃), 7.87 (d, *J*=6.4 Hz, 2 H, NCHCHCCH₃), 7.95 (dd, *J*=8.9/5.9 Hz, 1 H, NCHCHCH), 8.06 (ddd, *J*=8.9/2.6/0.8 Hz, 1 H, NCHCHCH), 8.69 (d, *J*=5.9 Hz, 1 H, NCHCHCH), 8.97 (d, *J*=6.8 Hz, 2 H, NCHCHCCH₃), 9.05–9.07 ppm (m, 1 H, NCHCOCH₃); ¹³C NMR (100 MHz, CD₃CN): δ =22.37 (CCH₃), 33.80 (NCH₂CH₂), 57.63 (CH₃CCHCHNCH₂), 58.66 (CH₂NCHCOCH₃), 59.13 (OCH₃), 129.73 (NCHCHCH), 129.91 (NCHCHCCH₃), 132.52 (NCHCHCH), 133.26 (NCHCOCH₃), 138.30 (NCHCHCH), 144.77 (NCHCHCCH₃), 159.96 (NCHCOCH₃), 161.49 ppm (NCHCHCCH₃); IR (KBr): $\tilde{\nu}$ =3127, 3014, 2970, 2934, 1639, 1620, 1595, 1569, 1507, 1477, 1449, 1389, 1370, 1344, 1333, 1302, 1285, 1242, 1199, 1165, 1150, 1108, 1040, 1018, 997, 963, 916, 877, 848, 828, 807, 730, 697, 671, 567, 550, 521, 477 cm⁻¹; HRMS-FAB *m/z* [M-I]⁺ calcd for C₁₅H₂₀IN₂O: 371.0615, found: 371.0636.

1-{3-[4-(Dimethylamino)pyridin-1-ium-1-yl]propyl}-3-methoxypyridin-1-ium diiodide (4 b)

According to GP2, with **10 b** (405 mg, 1.00 mmol, 1.0 eq.) and **18** (147 mg, 1.20 mmol, 1.2 eq.) in MeCN (2.2 mL) at 90 °C. Reaction time: 1 h. Purification by RP-MPLC (C18, MeOH/H₂O = 10:90) afforded **4 b** (368 mg, 70%) as a yellow solid.

RP-MPLC: *t_R*=800 s (MeOH/H₂O 10:90); mp: 147°C; ¹H NMR (400 MHz, CD₃CN): δ =2.58–2.69 (m, 2 H, NCH₂CH₂), 3.18 (s, 6 H, N(CH₃)₂), 4.07 (s, 3 H, OCH₃), 4.38–4.43 (m, 2 H, NCCHCHNCH₂), 4.79–4.84 (m, 2 H, CH₂NCHCOCH₃), 6.86–6.91 (m, 2 H, NCHCHCN), 7.94 (dd, *J*=8.9/5.9 Hz, 1 H, NCHCHCH), 8.05 (ddd, *J*=8.9/2.6/0.9 Hz, 1 H, NCHCHCH), 8.26–8.31 (m, 2 H, NCHCHCN), 8.63 (d, *J*=5.9 Hz, 1 H, NCHCHCH), 8.98–9.00 ppm (m, 1 H, NCHCOCH₃); ¹³C NMR (100 MHz,

CD₃CN): δ =33.50 (NCH₂CH₂), 40.83 ((CH₃)₂N), 54.55 (NCCHCHNCH₂), 58.98 (CH₂NCHCOCH₃), 59.08 (OCH₃), 108.93 (NCHCHCN), 129.71 (NCHCHCH), 132.36 (NCHCHCH), 133.23 (NCHCOCH₃), 138.24 (NCHCHCH), 142.89 (NCHCHCN), 157.55 (NCHCHCN), 159.94 ppm (NCHCOCH₃); IR (KBr): $\tilde{\nu}$ =3047, 3014, 1947, 1837, 1650, 1577, 1535, 1509, 1480, 1456, 1440, 1376, 1360, 1343, 1292, 1236, 1197, 1174, 1089, 1049, 1041, 1005, 942, 916, 866, 840, 821, 798, 755, 739, 679, 584, 565, 528, 502 cm⁻¹; HRMS-FAB m/z [M-I]⁺ calcd for C₁₆H₂₃IN₂O: 400.0880, found: 400.0889.

3-Methoxy-1-{3-[4-(trifluoromethyl)pyridin-1-ium-1-yl]propyl}pyridin-1-ium di-iodide (**4 c**)

According to GP2, with **10 c** (886 mg, 2.00 mmol, 1.0 eq.) and **7** (225 mg, 2.00 mmol, 210 μ L, 1.2 eq.) in MeCN (4 mL) at 90 °C. Reaction time: 1 h. Purification by RP-MPLC (C18, MeOH/H₂O = 15:85) and subsequent recrystallization of the resulting residue from EtOH (6 mL) afforded **4 c** (687 mg, 62%) as a yellow solid.

RP-MPLC: t_R =750 s (C18, MeOH/H₂O 15:85); mp: 184°C; ¹H NMR (500 MHz, CD₃CN): δ =2.84–2.92 (m, 2 H, NCH₂CH₂), 4.08 (s, 3 H, OCH₃), 4.92–4.97 (m, 2 H, CH₂NCHCOCH₃), 5.05–5.10 (m, 2 H, F₃CCCHCHNCH₂), 7.96 (dd, J =8.9/5.9 Hz, 1 H, NCHCHCH), 8.06 (ddd, J =8.9/2.6/0.9 Hz, 1 H, NCHCHCH), 8.41 (d, J =6.4 Hz, 2 H, NCHCHCCF₃), 8.70 (d, J =5.9 Hz, 1 H, NCHCHCH), 9.07–9.10 (m, 1 H, NCHCOCH₃), 9.54 ppm (d, J =6.6 Hz, 2 H, NCHCHCCF₃); ¹³C NMR (125 MHz, CD₃CN): δ =33.71 (NCH₂CH₂), 58.49 (CH₂NCHCOCH₃), 59.14 (OCH₃), 59.21 (F₃CCCHCHNCH₂), 122.31 (q, J =274.2 Hz, CF₃), 126.54 (q, J =2.9 Hz, NCHCHCCF₃), 129.77 (NCHCHCH), 132.60 (NCHCHCH), 133.27 (NCHCOCH₃), 138.31 (NCHCHCH), 145.74 (q, J =36.5 Hz, CCF₃), 147.96–148.39 (m, NCHCHCCF₃), 160.02 ppm (COCH₃); IR (KBr): $\tilde{\nu}$ =3029, 3012, 2872, 2849, 1624, 1596, 1583, 1515, 1481, 1470, 1458, 1445, 1415, 1324, 1294, 1250, 1232, 1193, 1172, 1151, 1098, 1082, 1061, 1043, 1005, 878, 864, 831, 767, 735, 685, 644, 612, 590, 567, 512 cm⁻¹; HRMS-ESI m/z [M-I]⁺ calcd for C₁₅H₁₇F₃IN₂O: 425.0332, found: 425.0330.

1-(*tert*-Butyl)-4-(3-chloropropyl)benzene (**36**)

Triethylsilane (1.78 g, 15.3 mmol, 2.45 mL, 4.0 eq.) was added to a solution of ketone **35** (861 mg, 3.83 mmol, 1.0 eq.) in TFA (22 mL) and the resulting mixture was stirred for 15 h at 75 °C under microwave conditions (100 W). The solvent was removed under reduced pressure and the residue was dissolved in CH₂Cl₂ (40 mL). The organic layer

was washed with H₂O (2 x 40 mL) and the combined aqueous layers were extracted with CH₂Cl₂ (50 mL). The combined organic layers were dried over MgSO₄, the solvent was removed under reduced pressure and the crude product was purified by MPLC (SiO₂, *n*-pentane) to afford **36** (725 mg, 90%) as a colorless liquid.

*R*_f=0.4 (*n*-pentane); MPLC: *t*_R=520 s (*n*-pentane); ¹H NMR (400 MHz, CDCl₃): δ=1.31 (s, 9 H, C(CH₃)₃), 2.04–2.12 (m, 2 H, CH₂CH₂Cl), 2.71–2.77 (m, 2 H, CH₂CH₂CH₂Cl), 3.53 (t, *J*=6.5 Hz, 2 H, CH₂Cl), 7.11–7.15 (m, 2 H, CHCCH₂), 7.30–7.34 ppm (m, 2 H, CHCHCCH₂); ¹³C NMR (100 MHz, CD₃Cl₃): δ=31.39 (C(CH₃)₃), 32.23 (CH₂CH₂CH₂Cl), 34.01 (CH₂CH₂Cl), 34.38 (C(CH₃)₃), 44.36 (CH₂Cl), 125.35 (CHCHCCH₂), 128.18 (CHCCH₂), 137.58 (CHCCH₂), 148.95 ppm (CC(CH₃)₃); IR (KBr): $\tilde{\nu}$ =3092, 3055, 3024, 2961, 2906, 2867, 1517, 1509, 1475, 1462, 1444, 1413, 1393, 1363, 1306, 1291, 1268, 1202, 1139, 1109, 1019, 972, 870, 845, 831, 812, 765, 731, 665, 649 cm⁻¹; HRMS-El *m/z* [M]⁺ calcd for C₁₃H₁₉Cl: 210.1170, found: 210.1177.

The analytical data were in accordance with those previously reported.¹

4-(*tert*-Butyl)-1-{3-[4-(*tert*-butyl)phenyl]propyl}pyridin-1-ium chloride (5**)**

Nal (102 mg, 0.679 mmol, 1.1 eq.) and **6** (100 mg, 0.740 mmol, 108 μ L, 1.2 eq.) were added to a solution of alkylchloride **36** (130 mg, 0.617 mmol, 1.0 eq.) in MeCN (1.2 mL) and the resulting mixture was stirred for 16 h at 90 °C under microwave conditions (150 W). The solvent was removed under reduced pressure and the residue was dissolved in H₂O bidest./MeOH (1:1, 100 mL). Amberlite® IRA-410 Cl⁻-form ion exchange resin (16.0 g) was added to the solution and the resulting suspension was vigorously stirred for 72 h at room temperature. The resin was removed by filtration and was washed with H₂O bidest. (100 mL). The solvent removed under reduced pressure and the crude product was purified by RP-MPLC (C18, MeOH/H₂O = 50:50). The resulting highly viscous liquid was dissolved in H₂O bidest. (10 mL) and lyophilized to obtain the corresponding chloride salt as a colorless hygroscopic solid. The purified material was treated repeatedly with EtOAc (3 x 15 mL) and the solvent was removed under reduced pressure to afford **5** (191 mg, 90%) as a colorless and less hygroscopic solid.

[1] J. I. Perlmutter, L. T. Forbes, D. J. Krysan, K. Ebsworth-Mojica, J. M. Colquhoun, J. L. Wang, P. M. Dunman, D. P. Flaherty, *J. Med. Chem.* **2014**, *57*, 8540–8562.

RP-MPLC: t_R =1600 s (MeOH/H₂O 50:50); mp: 202°C; ¹H NMR (500 MHz, CD₃OD): δ =1.29 (s, 9 H, CCHCHC(C(CH₃)₃)), 1.43 (s, 9 H, NCHCHC(C(CH₃)₃)), 2.34 (quin. J =7.6 Hz, 2 H, NCH₂CH₂), 2.72 (t, J =7.5 Hz, 2 H, NCH₂CH₂CH₂), 4.56–4.61 (m, 2 H, NCH₂), 7.13–7.16 (m, 2 H, CH₂CCH), 7.31–7.34 (m, 2 H, CH₂CCHCH), 8.08–8.11 (m, 2 H, NCHCH), 8.80–8.83 ppm (m, 2 H, NCH); ¹³C NMR (125 MHz, CD₃OD): δ =30.24 (NCHCHC(C(CH₃)₃)), 31.83 (CCHCHC(C(CH₃)₃)), 32.80 (NCH₂CH₂CH₂), 33.63 (NCH₂CH₂), 35.26 (CCHCHC(C(CH₃)₃)), 37.58 (NCHCHC(C(CH₃)₃)), 61.80 (NCH₂), 126.55 (CCHCH), 126.61 (NCHCH), 129.11 (CH₂CCH), 138.15 (CH₂CCH), 145.24 (NCH), 150.51 (CCHCHC(C(CH₃)₃)), 172.77 ppm (NCHCHC(C(CH₃)₃)); IR (KBr): $\tilde{\nu}$ =2963, 2867, 1640, 1562, 1516, 1465, 1392, 1364, 1271, 1232, 1189, 1112, 1053, 1021, 929, 850, 581, 567 cm⁻¹; HRMS-ESI m/z [M]⁺ calcd for C₂₂H₃₂N: 310.2529, found: 310.2527.

3.4 Unveröffentlichte Ergebnisse

3.4.1 Allgemeiner Teil

Vor Beginn der Methodenentwicklung von MB327-Bindungsassays wurden zunächst Filtrations-basierte MS-Bindungsexperimente mit nicht-markiertem, nativem Epibatidin als Markerverbindung am *Torpedo*-nAChR, analog zu Radioligand-Bindungsassays mit tritiummarkiertem Epibatidin von Niessen⁵¹, durchgeführt. Hiermit sollte gezeigt werden, dass sich solche Bindungsexperimente statt mittels Szintillationszählung des Radioliganden auch mithilfe massenspektrometrischer Detektion der entsprechenden nativen Markerverbindung durchführen lassen. Für diese Bindungsexperimente wurden Membranpräparationen nach dem Protokoll der Arbeitsgruppe Niessen am Institut für Pharmakologie und Toxikologie der Bundeswehr (InstPharmTox) in München aus dem Elektroplax von *Torpedo californica* extrahiert. Zur Herstellung der Bindungsproben wurden Aliquots einer Membranpräparation mit Epibatidin als Reporterligand (500 pmol L^{-1} – 50 nmol L^{-1} bzw. 1 nmol L^{-1} – 80 nmol L^{-1}) und Carbamoylcholin bzw. Nikotin als Kompetitor (jeweils 10 mmol L^{-1}), letztere zur Bestimmung der nichtspezifischen Bindung, hergestellt. Nach Inkubation von Reporterligand und Target, Isolierung des Target-Reporterligand-Komplexes durch Filtration und Freisetzung des gebundenen Reporterliganden wurden die Bindungsproben zuletzt per LC-MS analysiert. Die Auswertung der erhaltenen Sättigungsisotherme (vgl. Abb. 12) mithilfe der PRISM v. 5.0-Software ergab eine Gleichgewichtsdissoziationskonstante (K_d) von 3.9 nmol L^{-1} bzw. von 9.2 nmol L^{-1} für die Bindung von Epibatidin am *Torpedo*-nAChR, wenn Carbachol bzw. Nikotin zur Bestimmung der nichtspezifischen Bindung eingesetzt wurde.

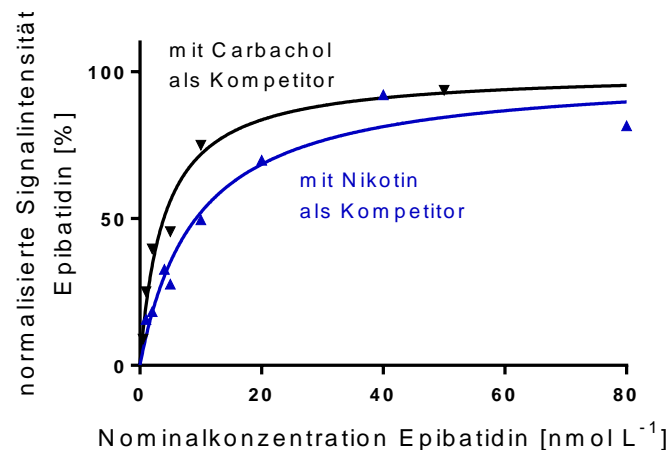


Abbildung 12: Sättigungsisothermen für die Bindung von Epibatidin als Reporterligand am *Torpedo*-nAChR. Die Bestimmung der nicht-spezifischen Bindung erfolgte in Anwesenheit von 10 mmol L^{-1} Carbachol bzw. Nikotin als Kompetitor in Bindungsproben. Für die spezifische Bindung, als Differenz von Gesamt- und nicht-spezifischer Bindung, im Reporterligand-Nominalkonzentrationsbereich $0.5 - 50 \text{ nmol L}^{-1}$ bzw. $1 - 80 \text{ nmol L}^{-1}$ ergab sich ein K_d -Wert von 3.9 nmol L^{-1} bzw. 9.2 nmol L^{-1} in Anwesenheit von Carbachol bzw. Nikotin als Kompetitor. Die Signalintensität, die als Fläche der Reporterligand-Signale ermittelt wurde, ist jeweils als prozentualer Anteil der maximal erreichten Signalfäche angegeben.

Beide Affinitätskonstanten stimmen gut mit bereits publizierten K_d -Werten zur Epibatidin-Bindung am *Torpedo*-nAChR überein.^{51,93,94}

Nebst Epibatidin- wurden auch Carbamoylcholin-Sättigungsexperimente, ebenfalls mittels Filtration zur Trennung des gebundenen von ungebundenem Reporterligand, durchgeführt. Nach Auswertung erhaltener Sättigungsisothermen wurde so ein K_d -Wert von $334 \pm 19 \text{ nmol L}^{-1}$ sowie ein B_{max} -Wert von $282 \pm 45 \text{ pmol mg}^{-1}$ Protein ($n = 3$, MW \pm SD) für die Bindung von Carbamoylcholin bzw. Carbachol am *Torpedo*-nAChR ermittelt. Eine repräsentative Sättigungsisotherme ist in Abbildung 13 dargestellt.

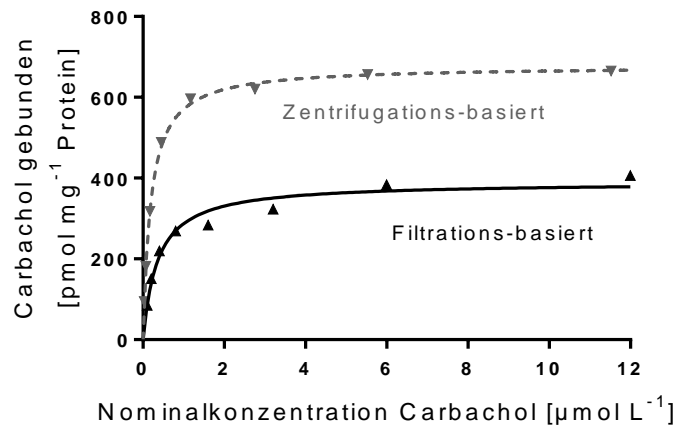


Abbildung 13: Sättigungsisothermen repräsentativer Carbachol-Bindungsexperimente mit Zentrifugation bzw. Filtration zur Trennung von gebundenem und ungebundenem Reporterligand. In den gezeigten Experimenten wurde ein K_d -Wert von 359 bzw. 188 nmol L $^{-1}$ und ein B_{max} -Wert von 390 bzw. 677 pmol mg $^{-1}$ Protein erreicht, wenn Bindungsproben filtriert bzw. zentrifugiert wurden.

Der Vergleich der Sättigungsisotherme eines repräsentativen Filtrations-basierten Bindungsexperiments mit der Sättigungsisotherme eines Zentrifugations-basierten Bindungsexperiments (vgl. Abschnitt 3.1), offenbart allerdings eine sichtliche Diskrepanz bezüglich der Anzahl maximaler Bindestellen bzw. der Affinität des Reporterliganden zum Target. Da es sich bei Carbachol um einen nAChR-Liganden mit vergleichbar geringer Affinität zum Target handelt ($K_d \geq 100 \text{ nmol L}^{-1}$)^{95,96} ist davon auszugehen, dass im Zuge der Waschschrte des Filter-Bindungsexperiments ein wesentlicher Teil des gebundenen Reporterliganden verloren geht und damit die spezifische Carbachol-Bindung unzureichend erfasst wird. So ist auch zu erklären, warum der B_{max} -Wert von $611 \pm 30 \text{ pmol mg}^{-1}$ Protein im Zentrifugations-basierten Bindungsexperiment (vgl. Abschnitt 3.1) auf $282 \pm 45 \text{ pmol mg}^{-1}$ Protein (jeweils $n = 3$, MW \pm SD) im Filter-Bindungsexperiment fällt bzw. der K_d -Wert von $171 \pm 18 \text{ nmol L}^{-1}$ auf $334 \pm 19 \text{ nmol L}^{-1}$ (jeweils $n = 3$, MW \pm SD) steigt. Das Zentrifugations-basierte Bindungsassay, bei dem eine derart umfangreiche Dissoziation des Reporterligand-Target-Komplexes während der Waschschrte nicht erfolgt, zeigt sich damit deutlich besser für die zuverlässige Bestimmung der spezifischen Carbachol-Bindung geeignet. Schließlich belegen beide Bindungsexperimente, mit Epibatidin bzw. Carbamoylcholin als nativem Reporterligand, dass eine Affinitätscharakterisierung von nAChR-Liganden am *Torpedo*-nAChR mithilfe von MS-Bindungsassays sehr gut möglich ist.

3.4.2 Experimenteller Teil

Geräte und Material

Die nAChR-Agonisten (+/-)-Epibatidin und Carbamoylcholinchlorid wurden von Tocris (Bristol, Vereinigte Staaten) bzw. von Sigma-Aldrich (Taufkirchen, Deutschland) bezogen. Die Beschaffung von gefrorenem Elektroplax-Material des *Torpedo californica* erfolgte durch die Firma Aquatic Research Consultants (San Pedro, CA, USA). Für die Herstellung von Inkubationspuffern sowie Puffern der mobilen Phase wurde demineralisiertes Wasser (hergestellt durch Reverse Osmose) verwendet, das außerdem destilliert und zusätzlich durch Filtermaterial mit 0.45 µm Porengröße filtriert wurde. Für die Herstellung der mobilen Phase wurde HPLC grade Acetonitril von VWR Prolabo (Darmstadt, Deutschland), sowie Ammoniumformiat von Sigma-Aldrich (für Massenspektrometrie, Taufkirchen, Deutschland) als Additiv für den wässrigen Anteil der mobilen Phase verwendet. Alle weiteren Chemikalien hatten den zu Analysezwecken erforderlichen Reinheitsgrad. Verbrauchsmaterialien wie 96-Well-Mikrotiterplatten aus Polypropylen bzw. Polystyrol, Reagiergefäße und Pipettenspitzen wurden von der Firma Sarstedt (Nümbrecht, Deutschland) bezogen. Die Beschaffung von Glasfaserfilterplatten im 96-Wellformat hingegen erfolgte über die Firma Pall (AcroPrep Advance, Glasfaser, 1.0 µm, 350 µL, Pall, Dreieich, Deutschland).

Für die LC-MS-Detektion stand eine Agilent 1200 HPLC (Agilent, Waldbronn, Deutschland) mit SIL-HT(A)-Autosampler (Shimadzu, Duisburg, Deutschland) und ein API 3200 Triple Quadrupol Massenspektrometer (AB Sciex, Darmstadt, Deutschland) mit Turbo V-Ionenquelle zur Verfügung. Als stationäre Phase wurde eine YMC-Pack Diol-NP (ME-03C, 50 × 3.0 mm) bzw. eine YMC-Triart Diol-HILIC (50 mm × 2.0 mm, 3 µm, 12 nm, YMC Europe GmbH, Dinslaken, Deutschland) eingesetzt. Für die Filtration in Bindungsassays stand eine 96-Well-Filtrationseinheit (Multiwellplatten-Vakuum-Absaugstation, Pall, New York, USA) zur Verfügung.

Massenspektrometrische Detektion von Epibatidin und Carbachol

Die Detektion von Carbachol bzw. Epibatidin in Bindungsproben erfolgte per LC-ESI-MS/MS an einem API 3200 der Firma AB Sciex. Proben zur Analyse wurden in 96-Deepwell-Platten (1.2 mL, PP) vorgelegt und mit Aluminiumfolie abgedeckt. Nach Äquilibrieren der stationären Phase in der entsprechenden mobilen Phase für mindestens 30 min wurden die Proben über einen SIL-HT(A) Autosampler in einem

Volumen von 10 μL in das HPLC-System und auf die stationäre Phase injiziert. Die Einstellungen des Autosamplers sind in Tabelle 2 aufgeführt. Bindungsproben der Epibatidin-Bindungsexperimente wurden in einer mobilen Phase aus Acetonitril und Ammoniumformiatpuffer (20 mmol L^{-1} , pH 3.0) im Verhältnis 85 : 15 in einer Flussrate von 600 $\mu\text{L min}^{-1}$ auf eine YMC-Pack-Diol-NP (50 mm \times 3.0 mm, 5 μm) als stationäre Phase gebracht und anschließend im Massenspektrometer mittels Massenübergang m/z 209.0 \rightarrow 126.0 detektiert. Bindungsproben der Carbachol-Bindungsexperimente wurden in einer mobilen Phase aus Acetonitril und Ammoniumformiatpuffer (20 mmol L^{-1} , pH 3.0) im Verhältnis 80 : 20 in einer Flussrate von 800 $\mu\text{L min}^{-1}$ auf eine Triart Diol-NP (50 mm \times 2 mm, 3 μm) gebracht. Im Anschluss wurde im Massenspektrometer der Massenübergang m/z 148.2 \rightarrow 88.0 aufgezeichnet. Der Säulenofen war stets auf 20 $^{\circ}\text{C}$ temperiert. Die Analysenzeit betrug dabei knapp 3 min. Substanzspezifische und quellenspezifische Parameter für die Analyse von Epibatidin- bzw. Carbachol-Bindungsproben waren dabei wie folgt eingestellt (vgl. Tabelle 3 und 4).

Tabelle 2: Einstellungen des SIL-HT(A)-Autosamplers

Autosampler-Einstellungen	
Nadelspülvolumen [in μL]	200
Eintauchtiefe [in mm]	52
Nadelspülgeschwindigkeit [in $\mu\text{L s}^{-1}$]	35
Probennahmegeschwindigkeit [in $\mu\text{L s}^{-1}$]	5.0
Spülmodus mit MeCN/H ₂ O, 80 : 20	Vor und nach Probeninjektion
Injektionsvolumen [in μL]	10

Tabelle 3: Einstellungen der substanzspezifischen Parameter Declustering Potential (DP), Entrance Potential (EP), Collision Energy (CE) und Cell Exit Potential (CXP) für die massenspektrometrische Detektion von Carbachol und Epibatidin

Substanzspezifische Parameter	Epibatidin	Carbachol
DP [in V]	36	16
EP [in V]	11	8
CE [in eV]	37	23
CXP [in V]	4	2

Tabelle 4: Einstellungen der quellenspezifischen Parameter Nebulizer Gas (GS1), Auxiliary Gas (GS2), Curtain Gas (CUR), Collision Gas, Ion-Spray-Voltage (ISV), Temperatur (TEM) und Interface-Heater (ihe) für die massenspektrometrische Detektion von Carbachol und Epibatidin

Quellenspezifische Parameter	
GS1 [in psi]	50
GS2 [in psi]	40
CUR [in psi]	25
Collision Gas [in psi]	8
ISV [in V]	3000.0
TEM [in °C]	500
ihe	An

Herstellung des Torpedo-Membranmaterials für das Bindungsexperiment

Membranpräparationen des elektrischen Organs von *Torpedo californica* wurden mittels fraktionierter Zentrifugation zunächst durch die Arbeitsgruppe von Karin Niessen am Institut für Pharmakologie und Toxikologie (InstPharmTox) der Sanitätsakademie der Bundeswehr hergestellt und zu Versuchszwecken zur Verfügung gestellt bzw. später unter Anleitung am InstPharmTox nach bestehendem Protokoll hergestellt. Das Material wurde gemäß Originalprotokoll^{51,93} zur Aufarbeitung für [³H]Epibatidin-Bindungsexperimente, mit geringen Modifikationen, hergestellt. Im ersten Schritt wurde, anstelle eines dreifachen Volumens ein zweifaches Volumen

Extraktionspuffer zum gefrorenen Elektroplax-Gewebe gegeben. Die Zentrifugation des Homogenats in Waschpuffer wurde nur einmal statt zweimal wiederholt, sodass insgesamt zwei Waschschr tte durchgef hrt wurden. Extrahierte Zellmembranen wurden nach den Waschschr tten, im Gegensatz zum Originalprotokoll, in einem sogenannten Dounce Homogenisator (Wheaton, NJ, USA) mit 50 H ben pro Volumen zus tzlich homogenisiert. Zuletzt wurde das gewonnene Material unter st ndigem Auf- und Abpipettieren im Lagerungspuffer   1 mL aliquotiert, mit fl ssigem Stickstoff schockgefroren und bei -150  C gelagert. Zur Proteinbestimmung wurde die BCA-Methode nach Smith⁹⁷ mit Bovinem Serumalbumin als Standard und mit den Reagenzien des BCA-Assay-Protein-Quantification Kits (Uptima/ INTERCHIM, Montlucon, Frankreich) gem   Protokoll des Herstellers angewandt.

Durchf hrung von Bindungsassays mit Epibatidin als Reporterligand

Die Durchf hrung der Filtrations-basierten Epibatidin-Bindungsassays erfolgte analog zur Vorgehensweise, die von Grimm⁸⁷ f r MS-Bindungsstudien mit Indatralin etabliert wurde. Zur Herstellung der Bindungsproben wurden Aliquots der *Torpedo*-Membranpr paration (entsprechend ca. 6 – 12  g Protein pro Well) mit Epibatidin in Tris-Puffer (30 mmol L⁻¹ Tris, 100 mmol L⁻¹ NaCl, 3 mmol L⁻¹ EDTA, 1 mmol L⁻¹ EGTA, mit HCl auf pH 7,4 eingestellt) in Deepwell-Platten (PP, 1.2 mL) bei 25  C f r 2 h im Wasserbad inkubiert. In Bindungsproben zur Bestimmung der nicht-spezifischen Bindung wurde in einem der beiden Experimente 10 mmol L⁻¹ Carbachol, in dem anderen Experiment 10 mmol L⁻¹ Nikotin als Kompetitor eingesetzt. Die Glasfilterplatten wurden mit je 100  L pro Well einer w ssrigen 0.5% Polyethyleniminl sung (m/v) beschickt, die nach einer Einwirkungszeit von 60 min bei Raumtemperatur durch Filtration mittels einer Vakuumstation abgesaugt wurde. Anschlie end wurde jeweils ein Aliquot (200  L) der Bindungsproben (Probenansatz 250  L) pro Well auf die Filterplatten  bertragen und unter Vakuum abgesaugt. Das Filtrat wurde in 96-Megablocks (2.2 mL, PP) gesammelt und verworfen. Die auf dem Filter verbleibenden R ckst nde wurden mit eiskaltem Inkubationspuffer in drei m glichst kurzen Intervallen (3   100  L) gewaschen. Nach Trocknen der Platten f r 60 min bei 50  C wurde der ehemals gebundene Reporterligand durch Elution mit Acetonitril in drei Schritten (3   100  L) eluiert (96-Deepwell-Platte, PP, 1.2 mL). Anschlie end wurden die erhaltenen Eluate f r die LC-MS/MS-Analyse durch Zugabe

von 33 μL Ammoniumformiatpuffer (20 mmol L^{-1} , pH 3.0) auf ein Probenmilieu von Acetonitril zu Puffer im Verhältnis von 90 : 10 gebracht.

Durchführung von Bindungsassays mit Carbachol als Reporterligand

Für Filtrations-basierte Bindungsversuche mit Carbachol als Reporterligand wurden Aliquots der *Torpedo*-Membranpräparation (entsprechend ca. 6 – 12 μg Protein pro Well) mit Carbachol in Phosphatpuffer (120 mmol L^{-1} NaCl, 5 mmol L^{-1} KCl, 8.05 mmol L^{-1} Na_2HPO_4 und 1.95 mmol L^{-1} NaH_2PO_4 , pH 7.4) in Deepwell-Platten (PP, 1.2 mL) bei 25 °C für 2 h im Wasserbad inkubiert. Im weiteren Verlauf wurde mit Bindungsproben analog zu Filter-Bindungsexperimenten mit Epibatidin verfahren. Die Bestimmung der nichtspezifischen Bindung erfolgte in diesem Fall allerdings mittels Hitzedenaturierung über vier experimentell ermittelte Datenpunkte mit anschließender Extrapolation durch lineare Regression, wie für Zentrifugations-basierte MB327- bzw. Carbachol-Bindungsexperimente beschrieben (vgl. Abschnitt 3.1). Für die Kalibrierung wurden Matrixproben, mit der Zugabe des Ammoniumformiatpuffers, zuletzt mit Reporterligand in vier Konzentrationen im Bereich 0.5 – 30 nmol L^{-1} gespikt.

Datenanalyse

Daten aus den LC-MS/MS Analysen wurden mittels der Software Analyst v. 1.6.1 (AB Sciex, Darmstadt, Deutschland) gespeichert und ausgewertet. Zur Auswertung von Bindungsexperimenten wurde die PRISM v. 5.0-Software (Graph Pad Software, San Diego, USA) verwendet. So wurde die Gleichgewichtsdissoziationskonstante (K_d) und die maximale Dichte der Bindestellen (B_{max}) mithilfe des PRISM-Tools „one site – specific binding“ (nichtlineare Regression) berechnet. Die spezifische Bindung war als Differenz der Gesamtbindung und nicht-spezifischer Bindung definiert.

ZUSAMMENFASSUNG DER ARBEIT

4. Zusammenfassung der Arbeit

Phosphororganische Verbindungen bewirken eine dauerhafte Blockade der Acetylcholinesterase (AChE), einem Enzym, das für den Abbau des Neurotransmitters Acetylcholin (ACh) verantwortlich ist. Die Akkumulation von ACh an cholinergen Synapsen verursacht wiederum eine Dauererregung nikotinischer sowie muskarinischer Acetylcholinrezeptoren (nAChRs und mAChRs), wodurch das sogenannte cholinerge Syndrom ausgelöst wird. Zur Therapie einer Organophosphat(OP)-Vergiftung werden derzeit Atropin, zur Antagonisierung der muskarinergen Übererregung, und ein Oxim z.B. Obidoxim, zur Reaktivierung der AChE, als Antidote verabreicht. In einigen Fällen z.B. bei Vergiftung mit Tabun oder Soman ist eine AChE-Reaktivierung nicht möglich, sodass die andauernde Überaktivierung der nikotinischen Acetylcholinrezeptoren dazu führt, dass der nAChR schließlich dauerhaft in einen inaktiven, desensitisierten Zustand übergeht.

Um diese therapeutische Lücke, dass die nAChR-Übererregung bei erfolgloser AChE-Reaktivierung unbehandelt bleibt, zu schließen, rücken zunehmend alternative Therapieoptionen wie eine direkte pharmakologische Intervention am nAChR in den Fokus der Antidotforschung. In diesem Kontext zeigte die Bispyridiniumverbindung MB327 bereits einen vielversprechenden therapeutischen Effekt gegen OP-Vergiftungen *in vitro* wie auch *in vivo*. Durch allosterische Modulation scheint MB327 in der Lage den desensitisierten Muskeltyp-nAChR zu reaktivieren bzw. zu „resensibilisieren“. Allerdings fehlt es MB327 für den Einsatz als Antidot sowohl an Potenz als auch an Selektivität. Daher sollten, ausgehend von MB327 als Leitstruktur, neue potentielle nAChR-„Resensibilisierer“ entwickelt und in geeigneten biologischen Assays getestet werden.

Ziel dieser Arbeit war die Entwicklung von Bindungsassays als solches Testsystem, mit massenspektrometrischer Detektion zur Quantifizierung des Reporterliganden in Bindungsproben (sogenannte MS-Bindungsassays), zur schnellen und zuverlässigen Bestimmung der Bindungsaffinitäten von MB327 und Derivaten an die MB327-Bindestelle des nAChR. Als Reporterligand wurde das sechsfach deuterierte Analogon [$^2\text{H}_6$]MB327, als Targetpräparation nAChR-reiche Membranen des elektrischen Organs aus *Torpedo californica*, eingesetzt.

Zur zuverlässigen und robusten Quantifizierung des Reporterliganden [$^2\text{H}_6$]MB327 in Bindungsproben wurde zunächst eine geeignete LC-ESI-MS/MS-Methode entwickelt. Die Proben wurden hierbei in einem Laufmittelgemisch von 20 mmol L⁻¹ Ammoniumformiatpuffer (pH 3.0) und Acetonitril im Verhältnis 20 : 80 an einer Diol-HILIC als stationäre Phase chromatographiert und mit einem API3200 Triple-Quadrupol-Massenspektrometer mit Elektrospray-Ionisierung analysiert. Zur selektiven Detektion des Reporterliganden wurde im Tandem-MS-Modus des Massenspektrometers gearbeitet und der Massenübergang m/z 159.2 \rightarrow 144.3 aufgezeichnet. Um Intensitätsschwankungen des Reporterligand-Signals bzw. suppressive Effekte der Bindungsproben-Matrix auf das Reporterligand-Signal (sog. Matrixeffekte) auszugleichen wurde das 18-fach deuterierte Analogon [$^2\text{H}_{18}$]MB327 als Interner Standard eingesetzt. Dabei wurde der Massenübergang m/z 165.2 \rightarrow 147.2 aufgenommen. Eine Validierung gemäß CDER-Richtlinien der FDA für bioanalytische Methoden, durchgeführt in markerfreien Proben des Bindungsexperiments, zeigte, dass die [$^2\text{H}_6$]MB327-Quantifizierungsmethode, über einen Konzentrationsbereich von 10 pmol L⁻¹ bis 10 nmol L⁻¹, alle Kriterien der Validierungsparameter Selektivität, Linearität, Richtigkeit und Präzision erfüllt. Mit den auf Basis dieser LC-MS-Methode entwickelten Zentrifugations-basierten MS-Bindungsassays gelang erstmals eine Charakterisierung der Bindung von MB327 bzw. [$^2\text{H}_6$]MB327 an den nAChR. Sättigungsexperimente lieferten einen K_d -Wert von 15.5 ± 0.9 $\mu\text{mol L}^{-1}$ für die [$^2\text{H}_6$]MB327-Bindung am *Torpedo*-nAChR. Der K_i -Wert für die native Bispyridiniumverbindung von 18.3 ± 2.6 $\mu\text{mol L}^{-1}$, der in Autokompetitionsexperimenten mit [$^2\text{H}_6$]MB327 als Markerverbindung und MB327 als Kompetitor ermittelt wurde, stimmte mit diesem gut überein. Interessanterweise deutete der Vergleich der B_{max} -Werte aus Sättigungsexperimenten mit MB327 bzw. Carbachol als Markerverbindung darauf hin, dass die Bispyridiniumverbindung, zumindest unter den gewählten Assaybedingungen, an nur eine einzige Bindungsstelle am *Torpedo*-nAChR bindet.

Vor Anwendung des entwickelten MS-Bindungsassays zur Affinitätscharakterisierung einer Reihe neu synthetisierter MB327-Derivate an die MB327-Bindestelle des *Torpedo*-nAChR, wurden die Versuchsbedingungen nochmals geringfügig angepasst. Um bei der Lagerung der Targetpräparation und deren Verwendung im

Bindungsversuch durchweg in einem Puffersystem arbeiten zu können, wurde der bislang verwendete Inkubationspuffer gegen den Lagerungspuffer ausgetauscht. Ein Vergleich von Sättigungs- und Autokompetitionsexperimenten, durchgeführt unter originären bzw. modifizierten Bedingungen, zeigte, dass auch unter den neuen Bedingungen eine zuverlässige Bestimmung von Affinitätskonstanten, mit vergleichbaren K_d - bzw. K_i -Werten wie zuvor ermittelt, möglich war. Die Methode wurde entsprechend umgestellt und im Anschluss erneut gemäß CDER-Richtlinien der FDA validiert, zum Nachweis, dass die Zuverlässigkeit der [$^2\text{H}_6$]MB327-Quantifizierung auch unter den neuen Assaybedingungen gegeben war.

Mit dem Ziel erste Struktur-Affinitätsbeziehungen an der MB327-Bindestelle aufzubauen waren von Sebastian Rappenglück, ausgehend von MB327 als Modellverbindung, 56 neue Zielstrukturen zur Untersuchung in MS-Bindungsassays synthetisiert worden. Alle neu synthetisierten MB327-Derivate erhielten eine PTM(Pharmazie und Toxikologie München)-Kennung. Die Strukturanaloga waren dabei entweder aus jeweils zwei identischen N-Heterocyclen (symmetrische MB327-Derivate) oder aus zwei strukturell verschiedenen bzw. verschieden substituierten Aromaten (nicht-symmetrische MB327-Derivate) aufgebaut. Von allen symmetrischen und nicht-symmetrischen Testverbindungen wurden die Bindungsaffinitäten bezüglich der MB327-Bindestelle in MS-Bindungsassays mit [$^2\text{H}_6$]MB327 als Reporterligand des *Torpedo*-nAChR bestimmt.

Die Bindungsdaten symmetrischer MB327-Derivate zeigten durchweg eine Tendenz zu höheren Bindungsaffinitäten an die MB327-Bindestelle, wenn Testverbindungen mit unpolaren statt polaren Gruppen substituiert waren. Die lipophile Verbindung PTM0022, mit zusätzlichem Phenylrest in 3-Position an beiden 4-*tert*-Butyl-substituierten Pyridiniumringen (MB327-Molekülgerüst), zeigte die höchste Bindungsaffinität an die MB327-Bindestelle, mit deutlichem Affinitätsgewinn gegenüber MB327 ($\text{p}K_i, \text{PTM0022} = 5.16 \pm 0.07$), das zwitterionische PTM0028 mit Carbonsäurefunktionen in 3-Position der Pyridiniumeinheiten des MB327-Molekülgerüsts die niedrigste Bindungsaffinität. Dabei nahm die Bindungsaffinität einer Zielstruktur an die MB327-Bindestelle mit sterischem Anspruch des lipophilen Substituenten zu, wie der Vergleich der Affinitätskonstanten von MB327 und PTM0013, PTM0001 und PTM0014 bzw. PTM0002 und PTM0003, mit einer *tert*-Butyl- bzw. einer

Isopropylgruppe in 4-, 3- oder 2-Position am Pyridiniumring, sowie von Bisimidazoliumverbindungen PTM0034 und PTM0059 mit Methyl- bzw. *tert*-Butylgruppe am N-Heteroatom, zeigt.

Innerhalb der biologischen Evaluation nicht-symmetrischer MB327-Derivate im MS-Bindungsassay zeigten allerdings auch solche Testverbindungen hohe Bindungsaffinitäten an die MB327-Bindestelle, die einen 4-*tert*-Butyl-substituierten Pyridiniumrest auf der einen und eine polar-substituierte (z.B. PTM0050, PTM0030 und PTM0056 mit 3-COOEt, 3- bzw. 4-NMe₂-Substitution) Pyridiniumeinheit auf der anderen Seite tragen. Diese Bindungsdaten stimmen mit Ergebnissen aus MB327-Docking-Studien an einem 3D-Strukturmodell des Muskeltyp-nAChR überein, dass putative MB327-Bindungstaschen asymmetrisch, mit überwiegend polaren Aminosäureseitenketten zur Interaktion mit dem Liganden auf der einen Seite und mehrheitlich lipophilen Resten auf der anderen Seite, aufgebaut sind. Wird der 4-*tert*-Butylsubstituent an einem der Pyridiniumringe des MB327-Molekülgerüsts beispielsweise durch einen 3- bzw. 4-Dimethylaminosubstituenten ersetzt (vgl. MB327 und PTM0030 bzw. PTM0056), steigt der entsprechende pK_i-Wert sichtlich. Die Dimethylaminogruppe lieferte bereits innerhalb der Testreihe symmetrischer MB327-Derivate überraschende Ergebnisse, indem sich deren Einführung als Ringsubstituent, im Gegensatz zu allen anderen polaren funktionellen Gruppen, nicht nachteilig auf die Bindung an der MB327-Bindestelle auswirkte. Vielmehr adressierte das 3-NMe₂-substituierte PTM0007 die MB327-Bindestelle mit ähnlich hoher Bindungsaffinität wie die Leitstruktur. Der Austausch einer *tert*-Butylgruppe gegen einen Methoxysubstituenten, hingegen, ob an einem oder an beiden Pyridiniumringen, ging in jedem Fall mit einem deutlichen Verlust an Bindungsaffinität an die MB327-Bindestelle einher (MB327 und PTM0008 bzw. PTM0040, PTM0001 und PTM0009 sowie PTM0002 und PTM0010). Interessanterweise konnte, sowohl innerhalb der Reihe symmetrischer wie auch nicht-symmetrischer MB327-Derivate, die Bindungsaffinität einer 3-Methoxysubstituierten Verbindung (PTM0009 bzw. PTM0040) durch Kombination mit einer *tert*-Butylgruppe als Zweitsubstituent in 4-Position am selben N-Heterocyclus (PTM0016 bzw. PTM0038) wieder deutlich, mit einer Differenz von jeweils 0.6 log Einheiten, gesteigert werden. Bei nicht-symmetrischer Substitution im Fall von PTM0038 hatte die Kombination des 3-Methoxy- und 4-*tert*-

Butylsubstituenten am N-Heterocyclus eine im Vergleich zu MB327 deutlich höhere Bindungsaffinität zur Folge ($pK_i, \text{MB327} = 4.73 \pm 0.03$; $pK_i, \text{PTM0038} = 4.97 \pm 0.02$).

Insgesamt deuten die Bindungsdaten darauf hin, dass die *tert*-Butylgruppe in 4-Position wie auch das positiv geladene Stickstoffatom am Pyridiniumring eine wichtige Rolle für die Bindung von MB327 und Derivaten an der MB327-Bindestelle spielen. Erstere erlaubt dabei lipophile Wechselwirkungen, während der positiv geladene Pyridiniumring sowohl ionische als auch Kation- π -Wechselwirkungen an der Bindetasche eingehen könnte. Die Tatsache, dass große konjugierte Ringsysteme ebenfalls mit hohen Bindungsaffinitäten einhergehen (PTM0022, PTM0032 und PTM0054) spricht außerdem dafür, dass auch π -Wechselwirkungen mit aromatischen oder positiv geladenen Aminosäureseitenketten für eine Bindung an der MB327-Bindestelle von Vorteil sind.

Mit der Bispyridiniumverbindung PTM0022 konnte im Rahmen dieses Projekts bereits eine erste Verbindung identifiziert werden, die mit deutlich höherer Affinität an die MB327-Bindestelle bindet als die Leitstruktur. Auf Basis der Bindungsdaten symmetrischer wie auch nicht-symmetrischer MB327-Derivate gelang es außerdem erste Struktur-Affinitätsbeziehungen an der MB327-Bindestelle abzuleiten. Um diese weiter zu verfeinern und auszubauen ist allerdings die Untersuchung weiterer, strukturell diverser Verbindungen im MS-Bindungsassay notwendig.

ABKÜRZUNGSVERZEICHNIS

5. Abkürzungsverzeichnis

ACh	Acetylcholin
AChE	Acetylcholinesterase
B _{max}	Anzahl maximal verfügbarer Bindungsstellen
BCA	Bicinchoninsäure
CDER	Center for Drug evaluation and research
ESI	Elektrospray-Ionisation
EDTA	Ethylendiamintetraessigsäure
FDA	Food and Drug Administration
GB	Gesamtbindung
HILIC	Hydrophilic-Interaction-Chromatography
(HP)LC	(Hochleistungs-) Flüssigkeitschromatographie
IC ₅₀	mittlere inhibitorische Konstante
IS	Interner Standard
K_d	Gleichgewichtsdissoziationskonstante
K_i	Inhibitionskonstante
LC-MS	Flüssigkeitschromatographie mit Massenspektrometrie- Kopplung
[L]	Reporterligandkonzentration
MeCN	Acetonitril
MS	Massenspektrometrie
MW	Mittelwert
m/z	Verhältnis Masse zu Ladung

mAChR	muskarinischer Acetylcholinrezeptor
nAChR	nikotinischer Acetylcholinrezeptor
NAM	negativ allosterischer Modulator
NB	nicht-spezifische Bindung
OP	Organophosphat
OPCW	Organisation for the Prohibition of Chemical Weapons
PAM	positiv allosterischer Modulator
PP	Polypropylen
PS	Polystyrol
PTM	Pharmazie und Toxikologie München
Q	Quadrupol
SB	spezifische Bindung
SD	Standardabweichung
SURFE ² R	Surface-Electrogenic-Event-Reader
[T]	Targetkonzentration
[TL] bzw. [TV]	Konzentration an Komplexen von Target und Reporterligand bzw. Testverbindung
TM	Transmembrandomäne
Tris	Tris(hydroxymethyl)-aminomethan
UE	Untereinheit
ZNS	zentrales Nervensystem

LITERATURVERZEICHNIS

6. Literaturverzeichnis

- ¹ Höfer, M. Chemische Kampfstoffe: Ein Überblick *Chemie in unserer Zeit* **2002**, 36, 148-155.
- ² Szinicz, L. History of chemical and biological warfare agents *Toxicology* **2005**, 214, 167-181.
- ³ Koelle, G. B. Organophosphate Poisoning - An Overview *Fundam. Appl. Toxicol.* **1981**, 1, 129-134.
- ⁴ deWittlaan, J. The Structure of the OPCW Fact Sheets. [Online] Nov, 2017. https://www.opcw.org/fileadmin/OPCW/Fact_Sheets/English/Fact_Sheet_3_-_OPCW_Structure.pdf (aufgerufen am 27.05.2018).
- ⁵ Chemical weapons watchdog wins Nobel Peace Prize for Syrian mission. *Reuters* [Online] Okt 11, 2013. <https://www.reuters.com/article/us-nobel-peace-opcw-annoucement/chemical-weapons-watchdog-wins-nobel-peace-prize-for-syrian-mission-idUSBRE99A07F20131011> (aufgerufen am 27.05.2018).
- ⁶ The poisoning of former Russian double agent Sergei Skripal. *Reuters* [Online] März 8, 2018. <https://www.reuters.com/article/us-britain-russia-explainer/the-poisoning-of-former-russian-double-agent-sergei-skripal-idUSKCN1GK1QI> (aufgerufen am 15.07.2018).
- ⁷ What is known, and not known, about poisoning of ex-spy in Britain. *Reuters* [Online] Apr. 5, 2018. <https://www.reuters.com/article/us-britain-russia-explainer/what-is-known-and-not-known-about-poisoning-of-ex-spy-in-britain-idUSKCN1HC148> (aufgerufen am 15.07.2018).
- ⁸ VX used in airport murder of Kim Jong Nam kills in minutes. *Reuters* [Online] Feb 24, 2017. <https://www.reuters.com/article/us-northkorea-malaysia-kim-nerveagent/vx-used-in-airport-murder-of-kim-jong-nam-kills-in-minutes-idUSKBN1630F4> (aufgerufen am 15.07.2018).
- ⁹ Dolgin, E. Syrian gas attack reinforces need for better anti-sarin drugs *Nature Med.* **2013**, 19, 1194–1195.
- ¹⁰ John, H.; van der Schans, M. J.; Koller, M.; Spruit, H. E. T.; Worek, F.; Thiermann, H.; Noort, D. Fatal sarin poisoning in Syria 2013: forensic verification within an international laboratory network *Forensic Toxicol.* **2018**, 36, 61–71.
- ¹¹ Bajgar, J. Organophosphates/ Nerve Agent poisoning: Mechanism of action, diagnosis, prophylaxis, and treatment. In

Advances in Clinical Chemistry; Makowski, G. S. Ed.; Elsevier: San Diego, 2004; Band 38; pp 151-216.

¹² Aurbek, N.; Worek, F.; Thiermann, H. Aktuelle Aspekte in der Behandlung der phosphororganischen Vergiftung, *Wehrmed. Mschr.* **2009**, 53, 340-349.

¹³ Tucker, J. B. War of Nerves: *Chemical Warfare from World War I to Al-Qaeda*, 1st ed.; Pantheon Books: New York, 2006.

¹⁴ Newmark, J. Nerve Agents *Neurologist* **2007**, 13, 20-32.

¹⁵ Balali-Mood, M.; Saber, H. Recent Advances in the Treatment of Organophosphorous Poisonings *Iran. J. Med. Sci.* **2012**, 37, 74–91.

¹⁶ Black, R. Development, Historical Use and Properties of Chemical Warfare Agents. In *Chemical Warfare Toxicology: Volume 1: Fundamental Aspects*; Worek, F.; Jenner, J.; Thiermann, H. Eds.; Royal Society of Chemistry: London, 2016; 1st ed.; pp 1-28.

¹⁷ Worek, F.; Thiermann, H.; Szinicz, L.; Eyer, P. Kinetic analysis of interactions between human acetylcholinesterase, structurally different organophosphorus compounds and oximes *Biochem. Pharmacol.* **2004**, 68, 2237-2248.

¹⁸ Mirzayanov, V. S. *Dismantling the Soviet/Russian Chemical Weapons Complex: An Insider's View*; Chemical Weapons Disarmament in Russia: Problems and Prospects, Report No. 17;

The Henry L. Stimson Center: Washington, DC, 1995.

¹⁹ Mirzayanov, V. S. *State secrets. An insider's chronicle of the Russian chemical weapons program*, Outskirts Press: Parker, 2008.

²⁰ Chai, P. R.; Hayes, B. D.; Erickson, T. B.; Boyer, E. W. Novichok agents: a historical, current, and toxicological perspective *Toxicol. Commun.* **2018**, 2, 45-48.

²¹ Weinbroum, A. A. Pathophysiological and clinical aspects of combat anticholinesterase poisoning *Br. Med. Bull.* **2005**, 72, 119-133.

²² Schmaltz, F. *Kampfstoff-Forschung im Nationalsozialismus: Zur Kooperation von Kaiser-Wilhelm-Instituten, Militär und Industrie*, Wallstein-Verlag: Göttingen, 2005.

²³ Newmark, J. Nerve Agents: Pathophysiology and Treatment of Poisoning *Semin. Neurol.* **2004**, 24, 185-196.

²⁴ Eddleston, M.; Buckley, N. A.; Eyer, P.; Dawson, A. H. Management of acute organophosphorus pesticide poisoning *Lancet* **2008**, 371, 597–607.

²⁵ Marrs, T. C. Organophosphate Poisoning *Pharmacol. Ther.* **1993**, 58, 51-66.

-
- ²⁶ Campbell, N. A.; Reece, J. B. *Biology*, 6th ed.; Benjamin Cummings: San Francisco, 2005.
- ²⁷ Sirin, G. S.; Zhou, Y.; Lior-Hoffmann, L.; Wang, S.; Zhang, Y. Aging Mechanism of Soman Inhibited Acetylcholinesterase, *J. Phys. Chem. B*. **2012**, *116*, 12199-12207.
- ²⁸ Kilby, B. A.; Kilby, M. The Toxicity of Alkyl Fluorophosphonates in man and animals, *Br. J. Pharmacol.* **1947**, *2*, 234-240.
- ²⁹ Brown, J. H.; Laiken, N. Muscarinic Receptor Agonists and Antagonists. In *Goodman & Gilman's The pharmacological basis of therapeutics*; Brunton, L. L.; Chabner, B. A.; Knollmann, B. C. Eds.; McGraw Hill Professional: New York, 2011; 12th ed.; pp 219-237.
- ³⁰ Zilker, T. Medical management of incidents with chemical warfare agents *Toxicology* **2005**, *214*, 221-231.
- ³¹ Worek, F.; Aurbek, N.; Koller, M.; Becker, C.; Eyer, P.; Thiermann, H. Kinetic analysis of reactivation and aging of human acetylcholinesterase inhibited by different phosphoramidates *Biochem. Pharmacol.* **2007**, *73*, 1807-1817.
- ³² Marrs, T. C. Diazepam in the Treatment of Organophosphorus Ester Pesticide Poisoning *Toxicol. Rev.* **2003**, *22*, 75-81.
- ³³ Murphy, M. R.; Blick, D. W.; Dunn, M. A.; Fanton, J. W.; Hartgraves, S. L. Diazepam as a treatment for nerve agent poisoning in primates *Aviat. Space Environ. Med.* **1993**, *64*, 110-5.
- ³⁴ Shafferman, A.; Ordentlich, A.; Barak, D.; Stein, D.; Ariel, N.; Velan, B. Aging of phosphorylated human acetylcholinesterase: catalytic processes mediated by aromatic and polar residues of the active centre *Biochem. J.* **1996**, *318*, 833-840.
- ³⁵ Karlin, A. Emerging Structure of the Nicotinic Acetylcholine Receptors, *Nature Rev. Neurosci.* **2002**, *3*, 102-114.
- ³⁶ Sine, S. M.; Engel, A. G. Recent advances in Cys-loop receptor structure and function *Nature* **2006**, *440*, 448-455.
- ³⁷ Chatzidaki, A.; Millar, N. S. Allosteric modulation of nicotinic acetylcholine receptors, *Biochem. Pharmacol.* **2015**, *97*, 408-417.
- ³⁸ Gotti, C.; Clementi, F. Neuronal nicotinic receptors: from structure to pathology, *Prog. Neurobiol.* **2004**, *74*, 363-396.
- ³⁹ Wang, H.; Yu, M.; Ochani, M.; Amella, C. A.; Tanovic, M.; Susarla, S.; Li, J. H.; Wang, H.; Yang, H.; Ulloa, L.; Al-Abed, Y.; Czura, C. J.; Tracey, K. J. Nicotinic acetylcholine receptor $\alpha 7$ subunit is an essential regulator of inflammation *Nature* **2003**, *421*, 384-388.
- ⁴⁰ Umana, I. C.; Daniele, C. A.; McGehee, D. S. Neuronal nicotinic receptors as analgesic targets: It's a winding road *Biochem. Pharmacol.* **2013**, *86*, 1208-1214.

-
- ⁴¹ Dani, J. A.; Bertrand, D. Nicotinic Acetylcholine Receptors and Nicotinic Cholinergic Mechanisms of the Central Nervous System *Annu. Rev. Pharmacol. Toxicol.* **2007**, *47*, 699-729.
- ⁴² Mantione, E.; Micheloni, S.; Alcaïno, C.; New, K.; Mazzaferro, S.; Bermudez, I. Allosteric modulators of $\alpha 4\beta 2$ nicotinic acetylcholine receptors: a new direction for antidepressant drug discovery *Future Med. Chem.* **2012**, *4*, 2217-2230.
- ⁴³ Haydar, S. N.; Dunlop, J. Neuronal Nicotinic Acetylcholine Receptors - Targets for the Development of Drugs to Treat Cognitive Impairment Associated with Schizophrenia and Alzheimer's Disease *Curr. Top. Med. Chem.* **2010**, *10*, 144-152.
- ⁴⁴ Gibbons, A.; Dean, B. The Cholinergic System: An Emerging Drug Target for Schizophrenia *Curr. Pharm. Des.* **2016**, *22*, 2124-2133.
- ⁴⁵ Mucchietto, V.; Crespi, A.; Fasoli, F.; Clementi, F.; Gotti, C. Neuronal Acetylcholine Nicotinic Receptors as New Targets for Lung Cancer Treatment *Curr. Pharm. Des.* **2016**, *22*, 2160-2169.
- ⁴⁶ Albuquerque, E. X.; Pereira, E. F. R.; Alkondon, M.; Rogers, S. W. Mammalian Nicotinic Acetylcholine Receptors: From Structure to Function *Physiol. Rev.* **2009**, *89*, 73-120.
- ⁴⁷ Noda, M.; Furutani, Y.; Takahashi, H.; Toyosato, M.; Tanabe, T.; Shimizu, S.; Kikuyotani, S.; Kayano, T.; Hirose, T.; Inayama, S.; Numa, S. Cloning and sequence analysis of calf cDNA and human genomic DNA encoding α -subunit precursor of muscle acetylcholine receptor *Nature* **1983**, *305*, 818-823.
- ⁴⁸ Millar, N. S. Assembly and subunit diversity of nicotinic acetylcholine receptors, *Biochem. Soc. Trans.* **2003**, *31*, 869-874.
- ⁴⁹ Navedo, M.; Nieves, M.; Rojas, L.; Lasalde-Dominicci, J. A. Tryptophan substitutions reveal the role of nicotinic acetylcholine receptor alpha-TM3 domain in channel gating: differences between *Torpedo* and muscle-type AChR *Biochemistry* **2004**, *43*, 78-84.
- ⁵⁰ Arias, H. R.; Xing, H.; MacDougall, K.; Blanton, M. P.; Soti, F.; Kem, W. R. Interaction of benzylidene-anabaseine analogues with agonist and allosteric sites on muscle nicotinic acetylcholine receptors *Br. J. Pharmacol.* **2009**, *157*, 320-330.
- ⁵¹ Niessen, K. V.; Seeger, T.; Tattersall, J. E.; Timperley, C. M.; Bird, M.; Green, A. C.; Thiermann, H.; Worek, F. Affinities of bispyridinium non-oxime compounds to [³H]epibatidine binding sites of *Torpedo californica* nicotinic acetylcholine receptors depend on linker length *Chem. Biol. Interact.* **2013**, *206*, 545-554.

- ⁵² Unwin, N. Refined structure of the nicotinic acetylcholine receptor at 4Å resolution *J. Mol. Biol.* **2005**, *346*, 967-989.
- ⁵³ Changeux, J. P. The Nicotinic Acetylcholine Receptor: The Founding Father of the Pentameric Ligand-gated Ion Channel Superfamily *J. Biol. Chem.* **2012**, *287*, 40207-40215.
- ⁵⁴ Papke, R. L. Merging old and new perspectives on nicotinic acetylcholine receptors *Biochem. Pharmacol.* **2014**, *89*, 1-11.
- ⁵⁵ Hurst, R.; Rollema, H.; Bertrand, D. Nicotinic acetylcholine receptors: From basic science to therapeutics *Pharmacol. Ther.* **2013**, *137*, 22-54.
- ⁵⁶ Berman, H. M.; Westbrook, J.; Feng, Z.; Gilliland, G.; Bhat, T. N.; Weissig, H.; Shindyalov, I. N.; Bourne, P. E. The Protein Data Bank *Nucleic Acids Res.* **2000**, *28*, 235-242.
- ⁵⁷ Rose, A. S.; Hildebrand, P. W. NGL Viewer: a web application for molecular visualization *Nucleic Acids Res.* **2015**, *43*, 576-579.
- ⁵⁸ Sheridan, R. D.; Smith, A. P.; Turner, S. R.; Tattersall, J. E. H. Nicotinic antagonists in the treatment of nerve agent intoxication *J. R. Soc. Med.* **2005**, *98*, 114-115.
- ⁵⁹ Arias, H. R. Allosteric modulation of nicotinic acetylcholine receptors. In *Pharmacology of Nicotinic Acetylcholine Receptors from the Basic and Therapeutic Perspectives*; Arias, H. R. Ed.; Research Signpost: Kerala, 2011; pp 151-173.
- ⁶⁰ Ng, H. J.; Whittemore, E. R.; Tran, M. B.; Hogenkamp, D. J.; Broide, R. S.; Johnstone, T. B.; Zheng, L.; Stevens, K. E.; Gee, K. W. Nootropic $\alpha 7$ nicotinic receptor allosteric modulator derived from GABA_A receptor modulators *Proc. Natl. Acad. Sci. U. S. A.* **2007**, *104*, 8059-8064.
- ⁶¹ Timmermann, D. B.; Grønlien, J. H.; Kohlhaas, K. L.; Nielsen, E. Ø.; Dam, E.; Jørgensen, T. D.; Ahring, P. K.; Peters, D.; Holst, D.; Christensen, J. K.; Malysz, J.; Briggs, C. A.; Gopalakrishnan, M.; Olsen, G. M. An Allosteric Modulator of the $\alpha 7$ Nicotinic Acetylcholine Receptor Possessing Cognition-Enhancing Properties in Vivo *J. Pharmacol. Exp. Ther.* **2007**, *323*, 294-307.
- ⁶² Hurst, R. S.; Hajós, M.; Raggenbass, M.; Wall, T. M.; Higdon, N. R.; Lawson, J. A.; Rutherford-Root, K. L.; Berkenpas, M. B.; Hoffmann, W. E.; Piotrowski, D. W.; Groppi, V. E.; Allaman, G.; Ogier, R.; Bertrand, S.; Bertrand, D.; Arneric, S. P. A Novel Positive Allosteric Modulator of the $\alpha 7$ Neuronal Nicotinic Acetylcholine Receptor: *In Vitro* and *In Vivo* Characterization *J. Neurosci.* **2005**, *25*, 4396-4405.
- ⁶³ Gee, K. W.; Olincy, A.; Kanner, R.; Johnson, L.; Hogenkamp, D.; Harris, J.; Tran, M.; Edmonds, S. A.; Sauer, W.; Yoshimura, R.; Johnstone, T.; Freedman, R.

First in human trial of a type I positive allosteric modulator of $\alpha 7$ -nicotinic acetylcholine receptors: Pharmacokinetics, safety, and evidence for neurocognitive effect of AVL-3288 *J. Psychopharmacol.* **2017**, *31*, 434-441.

⁶⁴ Monod, J.; Wyman, J.; Changeux, J. P. On the Nature of Allosteric Transitions: A Plausible Model *J. Mol. Biol.* **1965**, *12*, 88-118.

⁶⁵ Corradi, J.; Bouzat, C. Understanding the Bases of Function and Modulation of $\alpha 7$ Nicotinic Receptors: Implications for Drug Discovery *Mol. Pharmacol.* **2016**, *90*, 288–299.

⁶⁶ Zhang, J.; Xue, F.; Liu, Y.; Yang, H.; Wang, X. The Structural Mechanism of the Cys-Loop Receptor Desensitization *Mol. Neurobiol.* **2013**, *48*, 97-108.

⁶⁷ Quick, M. W.; Lester, R. A. J. Desensitization of Neuronal Nicotinic Receptors, *J. Neurobiol.* **2002**, *53*, 457–478.

⁶⁸ Niessen, K. V.; Muschik, S.; Langguth, F.; Rappenglück, S.; Seeger, T.; Thiermann, H.; Worek, F. Functional analysis of *Torpedo californica* nicotinic acetylcholine receptors in multiple activation states by SSM-based electrophysiology *Toxicol. Lett.* **2016**, *247*, 1-10.

⁶⁹ Seeger, T.; Eichhorn, M.; Lindner, M.; Niessen, K. V.; Tattersall, J. E.; Timperley, C. M.; Bird, M.; Green, A. C.; Thiermann, H.; Worek, F. Restoration of soman-blocked

neuromuscular transmission in human and rat muscle by the bispyridinium non-oxime MB327 in vitro *Toxicology* **2012**, *294*, 80-84.

⁷⁰ Timperley, C. M.; Bird, M.; Green, C.; Price, M. E.; Chad, J. E.; Turner, S. R.; Tattersall, J. E. H. 1,1'-(Propane-1,3-diyl)bis(4-*tert*-butylpyridinium) di(methanesulfonate) protects guinea pigs from soman poisoning when used as part of a combined therapy *Med. Chem. Commun.* **2012**, *3*, 352-356.

⁷¹ Kassa, J.; Pohanka, M.; Timperley, C. M.; Bird, M.; Green, A. C.; Tattersall, J. E. H. Evaluation of the benefit of the bispyridinium compound MB327 for the antidotal treatment of nerve agent-poisoned mice *Toxicol. Mech. Methods* **2016**, *26*, 334-339.

⁷² Price, M. E.; Docx, C. J.; Rice, H.; Fairhall, S. J.; Poole, S. J. C.; Bird, M.; Whiley, L.; Flint, D. P.; Green, A. C.; Timperley, C. M.; Tattersall, J. E. H. Pharmacokinetic profile and quantitation of protection against soman poisoning by the antinicotinic compound MB327 in the guinea-pig *Toxicol. Lett.* **2016**, *244*, 154-160.

⁷³ Turner, S. R.; Chad, J. E.; Price, M. E.; Timperley, C. M.; Bird, M.; Green, A. C.; Tattersall, J. E. H. Protection against nerve agent poisoning by a noncompetitive nicotinic antagonist, *Toxicol. Lett.* **2011**, *206*, 105-111.

- ⁷⁴ Niessen, K. V.; Seeger, T.; Rappenglück, S.; Wein, T.; Höfner, G.; Wanner, K. T.; Thiermann, H.; Worek, F. In vitro pharmacological characterization of the bispyridinium non-oxime compound MB327 and its 2- and 3-regioisomers *Toxicol. Lett.* **2018**, 293, 190-197.
- ⁷⁵ Niessen, K. V.; Tattersall, J. E. H.; Timperley, C. M.; Bird, M.; Green, C.; Thiermann, H.; Worek, F. Competition radioligand binding assays for the investigation of bispyridinium compound affinities to the human muscarinic acetylcholine receptor subtype 5 (hM₅) *Drug. Test. Anal.* **2012**, 4, 292–297.
- ⁷⁶ Silverman, R. B.; Holladay, M. W. *The Organic Chemistry of Drug Design and Drug Action*, 3rd ed.; Academic Press: San Diego, 2014.
- ⁷⁷ Hulme, E. C. *Receptor-Ligand Interactions: A practical Approach*; Oxford University: Oxford, 1992.
- ⁷⁸ de Jong, L. A. A.; Uges, D. R. A.; Franke, J. P.; Bischoff, R. Receptor ligand binding assays: Technologies and applications *J. Chromatogr. B Analyt. Technol. Biomed. Life Sci.* **2005**, 829, 1-25.
- ⁷⁹ Fang, Y. Ligand-receptor interaction platforms and their applications for drug discovery *Expert. Opin. Drug Discov.* **2012**, 7, 969-988.
- ⁸⁰ Núñez, S.; Venhorst, J.; Kruse, C. G. Target–drug interactions: first principles and their application to drug discovery *Drug Discov. Today* **2012**, 17, 10-22.
- ⁸¹ Leysen, J. E.; Langlois, X.; Heylen, L.; Lammertsma, A. A. Receptors: Binding Assays. In *Encyclopedia of Psychopharmacology*; Stolerman, I. P. Ed.; Springer-Verlag: Heidelberg, 2010; Vol. 1; pp 1134-1142.
- ⁸² Höfner, G.; Wanner, K. T. MS binding assays. In *Analyzing Biomolecular Interactions by Mass Spectrometry*; Kool, J.; Niessen, W. M. A. Eds.; Wiley-VCH: Weinheim, 2015; pp 165-198.
- ⁸³ Hulme, E. C.; Trevethick, M. A. Ligand binding assays at equilibrium: Validation and interpretation *Br. J. Pharmacol.* **2010**, 161, 1219-1237.
- ⁸⁴ Höfner, G.; Wanner, K. T. Competitive Binding Assays Made Easy with a Native Marker and Mass Spectrometric Quantification *Angew. Chem. Int. Ed. Engl.* **2003**, 42, 5235–5237.
- ⁸⁵ Zepperitz, C.; Höfner, G.; Wanner, K. T. MS-binding assays: Kinetic, saturation, and competitive experiments based on quantitation of bound marker as exemplified by the GABA transporter mGAT1 *ChemMedChem* **2006**, 1, 208–217.
- ⁸⁶ Hess, M.; Höfner, G.; Wanner, K. T. (S)- and (R)-Fluoxetine as Native Markers in Mass Spectrometry (MS) Binding Assays

Addressing the Serotonin Transporter
ChemMedChem **2011**, 6, 1900–1908.

⁸⁷ Grimm, S. H.; Höfner, G.; Wanner, K. T. MS Binding Assays for the Three Monoamine Transporters Using the Triple Reuptake Inhibitor (1R,3S)-Indatraline as Native Marker *ChemMedChem* **2015**, 10, 1027–1039.

⁸⁸ Neiens, P.; Höfner, G.; Wanner, K. T. MS Binding Assays for D 1 and D 5 Dopamine Receptors *ChemMedChem* **2015**, 10, 1924–1931.

⁸⁹ Cheng, Y.; Prusoff, W. H. Relationship between the inhibition constant (K_i) and the concentration of inhibitor which causes 50 percent inhibition (IC₅₀) of an enzymatic reaction *Biochem. Pharmacol.* **1973**, 22, 3099–3108.

⁹⁰ AB Sciex. Sensitivity, ruggedness, and simplicity. Together at last. API 5000™ LC/MS/MS SYSTEM. [Online] 2010. http://www.absciex.com/Documents/Downloads/Literature/mass-spectrometry-cms_040627.pdf (aufgerufen am 29.07.2015).

⁹¹ Food and Drug Administration Guidance for Industry: Bioanalytical method validation. [Online] 2001. <http://www.labcompliance.de/documents/FDA/FDA-Others/Laboratory/f-507-bioanalytical-4252fml.pdf> (aufgerufen am 27.05.2018).

⁹² Wein, T.; Höfner, G.; Rappenglück, S.; Sichler, S.; Niessen, K. V.; Seeger, T.; Worek, F.; Thiermann, H.; Wanner, K. T. Searching for putative binding sites of the bispiridinium compound MB327 in the nicotinic acetylcholine receptor *Toxicology Letters* **2018**, 293, 184–189.

⁹³ Niessen K. V.; Tattersall J. E. H.; Timperley C. M.; Bird M.; Green C.; Seeger T.; Thiermann H.; Worek F. Interaction of bispiridinium compounds with the orthosteric binding site of human $\alpha 7$ and *Torpedo californica* nicotinic acetylcholine receptors (nAChRs) *Toxicology Letters* **2011**, 206, 100–104.

⁹⁴ Kawai, H.; Dunn, S. M. J.; Raftery, M. A. Epibatidine binds to four sites on the *Torpedo* nicotinic acetylcholine receptor *Biochemical and Biophysical Research Communications* **2008**, 366, 834–839.

⁹⁵ Boyd, N. D.; Cohen, J. B. Kinetics of binding of [³H]acetylcholine and [³H]carbamoylcholine to *torpedo* postsynaptic membranes: Slow conformational transitions of the cholinergic receptor *Biochemistry* **1980**, 19, 5344–5353.

⁹⁶ Dunn, S. M. J.; Blanchard, S. G.; Raftery, M. A. Kinetics of carbamylcholine binding to membrane-bound acetylcholine receptor monitored by fluorescence changes of a covalently bound probe *Biochemistry* **1980**, 19, 5645–5652.

⁹⁷ Smith P. K., Krohn R. I., Hermanson G. T., Mallia A. K., Gartner F. H., Provenzano M. D., Fujimoto E. K., Goeke N. M., Olson

B. J., Klenk D. C. Measurement of protein using bicinchoninic acid *Analytical Biochemistry* **1985**, 150, 76–85.